

**MECHANISMS AND APPLICATIONS OF RECA-INDEPENDENT  
RECOMBINATION IN *LEGIONELLA PNEUMOPHILA***

by

**Andrew Bevan Brody Bryan**

A dissertation submitted in partial fulfillment  
of the requirements for the degree of  
Doctor of Philosophy  
(Microbiology and Immunology)  
in The University of Michigan  
2011

Doctoral Committee:

Professor Michele S. Swanson, Chair  
Professor Victor DiRita  
Associate Professor Matthew R. Chapman  
Associate Professor Mary X.D. O’Riordan

© Andrew Bevan Brody Bryan

---

2011

## **DEDICATION**

For Amanda

From elementary school to graduate school and beyond,  
may we continue to learn from and with each other for years to come.

## ACKNOWLEDGEMENTS

I wish to express my sincere thanks to all those who have helped and encourage me throughout the years. Thanks to my mentor, Prof. Michele Swanson, whose skills at critical thinking, writing, and speaking have undoubtedly improved my own, despite my incoherent ramblings. Her emphasis on maintaining a balanced work-life relationship have been critical for maintaining my sanity, while her mentoring at all levels of science and advocacy for women in science issues are truly admirable. Thanks to my foodie thesis committee, Drs. Matt Chapman, Vic DiRita, and Mary O’Riordan for many helpful conversations. Drs. Lyle Simmons, Donald Court, and David Friedman all deserve equal thanks to my committee for advising on my projects that often fell outside the expertise of most of the department. Thanks to all my labmates past and present, Zach Abbott, Brenda Byrne, Jeff Dubuisson, Rachel Edwards, Esteban Fernandez-Moreira, Maris Fonseca, Amrita Joshi, Ari Molofsky, J.D. Sauer, Natalie Whitfield, Brian Yagi, and especially Kaoru Harada, my undergraduate research assistant, for her patience working with me. Thanks to the Department of Microbiology and Immunology and the Medical Scientist Training Program for their collegiality and support, funding and otherwise. Special thanks to Drs. Mike Sadowsky and Rod Welch and their labs for mentoring me as an undergraduate—especially the Welch lab, where the scientific and familial atmosphere, along with the mentoring of Paula Roesch, Shai Pellett, and others can be directly credited for my choice to come to graduate school. A big hug to all my friends who helped me make it through, whether it be a rant about bugs not growing or an escape

to not think about school. Lastly, thanks to my family. To my parents Bill and Carol and all my grandparents for raising me to ask questions and to read books like *How Things Work*, and to my brother Nick, who makes an older brother proud and shares a pursuit of science, engineering, and creativity.

## TABLE OF CONTENTS

<b>DEDICATION</b> .....	<b>ii</b>
<b>ACKNOWLEDGEMENTS</b> .....	<b>iii</b>
<b>LIST OF FIGURES</b> .....	<b>viii</b>
<b>LIST OF TABLES</b> .....	<b>x</b>
<b>LIST OF APPENDICES</b> .....	<b>xi</b>
<b>ABSTRACT</b> .....	<b>xii</b>
<b>CHAPTER ONE: Introduction</b> .....	<b>1</b>
Thesis outline and context .....	1
An environmental pathogen.....	3
Burden of disease.....	4
Outbreaks.....	5
Clinical features, diagnosis and treatment.....	6
Serogroup epidemiology.....	8
A DNA-rich lifestyle; a dynamic genome riddled with eukaryotic DNA.....	9
Recombination and the exchange of genetic material .....	11
RecA-dependent recombination .....	12
Phage-mediated recombination .....	14
Site-specific recombination .....	16
Intersection of recombination, replication, and repair.....	18

<b>CHAPTER TWO: Efficient generation of unmarked deletions in</b> <i>Legionella pneumophila</i> .....	26
SUMMARY .....	26
INTRODUCTION.....	26
METHODS.....	27
Construction of null alleles with <i>FRT</i> -flanked antibiotic resistance cassettes. ....	27
<i>FRT</i> -flanked cassettes are excised using vectors that express Flp. ....	28
Flp-mediated excision of cassettes and removal of vector. ....	28
Motility. ....	29
Lysosomal degradation.....	29
RESULTS.....	30
pBSFlp-mediated excision and vector loss is highly efficient. ....	30
Mutations in multiple genes with redundant function reveal phenotypes. ....	30
Unmarked <i>fliA</i> deletion alleles are not polar on <i>motAB</i> . ....	31
DISCUSSION .....	33
Unmarked deletions in <i>Legionella</i> .....	33
Exonuclease and mismatch repair potential of <i>L. pneumophila</i> .....	33
<b>CHAPTER THREE: Oligonucleotides stimulate genomic alterations of</b> <i>Legionella pneumophila</i> .....	45
SUMMARY .....	45
INTRODUCTION.....	46
METHODS.....	49
Bacterial strains and resistance cassettes.....	49
Transformations.....	50

RESULTS.....	53
Oligo-induced mutagenesis in <i>L. pneumophila</i> is distinct from classical homologous recombination. ....	53
Oligo-induced mutagenesis is strand- and growth-phase dependent.....	56
Oligo-induced mutagenesis is limited by exonucleases. ....	58
Oligos stimulate RecA-independent excision of large DNA fragments.....	60
Oligo-stimulated excision is sensitive to orientation in the chromosome. ....	62
Oligo mutagenesis is not inhibited by 3' modified oligos that are non-extendable by DNA polymerase. ....	64
Oligo mutagenesis is not increased by 5' phosphate modification compared to 5' hydroxyl oligos.....	65
PriA and Pol I, but not RadA, contribute to oligo mutagenesis. ....	66
Homologous oligos flanked by non-homologous sequences have decreased, but not abolished, ability to stimulate oligo mutagenesis.....	68
Oligo-stimulated excision can be exploited to generate markerless chromosomal mutations by counter-selection.....	70
Oligo-induced mutagenesis can be harnessed to insert DNA onto the chromosome.....	71
DISCUSSION .....	72
<b>CHAPTER FOUR: Discussion</b> .....	101
Genetic engineering of <i>L. pneumophila</i> and beyond.....	101
Oligo-induced mutagenesis .....	107
Alternative models of oligo mutagenesis .....	111
Concluding remarks .....	114
<b>APPENDICES</b> .....	118
<b>BIBLIOGRAPHY</b> .....	185



## LIST OF FIGURES

<b>Figure 1.1.</b> Strand annealing/integration model of $\lambda$ Red recombination with an oligonucleotide as described in the text, where oligo is physically incorporated into the nascent strand.....	22
<b>Figure 1.2.</b> <i>Legionella</i> phage recombinase genes <i>orfBC</i> mediate recombination with oligos in a DNA- and strand-dependent manner, as predicted by $\lambda$ Red recombination, when expressed under <i>ptac</i> control in <i>E. coli</i> on a RSF1010-based shuttle plasmid.....	23
<b>Figure 1.3.</b> Flp recombination.....	24
<b>Figure 1.4.</b> Model for replication restart involving RecFOR, PriA, pol II and pol III proteins.....	25
<b>Figure 2.0.</b> Outline of strategy to construct an unmarked deletion in <i>fliA</i> .....	35
<b>Figure 2.1.</b> After efficiently curing antibiotic resistance cassettes from the <i>L. pneumophila</i> chromosome, plasmids expressing the Flp recombinase can be segregated from the host strain.....	36
<b>Figure 2.2.</b> Exonuclease double mutants are sensitive to 2-aminopurine and nalidixic acid.....	37
<b>Figure 2.3.</b> <i>fliA</i> transposon insertion mutant cells, but not <i>fliA::FRT</i> complete deletion mutant cells, evade degradation poorly when phagocytized by macrophages.....	38
<b>Figure 2.S1.</b> Growth of strains following Flp excision.....	44
<b>Figure 3.1.</b> Oligo-induced mutagenesis is RecA-independent and insensitive to lengths of homology $\geq 21$ nt.....	81
<b>Figure 3.2.</b> Oligo-induced mutagenesis is strand- and growth-phase dependent.....	82
<b>Figure 3.3.</b> Oligo-induced mutagenesis is limited by exonucleases.....	83
<b>Figure 3.4.</b> Oligo-induced mutagenesis can excise large fragments of DNA and is sensitive to orientation in the chromosome.....	85

<b>Figure 3.5.</b> Oligo mutagenesis is not inhibited by 3' modified oligos that are non-extendable by DNA polymerase.....	87
<b>Figure 3.6.</b> Oligo mutagenesis is not increased by 5' phosphate modification compared to unmodified 5' hydroxyl oligos.....	88
<b>Figure 3.7.</b> PriA and Pol I, but not RadA, contribute to oligo mutagenesis.....	89
<b>Figure 3.8.</b> Homologous oligos flanked by non-homologous sequences have decreased, but not abolished, mutagenic activity.....	90
<b>Figure 3.9.</b> Oligo-induced mutagenesis can be harnessed for genetic manipulation of the chromosome.....	91
<b>Figure 3.10.</b> Strand annealing model of oligo-induced mutagenesis in <i>L. pneumophila</i> as described in the text.....	92
<b>Figure 3.S1.</b> Growth curves of strains used in oligo mutagenesis assays and their recombinant derivatives.....	93
<b>Figure 4.1.</b> Template switch model of oligo-induced mutagenesis in <i>L. pneumophila</i> , an alternate model to that described in the text and in Figure 3.10.....	117

## LIST OF TABLES

<b>Table 1.1.</b>	Abbreviated list of absent and duplicate proteins in <i>Legionella</i> .....	21
<b>Table 2.1.</b>	Abbreviated list of bacterial strains and plasmids.....	39
<b>Table 2.2.</b>	Motility phenotypes.....	40
<b>Table 2.S1.</b>	Bacterial strains and plasmids.....	41
<b>Table 3.S1.</b>	Bacterial strains and plasmids.....	94
<b>Table 3.S2.</b>	Oligos used for direct mutagenesis in <i>L. pneumophila</i> and <i>E. coli</i> .....	96
<b>Table 3.S3.</b>	Oligos used for strain construction.....	98

## LIST OF APPENDICES

<b>APPENDIX A:</b> Inhibition of host vacuolar H <sup>+</sup> -ATPase activity by a <i>Legionella pneumophila</i> effector.....	118
<b>APPENDIX B:</b> <i>L. pneumophila</i> major facilitator superfamily protein Lpg0273 provides protection from toxic concentrations of nicotinic acid.....	177

## ABSTRACT

Recombination is fundamental to genome maintenance and contributes to diversity in all Domains of life by generating novel sequences from the breaking and joining of DNA. RecA is central to one of the best studied mechanisms of recombination, but RecA-independent pathways also have implications for genetic engineering, evolution, and DNA replication. Here, I harness two forms of RecA-independent recombination for engineering of *Legionella pneumophila*, while also probing replication and repair machinery. Specifically, I make unmarked deletions in *L. pneumophila* using the Flp site-specific recombinase while also examining single-stranded nucleases and mismatch repair. I also describe a distinct form of recombination that does not require expression of recombinase genes. Oligonucleotides (oligos) generate mutations on the *L. pneumophila* chromosome by a mechanism that requires homologous DNA, but not RecA, RadA or any known phage recombinase. Instead, DNA replication likely contributes, since oligo-induced mutagenesis required  $\geq 21$  nucleotides of homology, was strand-dependent, and was most efficient in exponential phase. Mutagenesis appeared to be distinct from previously described mechanisms of oligo recombination, as it did not require canonical 5' phosphate or 3' hydroxyl groups, but did require the primosomal protein PriA and DNA Pol I. After electroporation, oligos stimulated excision of 2.1 kb of chromosomal DNA or insertion of 18 bp, and can be exploited to generate chromosomal deletions and to insert an epitope into a chromosomal coding sequence. The frequency of mutagenesis also increased substantially when either

its RecJ and ExoVII nucleases were inactivated or the oligos were modified by nuclease-resistant bases.

*L. pneumophila* is a diverse species and has a surprising number of Eukaryotic-like genes. As the organism is naturally transformable, it is thought that the species acquired some of these genes by horizontal gene transfer. Since divergent Eukaryotic sequences may be inefficiently incorporated into the genome by RecA-mediated recombination due to the extensive homology required, oligo-induced mutagenesis may have evolutionary implications as a mechanism to incorporate divergent DNA sequences with only short regions of homology. Since oligo mutagenesis appears to be conserved, it may play a role in remodeling the genomes of *L. pneumophila* and species across the Bacterial Domain.

## CHAPTER ONE

### Introduction

#### Thesis outline and context

My thesis examines RecA-independent recombination in *Legionella pneumophila*, specifically its application for genetic engineering as well as testing the contribution of recombination, replication, and repair machinery to elucidate underlying mechanisms. Chapter Two focuses on harnessing phage recombination in *Escherichia coli* coupled with site-specific Flp recombination in *L. pneumophila* to construct unmarked deletions, while examining the role of single-stranded exonucleases in the process. Chapter Three analyzes a phenomenon I name oligo mutagenesis, a form of RecA-independent recombination that relies on short homologous sequences. I show that oligo mutagenesis can not only be applied to engineer *L. pneumophila*, but is likely conserved among Bacteria and could be harnessed for the study of organisms currently lacking genetic tools.

My work is among of the first to approach basic recombination and repair mechanisms in the intracellular pathogen *L. pneumophila*. Because most studies involving basic mechanisms involve model organisms, in the introduction I will highlight why *L. pneumophila* is of particular interest. Besides its often under-appreciated clinical importance and resultant impact on morbidity and mortality worldwide, the unique evolutionary history and lifestyle of the organism provide an opportunity to consider how

basic mechanisms of recombination can impact an organism's ecological niche and ability to parasitize its host. While I do not directly test evolutionary hypotheses, I have designed some experiments to indirectly examine these ideas and also consider it an important framework for evaluating the impact of my research.

A related consideration is the importance of examining basic mechanisms in non-model organisms and to emphasize that similarities do not necessarily indicate that the process will be the same. Acknowledging the limitations of extrapolating from model organisms is important, not only for the interpretation of my results, but for all of biology. Much research has focused on the convenient experimental models of *Escherichia*, *Bacillus*, *Drosophila*, *Danio*, *Mus*, Lambda, SV40, *et cetera*, but many of the assumptions drawn from these results have not been tested in other genera. Untested assumptions not only create bias in the literature, but can confound interpretations of specific data. For example, when considering error-prone replication as an explanation for mutation frequency, it becomes difficult to draw on data from *E. coli*, as *L. pneumophila* appears to have divergent SOS response machinery. While lacking LexA and SulA, *L. pneumophila* appears to have two copies of Pol V (Table 1.1). My data emphasize the risks inherent in bias toward previously published models by showing that, contrary to described mechanisms of oligo recombination in all three Domains of life, the process of oligo mutagenesis I describe depends on a distinct set of replication machinery, despite a superficial similarity.

A portion of this chapter was published by Swanson and Bryan, in "*Legionella pneumophila*, a Pathogen of Amoebae and Macrophages" in *Phagocyte-Pathogen*



*Interactions: Macrophages and the Host Response to Infection* by ASM Press (2009).

Used with permission.

### **An environmental pathogen**

*Legionella pneumophila* is a Gram-negative bacterium that has evolved strategies to parasitize professional phagocytes. Most *Legionella* species, including *L. pneumophila*, are aquatic microbes; other species thrive in soil. There the microbe naturally infects amoeba and protozoa. But, when given the opportunity, *L. pneumophila* can infect human alveolar macrophages and cause the severe pneumonia Legionnaires' disease.

Aerosols of contaminated water or soil transmit the disease agent to humans. Because the bacterium is ubiquitous in nature, water sources of all kinds can act as vehicles for transmission. The point source is most often identified in epidemic outbreaks, where exposures can be evaluated using case-control studies. Epidemiologists usually implicate man-made equipment, including water-cooling towers, whirlpools, and showers. The origin of sporadic disease is more difficult to assess, as is the contribution of natural water sources to disease burden.

A significant portion of Legionnaires' disease occurs in the health care setting, and these cases account for the highest fatality rates. Contributing factors include the vulnerability of the patient population and the institutional setting, where virulent isolates can be efficiently transmitted to the large number of susceptible individuals housed there.

Significantly, during the 35 years the Centers for Disease Control has tracked the disease, there have been no reports of human-to-human transmission. Evidently, factors that promote spread in fresh water microbial communities are not sufficient for *L. pneumophila* to pass safely and efficiently from the lungs of one susceptible human to another. It is also possible that amoebae are required for the biogenesis of infectious particles that can withstand transmission in aerosols.

### **Burden of disease**

Considered along with *Chlamydia pneumoniae* and *Mycoplasma pneumoniae* to be an “atypical” etiological agent of pneumonia, *L. pneumophila* actually causes considerable morbidity and mortality (Edelstein and Cianciotto, 2005). Legionellosis is a nationally notifiable disease, with 3,181 cases reported to the CDC in 2008 (Hall-Baker, *et al.*, 2010). The disease is widely under-reported and, although estimates vary widely, between 18,000 and 88,000 cases are thought to occur annually in the United States, or 2-15% of community acquired pneumonias (Foy, *et al.*, 1979, Mulazimoglu and Yu, 2001). Of these, between 8,000 and 18,000 require hospitalization (Marston, *et al.*, 1997). Mainly afflicting immunocompromised individuals, the disease carries a case fatality rate of 5-46%, the highest of the atypical pneumonias (Mulazimoglu and Yu, 2001), with the outcome primarily dependent on the immunological state of the person and the choice of therapy (Benin, *et al.*, 2002). While interpreting the trends in overall incidence of Legionnaires’ disease is complicated by increased diagnosis, it is clear that fatality rates are decreasing—a pattern likely attributable to more convenient diagnostic tools and

rising use of empiric antimicrobial therapy with activity against *L. pneumophila*. *L. pneumophila* is also associated with Pontiac Fever, a milder, febrile, non-pneumonic illness whose etiology is not clear. Since Pontiac Fever does not appear to require viable bacteria, it is beyond the scope of this thesis.

## **Outbreaks**

Although epidemics of Legionnaires' disease comprise only 25-35% of cases, they are a rich source of information about the illness (Edelstein and Cianciotto, 2005). The namesake 1976 outbreak, which occurred at a Philadelphia convention of American Legion members, highlights both the epidemic potential of the institutional setting and the predilection of disease in susceptible individuals. The convention was attended by approximately 4,000 members of the Pennsylvania State American Legion, a group predisposed primarily by age, but also by preexisting chronic lung disease and tobacco use. After exposure to contaminated aerosols from the convention hotel's air conditioning system, 149 Legionnaires and 33 non-Legionnaires were eventually diagnosed with the disease, and 29 died (Edelstein, 2008). Epidemic Legionnaires' disease continues to be a problem. For example, in October 2005, 127 residents of a home for the elderly in Toronto, Ontario became ill with Legionnaires' disease, and 20 of them died. The source of the outbreak was eventually determined to be a cooling tower on the roof that spread contaminated aerosols into the building's air handling system. Typically, the attack rate in epidemics is ~ 5%, and those who become ill have pre-existing damage to their airways or weakened cell-mediated immune systems. Healthy

individuals can clear the infection: Once activated by interferon- $\gamma$ , human macrophages can restrict *L. pneumophila* replication by limiting the microbe's iron supply (Byrd and Horwitz, 1989, Sporri, *et al.*, 2006, Yoshizawa, *et al.*, 2005).

### **Clinical features, diagnosis and treatment**

The clinical presentation of Legionnaires' disease can range from the average febrile pneumococcal-appearing pneumonia to symptoms less commonly associated with pneumonia, such as abdominal pain, diarrhea, memory loss, severe headache, and low serum sodium (Edelstein and Cianciotto, 2005). Cough may be unimpressive, and can range from non-productive to bloody. Chest radiography yields pathological changes, frequently confluent lobular and bilateral, but nothing diagnostic for Legionnaires' disease. Due to the inconsistent nature of symptoms, diagnostic formulas with acceptable positive predictive values have been elusive. Nevertheless, experienced clinicians with an appropriate index of suspicion are good judges of disease, and, by applying an appropriate diagnostic test, can identify the illness with reasonable frequency (Mulazimoglu and Yu, 2001).

Lung pathology is usually consistent with acute bronchiolitis and alveolitis. Histology of human, rodent, and primate animal models generally reveals fibrinopurulent infiltrates, with macrophages usually comprising a significant portion of the total leukocytes (Baskerville, *et al.*, 1983, Winn and Myerowitz, 1981). Neutrophils make up most of the remainder of the infiltrate. Erythrocytes are also commonly present, indicative of vascular damage that can accompany the disease. Lysed white blood cells

are also evident. Alveolar macrophages appear to phagocytose *L. pneumophila* to a greater extent than neutrophils. Phagosomes that contain multiple intact bacteria are often observed, suggestive of intracellular replication (Baskerville, *et al.*, 1983, Winn and Myerowitz, 1981). The *in situ* observations of macrophage infection, intracellular replication, and phagocyte lysis are mirrored by current *in vitro* experimental models, including interactions with primary macrophages derived from the bone marrow of A/J mice (Baskerville, *et al.*, 1983, Byrne and Swanson, 1998).

*Legionella* retains Gram's stain poorly, which can lead to false negative sputum smears and pathology sections. Culture is still the gold standard of diagnosis, but the advent of the urine antigen test has made Legionnaires' disease possibly the easiest respiratory illness to diagnose with speed and certainty (Edelstein and Cianciotto, 2005). The urine antigen test's specificity approaches 100%, but only detects *L. pneumophila* serogroup 1, leading to under-diagnosis of other species and serogroups (Benin, *et al.*, 2002). Especially in areas reporting a greater prevalence of non-serogroup 1 isolates, a negative urine antigen test should not absolutely rule out Legionnaire's Disease. This is particularly true in Australia and New Zealand, where serogroup 1 isolates only comprise 45% of cases (Yu, *et al.*, 2002). Alternatives to culture and the antigen test include direct fluorescent antibody staining, serology, and polymerase chain reaction assays (Benin, *et al.*, 2002, Diederer, *et al.*, 2008, Edelstein and Cianciotto, 2005, Hayden, *et al.*, 2001, Templeton, *et al.*, 2003).

Rapid therapeutic intervention is critical for resolution of disease with a low mortality rate, and the appropriate chemotherapeutic agent is necessary to achieve

clearance (Edelstein and Cianciotto, 2005). Due to its insensitivity to beta-lactam antibiotics, *Legionella* has contributed to a shift in empiric antimicrobial therapy for pneumonia. Rather than administer narrow range anti-pneumococcal agents, clinicians now rely first on drugs that cover a broad range of microorganisms. Macrolides and quinolones are the most common classes of antimicrobials with good activity against *Legionella*. Acquired resistance to antimicrobials has not been an issue, likely due to lack of human-to-human transmission and the acute nature of the illness. The susceptibility pattern of *Legionella* highlights the intracellular nature of the pathogen: The effective and commonly used drug gentamycin is efficacious *in vitro* and useful in the research laboratory, but its inability to penetrate host cells limits its clinical value.

### **Serogroup epidemiology**

The genus of *Legionella* is quite diverse, comprising 50 distinct species. Nevertheless, the species *L. pneumophila* contributes to over 90% of the human disease burden in the United States and Europe, with smaller percentages contributed by *L. micdadei*, *L. longbeachae*, and several others (Benin, *et al.*, 2002). Within *L. pneumophila*, there are at least 15 defined serogroups. Even though serogroup 1 strains account for less than 30% of environmental isolates, they cause the majority of Legionnaires' disease (Doleans, *et al.*, 2004). While all *Legionella* species are adept at infecting environmental phagocytes, amoebae and protozoa, it is interesting to consider what attributes equip serogroup 1 isolates to more readily infect the alveolar macrophage

and how they acquired these determinants.

### **A DNA-rich lifestyle; a dynamic genome riddled with eukaryotic DNA**

*L. pneumophila* is equipped to internalize foreign DNA and to recombine the genetic material onto its chromosome (Sexton and Vogel, 2004, Stone and Kwaik, 1999). Unlike the best studied naturally transformable Gram negative organisms, *N. gonorrhoeae* and *H. influenzae*, the process does not depend on a specific uptake sequence, and the organism appears to indiscriminately take up naked DNA from the environment (Johnsborg, *et al.*, 2007, Sexton and Vogel, 2004, Stone and Kwaik, 1999, Thomas and Nielsen, 2005). In nature, the microbe likely persists for extended periods within multispecies biofilms, potentially a rich source of both self and diverse foreign DNA (Declerck, 2009, Whitchurch, *et al.*, 2002). When phagocytic amoebae or protozoa graze on biofilms, the ingested *L. pneumophila* can establish a replication niche within a vacuole, leading to eventual nutrient exhaustion and host cell lysis—yet another source of exposure of *Legionella* to foreign DNA. Even during infection of a host, transfer of DNA could be envisioned. A Type IV pilus has been shown to be involved in adherence to mammalian and protozoan cells (Stone and Abu Kwaik, 1998), while also being essential for natural transformation (Stone and Kwaik, 1999). Other Type IV secretion systems could further contribute to the exposure of the bacterium to host DNA.

To establish a replication vacuole within a professional phagocyte, *L. pneumophila* relies on a specialized secretion system that can deliver bacterial proteins directly to the host cytosol (Vogel, *et al.*, 1998). Derived from machinery that transfers

plasmids during conjugation with another bacterium, Type IV secretion systems can transport DNA or protein across both the bacterial and the phagosomal membranes (Vincent, *et al.*, 2006). Such adapted conjugation systems are utilized by a variety of microbes, including the plant pathogen *Agrobacterium tumefaciens* and the mammalian pathogens *Helicobacter pylori*, *Bordetella pertussis*, *Bartonella henselae*, and *Coxiella burnetii*. In *L. pneumophila*, however, the secretion system also results in host membrane permeability, including accessibility of the nucleus to DNA tracking dyes (Whitfield, *et al.*, 2009), and could result in further association between host and bacterial DNA even if the apparatus is not directly involved in DNA transfer.

The DNA-rich life of this pathogen could contribute to the observed species diversity. Although the ~3.5 Mb *L. pneumophila* chromosome is predicted to encode ~3000 proteins, only ~ 2400 of these are common to four sequenced *L. pneumophila* (Cazalet, *et al.*, 2004). Moreover, there is an extraordinarily high frequency of eukaryotic motifs embedded in the *L. pneumophila* genome: Nearly 3.5% of the predicted proteins have eukaryotic motifs (Bruggemann, *et al.*, 2006, Cazalet, *et al.*, 2004, de Felipe, *et al.*, 2005, Gomez-Valero, *et al.*, 2009, Lurie-Weinberger, *et al.*, 2010). These include ankyrin domains, which mediate protein-protein interactions; F-box and U-box domains, a feature of components of the ubiquitination pathway; a homologue of sphingosine-1-phosphate lyase, an enzyme that modulates whether cells induce autophagy or cell death; two apyrases, secreted proteins that degrade extracellular nucleotide di- or triphosphates; and three serine-threonine kinases, signal transduction proteins. In a PCR screen of 77 *Legionella* isolates, most of the eukaryotic-like genes were conserved, suggesting



importance to the lifestyle of the organism (Lurie-Weinberger, *et al.*, 2010). Yet, a handful of unique eukaryotic-like genes were found even amongst strains within the same serogroup—suggesting recent and continuing gene acquisition (Lurie-Weinberger, *et al.*, 2010). Presumably, the organism’s environmental hosts supply ample eukaryotic DNA which *L. pneumophila* efficiently incorporates, ultimately retaining those DNA sequences that increase fitness and losing those that decrease it. It is tempting to speculate that eukaryotic motifs that are broadly conserved in the species equip *L. pneumophila* to modulate the biology of its host phagocyte. Supporting this notion is the recent observation that the eukaryotic-like F-box containing Type IV secretion effector AnkB is necessary for intracellular bacterial growth and hijacks the polyubiquitination machinery of the host (Price, *et al.*, 2009). One of the many outstanding questions, however, is how *Legionella* incorporates these divergent sequences into its chromosome and whether previously described mechanisms can account for the observed diversity.

### **Recombination and the exchange of genetic material**

*L. pneumophila* can take up free DNA from the environment and incorporate it into its genome, an ability restricted to approximately 1% of known bacterial species (Thomas and Nielsen, 2005). Independently of the ability to take up naked DNA, nearly all organisms have the potential for recombination, or the breakage and joining of DNA molecules that can result in exchange of genetic information. Although critical for repair processes and maintenance of a stable genome, recombination also contributes to evolution. Genetic drift, or small changes in DNA sequence, is typically due to the error

rate of DNA polymerases, whereas genetic shift, or bigger evolutionary jumps, often requires mechanisms of recombination to rearrange existing sequences, incorporate new ones, or remove sequences that decrease fitness (Thomas and Nielsen, 2005). The simplest example is the rearrangement of parental DNA to form a single DNA molecule that makes every human unique; aberrant recombination events can lead to cancer or inherited diseases (Chen, *et al.*, 2010). Understanding the mechanisms of recombination is fundamental to understanding biology from the basic microbe to the human. While some forms of recombination, such as non-homologous end joining, do not require specific DNA sequences, I focus here on common forms of recombination that require homologous DNA molecules or specific recognition sequences.

### **RecA-dependent recombination**

Perhaps the most ubiquitous and well-studied type of recombination relies on RecA/RadA/Rad51-like proteins and related machinery that execute many aspects of recombination, repair, and replication, as well as contribute to horizontal gene transfer and the experimentalists' genetic engineering tool kit (Kuzminov, 1999, Lusetti and Cox, 2002, Thomas and Nielsen, 2005, Volodin, *et al.*, 2005). These well-described recombination systems support the exchange between two DNA molecules that have large regions of homology to mediate efficient cross over or gene conversion events (Kuzminov, 1999, Lovett, *et al.*, 2002, Thomas and Nielsen, 2005). The RecA protein forms a nucleoprotein filament on single-stranded DNA (ssDNA), which facilitates strand invasion and annealing to complementary double-stranded target DNA (dsDNA),

followed by strand transfer, branch migration, and resolution (Snyder and Champness, 2007b, Volodin, *et al.*, 2005). The process is generally considered to proceed in a RecBCD- or RecFOR-dependent manner (Lovett, *et al.*, 2002). RecBCD has nuclease and helicase activity, with a particular affinity to double-stranded breaks, where it digests one strand, thereby allowing RecA filament formation and strand invasion (Lovett, *et al.*, 2002). On the other hand, RecFOR is thought to play a dominant role in assisting the loading of RecA in single-stranded gaps that have been stabilized by Single-Stranded Binding Protein and have had the RecJ single-stranded nuclease digest the exposed 5' terminus (Corrette-Bennett and Lovett, 1995, Han, *et al.*, 2006, Lovett, *et al.*, 2002). Both RecBCD and RecFOR pathways lead to branched intermediates called Holliday junctions, which can migrate to increase pairing, followed by cleavage and ligation to resolve the complex 4-stranded intermediate (Lovett, *et al.*, 2002, Snyder and Champness, 2007b). It is noteworthy that *L. pneumophila* does not appear to have RecBCD (Table 1.1), and thus the *E. coli* literature would suggest that most of its RecA-dependent recombination proceeds by the RecFOR pathway. Interestingly, when using standard laboratory conditions for natural transformation, formation of recombinant colonies is dependent on RecA but is not significantly decreased in the absence of RecF or RecJ (data not shown). While more careful examination of the frequencies of recombination in these different genetic backgrounds is needed, these data suggest that even canonical RecA-dependent recombination in *L. pneumophila* may differ from that of model organisms.

## Phage-mediated recombination

Bacteriophages often utilize host machinery for necessary recombination functions, but they can also encode their own enzymes to facilitate the process. While a discussion of the many decades of phage biology is beyond the scope of this thesis, understanding the Red genes of phage  $\lambda$  (and related genes of the Rac phage) is important for many of the underlying assumptions of oligo mutagenesis (Chapter 3), as well as the justification for studying it in the first place. The Red system is comprised of  $\beta$ ,  $\gamma$ , and *exo* genes, producing the Beta, Gam, and Exo proteins (Datsenko and Wanner, 2000). Gam protects linear double-stranded DNA from host RecBCD nucleolytic degradation, and *exo* encodes an exonuclease activity that degrades the 5' end of a double-stranded molecule, leaving a 3' single-stranded overhang (Snyder and Champness, 2007b). Beta then binds the exposed 3' single-stranded tail, protecting it from degradation and facilitating strand annealing to a homologous DNA molecule (Yu, *et al.*, 2000). Though RecA is important for some  $\lambda$  recombination that occurs by strand invasion, the process can also occur in a RecA-independent fashion—particularly when utilizing short regions of homology (Poteete and Fenton, 1993, Poteete and Fenton, 2000, Stahl, *et al.*, 1997, Yu, *et al.*, 2000).

The most commonly accepted model of RecA-independent  $\lambda$  Red recombination is the ‘annealing/integration’ model (Fig. 1.1), which dictates that Beta binds single-stranded DNA in the cell and, in lieu of strand invasion, facilitates its annealing to exposed single-stranded DNA at the replication fork (Costantino and Court, 2003, Ellis, *et al.*, 2001, Huen, *et al.*, 2006). If the substrate is ssDNA, only Beta is required, whereas

a dsDNA substrate requires Exo. If the host strain is RecBCD<sup>+</sup>, Gam is required for optimal efficiency (Datta, *et al.*, 2008, Ellis, *et al.*, 2001). In the case of ssDNA oligonucleotides (oligos), complementary oligos undergo recombination with differing frequencies. Recombination with oligos annealing to the lagging strand in the replication fork is thought to occur more readily due to greater expanse of chromosomal ssDNA (Ellis, *et al.*, 2001). Evidence suggests that following annealing, DNA polymerase extends the oligo during its ligation into the nascent strand and physical incorporation into the target DNA molecule (Grogan and Stengel, 2008, Huen, *et al.*, 2006).

The striking ability of  $\lambda$  Red to catalyze efficient recombination with lengths of homology as few as 36 nucleotides is particularly convenient for genetic engineering. In particular, the Red genes can be expressed from a prophage or plasmid, and regions of homology can be encoded by synthetic oligonucleotides at low cost (Datsenko and Wanner, 2000, Datta, *et al.*, 2008, Thomason, *et al.*, 2007a, Yu, *et al.*, 2000). This process of recombination using short homologies and phage recombinases is referred to as ‘recombineering.’ Advantages over traditional restriction enzyme based cloning and allelic exchange are increased efficiency and precision without having to use existing restriction sites or incorporate new ones. The drawbacks of recombineering are two-fold, however. The system is only functional in *E. coli* and closely related organisms, and it requires exogenous expression of the recombinase genes, which then usually need to be removed from the host strain. The first drawback has led to a search for phage recombinase genes in other organisms that may support a similar application, with the most notable success being in the *Mycobacteria* field (Datta, *et al.*, 2008, van Kessel and

Hatfull, 2007). In fact, a pair of Rac prophage-like recombinase genes has been isolated from a putative defective prophage region of a strain of *L. pneumophila* that undergoes phase variation of virulence traits due to a 30 kb episome that undergoes RecA-independent integration and excision (Datta, *et al.*, 2008, Luneberg, *et al.*, 2001). Datta *et al.* (2008) showed these *L. pneumophila* phage recombinases can function similar to Beta and Exo when expressed in an optimal system in *E. coli*. We have also cloned these genes into a *Legionella* shuttle vector and demonstrated recombination activity when expressed in *E. coli* (Fig. 1.2). However, I did not observe activity in *L. pneumophila* in any of the conditions tested (data not shown). To circumvent the obstacle of discovering phage recombinase genes, Chapter 2 describes how existing tools in *E. coli* can facilitate engineering of *L. pneumophila*, while Chapter 3 describes a recombineering-like activity that does not require expression of exogenous phage genes. Incidentally, this phage-independent activity was initially observed as a low-level background frequency of recombination in strains containing ‘no insert’ control vectors when searching for conditions optimal for expression of the *Legionella* phage genes.

### **Site-specific recombination**

Yet another broad category of recombination is site-specific. Rather than rely on general homologous sequences, this pathway relies on specific proteins to recognize specific target sequences and can result in integration, excision, inversions, or other genomic rearrangements. Although notably absent from *L. pneumophila* (Table 1.1), the broadly conserved XerCD recombinases facilitate resolution of multimers during DNA

replication in *E. coli*, integration of the cholera toxin phage in *Vibrio cholerae*, and loss of the 57-kb gonococcal genetic island in *Neisseria gonorrhoeae* (Blakely, *et al.*, 1993, Dominguez, *et al.*, 2010, Huber and Waldor, 2002). Site-specific recombination plays other roles in pathogenesis, such as regulation of the Type 1 fimbriae in uropathogenic *E. coli* (Bryan, *et al.*, 2006, Klemm, 1986). Perhaps two of the best known site-specific recombinases, however, are the Cre recombinase from bacteriophage P1 and the Flp recombinase of *Saccharomyces cerevisiae*, due to their utility for genetic engineering in a vast array of organisms (Schweizer, 2003). *flp* was discovered on the 2- $\mu$ m plasmid of *S. cerevisiae*, where it encodes a recombinase that recognizes two 48 bp *FRT* sites and catalyzes the interconversion of the plasmid between two isoforms (Schweizer, 2003, Senecoff, *et al.*, 1985). The minimal *FRT* site is only 34 bp and contains two inverted symmetry sequences flanking an 8 bp core (Fig. 1.3; Schweizer, 2003, Senecoff, *et al.*, 1985). When two *FRT* sites flank a DNA sequence and are in the same orientation, Flp-mediated recombination excises the intervening sequence; in contrast, if the *FRT* sites are inverted relative to each other, the entire sequence is inverted (Fig. 1.3; Schweizer, 2003). This versatility, combined with high activity in a large number of organisms, make the Flp/*FRT* system a useful genetic engineering tool, particularly for the deletion of antibiotic resistance cassettes. In Chapter 2, we apply Flp for the engineering of *L. pneumophila* for the first time.

## **Intersection of recombination, replication, and repair**

Central to all organisms is the ability to replicate their chromosome with high enough fidelity that essential genes do not suffer inactivating mutations. While the processive replicative DNA polymerase of most organisms (DNA Pol III in *E. coli*) is highly accurate at synthesizing DNA from the template strand, it cannot on its own accord overcome the many obstacles to chromosome replication with minimal error. Nearly every round of replication is thought to be interrupted by chromosomal insults, including single-stranded nicks or gaps, double-stranded breaks, base dimers, chromosomal multimers, and other lesions (Kuzminov, 1999, Lusetti and Cox, 2002). Circumvention of these insults can involve site specific recombinases, RecA-mediated recombination, and many other replication and repair proteins. While RecA can contribute to horizontal gene transfer and incorporation of transformed sequences, its role in replication is probably its most important function.

One of the interactions between replication and recombination well illustrated by Rangarajan *et al.* (Fig 1.4; 2002) and more generally reviewed elsewhere (Kuzminov, 1999, Lusetti and Cox, 2002) is the ability of replication to continue when the fork encounters UV-induced damage. When the replication fork encounters a DNA lesion, synthesis is uncoupled, creating ssDNA and fork arrest. RecFOR then facilitates the loading of RecA in this single-stranded gap, followed by a fork regression facilitated by RecG and synthesis by DNA Pol II. Although DNA Pol II can synthesize up to ~ 1.6 kb, it is not sufficient for restarting and continuing normal replication. Since DnaA can only initiate replication at the origin, the replication restart protein PriA is required, as it can



recognize the stalled structure that has been re-modeled by RecG and then load the primary replicative polymerase Pol III. This complex process avoids having to employ one of the error-prone translesion polymerases to overcome the obstacle to replication and can also provide time for nucleotide excision repair to remove the lesion (Rangarajan, *et al.*, 2002).

Yet another repair pathway that is coupled with replication is methyl directed mismatch repair (MDMR). MDMR recognizes slight DNA helix distortions including those involving mismatches, frameshifts, and incorporation of base analogs such as 2-aminopurine that can occur during replication (Modrich, 1991, Snyder and Champness, 2007a). When the system is absent, cells accumulate a high number of mutations and are often referred to as having a ‘mutator’ phenotype. Key features of MDMR are the ability to differentiate between template and nascent strands during replication, recognize and excise mismatches, and fill in the resultant gap using the original template. Initiating the MDMR pathway is recognition and binding of the helix distortion by a MutS dimer, followed by MutL and MutH binding (Modrich, 1991, Snyder and Champness, 2007a). MutH is the active nuclease that cleaves the newly synthesized error-containing strand, which it accomplishes by recognizing the methylation status of the strands (Modrich, 1991, Snyder and Champness, 2007a). During the normal life cycle of the cell, the Dam DNA methylase selectively methylates the adenine of GATC sequences; however, this process lags behind DNA replication such that newly synthesized dsDNA is hemi-methylated (Barras and Marinus, 1989). Following MutH cleavage, redundant single stranded exonucleases (ssExos) degrade the cleaved strand facilitated by helicase II

unwinding (Burdett, *et al.*, 2001, Modrich, 1991, Viswanathan, *et al.*, 2001). DNA Pol III then fills in the gap (Modrich, 1991). Three considerations relevant to this thesis are that MDMR is highly active at repairing base mismatches in *E. coli*, mismatches are not all recognized with the same efficiency, and only small (< 5 bp) lesions are recognized (Costantino and Court, 2003, Modrich, 1991, Swingle, *et al.*, 2010b).

When considering any individual component related to replication, homologous recombination, or repair processes, it is important to remember these elaborate interactions and how species differences can inform conclusions. For example, RecA-independent recombination often requires replication, even if only to expose ssDNA, since it lacks the strand invasion activity of RecA.  $\lambda$  recombination and oligo mutagenesis both exhibit this requirement, yet differ in how they accomplish the mutagenic event. Chapter 3 demonstrates that, unlike  $\lambda$  recombination, where DNA polymerase extends oligos like an Okazaki fragment, polymerase does not likely extend the oligo during oligo-induced mutagenesis; instead, it may slip/hop over the oligo and re-start downstream. Both Chapter 2 and 3 demonstrate that compared to *E. coli*, *L. pneumophila* has fewer single-stranded nucleases and a less active mismatch repair system, observations consistent with an evolutionary history of utilizing a dynamic genome to adapt strategies of parasitizing its hosts.

**Table 1.1. Abbreviated list of absent and duplicate proteins in *Legionella*.\***

<b>Notable proteins not present in <i>L. pneumophila</i>.</b>
RecBCD ( <i>E. coli</i> )
AddAB ( <i>Bacillus</i> )
MutS2 ( <i>Bacillus</i> )
Ku ( <i>Bacillus</i> )
RecET (Rac/ <i>E. coli</i> )
Bet, Exo (Lambda/ <i>E. coli</i> )
UvsX (T4/ <i>E. coli</i> )
SbcCD ( <i>E. coli</i> )
ExoI/SbcB ( <i>E. coli</i> )
ExoX ( <i>E. coli</i> )
PriB, PriC, DnaT ( <i>E. coli</i> )
Pol II ( <i>E. coli</i> )
LexA, Sula ( <i>E. coli</i> )
XerCD ( <i>E. coli</i> )

<b>Notable duplicate proteins in <i>L. pneumophila</i>.</b>
UmuC [lpg1232 and lpg1704] ( <i>E. coli</i> )
UmuD [lpg1231 and lpg1704] ( <i>E. coli</i> )

\*Abbreviated list of notable recombination, repair, or proteins of related function either absent or present in duplicate in *L. pneumophila* as assessed by searching the genome sequence of *L. pneumophila* Philadelphia (NC\_002942) by psi-BLAST using the model organism indicated. Not present defined as: no BLAST hits with expect values  $< 1 \times 10^{-10}$ , closest hit missing critical domain or components, or closest hit matches another well-defined protein.

**Figure 1.1**

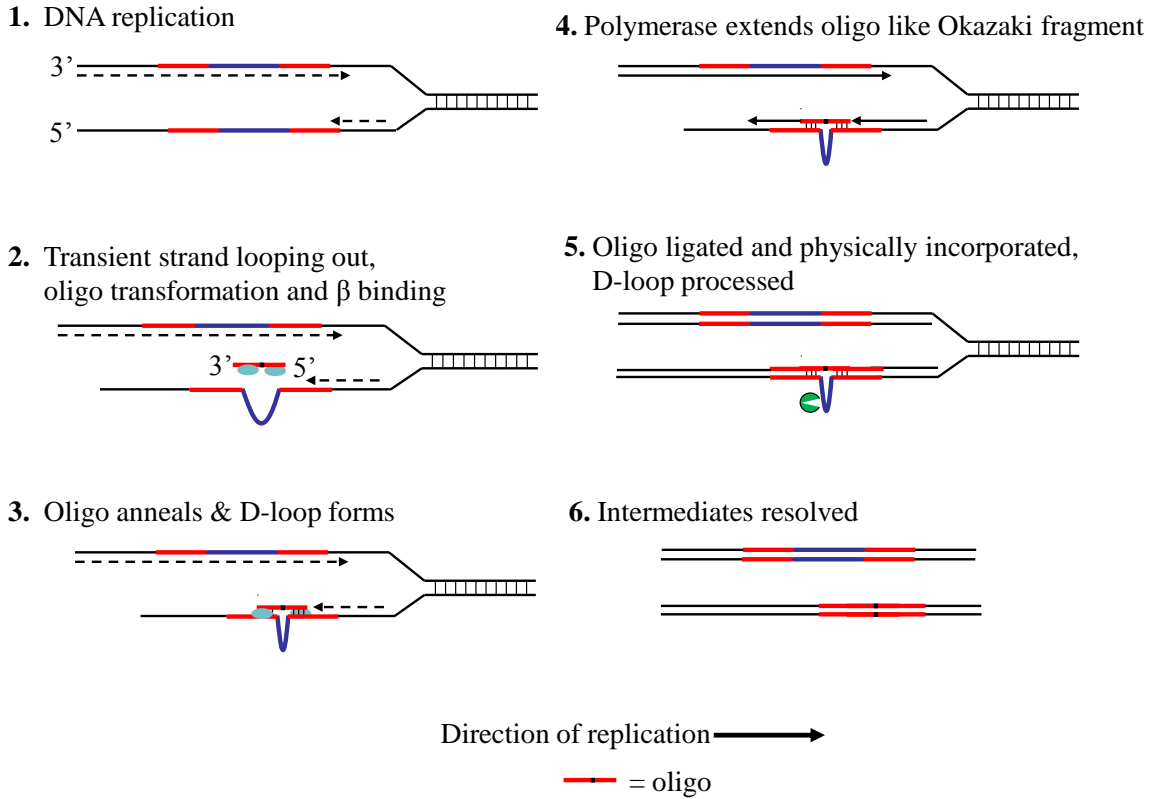


**Figure 1.1.** Strand annealing/integration model of  $\lambda$  Red recombination with an oligonucleotide as described in the text, where oligo is physically incorporated into the nascent strand. Red line with black center represents an oligo with homology to a chromosomal sequence (red) and a foreign sequence (black). Light blue ovals indicates  $\beta$  binding protein. Green Pac-Man indicates repair enzymes. Loop represents sequence as small as a single nucleotide or as long as several kilobases. Model based primarily on (Costantino and Court, 2003, Ellis, *et al.*, 2001, Grogan and Stengel, 2008, Huen, *et al.*, 2006, Li, *et al.*, 2003, Yu, *et al.*, 2000).

**Figure 1.2**

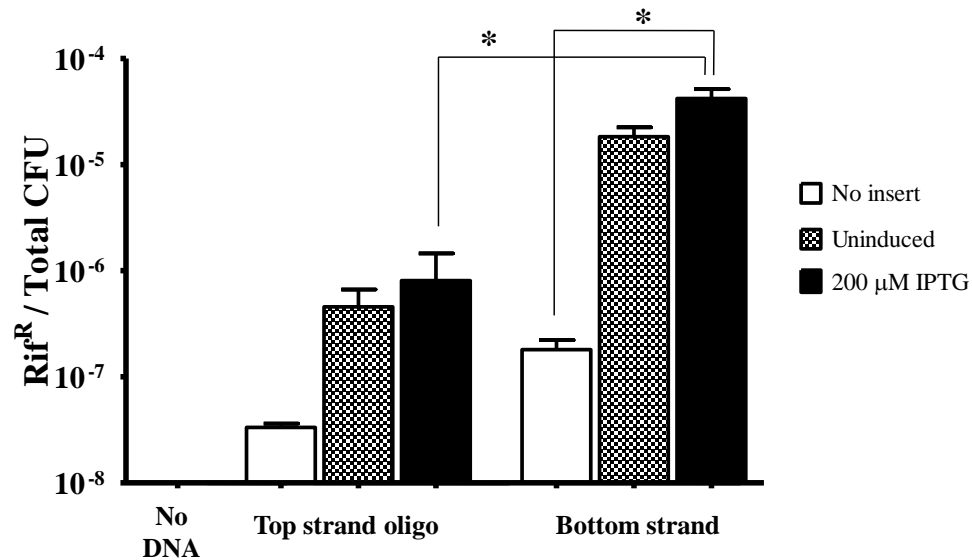


**Figure 1.2.** *Legionella* phage recombinase genes *orfBC* mediate recombination with oligos in a DNA- and strand-dependent manner, as predicted by  $\lambda$  Red recombination, when expressed under *ptac* control in *E. coli* on a RSF1010-based shuttle plasmid. Oligos corresponding to RpoB encode a point mutation conferring rifampin resistance. Assay is analogous to the rifampin resistance assay described in more detail in Chapter 3. When tested in *L. pneumophila*, no conditions were observed where expression of recombinase genes resulted in frequencies above ‘no insert’ controls, but a low frequency of DNA-dependent mutagenesis was observed that was independent of phage gene expression (data not shown, Chapter 3). Data represent mean  $\pm$  SEM of 3 independent experiments. \* indicates *P* value < 0.05 by two-tailed t test. Kaoru Harada contributed to these data.

**Figure 1.3**

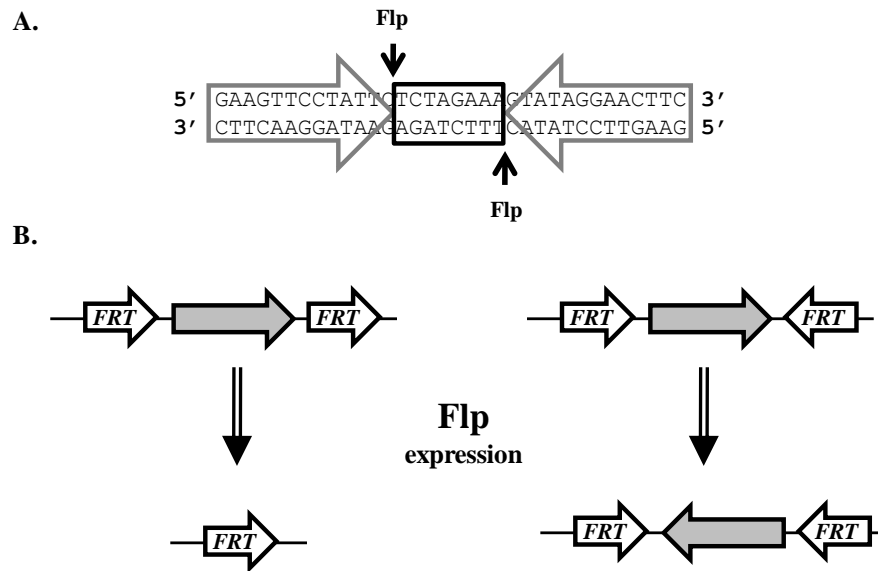


**Figure 1.3.** Flp recombination. **A)** 34 bp minimal *FRT* site. Large arrows indicate inverted symmetry elements; box indicates asymmetric core; small arrows indicate Flp cleavage sites. **B)** Orientation of *FRT* sites dictates fate of intervening DNA. Adapted from Schweizer 2003.

**Figure 1.4**

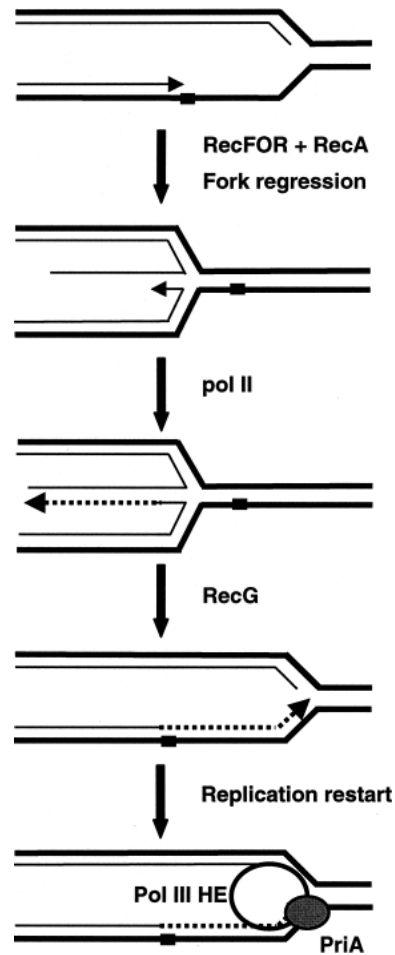


**Figure 1.4.** Model for replication restart involving RecFOR, PriA, pol II and pol III proteins. Lesions in DNA cause uncoupling of DNA synthesis leading to regions of ssDNA. These regions are subsequently coated by RecA, with the assistance of RecFOR proteins. The arrested replication fork regresses so that the uncoupled lagging strand becomes a template for DNA synthesis by pol II. After pol II dissociates from the template, RecG promotes fork regression in the opposite direction to RecA/RecFOR, and thereby facilitates lesion bypass without translesion replication. PriA recognizes this structure and promotes loading of pol III holoenzyme to the nascent DNA, in order to reconstitute a processive replication fork capable of complete genome duplication. Figure and legend from Rangarajan 2002, used with permission.

## CHAPTER TWO

### Efficient generation of unmarked deletions in *Legionella pneumophila*

#### SUMMARY

Unmarked gene deletions facilitate studies of *Legionella pneumophila* multi-component processes, such as motility and exonuclease activity. For this purpose, *FRT*-flanked alleles constructed in *Escherichia coli* using  $\lambda$ -Red recombinase were transferred to *L. pneumophila* by natural transformation. Resistance cassettes were then efficiently excised using the Flp site-specific recombinase encoded on a plasmid that is readily lost from the host strain. This chapter is published in part by Bryan, Harada, and Swanson in *Applied and Environmental Microbiology* (2011). Used with permission.

#### INTRODUCTION

*Legionella pneumophila* virulence strategies can be studied by exploiting its genome sequence, natural competence, and growth in artificial media (Molofsky and Swanson, 2004, Newton, *et al.*, 2010). However, research has been complicated by limited selectable markers and the microbe's functional redundancy, including numerous secretion substrates (Cianciotto, 2009, Hubber and Roy, 2010, Isberg, *et al.*, 2009). To facilitate construction of strains with multiple unmarked non-polar deletions, we coupled



phage-mediated recombination in *Escherichia coli* with Flp-mediated excision in *L. pneumophila*. By exploiting a  $\lambda$  phage enzyme to mediate homologous recombination between DNA substrates with as few as 35 nucleotides of homology, so-called recombineering offers several advantages over restriction enzyme-based cloning, including increased efficiency and precision (Court, *et al.*, 2002, Datsenko and Wanner, 2000, Thomason, *et al.*, 2007a, Thomason, *et al.*, 2007b, Yu, *et al.*, 2000). The *Saccharomyces cerevisiae* Flp site-specific recombinase excises DNA flanked by directly repeated 34 bp *FRT* sites (Cox, 1983, Falco, *et al.*, 1982, Golic and Lindquist, 1989, Morschhauser, *et al.*, 1999, O'Gorman, *et al.*, 1991, Schweizer, 2003, Senecoff, *et al.*, 1985). Here we efficiently generate unmarked deletions in *L. pneumophila* using Flp induced from plasmids, which are then cured from the strain. Compared to traditional methods, this approach generated unmarked deletions at a higher frequency and with greater consistency.

## **METHODS**

### **Construction of null alleles with *FRT*-flanked antibiotic resistance cassettes.**

To construct alleles, 500-1000 bp flanking each gene to be deleted was amplified by PCR from the chromosome of wild-type *L. pneumophila* and cloned into pGEM T easy (Promega) using *E. coli* DH5 $\alpha$  as the host (Fig 2.0, Table 2.1). The gene of interest was replaced by an *FRT*-flanked *cat* or *kan* cassette from pKD3 or pKD4, respectively (Datsenko and Wanner, 2000), using recombineering and *E. coli* DY330 (Fig 2.0, Table 2.1; Thomason, *et al.*, 2007a, Thomason, *et al.*, 2007b). The recombinant allele from

pGEM was then transferred to the Lp02 chromosome by natural transformation (Fig 2.0; Sexton and Vogel, 2004, Stone and Kwaik, 1999). An *FRT*-flanked gentamycin resistance cassette was also constructed that can be amplified with the same primers used for the *cat* and *kan* genes (Table 2.1).

### ***FRT*-flanked cassettes are excised using vectors that express Flp.**

To construct a shuttle vector for efficient expression of the Flp recombinase by *L. pneumophila*, *flp* was cloned into a gentamycin-resistant and sucrose-sensitive derivative of the broad host range plasmid pMMB206, yielding pMMBFlp (Table 2.S1). Vector pMMBFlp encodes an inducible and functional Flp recombinase (Fig 2.1A, Table 2.S1). However, since this plasmid was difficult to cure from the host strain (Fig 2.1B), it is suitable for stable *flp* expression in *L. pneumophila* or for development of tools in other species (Table 2.S1). For both transient Flp expression and ready segregation from *L. pneumophila*, pBSFlp was constructed by replacing the RSF1010 origin of replication of pMMBFlp with the ColE1 *ori* from pBluescript KS- (Table 2.1).

### **Flp-mediated excision of cassettes and removal of vector.**

pBSFlp was transferred by electroporation (Bryan and Swanson, 2011, Chen, *et al.*, 2006, Marra, *et al.*, 1992) to *L. pneumophila* strains harboring *FRT*-flanked deletion constructs, and transformants were selected on ACES-buffered charcoal yeast extract (Pasculle, *et al.*, 1980) supplemented with 100 µg/mL thymidine (CYET), gentamycin (10 µg/mL), and IPTG (200 µM) (Fig 2.0). After 5-6 days incubation, individual

colonies from the transformation were patched onto medium without antibiotics and IPTG and incubated overnight. Next, clones were isolated by streaking onto CYET containing 5% sucrose, and their phenotypes and genotypes determined (Fig 2.0). To verify the versatility of the method, deletions were constructed in *lpg1782 (fliA)*, *lpg2217*, *lpg0826 (xseA)*, *lpg1461 (recJ)*; an *xseA recJ* double mutant was also generated (Table 2.1).

### **Motility.**

Bacterial strains were grown to the exponential stage of growth, then back-diluted and grown to an initial OD<sub>600</sub> of ~3.5. Wet mounts were observed through an inverted phase microscope at 400X magnification at least three times as the broth cultures achieved OD<sub>600</sub> = 3.70 - 4.70.

### **Lysosomal degradation.**

Percentage of intact bacteria after 2 hour infection of murine bone marrow-derived macrophages was assessed by fluorescence microscopy at an MOI ~1 as previously described (Dalebroux, *et al.*, 2009).

## RESULTS

### **pBSFlp-mediated excision and vector loss is highly efficient.**

For every locus examined, the vast majority of clones had excised the resistance cassette and lost the plasmid when utilizing pBSFlp. When generating mutants in *fliA*, *lpg2217*, *xseA*, and *recJ*, 100% of the total clones (n=96) lost the desired resistance cassette when plated on medium containing IPTG, whereas 89% (n=44) of the isolates on medium without IPTG had done so. Loss of vector was also highly efficient: 100% (n=96) of clones lacked the vector after re-streaking on sucrose-containing medium.

The ability of Flp recombinase to excise two cassettes in one step was also examined. A double *recJ::FRT xseA::FRT* unmarked deletion mutant was constructed in three steps: one step for each cassette insertion, then Flp-mediated excision of both cassettes in a single final step (Table 2.1). In contrast, traditional allelic exchange methods utilizing counter selection would require four selection steps, costing the researcher more time while increasing the chances of second-site mutations. Minimizing strain passage was particularly important for the nuclease mutants, whose DNA repair is predicted to be defective.

### **Mutations in multiple genes with redundant function reveal phenotypes.**

To examine whether functionally redundant genes can be studied by constructing multiple unmarked deletions in a single strain, we investigated the individual and combined effects of the RecJ and ExoVII (XseA) nucleases. *E. coli* has four canonical

single-stranded nucleases (ssExos) with a great deal of redundancy (Burdett, *et al.*, 2001, Dutra, *et al.*, 2007, Viswanathan, *et al.*, 2001, Viswanathan and Lovett, 1998), whereas only two of these enzymes are annotated in the *L. pneumophila* genome (Bryan and Swanson, 2011, Chien, *et al.*, 2004). In *E. coli*, increased sensitivity to the base analog 2-aminopurine (2-AP) is not revealed until three or four of its ssExos are mutated (Burdett, *et al.*, 2001, Viswanathan, *et al.*, 2001). High concentrations of 2-AP saturate methyl-directed mismatch repair, with mismatches recognized by MutS leading to MutH-mediated strand cleavage (Burdett, *et al.*, 2001, Modrich, 1991). Subsequent strand processing requires exonucleolytic cleavage or else the repair event is aborted and toxic intermediates accumulate (Burdett, *et al.*, 2001, Viswanathan, *et al.*, 2001). Nuclease mutants also exhibit increased sensitivity to nalidixic acid (Chase and Richardson, 1977, Viswanathan, *et al.*, 2001). To test genetically if the *L. pneumophila* RecJ and ExoVII nucleases are redundant and together provide the majority of ssExo activity, we examined the susceptibility of single and double mutants to 2-AP and nalidixic acid. When treated with either DNA damaging agent, the plating efficiency of the double mutant was decreased compared to either single mutant, suggesting overlapping function (Fig 2.2).

### **Unmarked *fliA* deletion alleles are not polar on *motAB*.**

Compared to insertion mutations, unmarked mutations pose a lower risk of polar effects on downstream genes. For example, a transposon mutation in the gene encoding the flagellar sigma factor, *fliA*, completely eliminates flagella and motility, and these defects are only partially complemented (Table 2.2; Molofsky, *et al.*, 2005). Positioned 9

bp 3' of *fliA* is the *motAB* locus (Fig 2.3A), which encodes ion channels critical for flagellar motion, as < 5% of *motAB* mutant *L. pneumophila* exhibit motility (Table 2.2; Molofsky, *et al.*, 2005).

To test polarity of *fliA* mutations generated with Flp, we compared the resulting motility phenotypes to those of the *fliA* transposon mutant (Table 2.1). Motility was scored microscopically, since soft agar assays are not applicable for the non-chemotactic *L. pneumophila* (Byrne and Swanson, 1998). Plasmid-born *fliA* restored full motility only to the *fliA* unmarked mutant strain (Table 2.2). Since the partial motility of both the *fliA* transposon and the *FRT-cat-FRT* mutant strains carrying *fliA in trans* resembled that of the *motAB* mutant (Table 2.2), both of the insertion mutations are likely polar.

In addition to reducing polar effects, complete unmarked deletions reduce the chances that sequences not deleted by transposon insertions may still be transcribed and translated, occasionally leading to a protein with aberrant activity. We examined this possibility by observing whether the various mutants in *fliA* were able to avoid lysosomal degradation by murine macrophages at two hours post-infection. The *fliA::kan* transposon insertion mutant contains an insertion at residue 201 of 239—leaving most of the protein unaltered by the mutation, yet the strain is more susceptible to lysosomal degradation than wild-type cells (Fig 2.3; Molofsky, *et al.*, 2005). This defect is fully complemented, however, suggesting that polarity on *motAB* is unlikely to be responsible for the phenotype (Molofsky, *et al.*, 2005). In contrast to the insertion mutation, a mutant strain with a complete deletion of the coding sequence of *fliA* does not have a defect in lysosomal avoidance (Fig 2.3). While there are many possible explanations for these

differences, one consistent with our results is that the transposon insertion strain produces a truncated and functionally altered protein that results in the observed degradation phenotype, but this phenotype is recessive when the wild-type protein is over-expressed. These data illustrate the value of unmarked non-polar and complete deletions by demonstrating that, even when a phenotype of a mutation can be genetically complemented, it can still be difficult to assign a phenotype to a gene with confidence when less precise genetic inactivation tools are utilized.

## **DISCUSSION**

### **Unmarked deletions in *Legionella*.**

A powerful approach to study fundamental bacterial processes is the construction and analysis of unmarked non-polar mutations. Certain experimental questions, including whether factors are functionally redundant, require that multiple mutations be constructed in a single strain. To facilitate the genetic manipulation, we developed an efficient tandem approach in which recombinant alleles are first constructed in *E. coli* using the  $\lambda$ -Red recombinase system, and then Flp-mediated excision is induced in *L. pneumophila*.

### **Exonuclease and mismatch repair potential of *L. pneumophila*.**

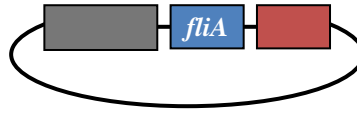
Genome sequences suggest *L. pneumophila* has a reduced exonucleolytic potential, at least as assessed by the number of major single-stranded exonucleases

compared to model organisms (Altschul, *et al.*, 2009, Cazalet, *et al.*, 2004, Chien, *et al.*, 2004). Our observations that *L. pneumophila* exonuclease double mutant cells are sensitive to DNA damaging agents support this genomic prediction. It was notable, however, that the *L. pneumophila* double mutant was more susceptible to 2-AP than the corresponding *E. coli* double mutant, yet it was more resistant than the *E. coli* quadruple mutant (Burdett, *et al.*, 2001). Since in *E. coli* nucleases are necessary for methyl-directed mismatch repair (MDMR) and the susceptibility to 2-AP is dependent on recognition of mismatches by repair machinery (Burdett, *et al.*, 2001, Viswanathan, *et al.*, 2001), *L. pneumophila* may have a less responsive MDMR system than *E. coli* or recruit non-canonical mechanisms to repair base mismatches. These observations are consistent with mismatch repair playing a relatively minor role in correcting base changes induced by oligo mutagenesis in *L. pneumophila* (Bryan and Swanson, 2011). Alternatively, this pathogen may have unrecognized ssExos. Interestingly, indirect data from oligo mutagenesis experiments may also suggest a contributing, but minor, role of unrecognized exonucleases (Bryan and Swanson, 2011). Nevertheless, the extreme sensitivity of the double mutant to nalidixic acid suggests that RecJ and ExoVII are *L. pneumophila*'s main ssExos. In concert with the organism's ability to undergo natural transformation, a reduced exonucleolytic potential and less sensitive mismatch repair system provide mechanistic support for epidemiological genomic studies (Bruggemann, *et al.*, 2006, Cazalet, *et al.*, 2008, Cazalet, *et al.*, 2004) that suggest *Legionella pneumophila* occupies an evolutionary niche that relies on a diverse and dynamic genome to exploit its eukaryotic hosts.

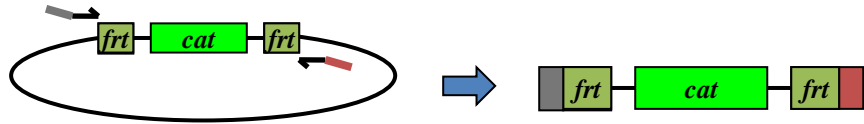


**Figure 2.0**

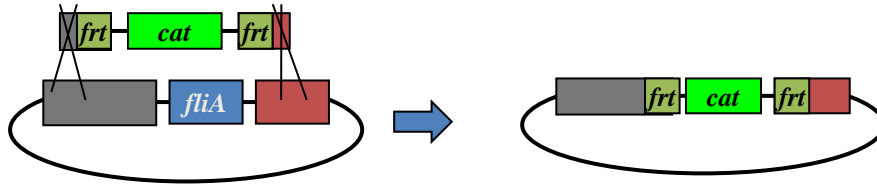
1. Clone gene with >500 bp flanking



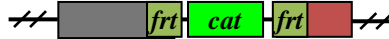
2. Amplify antibiotic cassette flanked by FRT sites, incorporating >35 bp homology by oligo design



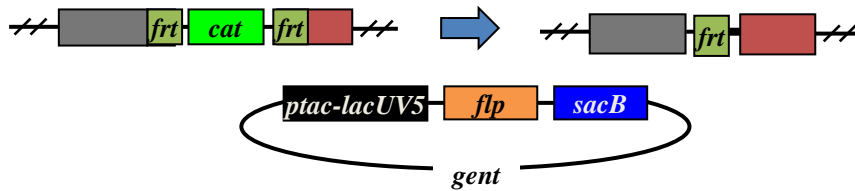
3. Co-electroporate into *E. coli* expressing  $\lambda$ -Red recombinase genes:  
- Cloned gene with flanking sequence  
- Linear resistance cassette



4. Move allele into *L. pneumophila* by natural transformation



5. Introduce Flp expression plasmid (pBSFlp), select on plates containing gentamycin and IPTG



6. Patch on plates without antibiotics or sucrose, then re-streak on plates containing sucrose to select for loss of plasmid



**Figure 2.0. Outline of strategy to construct an unmarked deletion in *fliA*.**

**Figure 2.1**

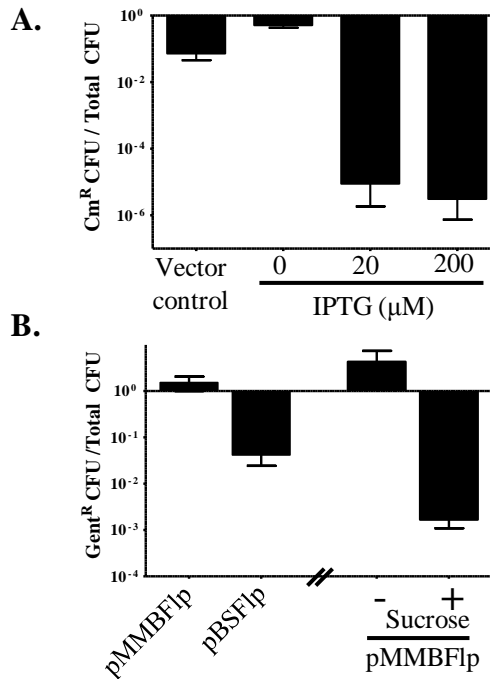


**Figure 2.1. After efficiently curing antibiotic resistance cassettes from the *L. pneumophila* chromosome, plasmids expressing the Flp recombinase can be segregated from the host strain. A)** Flp-mediated excision of a *cat* cassette was examined in a *letA::FRT-cat-FRT* strain using pMMBFlp and IPTG induction in broth, and then plating on medium with and without chloramphenicol (Table 2.S1). **B)** Loss of Flp-encoding plasmids with either an RSF1010 (pMMBFlp) or Cole1 (pBSFlp) origin of replication. For cultures that were selected for plasmid loss with sucrose, overnight cultures were first grown in the absence of sucrose, then exponential phase cultures were normalized, resuspended, and grown overnight in AYET + 5% sucrose without antibiotics. After plating on media with and without gentamycin, the presence of the resistance cassette encoded on the vector was scored. Data represent mean  $\pm$  SEM of  $\geq 3$  experiments.

**Figure 2.2**

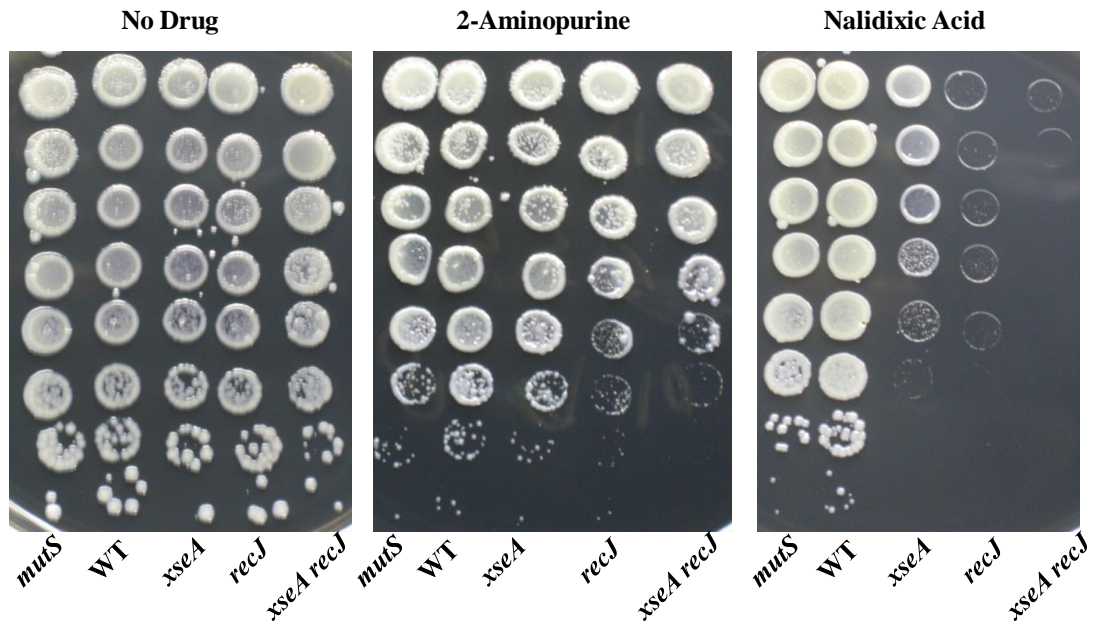


**Figure 2.2. Exonuclease double mutants are sensitive to 2-aminopurine and nalidixic acid.** Indicated strains were grown to the post-exponential phase of growth, as assessed by motility, cultures normalized to an  $OD_{600}$  of 1.0, and 10-fold serial dilutions plated on CYET without drug or CYET supplemented with 350  $\mu\text{g}/\text{ml}$  of 2-AP or 2  $\mu\text{g}/\text{ml}$  of nalidixic acid. A *mutS::cat* strain (Bryan and Swanson, 2011) is shown as a specificity control.

**Figure 2.3**

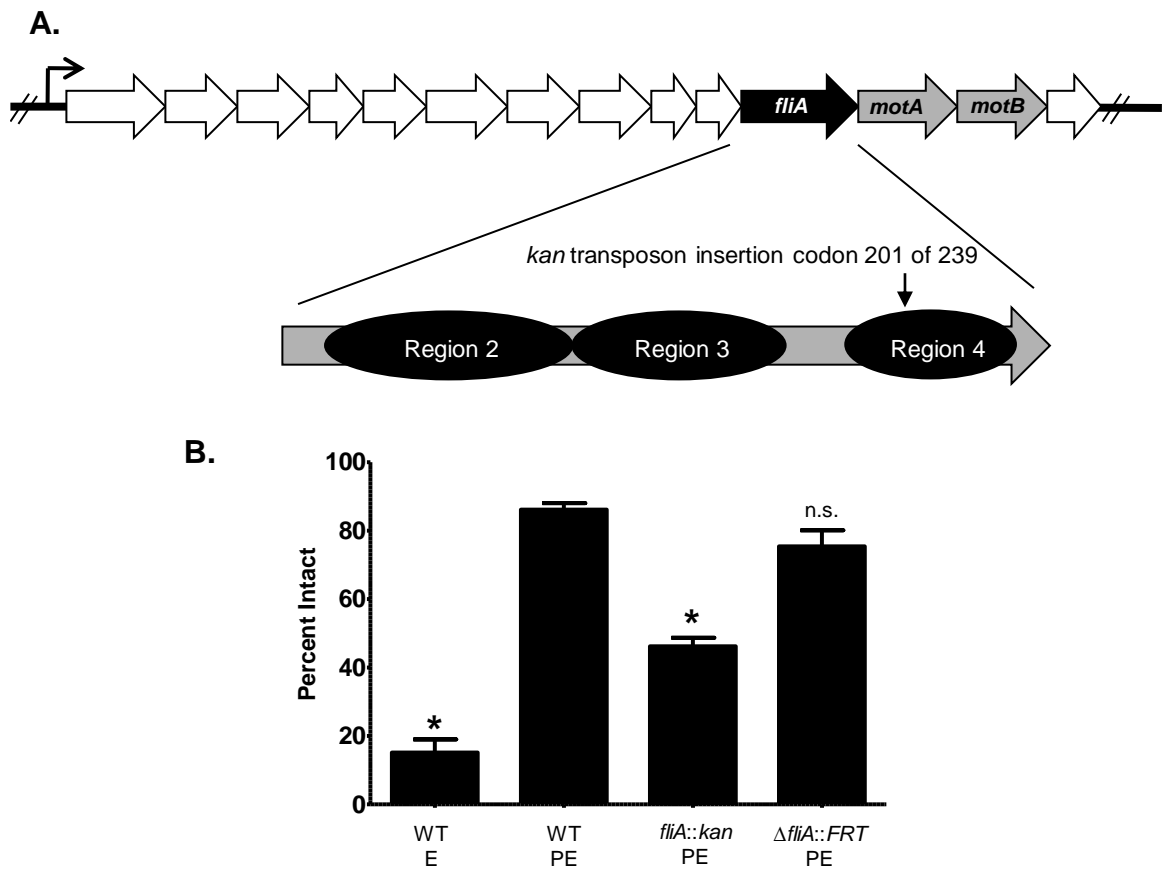


**Figure 2.3. *fliA* transposon insertion mutant cells, but not *fliA::FRT* complete deletion mutant cells, evade degradation poorly when phagocytized by macrophages.** **A)** Putative *fliA* operon structure and relative location of transposon insertion into the protein. Regions are predicted from alignment with *E. coli*  $\sigma^{70}$ : region 2 contains the -10 promoter recognition helix and the main core RNA polymerase binding domain, region 3 is involved in binding the core RNA polymerase and occasionally -10 sequences, and region 4 binds the -35 promoter element. **B)** Murine bone marrow-derived macrophages were infected for 2 hours with wild-type *L. pneumophila* or indicated strain grown to the exponential (E) or post-exponential (PE) growth phase. >100 infected macrophages were scored for the presence of intact or degraded *L. pneumophila*. Data represents the mean  $\pm$  SEM of 3 independent experiments. \* Indicates statistically significant from WT PE at  $\alpha = 0.05$  using one-way ANOVA and Bonferroni post-hoc. N.S. indicates not significant.

**Table 2.1. Abbreviated list of bacterial strains and plasmids.\***

Strain	Genotype or plasmid	Source
<i>E. coli</i> and plasmids		
DH5 $\alpha$	<i>supE44</i> $\Delta$ <i>lacU169</i> (80 <i>lacZ</i> $\Delta$ M15) <i>hsdR17</i> <i>recA1 endA1 gyrA96 thi-1 relA1</i>	Laboratory collection
DY330	W3110 $\Delta$ <i>lacU169 gal490</i> $\lambda$ <i>cI857</i> $\Delta$ ( <i>cro-bioA</i> ) pGEM-T easy pKD3 ( <i>FRT-cat-FRT</i> allele) pKD4 ( <i>FRT-kan-FRT</i> allele)	(Yu, <i>et al.</i> , 2000) Promega (Datsenko and Wanner, 2000) (Datsenko and Wanner, 2000)
MB838	DH5 $\alpha$ $\lambda$ <i>pir endA::FRT</i> pR6K $\gamma$ <i>FRT-gent-FRT</i>	This work
MB790	DH5 $\alpha$ pMMBFlp	This work
MB791	DH5 $\alpha$ pBSFlp	This work
MB750	DH5 $\alpha$ pGEM <i>fliA</i>	This work
MB751	DH5 $\alpha$ pGEM $\Delta$ <i>fliA::FRT-cat-FRT</i>	This work
<i>L. pneumophila</i>		
MB110	Lp02 wild type, <i>thyA</i> , <i>hsdR</i> , <i>rpsL</i> (Str <sup>R</sup> )	(Berger and Isberg, 1993)
MB811	Lp02 $\Delta$ <i>fliA::FRT-cat-FRT</i>	This work
MB818	Lp02 $\Delta$ <i>fliA::FRT</i>	This work
MB758	Lp02 <i>recJ::FRT-cat-FRT</i>	(Bryan and Swanson, 2011)
MB819	Lp02 $\Delta$ <i>recJ::FRT</i>	This work
MB759	Lp02 <i>xseA::FRT-kan-FRT</i>	(Bryan and Swanson, 2011)
MB820	Lp02 $\Delta$ <i>xseA::FRT</i>	This work
MB760	Lp02 <i>recJ::FRT-cat-FRT, xseA::FRT-kan-FRT</i>	(Bryan and Swanson, 2011)
MB821	Lp02 <i>recJ::FRT, xseA::FRT</i>	This work

\*See Table 2.S1 for complete strain table.

**Table 2.2. Motility phenotypes.**

Strain			Percent
Strain designation	Chromosome	Plasmid	Motile*
Lp02	Wild-type post-exponential	None	> 95%
Lp02	Wild-type exponential	None	0 %
MB560	<i>motAB::gent</i>	None	< 5%
MB808	<i>fliA::kan</i> transposon insertion	pMMBGent-empty	0 %
MB510	<i>fliA::kan</i> transposon insertion	pMMBGent-FliA	< 5%
MB814	$\Delta$ <i>fliA::FRT-cat-FRT</i>	pMMBGent-FliA	< 5%
MB816	$\Delta$ <i>fliA::FRT</i>	pMMBGent-empty	0 %
MB817	$\Delta$ <i>fliA::FRT</i>	pMMBGent-FliA	> 95%

\*Motility of  $> 10^4$  cells scored as a population in two independent experiments, as observed periodically from  $OD_{600} = 3.70 - 4.70$ , except WT exponential, which was observed at  $OD_{600} = 0.90-1.00$ . Kaoru Harada contributed to these data.

**Table 2.S1. Bacterial strains and plasmids.***E. coli* and plasmids

DH5 $\alpha$	<i>supE44 <math>\Delta</math>lacU169 (80 lacZ<math>\Delta</math>M15) hsdR17 recA1 endA1 gyrA96 thi-1 relA1 <math>\lambda</math>pir</i>	Laboratory collection
DH5 $\alpha$ $\lambda$ pir	<i>supE44 <math>\Delta</math>lacU169 (80 lacZ<math>\Delta</math>M15) hsdR17 recA1 endA1 gyrA96 thi-1 relA1 <math>\lambda</math>pir</i>	Laboratory collection
DY330	W3110 $\Delta$ lacU169 gal490 $\lambda$ c1857 $\Delta$ ( <i>cro</i> - <i>bioA</i> )	(Yu, <i>et al.</i> , 2000)
	pGEM-T easy	Promega
	pKD3 ( <i>FRT-cat-FRT</i> allele)	(Datsenko and Wanner, 2000)
	pKD4 ( <i>FRT-kan-FRT</i> allele)	(Datsenko and Wanner, 2000)
MB838	pR6K $\gamma$ <i>FRT-gent-FRT</i>	This work
	pCP20 (source of <i>flp</i> gene)	(Datsenko and Wanner, 2000)
	pMM237 (source of <i>sacB</i> gene)	(McClain, <i>et al.</i> , 1996)
	pBluescript KS- (source of ColE1 <i>ori</i> )	Stratagene
	pMMB206 $\Delta$ mob	(Molofsky and Swanson, 2003)
	pMMBGent-empty	(Molofsky, <i>et al.</i> , 2005)
	pMMBGent-FliA	(Molofsky, <i>et al.</i> , 2005)
MB741	pMMBGent (pMMB206 $\Delta$ mob with gentamycin resistance cassette replacing <i>cat</i> )	This work
MB789	pMMBbve (pMMBGent with <i>sacB</i> cloned downstream of the MCS)	This work
MB790	pMMBFlp (pMMBbve with <i>flp</i> cloned under ptac control)	This work
MB791	pBSFlp (pMMBFlp with ColE1 <i>ori</i> replacing RSF1010 <i>ori</i> )	This work
MB792	pGEM <i>letA</i>	This work
MB793	pGEM $\Delta$ <i>letA::FRT-cat-FRT</i>	This work
MB750	pGEM <i>fliA</i>	This work
MB751	pGEM $\Delta$ <i>fliA::FRT-cat-FRT</i>	This work
MB748	pGEM <i>xseA</i>	(Bryan and Swanson, 2011)
MB749	pGEM $\Delta$ <i>xseA::FRT-kan-FRT</i>	(Bryan and Swanson, 2011)
MB747	pGEM $\Delta$ <i>recJ::FRT-cat-FRT</i>	(Bryan and Swanson, 2011)
MB794	pGEM <i>lpg0558</i>	This work
MB795	pGEM $\Delta$ <i>lpg0558::FRT-cat-FRT</i>	This work

MB796	pGEMlpg1116	This work
MB797	pGEMΔlpg1116::FRT-cat-FRT	This work
MB798	pGEMlpg1889	This work
MB799	pGEMΔlpg1889::FRT-cat-FRT	This work
MB800	pGEMlpg1918	This work
MB801	pGEMΔlpg1918::FRT-cat-FRT	This work
MB802	pGEMlpg2217	This work
MB803	pGEMΔlpg2217::FRT-cat-FRT	This work
MB804	pGEMlpg2343	This work
MB805	pGEMΔlpg2343::FRT-cat-FRT	This work
MB806	pGEMlpg2918	This work
MB807	pGEMΔlpg2918::FRT-cat-FRT	This work

*L. pneumophila*\*

MB110	Lp02 wild type, <i>thyA</i> , <i>hsdR</i> , <i>rpsL</i> (Str <sup>R</sup> )	(Berger and Isberg, 1993)
MB413	<i>letA</i> :: <i>kan</i> transposon insertion	(Hammer, <i>et al.</i> , 2002)
MB808	Lp02 <i>fliA</i> :: <i>kan</i> transposon insertion, pMMBGent-empty	(Molofsky, <i>et al.</i> , 2005)
MB510	Lp02 <i>fliA</i> :: <i>kan</i> transposon insertion, pMMBGent-FliA	(Molofsky, <i>et al.</i> , 2005)
MB560	Lp02 <i>motAB</i> :: <i>gent</i>	(Molofsky, <i>et al.</i> , 2005)
MB809	Lp02 Δ <i>letA</i> ::FRT-cat-FRT, pMMBbve (vector control)	This work
MB810	Lp02 Δ <i>letA</i> ::FRT-cat-FRT, pMMBFlp	This work
MB811	Lp02 Δ <i>fliA</i> ::FRT-cat-FRT	This work
MB812	Lp02 Δ <i>fliA</i> ::FRT-cat-FRT, pMMBFlp	This work
MB813	Lp02 Δ <i>fliA</i> ::FRT-cat-FRT, pBSFlp	This work
MB814	Lp02 Δ <i>fliA</i> ::FRT-cat-FRT, pMMBGent-FliA	This work
MB815	Lp02 Δ <i>fliA</i> ::FRT, Supplemental Method	This work
MB816	Lp02 Δ <i>fliA</i> ::FRT, Supplemental Method, pMMBGent-empty	This work
MB817	Lp02 Δ <i>fliA</i> ::FRT, Supplemental Method, pMMBGent-FliA	This work
MB818	Lp02 Δ <i>fliA</i> ::FRT	This work
MB758	Lp02 Δ <i>recJ</i> ::FRT-cat-FRT	(Bryan and Swanson, 2011)
MB819	Lp02 Δ <i>recJ</i> ::FRT	This work
MB759	Lp02 Δ <i>xseA</i> ::FRT- <i>kan</i> -FRT	(Bryan and Swanson, 2011)
MB820	Lp02 Δ <i>xseA</i> ::FRT	This work
MB760	Lp02 Δ <i>recJ</i> ::FRT-cat-FRT, Δ <i>xseA</i> ::FRT- <i>kan</i> -FRT	(Bryan and Swanson, 2011)
MB821	Lp02 Δ <i>recJ</i> ::FRT, Δ <i>xseA</i> ::FRT	This work
MB822	Lp02 Δlpg0558::FRT-cat-FRT	This work



MB823	Lp02 $\Delta$ <i>lpg0558</i> :: <i>FRT</i> , Supplemental Method	This work
MB824	Lp02 $\Delta$ <i>lpg1116</i> :: <i>FRT-cat-FRT</i>	This work
MB825	Lp02 $\Delta$ <i>lpg1116</i> :: <i>FRT</i> , Supplemental Method	This work
MB826	Lp02 $\Delta$ <i>lpg1889</i> :: <i>FRT-cat-FRT</i>	This work
MB827	Lp02 $\Delta$ <i>lpg1889</i> :: <i>FRT</i> , Supplemental Method	This work
MB828	Lp02 $\Delta$ <i>lpg1918</i> :: <i>FRT-cat-FRT</i>	This work
MB829	Lp02 $\Delta$ <i>lpg1918</i> :: <i>FRT</i> , Supplemental Method	This work
MB830	Lp02 $\Delta$ <i>lpg2217</i> :: <i>FRT-cat-FRT</i>	This work
MB831	Lp02 $\Delta$ <i>lpg2217</i> :: <i>FRT</i> , Supplemental Method	This work
MB832	Lp02 $\Delta$ <i>lpg2217</i> :: <i>FRT</i>	This work
MB833	Lp02 $\Delta$ <i>lpg2343</i> :: <i>FRT-cat-FRT</i>	This work
MB834	Lp02 $\Delta$ <i>lpg2343</i> :: <i>FRT</i> , Supplemental Method	This work
MB835	Lp02 $\Delta$ <i>lpg2918</i> :: <i>FRT-cat-FRT</i>	This work
MB836	Lp02 $\Delta$ <i>lpg2918</i> :: <i>FRT</i> , Supplemental Method	This work

\*Strains were constructed as described in text, except for those listed as constructed with the Supplemental Method (also see Fig 2.1 and Fig 2.S1).

#### Supplemental Method for Table 2.S1:

To induce Flp expression and excision of resistance cassettes, pMMBFlp was transferred by electroporation to strains containing *FRT*-flanked deletion constructs, which were then cultured overnight in AYET containing IPTG (200  $\mu$ M) and gentamycin (10  $\mu$ g/mL). To remove IPTG and antibiotic, cells were washed twice and then cultured overnight in AYET to mid-exponential phase. To enrich for bacteria that had lost pMMBFlp, cells were diluted into AYET + 5% sucrose, cultured overnight or until growth was visible, and then isolated on CYET + 5% sucrose. Finally, colonies which were likely to have lost or inactivated *sacB*, identified by their non-mucoid morphology were screened for gentamycin and chloramphenicol sensitivity, and the size of the putative unmarked deletion allele was verified by PCR. The predicted scar sequence following Flp-mediated excision was confirmed by sequencing two independent deletions. To test the fidelity of the method, deletions were constructed in numerous loci that were relevant to other projects in our laboratory: *letA*, *fliA*, *lpg0558*, *lpg1116*, *lpg1889*, *lpg1918*, *lpg2217*, *lpg2343* and *lpg2918*. Although we occasionally observed unusual growth characteristics after the antibiotic cassette was excised by this method (Fig 2.S1), we nevertheless describe the unmarked strains here in the event they are of interest to others in the community. On the other hand, we have not observed unusual growth patterns for the corresponding antibiotic-resistant progenitors or the unmarked mutants generated using the less stable plasmid pBSFlp as described in the main text.

**Figure 2.S1**

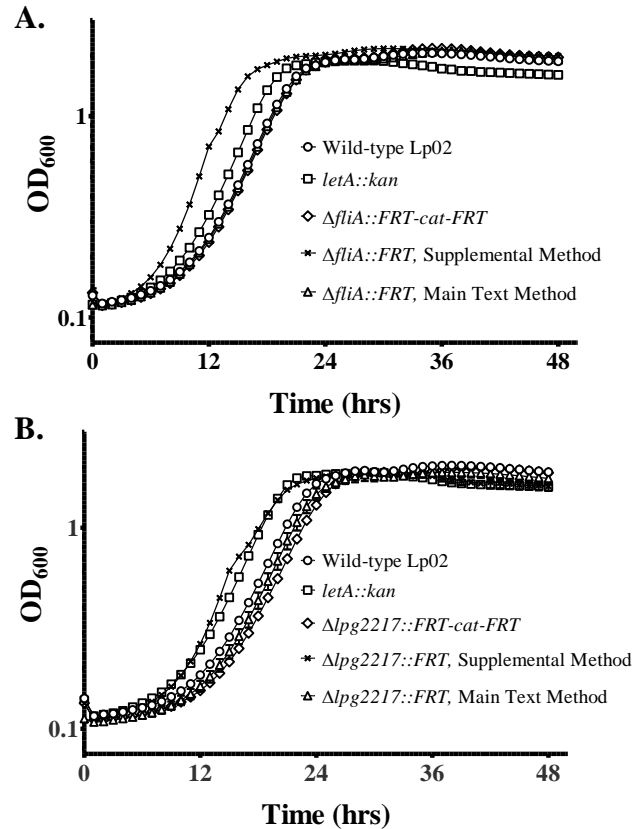


**Figure 2.S1. Growth of strains following Flp excision.** Aberrant growth was observed for *fliA* (A) and *lpg2217* (B) mutants obtained before and after Flp-mediated excision and sucrose selection when utilizing pMMBFlp in broth (Supplemental Method, described in Table 2.S1), but not pBSFlp on plates (described in text). Shown are the mean  $\pm$  SD for triplicate wells in one experiment representative of two assays performed on separate days. Error bars are typically masked by the indicator symbols. A *letA::kan* mutant is shown as a specificity control for its characteristic growth phenotype (Hammer, *et al.*, 2002). Kaoru Harada contributed to these data.

Data indicate no unusual growth characteristics for strains cultured to induce Flp expression and lose vector as described in the text. In contrast, the extra passages or some unknown effect of sucrose selection in broth for the Supplemental Method from Table 2.S1 often yielded strains exhibiting a fast-growth phenotype, with occasional decline in OD in late post-exponential phase, as illustrated by the *letA* mutant.

## CHAPTER THREE

### Oligonucleotides stimulate genomic alterations of *Legionella pneumophila*

#### SUMMARY

Genetic variation generates diversity in all kingdoms of life. The corresponding mechanisms can also be harnessed for laboratory studies of fundamental cellular processes. Here we report that oligonucleotides (oligos) generate mutations on the *L. pneumophila* chromosome by a mechanism that requires homologous DNA, but not RecA, RadA or any known phage recombinase. Instead we propose that DNA replication contributes, since oligo-induced mutagenesis required  $\geq 21$  nucleotides of homology, was strand-dependent, and was most efficient in exponential phase. Mutagenesis did not require canonical 5' phosphate or 3' hydroxyl groups, but the primosomal protein PriA and DNA Pol I contributed. After electroporation, oligos stimulated excision of 2.1 kb of chromosomal DNA or insertion of 18 bp, and non-homologous flanking sequences were also processed. We exploited this endogenous activity to generate chromosomal deletions and to insert an epitope into a chromosomal coding sequence. Compared to *E. coli*, *L. pneumophila* encodes fewer canonical single-stranded exonucleases, and the frequency of mutagenesis increased substantially when either its RecJ and ExoVII nucleases were inactivated or the oligos modified by nuclease-resistant bases. In addition to genetic engineering, oligo-induced mutagenesis may have evolutionary implications as

a mechanism to incorporate divergent DNA sequences with only short regions of homology. This chapter was published by Bryan and Swanson in *Molecular Microbiology* (2011). Used with permission.

## INTRODUCTION

The strategies that equip *Legionella pneumophila* to infect human alveolar macrophages evolved during its co-evolution with freshwater amoebae. This environmental pathogen has an unusually diverse genome, with numerous eukaryotic-like motifs and hundreds of genes unique to individual strains, even within the same species and serogroup (Cazalet, *et al.*, 2008, Cazalet, *et al.*, 2004, Chien, *et al.*, 2004, Gomez-Valero, *et al.*, 2009, Lurie-Weinberger, *et al.*). Horizontal transmission has contributed a number of genes that are critical to the bacterium's ability to replicate within phagocytes, evade host defenses, and cause disease (Cazalet, *et al.*, 2008, Cazalet, *et al.*, 2004, Chien, *et al.*, 2004, Gomez-Valero, *et al.*, 2009, Isberg, *et al.*, 2009, Shin and Roy, 2008).

Although horizontal gene transfer can occur by several mechanisms, it frequently depends on homologous recombination mediated primarily by either the bacterial RecA enzyme or bacteriophage recombinases (Thomas and Nielsen, 2005). Experimentalists harness these recombination systems to engineer the bacterial genome to study fundamental cellular processes. In general, RecA-mediated recombination is inefficient for substrates with < 50 bp of homology (Dutra, *et al.*, 2007, Lovett, *et al.*, 2002, Lusetti and Cox, 2002); in *L. pneumophila*, directed mutagenesis typically requires > 250 bp of homology (Sexton and Vogel, 2004). In contrast, phage-encoded single-stranded binding

proteins, primarily RecT and Beta homologs, can mediate recombination with < 50 bp of homology, thereby facilitating use of synthetic oligonucleotides (oligos) as substrates (van Kessel and Hatfull, 2007, Yu, *et al.*, 2000, Zhang, *et al.*, 1998). Indeed, in *E. coli* and a few other species, phage recombinases will mediate high frequency pinpoint recombination within short regions of homology (Datsenko and Wanner, 2000, Lesic and Rahme, 2008, Ranallo, *et al.*, 2006, van Kessel and Hatfull, 2007, Yu, *et al.*, 2000). Although the so called recombineering or  $\lambda$ -Red method is highly efficient for genetic engineering, its application is limited to these phages' host or closely related bacteria and necessitates expression of exogenous genes in the species of interest.

Recently Dutra *et al* (Dutra, *et al.*, 2007) and Swingle *et al* (Swingle, *et al.*, 2010b) described recombination in bacteria stimulated by oligos by a process that is independent of both RecA and exogenous phage recombinases. Swingle and colleagues introduced small nucleotide changes in the chromosomes of four different bacterial species, suggesting that the process of RecA- and phage-independent oligo recombination is likely conserved among bacteria. Moreover, by a mechanism that remains to be determined, oligos can stimulate deletion of ~ 500 bp from the *Pseudomonas syringae* chromosome, albeit with low efficiency and fidelity (Swingle, *et al.*, 2010b).

RecA- and phage-independent oligo recombination has been proposed to occur via a similar mechanism as  $\lambda$ -Red mediated recombination, but without the necessity of a single-stranded binding protein (Murphy and Marinus, 2010, Swingle, *et al.*, 2010b). The annealing/integration model for  $\lambda$ -Red mediated recombination holds that oligos anneal at the replication fork and are incorporated into the nascent strand by direct extension and

ligation by DNA polymerase and ligase, respectively (Ellis, *et al.*, 2001, Huen, *et al.*, 2006, Li, *et al.*, 2003). In all three Domains of life, as illustrated by *E. coli*  $\lambda$ -Red (Grogan and Stengel, 2008, Huen, *et al.*, 2006), mammalian cells (Radecke, *et al.*, 2006), and the Archaeon *Sulfolobus acidocaldarius* (Grogan and Stengel, 2008), the annealing/integration model has been empirically supported by the decrease in recombination frequency observed for oligos that are non-extendable by DNA polymerase, despite particular mechanistic differences in these divergent oligo recombination systems.

Here we extend knowledge of oligo-induced chromosomal mutagenesis by analyzing in *L. pneumophila* both native and heterologous genomic alleles, excision of large DNA segments, and insertion of short sequences. Furthermore, we exploit this pathway to construct defined markerless mutations and to insert an epitope tag. Our data also highlight notable mechanistic differences from previously described recombination systems, as we document mutagenesis by oligos that are non-extendable by DNA polymerase. These observations emphasize the value of testing directly whether observations in model organisms hold for other species of bacteria. The implications of oligo-induced chromosomal mutation for genetic engineering as well as the evolution of highly divergent *L. pneumophila* genomes are also discussed.

## METHODS

### Bacterial strains and resistance cassettes.

*Legionella pneumophila* strain Lp02 and derivatives were cultured as previously described (Byrne and Swanson, 1998); *E. coli* DH5 $\alpha$ , BW25113, JW2669, HB101 and derivatives were cultured using standard laboratory conditions. Chloramphenicol (5 and 25  $\mu$ g/ml), gentamycin (10  $\mu$ g/ml), rifampin (5 and 50  $\mu$ g/ml), ampicillin (100  $\mu$ g/ml), streptomycin (0.5 and 1 mg/ml), and metronidazole (10  $\mu$ g/ml) were used for selection of *L. pneumophila* and *E. coli*, respectively. Metronidazole-streptomycin plates were poured fresh and either immediately used or refrigerated for use within one week. Isogenic mutations in strain Lp02 were generated by constructing recombinant alleles in *E. coli* after cloning into pGEM T easy (Promega, Madison, WI) and replacing the desired sequence with a resistance cassette by recombineering (Bryan, *et al.*, 2011, Datsenko and Wanner, 2000, Thomason, *et al.*, 2007a), except for the *recJ::cat* allele, which was made by overlap-extension PCR. Recombinant alleles were transferred to Lp02 by natural transformation (Bryan, *et al.*, 2011, Sexton and Vogel, 2004). Where necessary, resistance cassettes were removed by FLP recombinase-mediated excision (Bryan, *et al.*, 2011). See supplementary information for complete strain and oligo list (Tables 3.S2-4). The *recA* mutants were confirmed by their inability to undergo natural transformation under standard laboratory conditions and slightly decreased growth phenotype (Luneberg, *et al.*, 2001). The *cat-rdxA-rpsL* cassette was assembled by overlap-extension PCR by amplifying the appropriate fragments from pKD3 (Datsenko and Wanner, 2000), pRDX (Goodwin, *et al.*, 1998, LeBlanc, *et al.*, 2006), and *E. coli*

DH5 $\alpha$ . In a second overlap-extension step, the *cat-rdxA-rpsL* cassette was fused with ~500 bp of flanking DNA 5' and 3' to the *L. pneumophila fliA* gene. The *fliA::cat-rdxA-rpsL* allele was cloned into pGEM T easy and used as a template to construct another allele in which *cat-rdxA-rpsL* was inserted at the start of *fliA* by recombineering in *E. coli*, as above. The *cat-rdxA-rpsL* cassette flanked with several restriction sites has also been cloned using an R6K $\gamma$  origin of replication, creating pR6K*catrdxArpsL* (Table 3.S1). The cassette can be amplified using the forward primer sequence 5'-tgtgacggaagatcacttcg-3' and the reverse primer sequence 5'-ttaagccttaggacgcttcacg-3'. To support replication and allow phenotype verification in a streptomycin resistant background strain, the plasmid is carried by an HB101 $\lambda$ *pir endA::frt* strain (Table 3.S1). To rescue sub-clones with different origins of replication and allow phenotype verification, an HB101 *endA::frt* strain is used (Table 3.S1). The colony morphology of clones containing the *cat-rdxA-rpsL* cassette were often observed to be slightly heterogeneous in both *L. pneumophila* and *E. coli*, with clones yielding smaller colonies displaying the strongest counter-selectable phenotype. The growth of strains containing the *cat-rdxA-rpsL* cassette was also slightly retarded (Fig 3.S1).

### **Transformations.**

For electroporation, *L. pneumophila* cells were cultured overnight to exponential phase and diluted ~ 25- to 100-fold into 35 mL of AYET without antibiotics in a 250 mL flask at 37 °C with shaking at 250 rpm. Strains containing plasmids were maintained by selecting for thymidine prototrophy. Unless noted, cells were cultured overnight to



OD<sub>600</sub> = 1.00 ± 0.05 and then chilled on ice for ~10 min prior to centrifugation of 30 ml of the culture at 4600 g for 7 min at 4 °C. Cells were washed once with 30 ml ice-cold sterile distilled deionized water and transferred to a 1.5 ml tube. After centrifugation at full speed for 50-60 sec at 4 °C in a microcentrifuge, cells were washed twice with 1 ml of water and then resuspended in a final volume of ~ 240 µL. 50 µL of cells were electroporated with 1 – 5000 pmol of oligo in 1 cm path length cuvettes at 1.8 kV, 100 ohms, and 25 µF and immediately transferred to 5 mL of broth. Cultures were incubated at 37 °C on a rotating wheel without selection overnight or until at least the late exponential growth phase (~ 10 doublings). 100 µl of each culture was spread onto 1-3 plates with and without the appropriate antibiotic. Data for the rifampin-resistance assay likely under represents the true frequency, since the growth rate of rif<sup>R</sup> cells was slower compared to wild-type cells (Fig 3.S1). In contrast, the growth rate of the *cat::kan* strain and derivative *cat* recombinants were comparable (Fig 3.S1).

*E. coli* cells were cultured as for λ-Red induction (Thomason, *et al.*, 2007a), with some modification. Cells were grown overnight, then diluted 70-fold into 55 ml of fresh LB containing ampicillin selection for plasmid backbone in a 250 mL flask at 37 °C with shaking at 250 rpm. Cultures were grown to OD<sub>600</sub> = 0.42 ± 0.02 and then chilled on ice for ~10 min prior to centrifugation of 50 ml of the culture at 4600 g for 7 min at 4 °C. Cells were washed once with 35 ml ice-cold sterile distilled deionized water and transferred to a 1.5 ml tube. After centrifugation at full speed for 30-40 sec at 4 °C in a microcentrifuge, cells were washed once with 1 ml of water and then resuspended in a final volume of ~ 400 µL. 50 µL of cells were electroporated with 1 nmol of oligo in 1

cm path length cuvettes at 1.8 kV, 200 ohms, and 25  $\mu$ F and immediately transferred to 1 mL of LB. Cultures were incubated for 4 h at 37 °C on a rotating wheel maintaining selection for plasmid backbone, but without selection for parental ( $\text{kan}^{\text{R}}$ ) or derivative recombinant allele ( $\text{cm}^{\text{R}}$ ). 100  $\mu$ l of each culture was spread onto 1-3 plates with and without the appropriate antibiotic.

Oligos were purchased as standard de-salted reagents without further purification from either Invitrogen (Carlsbad, CA) or IDT (Coralville, IA), except for the 130mer and 161mer oligo, which were purchased as Ultramers from IDT. To produce double-stranded DNA, oligos were heated and then slowly cooled in the presence of 10 mM TrisHCl/50mM NaCl, dialyzed, and final concentration adjusted to 0.1 nmol/ $\mu$ L. To assess whether single stranded DNA remained after annealing, oligos were examined by agarose gel migration pattern and ethidium bromide staining (Goedhart and Gadella, 2005) and determined to have  $\leq 10$  pmol of ssDNA (data not shown)—a molar quantity insufficient to mediate observable mutagenesis over *no DNA* controls (Fig 3). Oligos modified by a 3' inverted thymidine nucleotide (invT), 3' phosphate (3'  $\text{PO}_4^-$ ), and a 3' dideoxy (ddC) were verified to be non-extendable by DNA polymerase using PCR with *L. pneumophila* genomic DNA as a template. PCR reactions were conducted with each of following enzymes whose exonuclease activity varies: *Taq* DNA polymerase (NEB); Platinum Taq High Fidelity, a mixture of *Taq* DNA polymerase and *Pyrococcus species* GB-D polymerase (Invitrogen); and Deep Vent Polymerase (NEB), comprised of only the *Pyrococcus species* GB-D polymerase containing an intact 3'→5' exonuclease domain. PCR reactions using unmodified oligos or those protected by phosphorothioate bonds

alone yielded product as expected. Oligos with invT and 3' PO<sub>4</sub><sup>-</sup> never yielded product, while ddC oligos yielded a faint band only when Deep Vent Polymerase was supplied at high concentration.

All data shown are the mean ± SEM of independent experiments, except for Fig 3.9C, in which 2-3 individual experiments are shown because of colony heterogeneity, spontaneous resistance, and variability in solid medium freshness confounded calculating means that accurately represented frequency. Since individual electroporations occasionally varied due to conditions unrelated to mutagenesis frequency (i.e. air bubble in cuvette, inexplicable slower recovery compared to similar cultures, etc), data from individual electroporations were excluded if the time constant was less than 2.0 for *L. pneumophila* or 4.0 for *E. coli* or, when ≥ 4 electroporations were conducted for a given condition, the Grubbs test for outliers was significant at  $p < 0.05$ . No more than one value was excluded per condition using the Grubbs test.

## RESULTS

### **Oligo-induced mutagenesis in *L. pneumophila* is distinct from classical homologous recombination.**

While investigating a *L. pneumophila* RecT-like phage recombinase (Datta, *et al.*, 2008, Luneberg, *et al.*, 2001), we observed that, after electroporation, oligos stimulated a modest increase in the corresponding mutation frequency, independently of an exogenous recombinase. To monitor the frequency of an oligo-induced point mutation, 1 nmol of a

71 nucleotide (nt) oligo homologous to *rpoB* and containing a point mutation that confers rifampin resistance (Nielsen, *et al.*, 2000) was introduced by electroporation into wild-type *L. pneumophila* strain Lp02. The oligo corresponding to the top (+) strand encodes a C→T transition and a T-G mismatch, while the oligo corresponding to the bottom (-) strand encodes a G→A transition and A-C mismatch. Oligos corresponding to each DNA strand or their annealed dsDNA product (+/-) each increased the frequency of rifampin resistance compared to samples that were not exposed to exogenous DNA (Fig 3.1A). Consistently, the oligo corresponding to the bottom strand was more mutagenic (- ; Fig 3.1A). We predict that the bottom (-) oligos anneal to the lagging strand during DNA synthesis, based on the single predicted *L. pneumophila* origin of replication (Gao and Zhang, 2007) and its position and orientation in the chromosome. However, because no empirical evidence has verified the predicted origin or distinguished the lagging versus leading strands of the *L. pneumophila* chromosome, we will simply designate strands as top (+) or bottom (-). We shall refer to the transfer of information from a synthetic oligo to the chromosome of *L. pneumophila* as “oligo-induced mutagenesis” for brevity, without implying mechanism.

To test whether classical homologous recombination pathways contribute to oligo-induced mutagenesis, three approaches were applied. First, an isogenic *recA::cat* strain was constructed and compared to wild type, revealing that RecA did not affect the frequency of rifampin resistance (Fig 3.1A). Most, but not all (Lovett, *et al.*, 2002), RecA-dependent homologous recombination proceeds by one of two different mechanisms, the RecBCD or RecFOR pathways (Kuzminov, 1999). Since *L.*

*pneumophila* does not encode a canonical RecBCD enzyme (Table 1.1; Altschul, *et al.*, 1997, Cazalet, *et al.*, 2004, Chien, *et al.*, 2004), oligo mutagenesis is likely independent of this pathway. To assess the contribution of RecFOR, we analyzed an isogenic *recF::cat* mutant. Similar to the *recA* mutant, no reduction in oligo-induced mutagenesis was observed in the *recF* mutant relative to wild-type cells (mean of  $n \geq 4$  experiments:  $2 \times 10^{-5}$  rif<sup>R</sup>/total CFU for *recF* versus  $8 \times 10^{-6}$  for WT). As a third test of the similarity to classical recombination pathways, we analyzed the impact of the length of homology. The frequency of rifampin resistance was similar when cells were treated with oligos between 21 and 161 nt of homology (Fig 3.1B), a pattern distinct from RecA- and phage-based recombination systems (Lovett, *et al.*, 2002, Sexton and Vogel, 2004, Yu, *et al.*, 2000). The dependence on homology but not canonical recombination enzymes indicates that oligo-induced mutagenesis is distinct from classical homologous recombination.

We next assessed whether the selectable mutation must be encoded by the oligo, or exposure to excessive single-stranded DNA was sufficient for mutagenesis. After treatment with a 71 nt oligo encoding the wild-type *rpoB* sequence, the frequency of rifampin resistance increased slightly over background, but remained well below the frequencies generated by oligos that encode the point mutation (Fig 3.1A). Similar results have been reported for *P. syringae* (Swingle, *et al.*, 2010a). Therefore, we tested whether this slight increase in mutation frequency was either restricted to sequences encoded by the oligo, a general response to an influx of single-stranded DNA, or a local but indirect effect. For this purpose, we introduced 31 nt oligos of wild-type sequence that corresponded to a region that was either centered on the target nucleotide, directly 5'

or 3' of the target base, or elsewhere on the chromosome but matched for GC content. In each condition tested, only those oligos encompassing the mutation resulted in mutation frequencies greater than the *no DNA* control (Fig 3.1C). Furthermore, a higher mutation frequency was measured at the trend level for *no mutation* oligos of 71 nt compared to 31 nt ( $9.7 \times 10^{-8}$  vs.  $4.8 \times 10^{-8}$ , respectively,  $p = 0.0505$ ), again implicating a role for the oligo at the specific target sequence. A similar pattern has been observed in *E. coli* (Donald L. Court, personal communication; Oppenheim, *et al.*, 2004). This background mutation rate could be due to the error rate of either chemical synthesis, which is greater for longer oligos (manufacturer's information), or one of *L. pneumophila*'s three annotated translesion polymerases (Table 1.1; Chien, *et al.*, 2004). Whatever the process, these results provide no evidence for either a local indirect process, such as a repair mechanism within the replication fork, or a general response to single-stranded DNA, such as SOS (Table 1.1).

### **Oligo-induced mutagenesis is strand- and growth-phase dependent.**

Strand dependence (Fig 3.1A) has been used to infer that a recombination event occurs at the replication fork. However, interpreting strand dependence is complicated by the observation that the efficiency of the *E. coli* mismatch repair system is affected by the DNA sequence (Costantino and Court, 2003, Ellis, *et al.*, 2001, Li, *et al.*, 2003, Modrich, 1991, Su, *et al.*, 1988). Therefore, as a more stringent probe of strand-dependence, we inactivated mismatch repair of *L. pneumophila* by mutating *mutS*, the component of the repair complex that initially recognizes and binds a single base

mismatch or insertion and deletion loops (Su and Modrich, 1986). Consistent with the pattern observed in wild-type *L. pneumophila* (Fig 3.1A), the oligo corresponding to the bottom (-) strand of the annotated sequence (AE017354; Chien, *et al.*, 2004) stimulated a slightly higher frequency of rifampin resistance (3-fold) in the mutant than did the complementary oligo (Fig 3.2A). Thus, the strand-dependence observed in both wild-type and *mutS L. pneumophila* is consistent with the hypothesis that oligos induce mutation at the replication fork (Costantino and Court, 2003, Li, *et al.*, 2003).

In general, the *mutS* strain yielded a higher frequency of rifampin resistance than wild type. We measured a 2.5-fold increase for the control sample electroporated without DNA, a 5.6-fold increase for the top strand (T-G mismatch), and a 4.6-fold increase for the bottom strand (A-C mismatch; Fig 3.2A). Accordingly, the *L. pneumophila* mismatch repair system may actively repair the base change encoded by the oligo. Interestingly, even though the A-C and T-G mismatches are considered good substrates for repair (Modrich, 1991, Su, *et al.*, 1988), the efficiency of mismatch repair in *L. pneumophila* appeared to be significantly lower than in *E. coli*, where a >100-fold difference between *mutS* and wild-type cells has been observed (Costantino and Court, 2003, Swingle, *et al.*, 2010b). There is no evidence for a second *mutS* homolog in the genome of *L. pneumophila* to explain this difference (Table 3.S1). Instead, compared to model organisms, this pathogen may rely on some unrecognized repair system or endure more frequent base mismatches (Bryan, *et al.*, 2011).

To investigate by an independent approach the model that oligos induce mutations at replication forks, we compared exponential and post-exponential phase cultures.

Unlike replicating bacteria, post-exponential phase cells did not acquire rifampin resistance at an elevated rate (Fig 3.2B). To a first approximation, the growth phase difference did not reflect electroporation efficiency, since the frequency of transformation with an autonomously replicating plasmid was similar for exponential and post-exponential phase cultures (Fig 3.2B). Together, both the strand- and growth phase-dependence are consistent with the hypothesis that oligo-induced mutagenesis occurs at the replication fork, a feature that can be exploited to optimize its application and gain insight to its underlying mechanism.

### **Oligo-induced mutagenesis is limited by exonucleases.**

While important for chromosome fidelity and processing of DNA repair intermediates, single-stranded exonucleases significantly decrease the efficiency of RecA-independent recombination in *E. coli* (Dutra, *et al.*, 2007). Whereas *E. coli* encodes four major single-stranded exonucleases (Dutra, *et al.*, 2007), the *L. pneumophila* genome bears only the canonical RecJ and ExoVII (XseA) nucleases (Table 1.1; Altschul, *et al.*, 1997, Cazalet, *et al.*, 2004, Chien, *et al.*, 2004). Exonucleases often exert redundant activity, since a mutant phenotype is typically observed only after several enzymes have been inactivated (Dutra, *et al.*, 2007). Therefore, to determine the impact of exonuclease activity on oligo-induced mutagenesis in *L. pneumophila*, we constructed and analyzed a *recJ xseA* double mutant strain. Consistent with the prediction of genomic instability in exonuclease-deficient cells (Dutra, *et al.*, 2007), the exonuclease double mutant had a higher percentage of stringy cells, less predictable growth patterns,



and lower numbers of viable cells than wild-type cultures. Unlike wild-type cultures, which acquired rifampin resistance at measurable frequencies only when exposed to high DNA concentrations ( $\geq 100$  pmol per electroporation for statistically significant differences from the *no DNA* control), *recJ xseA* mutants sustained oligo-induced mutations at lower DNA concentrations ( $\geq 10$  pmol per electroporation for frequencies significantly different from *no DNA* control; Fig 3.3).

As an independent test of the impact of exonucleases, we incorporated one Locked Nucleic Acid (LNA) and three phosphorothioate bonds (PT) at both the 5' and 3' ends of a 45 nt oligo. A phosphorothioate bond contains a sulfur in place of a non-bridging oxygen in the oligo backbone, whereas LNAs contain a methylene bridge between the 2'-O atom and the 4'-C atom of the nucleotide (manufacturer's information). Both DNA modifications limit degradation by nucleases in an oligo recombination system in eukaryotic cells (Parekh-Olmedo, *et al.*, 2002); PT bonds have also been used in prokaryotes (Grogan and Stengel, 2008, Huen, *et al.*, 2006). The LNA modification also stabilizes the annealed oligo-DNA molecule, as judged by melting temperature (manufacturer's information). When examined in oligo mutagenesis of *L. pneumophila*, the modified oligos stimulated a higher frequency of rifampin resistance in both wild-type and exonuclease-deficient bacteria (Fig 3.3). The elevated frequency of oligo-induced mutagenesis by the modified oligos may reflect either the higher stability of the LNA oligo-DNA complex or the ability of some unidentified *L. pneumophila* exonuclease to degrade ssDNA. In either case, the increased mutation frequencies observed with modified oligos will facilitate application of oligo-induced mutagenesis for

genetic engineering.

### **Oligos stimulate RecA-independent excision of large DNA fragments.**

While point mutations contribute to evolutionary drift, the mechanisms underlying larger genomic changes are of particular interest for *L. pneumophila* given the diversity documented within the species (Cazalet, *et al.*, 2008, Cazalet, *et al.*, 2004, Chien, *et al.*, 2004, Gomez-Valero, *et al.*, 2009, Lurie-Weinberger, *et al.*). Deletions of more than a few nucleotides have been observed (Dutra, *et al.*, 2007, Swingle, *et al.*, 2010b) but remain to be examined in detail. Therefore, to investigate whether oligos can stimulate large deletions in the chromosome of *L. pneumophila*, we first disrupted a chloramphenicol-resistance gene with a 950 bp kanamycin-resistance gene and then replaced the *fliA* locus with this cassette (Fig 3.4A). Next, *L. pneumophila* was treated with an oligo homologous to the *cat* sequences that directly flank the kan-resistance insertion. Fidelity of excision of the *kan* gene was then measured as the number of chloramphenicol-resistant colonies per total colonies. Oligos with as few as 22 nt of homology on each side of the insertion (44 nt total length) stimulated excision of the 950 bp kan gene, as measured by chloramphenicol-resistance. No chloramphenicol-resistant colonies were detected when DNA was omitted. Oligos  $\geq 60$  nt in length generated a slightly higher frequency of excision, but the frequency of excision from the chromosome was no greater with longer oligos (Fig 3.4B). Typically, between 15 and 50 recombinant colonies were observed per plate using unmodified 60mer oligos, while  $>200$  CFU was sometimes observed with certain modifications. To verify that oligos stimulate excision

of chromosomal DNA, several colonies obtained in two independent experiments were analyzed in more detail. The chloramphenicol-resistance phenotype was confirmed for all isolates ( $> 20$  per experiment), as judged by robust growth on appropriate medium. Furthermore, the *fliA* locus was the size expected for all isolates screened ( $\geq 7$  per experiment), as determined by PCR. Therefore, oligos with only short sequences of homology can stimulate large chromosomal deletions.

Since oligos may promote chromosomal deletions and point mutations by different processes, we investigated several additional parameters. By constructing a *recA::gent* derivative of the strain containing the *cat::kan* cassette, we determined that RecA does not appear to contribute to the generation of either chromosomal deletions or point mutations stimulated by the corresponding oligos (Fig 3.4B, Fig 3.1A). Compared to oligos designed to introduce a single base change, a stronger strand-dependence was observed for oligos that stimulate excision of the 950 bp kanamycin resistance gene ( $\sim 3$ -fold versus  $\sim 70$ -fold difference). This greater differential between complementary oligos is expected due to the predicted requirement of strand annealing across larger regions of ssDNA and subsequent D-loop formation (Fig 3.10). Another difference between the point mutation and large deletion assay is that chloramphenicol-resistant colonies were not generated by the corresponding annealed dsDNA for the large deletions (+/-; Fig 3.4B versus Fig. 3.1A). Large excisions mediated by a homologous ssDNA may contribute to bacterial evolution, since natural transformation of dsDNA substrates can generate ssDNA in the cytoplasm (Johnsborg, *et al.*, 2007).

Since many bacteria harbor plasmids, we next investigated whether circular DNA is a substrate for oligo mutagenesis. This experiment also addressed the potential contribution of other processing enzymes, such as endonucleases. To this end, we cloned annealed dsDNA oligos into an RSF1010-based plasmid and examined its ability to confer chloramphenicol resistance to cells containing the *cat::kan* allele. This plasmid is predicted to supply short regions of homology either as both circular double-stranded molecules or as circular single-stranded molecules generated during plasmid replication. No recombinant colonies were obtained in two independent experiments performed with and without selection for the plasmid backbone (limit of detection  $\sim 3 \times 10^{-10}$  CFU/ml). That no recombinants were observed could be due to either a very low efficiency or a mechanistic requirement for linear DNA. In either case, in nature intact plasmids are unlikely to stimulate appreciable mutagenesis by processes akin to oligo mutagenesis.

#### **Oligo-stimulated excision is sensitive to orientation in the chromosome.**

Although models in which oligos induce mutagenesis at the replication fork are supported by both strand- and growth phase-dependence (Fig 3.2), it is also possible that the transcription machinery or growth phase-specific factors contribute. Transcription does promote non-canonical recombination pathways in yeast (Liu, *et al.*, 2002) and *E. coli* (Ikeda and Matsumoto, 1979), but not  $\lambda$ -Red mediated recombination (Li, *et al.*, 2003). Therefore, to test whether transcription enhances oligo-stimulated excision, the *cat::kan* cassette was also inserted in the reverse orientation at the *fliA* locus, and then the frequency of excision was measured using the identical set of oligos (+ and -; Fig 3.4A).

If the direction that the replication fork moves affects oligo insertion, we predicted that the relative efficiency of mutagenesis by each oligo pair would switch. Indeed, the reverse pattern that we observed, namely in this case the bottom strand oligo (+) was more mutagenic than the top strand (-; Fig 3.4B), is consistent with models in which exogenous oligos mediate mutagenesis during DNA replication, not transcription.

We next tested whether oligo mutagenesis was also strand-dependent when the substrate was plasmid DNA. Using this approach we also tested whether our observations were species-specific. For this experiment, we cloned the *cat::kan* allele in both orientations into an RSF1010-based broad host range plasmid. Oligo-induced mutagenesis of this plasmid substrate was then examined in *recA* mutants of *L. pneumophila* and *E. coli* (BW25113 derivative, Table 3.S1) using the same set of oligos as the chromosomal assay. In both species, oligo mutagenesis of the plasmid was more efficient, and strand dependence was consistent, though more modest, than for the *L. pneumophila* chromosomal substrate (Fig 3.4C). Therefore, the ability of oligo mutagenesis to excise large fragments of DNA is not unique to *L. pneumophila*. Accordingly, these data verify and extend the observations of Swingle *et al.* who documented oligo-induced point mutations in four different bacterial genera (Swingle, *et al.*, 2010b).

**Oligo mutagenesis is not inhibited by 3' modified oligos that are non-extendable by DNA polymerase.**

Oligo recombination by divergent systems in all three Kingdoms relies on extension of the oligo by DNA polymerase, as judged by the decreased mutation rate of oligos that contain 3' dideoxy modifications (Grogan and Stengel, 2008, Huen, *et al.*, 2006, Radecke, *et al.*, 2006). Therefore, we sought to determine if a similar annealing/integration model holds for the RecA- and phage-independent oligo mutagenesis observed in *L. pneumophila*. To this end, we utilized three different 3' modifications to generate oligos that are non-extendable by DNA polymerase and protected from exonucleolytic cleavage by three sequential phosphorothioate modifications. To rule out any modification-specific effects, we examined oligos whose extension was blocked by either a 3' inverted thymidine nucleotide (invT), a 3' phosphate (3' PO<sub>4</sub><sup>-</sup>), or a 3' dideoxy (ddC). The 3' inverted thymidine nucleotide and 3' phosphate modifications also increase nuclease resistance (Ortigao, *et al.*, 1992; manufacturer's information). To reduce exonucleolytic cleavage of the modifications, which would allow extension from internal nucleotides, we also utilized *recJ xseA* double nuclease mutant *L. pneumophila*. Since  $\lambda$ -Red recombination in *E. coli* is sensitive to the concentration of oligo (Huen, *et al.*, 2006), we performed experiments with both limiting (0.1 nmol per electroporation) and near-saturating amounts (1 nmol per electroporation, our standard condition). In no experiment did non-extendable oligos reduce the frequency of mutagenesis; indeed, the frequency typically increased (Fig 3.5A).

To assess whether the increase in mutation frequency from non-extendable oligos is specific to RecA- and phage-independent oligo mutagenesis in *L. pneumophila* or instead is a conserved feature of the bacterial process, we examined the 3' inverted thymidine modified oligo in our plasmid system in both *L. pneumophila* and *E. coli*. Consistent with mutagenesis of the *L. pneumophila* chromosome, the frequency of mutagenesis by non-extendable oligos was increased in both species, not decreased (Fig 5B). To confirm that our inverted thymidine oligo decreased recombination frequencies in a  $\lambda$ -dependent system, we employed our plasmid assay in *E. coli* DY330 and used limiting oligo concentrations (1 pmol per electroporation) to reduce confounding effects of oligo mutagenesis. In three independent experiments, we observed a mean 4.3-fold reduction in recombination frequency with the invT oligo compared to the unmodified oligo, as expected from previous studies using dideoxy oligos (Grogan and Stengel, 2008, Huen, *et al.*, 2006) and in stark contrast to the ~10-fold increase in phage-independent oligo mutagenesis measured in *E. coli* (Fig 3.5B).

**Oligo mutagenesis is not increased by 5' phosphate modification compared to 5' hydroxyl oligos.**

To test if other parameters of the annealing/integration model apply to oligo-induced mutagenesis in *L. pneumophila*, we investigated whether oligos are directly ligated into the nascent strand by comparing mutagenesis by oligos that contain either 5' phosphate or hydroxyl groups. To reduce degradation of the 5' end, the terminus was protected by three sequential phosphorothioate modifications and a *recJ xseA* double

nuclease mutant was employed. In both wild-type and exonuclease mutant cells, the mutagenesis frequencies were similar for oligos with 5' phosphate versus 5' hydroxyl groups (Fig 3.6). Likewise, LNA-protected oligos, which have a 5' hydroxyl, supported high frequencies of oligo-induced point mutations (Fig 3.3). Thus, the effect of modifications of both the 5' and 3' ends of the oligos on *L. pneumophila* mutagenesis was opposite that reported for  $\lambda$ -Red mediated recombination in *E. coli* and *S. acidocaldarius* (Grogan and Stengel, 2008).

### **PriA and Pol I, but not RadA, contribute to oligo mutagenesis.**

Since the features of oligo-induced mutagenesis of *L. pneumophila* differ from previously described recombination systems, we applied genetics to investigate its mechanistic requirements. Having no evidence for either classical homologous recombination or contributions by a phage-encoded single-stranded binding protein (Table 3.S1), we tested the RecA paralog RadA, which contributes to recombination in different systems to varying degrees (Beam, *et al.*, 2002, Lovett, 2006, Seitz, *et al.*, 1998, Slade, *et al.*, 2009). Under the conditions tested, the *radA* and wild-type cells exhibited similar frequencies of oligo mutagenesis (Fig 3.7).

Since oligo-induced mutagenesis was strand dependent but elongation independent, we reasoned that when oligos anneal at the fork, the advancing replicative polymerase hops over the oligo and re-starts downstream. Initiation of replication outside of the origin requires the primosomal proteins PriA or PriC (Gabbai and Marians, Lovett, 2005). Since *L. pneumophila* does not appear to have PriC (Table 1.1), we



analyzed the impact of a *priA* mutation in our *cat::kan* assay strain. Consistent with a defect in replication restart, compared to wild type the *priA*-deficient strain had a higher number of filamentous cells, slower growth, and plateaued at lower culture densities. When subjected to oligo-induced mutagenesis, *priA* mutant cells had a significantly reduced mutation frequency compared to wild-type cells (Fig 3.7). In contrast, *E. coli priA* mutants are not impaired for  $\lambda$ -Red dependent recombination (Huen, *et al.*, 2006). The low background frequency of mutagenesis observed in the *priA* mutant may reflect accumulation of suppressor mutations, given that mutant colonies were more heterogeneous than normal.

Rather than extend, if the replicative polymerase hops over an annealed oligo, and then PriA directs the enzyme to restart, a single-stranded gap would remain after passage of the replisome. Since many gap-repair systems require DNA polymerase I (Kuzminov, 1999), we constructed a strain which lacks the entire predicted polymerase domain. Similar to the *priA* strain, these *polA* mutant cells displayed characteristics typical of replication and repair mutants, although the cultures grew to normal cell densities. When subjected to oligo mutagenesis, the *polA* polymerase domain mutant exhibited a mutation frequency significantly lower than wild type (Fig 3.7). These data are consistent with a requirement for proficient single-strand gap repair. However, we have not ruled out other potential roles or confounding effects for DNA Pol I activity, such as oligo extension or limitation of the region of ssDNA available. It remains possible that the reduced rate of oligo mutagenesis for both the *priA* and *polA* polymerase domain mutant strains reflects a paucity of replication forks due to their poor growth. However, we find this explanation

unlikely, since the *recJ xseA* nuclease mutant cells displayed a similarly high proportion of filamentous cells, reduced growth rate, and variable recovery after electroporation, yet sustained oligo mutagenesis more frequently than wild-type cells did (Fig 3.3).

**Homologous oligos flanked by non-homologous sequences have decreased, but not abolished, ability to stimulate oligo mutagenesis.**

In its natural aquatic reservoir, the DNA *L. pneumophila* encounters and takes up via natural transformation is unlikely to contain perfectly homologous DNA. More likely, DNA substrates may include small conserved motifs flanked by non-homologous sequences. Therefore, to gain insight to both potential evolutionary impact and mechanism, we tested whether oligos with non-homologous ends are mutagenic. *L. pneumophila* was exposed to oligos containing 60 nt of homology (30 nt on either side of kan cassette, as above) and flanked by either 10 or 35 nt of non-homologous sequence on both the 5' and 3' ends. To control for amount of homology, as well as for the total length of the oligo, we also introduced entirely homologous 60mer, 80mer or 130mer oligos. To test the contribution of classical homologous recombination, we analyzed a *recA* mutant strain. In general, the addition of non-homologous sequences decreased, but did not abolish, mutagenesis (Fig 3.8). The slightly higher frequency observed for the 130mer compared to 60-80mer entirely homologous oligos may be due to the higher purity of the 130mer Ultramer compared to standard de-salted 60-80mers (manufacturer's information). To ascertain whether recombinant colonies incorporated any non-homologous nucleotides, we sequenced the corresponding locus of mutants generated

with either the entirely homologous 80mer oligo (6 clones), the oligo containing 10 nt of non-homologous sequence on both 5' and 3' ends (6 clones), or the oligo with 10 nt of non-homologous sequence plus 3' nuclease-resistant cap (8 clones). In all cases, the identical *cat* sequence was obtained, and non-homologous sequences were not inserted. Together, these results indicate that non-homologous flanking DNA can be processed from the homologous sequences, which stimulate the mutagenic process.

Natural DNA substrates could have much longer non-homologous sequences than the 10-35 nt investigated here. Since synthesis of longer oligos is a technical and economic hurdle, as a surrogate for longer non-homologous sequences, we genetically inactivated exonucleases and/or protected the 3' ends from nucleases. Unmodified oligos bearing non-homologous ends stimulated a similar mutation frequency in the *recJ xseA* exonuclease mutants and wild-type cells, suggesting enzymes other than RecJ or XseA can process the oligo. However, when the exonuclease mutant was treated with 3' nuclease-resistant oligos bearing non-homologous ends, the mutation frequency decreased to near the limit of detection. These data suggest that the oligos are likely processed by RecJ, XseA, and/or other exonucleases, but are less likely to be processed by endonucleases. Taken together, our results indicate that, to facilitate exchange of genetic information and acquisition of selectable phenotypes, *L. pneumophila* can process single-stranded DNA molecules, including non-homologous sequences that may inhibit either the reaction or expression of a new gene product.

**Oligo-stimulated excision can be exploited to generate markerless chromosomal mutations by counter-selection.**

Having observed excision of large DNA fragments by a direct gain-of-function selection (Fig 3.4-8), to approximate what occurs in the environment we tested whether deletions can be obtained with a less stringent loss-of-function selection. While doing so, we investigated whether oligo mutagenesis can be harnessed to construct markerless mutations without expression of phage recombinase proteins, an application that has been proposed but not yet realized in bacteria (Dutra, *et al.*, 2007, Murphy and Marinus, Swingle, *et al.*, 2010b). To accommodate the low frequency of excision (Fig 3.4) and high frequency of spontaneous mutation of many counter-selectable cassettes, we first constructed a cassette containing three genes in tandem: *cat*, conferring chloramphenicol resistance; *rdxA*, conferring metronidazole sensitivity; and *rpsL*, conferring streptomycin sensitivity. Next, the chromosomal *fliA* locus was replaced by natural transformation with this 2.1 kb double counter-selectable cassette by isolating chloramphenicol-resistant colonies. After electroporation with an oligo homologous to the *fliA* sequences directly flanking the cassette, cells that had excised the counter-selectable markers were isolated on medium containing metronidazole and streptomycin. Indeed, defined markerless deletions of *fliA* were obtained in each of three independent experiments, as determined by PCR (Fig 3.9A, C). Two isolates obtained in one experiment were also confirmed by sequencing.

### **Oligo-induced mutagenesis can be harnessed to insert DNA onto the chromosome.**

Next we assessed whether oligos also stimulate insertion of foreign DNA—an important and previously unexplored activity that could inform mechanism, evolution, and genetic engineering. The *cat-rdxA-rpsL* cassette was first placed at the translational start of the *fliA* gene. Next, bacteria were electroporated with an oligo having 36 nt of homology to the sequences flanking the cassette as well as 18 nt encoding a 6(x)His tag (Fig 3.9B). In each of two independent experiments, clones were isolated in which the *cat-rdxA-rpsL* cassette was excised and the 18 nt 6(x)His-tag sequence was inserted. Each of four clones obtained in one experiment were confirmed by sequencing. Thus, *L. pneumophila* can insert into the chromosome at least short sequences of foreign DNA, provided the elements are flanked by short regions of homology (Fig 3.9B, C).

To investigate the fidelity of the oligo insertion process, we performed phenotypic and molecular analysis of the engineered *fliA* locus. By screening metronidazole- and streptomycin-resistant clones obtained after electroporation of the oligo encoding the His tag (Fig 3.9B), we determined that the majority, though not all, of the clones had also lost the chloramphenicol resistance phenotype (Fig 3.9C). A portion of these chloramphenicol-sensitive clones were confirmed by PCR and/or sequencing to have the desired 6(x)His tag sequence (Fig 3.9B, C), whereas a separate class of mutants were chloramphenicol sensitive, but did not encode the His tag. To distinguish between excision of a large fragment of DNA and acquisition of point mutations in the counter-selectable cassettes, the chloramphenicol-sensitive recombinants were screened by PCR. A striking degree of heterogeneity in the size of the products was observed. Some clones

yielded products larger or smaller than expected; other clones yielded no product, suggesting loss of one or both of the primer sites. To further investigate these clones, five representative *fliA* alleles of aberrant sizes were sequenced. All five isolates contained deletions of various lengths, consistent with the inactivation of the *cat*, *rdxA*, and *rpsL* alleles, but no other patterns were obvious (Fig 3.9D). Similar results were observed when the *cat-rdxA-rpsL* strain was simply grown overnight and selected on metronidazole-streptomycin plates—suggesting these large deletions also occur independently of exposure to oligo DNA. Despite the high degree of heterogeneity, 100% of the clones derived from oligo transformations that yielded in the initial PCR screen a product of the correct size also encoded the desired sequence modification, as determined by an independent PCR strategy and/or the nucleotide sequence of the allele. Thus, the strong pressure for metronidazole and streptomycin resistance selects for rare large and variable chromosomal deletions. However, when homologous foreign DNA in the form of an oligo is also present, the propensity for the corresponding sequence to be deleted from the chromosome increases.

## **DISCUSSION**

Here we report that *L. pneumophila* sustains a moderate frequency of mutation when exposed only to short sequences of homologous DNA at high concentrations (Fig 3.1, 3.4). This oligo-induced mutagenesis is RecA- and RadA-independent (Fig 3.1, 3.5-7). The mutation frequency increases when exonucleases are inactivated and moderately decreases when non-homologous sequences flank the regions of homology (Fig 3.7, 3.8).

Although phage-like sequences are detectable within the genome (Cazalet, *et al.*, 2004), no phage recombinases homologous to RecT or Beta have been identified within our wild-type strain sequence (Table 3.S1; Altschul, *et al.*, 1997, Chien, *et al.*, 2004). While unknown phage genes may underlie our observations, it is difficult to test, and we have no evidence to support that possibility. Oligo mutagenesis does not appear to utilize canonical 5' phosphate or 3' hydroxyl groups, but the primosomal protein PriA and DNA polymerase I each contribute (Fig 3.5-7). As a genetic engineering tool, short oligos can direct precise deletions and insertions, and the desired recombinants be identified by a PCR screen (Fig 3.9). Taken together, our results suggest that both single nucleotide changes as well as larger chromosomal deletions likely occur at the replication fork, rather than during transcription or by canonical recombination (Fig 3.2, 3.4, 3.7).

Certain aspects of oligo-induced mutagenesis of *L. pneumophila* are similar to classical homologous recombination and phage recombination systems, but other features are distinct. Like both RecA- and phage-mediated recombination, oligo-induced mutagenesis requires DNA homology. Homologous recombination is conserved among all kingdoms of life, with most organisms possessing a RecA/RadA/Rad51-like recombination system that executes many aspects of recombination, repair, and replication (Kuzminov, 1999, Lusetti and Cox, 2002). These well-described recombination systems usually rely on large regions of homology to mediate efficient cross over or gene conversion events (Kuzminov, 1999, Lovett, *et al.*, 2002, Thomas and Nielsen, 2005). In contrast, the use of  $\lambda$ -Red phage recombination system as a genetic engineering tool continues to increase because homologous recombination is stimulated

by sequences with < 50 bp of homology (Yu, *et al.*, 2000). Likewise, oligo-induced mutagenesis requires only short regions of homology. However, in contrast to the known phage systems, the relationship between efficiency of oligo-induced mutation and length of homology is not linear (Fig 3.1B; Lovett, *et al.*, 2002, Yu, *et al.*, 2000). Oligo-induced mutagenesis also differs from both RecA- and phage-dependent recombination in its requirement for higher concentrations of DNA, possibly due to greater susceptibility to exonucleases (Fig 3.3; Dutra, *et al.*, 2007, Swingle, *et al.*, 2010b).

Mechanistic requirements also distinguish oligo-induced mutagenesis from  $\lambda$ -Red mediated recombination. While  $\lambda$ -Red requires a free 5' phosphate and a 3' terminus that can be extended by DNA polymerase (Grogan and Stengel, 2008, Huen, *et al.*, 2006), phage-independent oligo mutagenesis does not (Fig 3.5, 3.6). While sensitivity to 5' and 3' end modifications may be masked by nucleolytic cleavage, several indirect results suggest this is not the case. First, non-extendable oligos were mutagenic in both *L. pneumophila* and *E. coli*, ruling out cleavage by a species-specific nuclease. Second, similar mutation frequencies were obtained whether or not modifications were protected by either sequential phosphorothioate bonds or potent nuclease-resistant nucleotides, even in the *recJ xseA* double nuclease mutant. Third, when oligos with non-homologous ends were protected with 3' caps, the frequency of mutagenesis decreased to near limit-of-detection in the *recJ xseA* mutants. Fourth, no recombinants were observed when homologous donor DNA was provided as a circular molecule. Fifth, since the lengths of homology present just met the threshold needed for maximal efficiency (Fig 3.4-6), endonucleolytic cleavage was predicted to decrease the length of homology and decrease



mutation frequency, but this pattern was not observed. The requirement for PriA in oligo mutagenesis (Fig 3.7), but not in  $\lambda$ -Red recombination (Huen, *et al.*, 2006), is also consistent with the notion that, whereas polymerase extends an oligo as an Okazaki fragment during  $\lambda$ -Red recombination, replication re-starts downstream of the oligo during phage-independent oligo mutagenesis. Based on this series of results, we propose that during oligo-induced mutagenesis, DNA polymerase does not directly extend oligos and DNA ligase does not directly ligate the oligo to the nascent strand.

Taking into consideration its similarities and differences from both classical homologous recombination and phage recombination systems, we currently favor a modified strand annealing mechanism for oligo-induced mutagenesis (Fig 3.10). In this model, DNA replication generates single-stranded DNA at the replication fork, followed by transient looping out of predominantly the lagging strand (Fig 3.1, 3.2, 3.4). The exposed ssDNA provides a substrate for homologous oligos to anneal and stabilize minor or more extensive “D-loops”. In turn, the replication fork stalls due to the secondary structure of the D-loop and the dsDNA encountered by DNA polymerase (Bzymek and Lovett, 2001, Canceill and Ehrlich, 1996, Saveson and Lovett, 1997, Swingle, *et al.*, 2010b, Viguera, *et al.*, 2001). Exonucleases digest any flanking non-homologous sequences, either before or after the oligo anneals (Fig 3.8). The mutagenesis frequency could be reduced when helicases at the fork recognize non-homologous flaps, thereby dislodging the annealed oligo and aborting the event. Regardless of oligo processing, PriA mediates replication re-start downstream of the annealed oligo (Fig 3.3, 3.5-7). An unknown post-replication repair mechanism then processes the D-loop using the oligo as

a template. Finally, the oligo itself is processed, or possibly excised entirely (Fig 3.5, 3.6, 3.8). The resultant single-stranded gap is repaired by DNA Pol I (Fig 3.7). Strong antibiotic or other evolutionary pressures can capture the rare excision of large fragments of DNA. By stabilizing D-loops, homologous DNA that anneals increases the propensity for deletion of the corresponding nucleotides; alternatively, the oligos could insert any intervening sequences (Fig 3.4-9). By incorporating mismatch repair, the same model can account for point mutations or other minor genetic changes (Fig 3.1-3). Nevertheless, a template switch model similar to that proposed for  $\lambda$ -Red (Poteete, 2008) also accommodates our data (Fig 3.11), and distinguishing between the two mechanisms would be difficult with the tools currently available for *L. pneumophila*.

That physical annealing of homologous oligos contributes to mutagenesis is inferred by a number of observations. By manipulating GC content of the oligos, Swingle *et al* correlated predicted binding affinity and mutagenesis frequency (Swingle, *et al.*, 2010b). Our observation that the frequency of mutagenesis in exonuclease mutant bacteria was increased by LNA-modification (Fig 3.3), which stabilizes binding to template DNA, is also consistent with direct annealing of the oligo. The homologous DNA template could potentially originate from a second chromosomal copy during replication, foreign DNA taken up via natural transformation, or a synthetic oligonucleotide introduced via electroporation, as we have shown here. Even in the absence of exogenous homologous DNA sequences, excision of ssDNA loops likely occurs as a stochastic process, as judged by the chloramphenicol-sensitive phenotype of colonies selected with metronidazole and streptomycin in the control samples that were

not treated with DNA (data not shown). Whether stimulated by exogenous DNA or not, such infidelity during DNA replication would equip bacteria with a mechanism to alter the size of their chromosomes, conferring an advantage to cells that incorporate beneficial DNA or excise sequences that are unnecessary or harmful in particular environmental conditions.

Oligo recombination can be a powerful genetic engineering tool for organisms that lack efficient phage recombinase systems. Here we exploited oligos to construct defined markerless mutations within the chromosome or to insert short sequences that encode an epitope tag. This enables the researcher to order custom-designed oligos of precise sequence, thereby reducing allele construction steps. By engineering a novel counter-selectable cassette (Fig 3.9), we decreased the background of spontaneously resistant isolates, permitting plating cells at high density on selective media. As a result, we obtained the desired mutants in every experiment conducted. To increase the frequency of the desired mutation, oligo modifications predicted to limit exonucleolytic attack and increase annealing strength can be incorporated (Fig 3.3, 3.5). Oligos have been shown to promote chromosomal point mutations in several genera (Swingle, *et al.*, 2010b), and we extend those observations by demonstrating that oligos induce large deletions in both *L. pneumophila* and *E. coli* (Fig 3.4, 3.5). While the application beyond Gram negative organisms is unknown, the apparent contributions by conserved replication components rather than specific phage genes suggests broad applicability. Therefore, oligo mutagenesis techniques are likely applicable to a large range of organisms, including those where genetic tools are limited. While adaptation to different

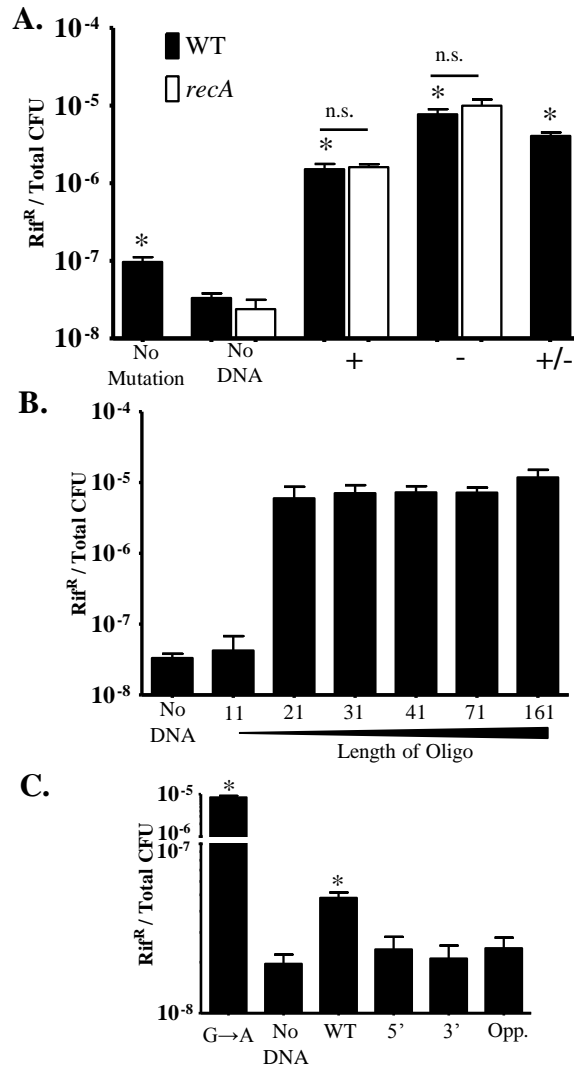
species may require tailored selectable markers and transformation conditions and has thus far been less efficient than phage-based recombineering, it may be less cumbersome than the herculean task of searching for and optimizing a species-specific phage recombinase that supports efficient recombination, as van Kessel and Hatfull have done for the Mycobacteria community (van Kessel and Hatfull, 2007).

*L. pneumophila* exhibits extraordinary genomic diversity and high plasticity, including the presence of eukaryotic-like motifs that contribute to pathogenesis (Cazalet, *et al.*, 2008, Cazalet, *et al.*, 2004, Chien, *et al.*, 2004, Gomez-Valero, *et al.*, 2009, Lurie-Weinberger, *et al.*, 2010, Price, *et al.*, 2009). The species' variability may reflect the organism's ability to take up foreign DNA in its natural reservoir of aquatic biofilms and phagocytic amoebae and protozoa. Indeed, Ogata and colleagues identified in the *Rickettsia bellii* genome several open reading frames similar to either eukaryotic or Legionellaceae sequences, which may indicate promiscuous and reciprocal gene exchange within host amoebae (Ogata, *et al.*, 2006). Natural isolates of *L. pneumophila* do undergo both intergenic (Coscolla and Gonzalez-Candelas, 2007) and intragenic recombination (Ko, *et al.*, 2003), including at loci associated with virulence. In addition to classical homologous recombination, we speculate that, in concert with its ability to take up free DNA from the environment, a process akin to oligo-induced mutagenesis may also contribute to emergence of pathogenic strains. In particular, short homologous sequences can facilitate the incorporation of novel DNA sequences, including those that encode eukaryotic-like motifs, even if flanked by non-homologous sequences (Fig 3.8, 3.9). Although in initial studies we did not detect oligo-induced mutagenesis after natural

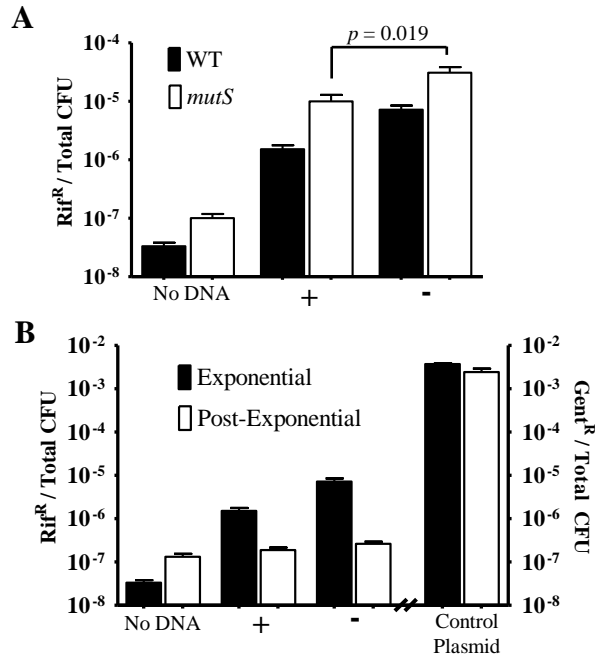
transformation, most likely because of the high DNA concentrations needed, we did not pursue this possibility exhaustively. Nevertheless, considering evolutionary time scales, as well as environmental conditions that may stimulate natural transformation or suppress exonucleases, it is feasible that oligo-induced mutagenesis generates diversity within the species. Furthermore, compared to model organisms, *L. pneumophila* encodes a minimal mismatch repair system and fewer single stranded nucleases (Figs 3.2, 3.3, Table 1.1; Altschul, *et al.*, 1997, Bryan, *et al.*, 2011, Cazalet, *et al.*, 2004, Chien, *et al.*, 2004). Perhaps natural competence, an extended half-life of single-stranded DNA molecules, and a modest editing machinery comprise an evolutionary strategy by which *L. pneumophila* increases the propensity to modify its genome to adapt to a broad array of eukaryotic hosts—including at least 13 species of amoeba, 2 species of ciliated protozoa, and the immunocompromised human (Fields, 1996).

**Figure 3.1. Oligo-induced mutagenesis is RecA-independent and insensitive to lengths of homology  $\geq 21$  nt.** **A)** Wild-type or *recA::cat* mutant *L. pneumophila* were transformed with 1 nmol of an oligo corresponding either to the top (+) or bottom (-) strand of the annotated genomic *rpoB* sequence or to their dsDNA annealed product (+/-). Oligos of 71 nt encoded either wild-type *rpoB* sequence or a point mutation that confers rifampin resistance (Rif<sup>R</sup>; RpoB H541Y). **B)** Wild-type cells were electroporated with RpoB H541Y oligos of the lengths indicated. **C)** Wild-type cells were electroporated with oligos 31 nt in length corresponding to the bottom (-) strand. Oligo A→G corresponds to the oligo encoding the point mutation conferring rifampin resistance. WT represents the *no mutation* control oligo with wild-type *rpoB* sequence centered around the nucleotide that confers rifampin resistance. 5', 3', and Opp. indicate oligos directly 5', directly 3', or on the opposite side of the chromosome as the mutation conferring rifampin resistance. Rif<sup>R</sup> values represent the mean  $\pm$  SEM  $\geq 3$  independent experiments performed on separate days. \* Indicates statistically significant difference from *no DNA* control at  $\alpha = 0.05$  by two-tailed t-test with Welch's correction, where appropriate, and adjusted by Bonferroni's correction for multiple comparisons. n.s., not significant.

Figure 3.1



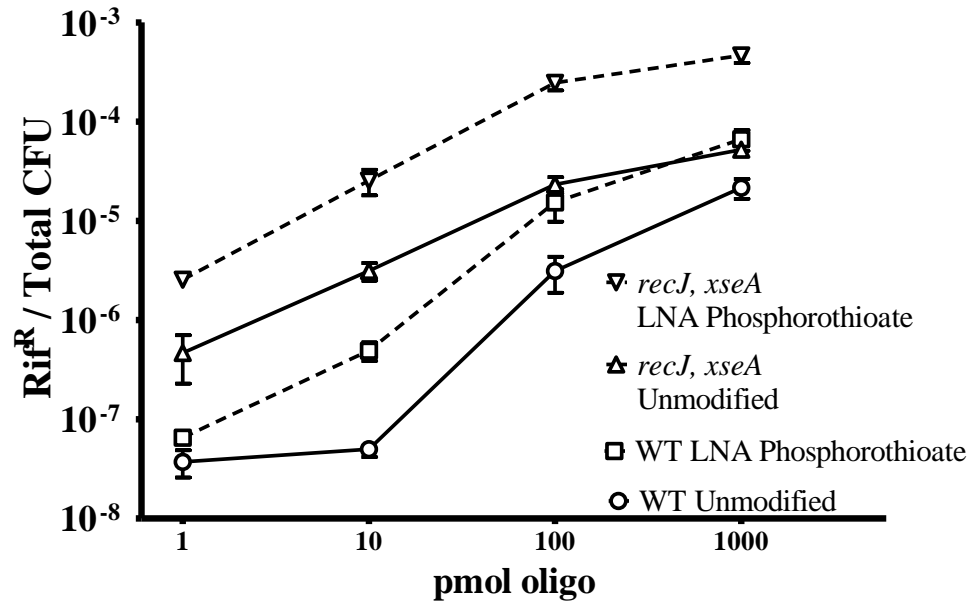
**Figure 3.2**



**Figure 3.2. Oligo-induced mutagenesis is strand- and growth-phase dependent.** **A)** Wild-type or *mutS::cat* mutant *L. pneumophila* were electroporated with RpoB H541Y oligos corresponding to the top (+) or bottom (-) strand as in Fig. 1. *P*-value was determined by two-tailed t-test with Welch's correction. **B)** Wild type cultured to exponential ( $OD_{600} \sim 1.00 \pm 0.05$ ) or post-exponential (> 95% motile,  $OD_{600} > 4.0$ ) growth phase were electroporated with either an oligo or a control plasmid that confers gentamycin resistance (Gent<sup>R</sup>) and cultured overnight or for 1.5 h, respectively, before plating on selective medium. Values represent the mean  $\pm$  SEM of  $\geq 3$  independent experiments performed on separate days.



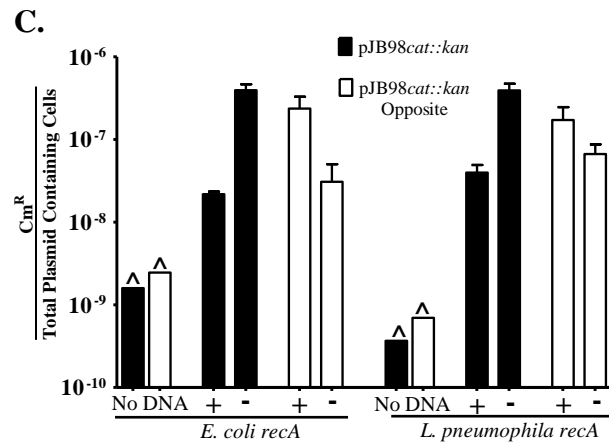
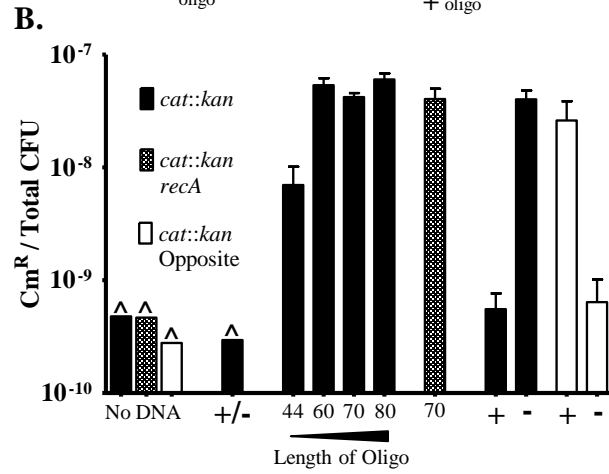
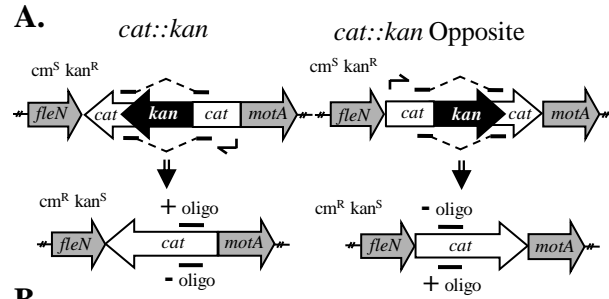
Figure 3.3



**Figure 3.3. Oligo-induced mutagenesis is limited by exonucleases.** Wild-type or *recJ::cat xseA::kan* double mutant *L. pneumophila* were electroporated with the concentration shown of either a standard 45 nt oligo (solid line) or a corresponding oligo containing a single Locked Nucleic Acid (LNA) and 3 phosphorothioate bonds at both the 5' and 3' ends (dashed line). Each data point represents the mean  $\pm$  SEM of  $\geq 4$  independent experiments performed on separate days.

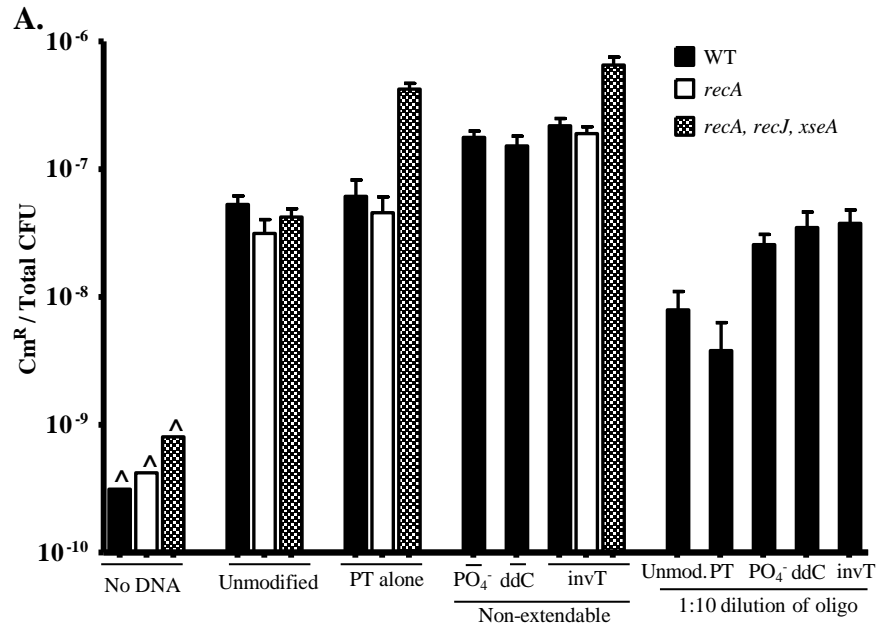
**Figure 3.4. Oligo-induced mutagenesis can excise large fragments of DNA and is sensitive to orientation in the chromosome.** **A)** The genomic orientations and expected phenotypes of *L. pneumophila* whose *fliA* gene is replaced by a *cat* gene containing an insertion of a 950 bp *kan* gene. **B)** The *cat::kan* strains with cassette in orientation shown and either the wild-type or *recA::gent* allele were cultured and treated as before. Experiments testing dsDNA used 1 nmol of annealed 70 nt oligos; tests of oligo length and RecA-dependence used 1 nmol of bottom (-) oligo; tests of orientation in the chromosome used 5 nmol of a 70 nt oligo. **C)** The same set of oligos was introduced into *recA* mutants of *E. coli* and *L. pneumophila* containing the *fliA::cat::kan* allele cloned in either orientation on a RSF1010-based plasmid. Total plasmid containing colonies indicates colonies exhibiting phenotypes conferred by the plasmid backbone—ampicillin resistance for *E. coli* and thymidine prototrophy for *L. pneumophila*. Values represent the mean  $\pm$  SEM of  $\geq 3$  independent experiments performed on separate days. ^, approximate limit of detection when no recombinant colonies were obtained; +/-, annealed oligos.

Figure 3.4



**Figure 3.5. Oligo mutagenesis is not inhibited by 3' modified oligos that are non-extendable by DNA polymerase.** **A)** Wild-type, *recA* mutant, and *recA xseA recJ* triple mutant bacteria were electroporated with either 1 nmol or 0.1 nmol (1:10 dilution) of 60mer oligos that were unmodified, protected at the 3' end by 3 sequential phosphorothioate modifications (PT alone), or protected at the 3' end by 3 sequential phosphorothioate modifications with either a 3' phosphate (PO<sub>4</sub><sup>-</sup>), 3' dideoxy (ddC), or 3' inverted thymidine (invT). **B)** Unmodified or 3' inverted thymidine capped oligos were introduced into *recA* mutants of *E. coli* and *L. pneumophila* containing the *fliA::cat::kan* allele cloned in either orientation on a RSF1010-based plasmid. Total plasmid containing colonies indicates colonies exhibiting phenotypes conferred by the plasmid backbone—ampicillin resistance for *E. coli* and thymidine prototrophy for *L. pneumophila*. Values represent the mean ± SEM of ≥ 3 independent experiments performed on separate days. ^, approximate limit of detection when no recombinant colonies were obtained.

Figure 3.5



**B.**

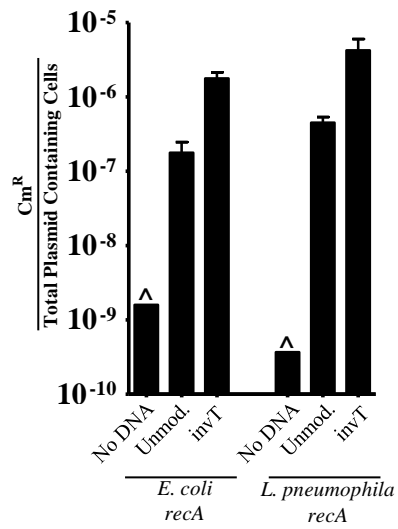


**Figure 3.6**

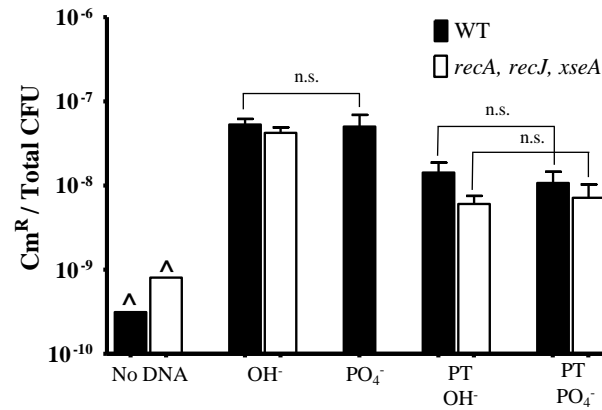


**Figure 3.6. Oligo mutagenesis is not increased by 5' phosphate modification compared to unmodified 5' hydroxyl oligos.** Wild-type and *recA xseA recJ* triple mutant bacteria were electroporated with 1 nmol of 60mer oligos that were either unmodified, and therefore contained a 5' hydroxyl (OH<sup>-</sup>), or contained a 5' phosphate (PO<sub>4</sub><sup>-</sup>) modification. PT indicates that the 5' end was protected from nucleolytic cleavage by 3 sequential phosphorothioate bonds. Values represent the mean ± SEM of ≥ 3 independent experiments performed on separate days. ^, approximate limit of detection when no recombinant colonies were obtained; n.s., not significantly different.

**Figure 3.7**

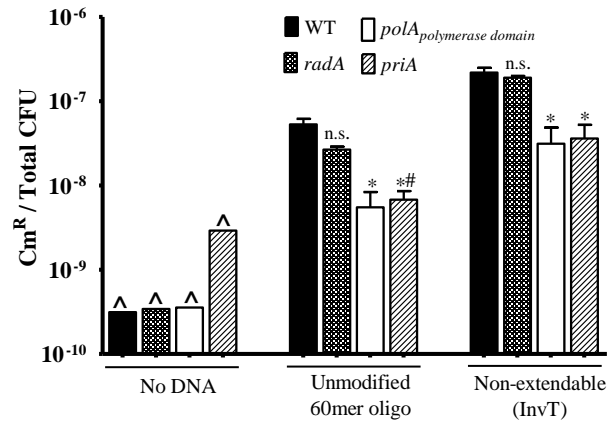


**Figure 3.7. PriA and Pol I, but not RadA, contribute to oligo mutagenesis.** Wild-type or bacteria with mutations in *radA*, *priA*, or the polymerase domain of *polA* (DNA Pol I) were electroporated with 1 nmol of the unmodified 60mer oligo or the oligo modified by 3 sequential phosphorothioate bonds at the 3' end and a 3' inverted thymidine. Values represent the mean  $\pm$  SEM of  $\geq 3$  independent experiments performed on separate days. ^, approximate limit of detection (LOD) when no recombinant colonies were obtained; #, in 1 out of 3 replicates no colonies were observed and the LOD was used in the calculation of the mean; \*, statistically significant difference from wild-type cells using the same oligo at  $\alpha = 0.05$  by two-tailed t-test with Welch's correction, where appropriate, and adjusted by Bonferroni's correction for multiple comparisons; n.s., not significant.

**Figure 3.8**

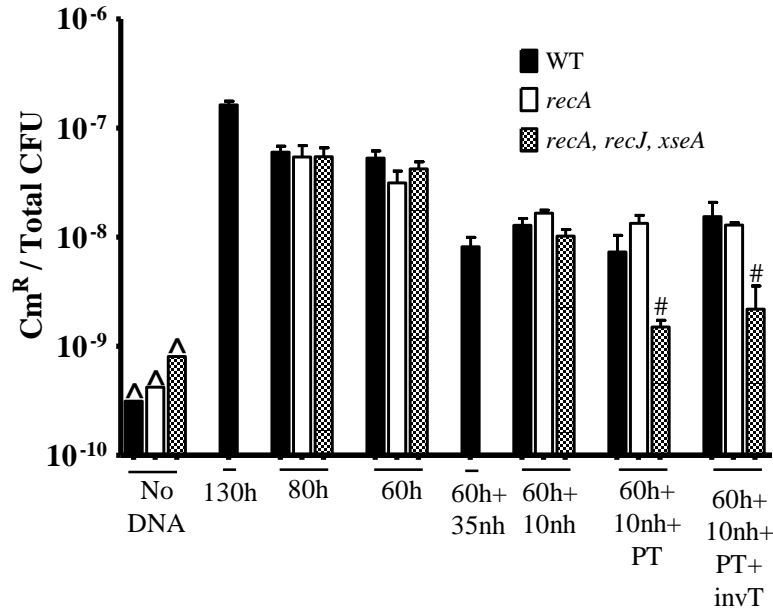


**Figure 3.8. Homologous oligos flanked by non-homologous sequences have decreased, but not abolished, mutagenic activity.** Wild-type, *recA* mutant, and *recA xseA recJ* triple mutant bacteria were electroporated with 1 nmol of the indicated oligo. Values represent the mean  $\pm$  SEM of  $\geq 3$  independent experiments performed on separate days. h, length of homologous sequence; nh, length of non-homologous sequence flanking the homologous DNA at both the 5' and 3' ends; PT, oligo was protected from nucleolytic digestion at the 3' end with 3 sequential phosphorothioate bonds; invT, oligo with a 3' inverted thymidine base; ^, approximate limit of detection (LOD) when no recombinant colonies were obtained; #, in 1 out of 3 replicates no colonies were observed and the LOD was used to calculate the mean.



**Figure 3.9**

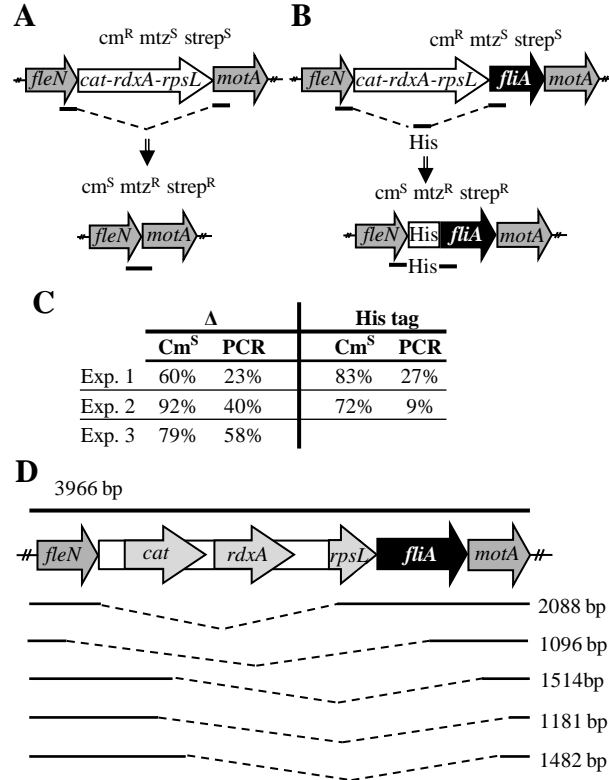


**Figure 3.9. Oligo-induced mutagenesis can be harnessed for genetic manipulation of the chromosome.** **A)** The genomic orientation and phenotype of *L. pneumophila* whose *fliA* gene is replaced by a *cat-rdxA-rpsL* selectable/counter-selectable cassette and an 84 nt oligo with homology directly flanking the *fliA* open reading frame. Excision of the cassette results in a defined markerless deletion. **B)** The genomic orientation and phenotype of *L. pneumophila* encoding the *cat-rdxA-rpsL* selectable/counter-selectable cassette at the translational start of the *fliA* gene and a 90 nt oligo with 36 nt of homology directly flanking the *fliA* open reading frame and 18 nt encoding a 6(x)His tag. **C)** The percentage of total restreaked metronidazole-resistant (Mtz<sup>R</sup>) and streptomycin-resistant (Strep<sup>R</sup>) colonies that were chloramphenicol-sensitive (Cm<sup>S</sup>), and the percentage of the Cm<sup>S</sup> clones whose deletions were confirmed by PCR in 2-3 representative experiments. **D)** Heavy line indicates position and size of PCR product of parental strain. The structure of five representative alleles from the same experiment that were chloramphenicol-sensitive and yielded PCR products of aberrant sizes as determined by DNA sequencing.

**Figure 3.10**

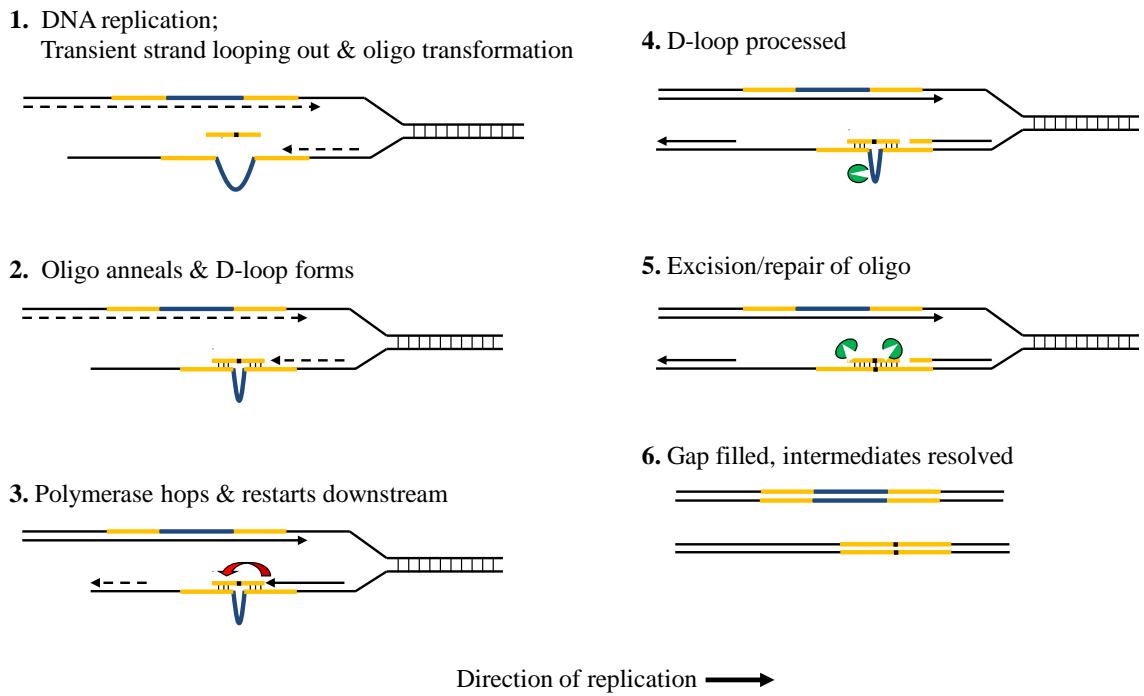


**Figure 3.10.** Strand annealing model of oligo-induced mutagenesis in *L. pneumophila* as described in the text. Yellow line with black center represents an oligo with homology to a chromosomal sequence (yellow) and a foreign sequence (black). Green Pac-Man characters indicate exonucleases or other unknown repair enzymes. Not shown are scenarios with non-homologous flanking DNA.

Figure 3.S1

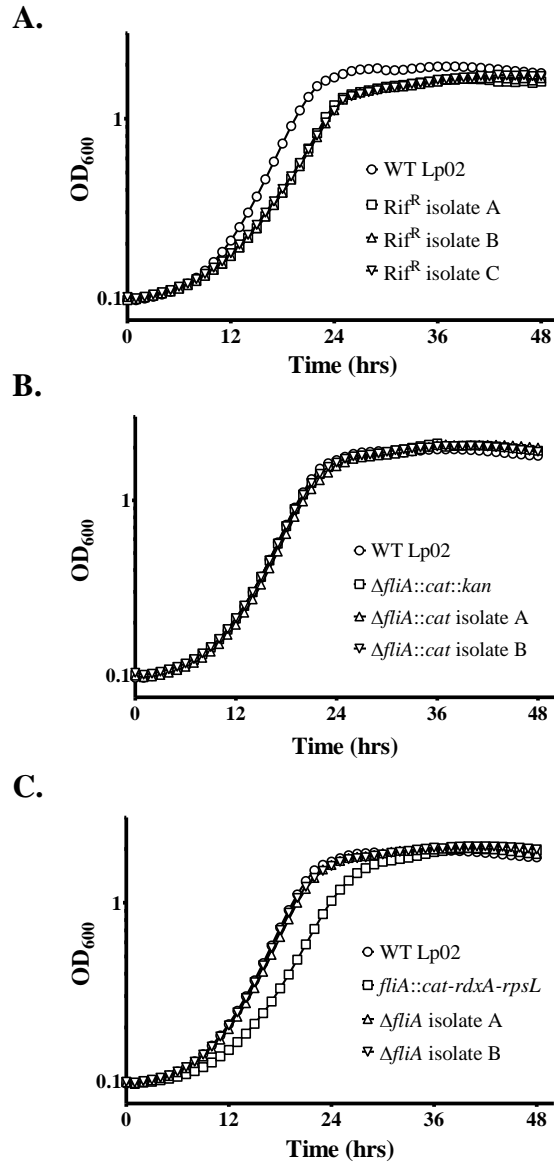


**Figure 3.S1. Growth curves of strains used in oligo mutagenesis assays and their recombinant derivatives.** Indicated strains were growth overnight in AYET, normalized, and OD<sub>600</sub> followed for 48 hours in a Bioscreen Growth Curve Analyzer. **A)** Wild-type Lp02 and three derivative rifampin resistant clones used in the point mutation assay, **B)** wild-type Lp02, *fliA::cat::kan* cells used in the large excision assay, and two derivative recombinant *fliA::cat* clones, and **C)** wild-type Lp02, *fliA::cat-rdxA-rpsL* strain used to construct the clean deletion in *fliA*, and resultant markerless deletion mutants in *fliA*. Data is representative of two independent experiments and represents the mean  $\pm$  SD of triplicate wells of a single experiment (In general, error bars are masked by time point symbols.).

**Table 3.S1. Bacterial strains and plasmids.***E. coli* and plasmids

DH5 $\alpha$	<i>supE44 <math>\Delta</math>lacU169 (80 lacZ<math>\Delta</math>M15) hsdR17 recA1 endA1 gyrA96 thi-1 relA1</i>	Laboratory collection
DY330	W3110 $\Delta$ lacU169 gal490 $\lambda$ cl857 $\Delta$ ( <i>cro-bioA</i> )	(Yu, <i>et al.</i> , 2000)
HB101	F <sup>-</sup> $\Delta$ ( <i>gpt-proA</i> )62 <i>leuB6 glnV44 ara-14 galK2 lacY1 <math>\Delta</math>(mcrC-mrr) rpsL20 (Str<sup>r</sup>) xyl-5 mtl-1 recA13</i>	(Lacks and Greenberg, 1977)
MB738	HB101 $\lambda$ pir	This work
MB739	HB101 <i>endA::frit</i>	This work
MB740	HB101 $\lambda$ pir <i>endA::frit</i>	This work
	pKD3	(Datsenko and Wanner, 2000)
	pKD4	(Datsenko and Wanner, 2000)
	pRDX	(Goodwin, <i>et al.</i> , 1998, LeBlanc, <i>et al.</i> , 2006)
	pGEM-T easy	Promega
MB442	DH5 $\alpha$ pMMB206 $\Delta$ mob	(Molofsky and Swanson, 2003)
MB741	DH5 $\alpha$ pMMBGent	This work
MB742	DH5 $\alpha$ pGEM <i>recA</i>	This work
MB743	DH5 $\alpha$ pGEM <i>recA::frit-cat-frit</i>	This work
MB744	DH5 $\alpha$ pGEM <i>recA::gent</i>	This work
MB773	DH5 $\alpha$ pGEM <i>recF</i>	This work
MB774	DH5 $\alpha$ pGEM <i>recF::frit-cat-frit</i>	This work
MB745	DH5 $\alpha$ pGEM <i>mutS</i>	This work
MB746	DH5 $\alpha$ pGEM <i>mutS::frit-cat-frit</i>	This work
MB747	DH5 $\alpha$ pGEM <i>recJ::frit-cat-frit</i>	This work
MB748	DH5 $\alpha$ pGEM <i>xseA</i>	This work
MB749	DH5 $\alpha$ pGEM <i>xseA::frit-kan-frit</i>	This work
MB750	DH5 $\alpha$ pGEM <i>fliA</i>	This work
MB751	DH5 $\alpha$ pGEM <i>fliA::frit-cat-frit</i>	This work
MB752	DH5 $\alpha$ pGEM <i>fliA::cat::kan</i>	This work
MB753	DH5 $\alpha$ pGEM <i>fliA::cat::kan</i> opposite orientation	This work
MB754	MB740 pGEM <i>fliA::cat-rdxA-rpsL</i> (cassette replacing <i>fliA</i> )	This work
MB755	MB740 pGEM <i>fliA::cat-rdxA-rpsL</i> (cassette inserted at start of FliA)	This work
MB776	HB101 $\lambda$ pir <i>endA::frit</i> , pR6K <i>catrdxArpsL</i>	This work
JW2669	BW25113 <i>recA::frit-kan-frit</i>	(Baba, <i>et al.</i> , 2006)
MB839	BW25113 <i>recA::frit</i>	This work
MB840	DH5 $\alpha$ pJB98 <i>cat::kan</i>	This work
MB841	DH5 $\alpha$ pJB98 <i>cat::kan-Opp</i>	This work
MB842	BW25113 <i>recA::frit</i> , pJB98 <i>cat::kan</i>	This work
MB843	BW25113 <i>recA::frit</i> , pJB98 <i>cat::kan</i>	This work
MB844	DH5 $\alpha$ pGEM <i>radA</i>	This work
MB845	DH5 $\alpha$ pGEM <i>radA::gent</i>	This work
MB846	DH5 $\alpha$ pGEM <i>polA</i> (polymerase domain)	This work

MB847	DH5α pGEM <i>polA</i> ( <i>polymerase domain</i> )::gent	This work
MB848	DH5α pGEM <i>priA</i>	This work
MB849	DH5α pGEM <i>priA</i> ::gent	This work

*L. pneumophila*

MB110	Lp02 wild type, <i>thyA</i> , <i>hsdR</i> , <i>rpsL</i> (Str <sup>R</sup> )	(Berger and Isberg, 1993)
MB756	Lp02 <i>recA</i> :: <i>frt-cat-frt</i>	This work
MB775	Lp02 <i>recF</i> :: <i>frt-cat-frt</i>	This work
MB757	Lp02 <i>mutS</i> :: <i>frt-cat-frt</i>	This work
MB758	Lp02 <i>recJ</i> :: <i>frt-cat-frt</i>	This work
MB759	Lp02 <i>xseA</i> :: <i>frt-kan-frt</i>	This work
MB760	Lp02 <i>recJ</i> :: <i>frt-cat-frt</i> , <i>xseA</i> :: <i>frt-kan-frt</i>	This work
MB761	Lp02 <i>fliA</i> :: <i>cat::kan</i>	This work
MB762	MB761 ( <i>fliA</i> :: <i>cat::kan</i> ), <i>recA</i> ::gent	This work
MB763	Lp02 <i>fliA</i> :: <i>cat::kan</i> opposite orientation	This work
MB764	Lp02 <i>fliA</i> :: <i>cat-rdxA-rpsL</i> (for precise deletion)	This work
MB765	Lp02 <i>fliA</i> clean deletion (MB764 cured with oligoAB201)	This work
MB766	Lp02 <i>fliA</i> :: <i>cat-rdxA-rpsL</i> (insertion at FliA start)	This work
MB767	Lp02 His-FliA (MB766 cured by oligoAB314)	This work
MB768	MB766 with 1878 bp excision (allele rdxA5)	This work
MB769	MB766 with 2870 bp excision (allele rdxA20)	This work
MB770	MB766 with 2452 bp excision (allele rdxA21)	This work
MB771	MB766 with 2785 bp excision (allele rdxA30)	This work
MB772	MB766 with 2482 bp excision (allele rdxA32)	This work
MB850	Lp02 <i>recA</i> ::gent	This work
MB851	Lp02 <i>recA</i> ::gent, pJB98-oligoAB243/4	This work
MB852	Lp02 <i>recA</i> ::gent, pJB98 <i>cat::kan</i>	This work
MB853	Lp02 <i>recA</i> ::gent, pJB98 <i>cat::kan-Opp</i>	This work
MB821	Lp02 <i>recJ</i> :: <i>frt</i> , <i>xseA</i> :: <i>frt</i>	(Bryan, <i>et al.</i> , 2011)
MB855	Lp02 <i>recJ</i> :: <i>frt</i> , <i>xseA</i> :: <i>frt</i> , <i>fliA</i> :: <i>cat::kan</i>	This work
MB856	Lp02 <i>recJ</i> :: <i>frt</i> , <i>xseA</i> :: <i>frt</i> , <i>fliA</i> :: <i>cat::kan</i> , <i>recA</i> ::gent	This work
MB857	Lp02 <i>fliA</i> :: <i>cat::kan</i> , <i>radA</i> ::gent	This work
MB858	Lp02 <i>fliA</i> :: <i>cat::kan</i> , <i>polA</i> ( <i>polymerase domain</i> )::gent	This work
MB859	Lp02 <i>fliA</i> :: <i>cat::kan</i> , <i>priA</i> ::gent	This work
MB838	DH5α λpir pR6K <i>frt-gent-frt</i>	(Bryan, <i>et al.</i> , 2011)

**Table 3.S2. Oligos used for direct mutagenesis in *L. pneumophila* and *E. coli*.**

oligoAB54	Top (+) strand, 71nt, RpoB H526Y	5' TTA TGG ATC AAG TGA ATC CAT TAT CTG GTG TTA CGT ATA AAA GAC GTG TAT CAG CTC TTG GGC CAG GTG GT 3'
oligoAB55	Bottom (-) strand, 71nt, RpoB H526Y	5' ACC ACC TGG CCC AAG AGC TGA TAC ACG TCT TTT ATA CGT AAC ACC AGA TAA TGG ATT CAC TTG ATC CAT AA 3'
oligoAB202	Bottom (-) strand, 71nt, No mutation control	5' ACC ACC TGG CCC AAG AGC TGA TAC ACG TCT TTT ATG CGT AAC ACC AGA TAA TGG ATT CAC TTG ATC CAT AA 3'
oligoAB221	Bottom (-) strand, 11nt, RpoB H526Y	5' TTT ATA CGT AA 3'
oligoAB220	Bottom (-) strand, 21nt, RpoB H526Y	5' CGT CTT TTA TAC GTA ACA CCA 3'
oligoAB219	Bottom (-) strand, 31nt, RpoB H526Y	5' ATA CAC GTC TTT TAT ACG TAA CAC CAG ATA A 3'
oligoAB203	Bottom (-) strand, 41nt, RpoB H526Y	5' AGC TGA TAC ACG TCT TTT ATA CGT AAC ACC AGA TAA TGG AT 3'
oligoAB204	Bottom (-) strand, 161nt, RpoB H526Y	5' TGT ATG TAC GTC ACG GAC TTC AAA TCC AGC CCG CTC ACG TGT TAA ACC ACC TGG CCC AAG AGC TGA TAC ACG TCT TTT ATA CGT AAC ACC AGA TAA TGG ATT CAC TTG ATC CAT AAA CTG TGA TAA CTG ACT GGA TCC AAA AAA CTC TTT AAT TGC GGC GG 3'
oligoAB253	Bottom (-) strand, 45nt, RpoB H526Y	5' AGA GCT GAT ACA CGT CTT TTA TAC GTA ACA CCA GAT AAT GGA TTC 3'
oligoAB256	Bottom (-) strand, 45nt, LNA (+), phosphorothioate (*), RpoB H526Y	5' +A*G*A* GCT GAT ACA CGT CTT TTA TAC GTA ACA CCA GAT AAT GGA* T*T*+C 3'
oligoAB243	Top (+) strand, 70nt, excise <i>kan</i> from <i>cat</i>	5' CTT TCA TTG CCA TAC GTA ATT CCG GAT GAG CAT TCA TCA GGC GGG CAA GAA TGT GAA TAA AGG CCG GAT A 3'
oligoAB244	Bottom (-) strand, 70nt, excise <i>kan</i> from <i>cat</i>	5' TAT CCG GCC TTT ATT CAC ATT CTT GCC CGC CTG ATG AAT GCT CAT CCG GAA TTA CGT ATG GCA ATG AAA G 3'
oligoAB201	Bottom (-) strand, 84nt, <i>fliA</i> precise deletion	5' CAA TCC TAT TAA AGT CAA AGT ATC CAT ACT TAT TTT GAT ACT CTC CTT ACA ATA ACA GCA GAT TGT AGT TAT TAG TAA TTT GGT 3'
oligoAB314	Bottom (-) strand, 90nt, 6(x)His-FliA	5' TTG TTG ATT TAC TTT GCT GTA TGC AGC CAA AGC ATC GTG ATG ATG ATG ATG CAC GAT ACT CTC CTT ACA ATA ACA GCA GAT TGT AGT 3'
oligoAB349	Bottom (-) strand, 31nt, No mutation control	5' ATA CAC GTC TTT TAT GCG TAA CAC CAG ATA A 3'
oligoAB350	Bottom (-) strand, 31nt, WT sequence, directly 5' to RpoB H526Y mutation	5' CGT AAC ACC AGA TAA TGG ATT CAC TTG ATC C 3'
oligoAB351	Bottom (-) strand, 31nt, WT sequence, directly 3' to RpoB H526Y mutation	5' CCT GGC CCA AGA GCT GAT ACA CGT CTT TTA T 3'
oligoAB407	Bottom (-) strand, 31nt, WT sequence, anneals in <i>lpg1846</i>	5' CCA AAG CGT AAG TTG CAT AAA TAT ACT CCA T 3'
oligoAB295	Bottom (-) strand, 44nt, excise <i>kan</i> from <i>cat</i>	5' TTC ACA TTC TTG CCC GCC TGA TGA ATG CTC ATC CGG AAT TAC GT 3'
oligoAB309	Bottom (-) strand, 60nt, excise <i>kan</i> from <i>cat</i>	5' GGC CTT TAT TCA CAT TCT TGC CCG CCT GAT GAA TGC TCA TCC GGA ATT ACG TAT GGC AAT 3'
oligoAB367	Bottom (-) strand, 80nt, excise <i>kan</i> from <i>cat</i>	5' AGT TTT ATC CGG CCT TTA TTC ACA TTC TTG CCC GCC TGA TGA ATG CTC ATC CGG AAT TAC GTA TGG CAA TGA AAG ACG GT 3'
oligoAB366	Bottom (-) strand, 130nt, excise <i>kan</i> from <i>cat</i>	5' AAG ACC GTA AAG AAA AAT AAG CAC AAG TTT TAT CCG GCC TTT ATT CAC ATT CTT GCC CGC CTG ATG AAT GCT CAT CCG GAA TTA CGT ATG GCA ATG AAA GAC GGT GAG CTG GTG ATA TGG GAT AGT GTT C 3'
oligoAB370	Bottom (-) strand, 60nt, excise <i>kan</i> from <i>cat</i> , phosphorothioate (*)	5' GGC CTT TAT TCA CAT TCT TGC CCG CCT GAT GAA TGC TCA TCC GGA ATT ACG TAT GGC* A*A*T 3'
oligoAB382	Bottom (-) strand, 60nt, excise <i>kan</i> from <i>cat</i> , phosphorothioate (*), 3' PO <sub>4</sub> <sup>-</sup>	5' GGC CTT TAT TCA CAT TCT TGC CCG CCT GAT GAA TGC TCA TCC GGA ATT ACG TAT GGC* A*A*T-PO <sub>4</sub> <sup>-</sup> 3'

oligoAB383	Bottom (-) strand, 60nt, excise <i>kan</i> from <i>cat</i> , phosphorothioate (*), 3' ddC	5' GGC CTT TAT TCA CAT TCT TGC CCG CCT GAT GAA TGC TCA TCC GGA ATT ACG TAT GGC* A*A*T-ddC 3'
oligoAB369	Bottom (-) strand, 60nt, excise <i>kan</i> from <i>cat</i> , phosphorothioate (*), 3' invT	5' GGC CTT TAT TCA CAT TCT TGC CCG CCT GAT GAA TGC TCA TCC GGA ATT ACG TAT GGC* A*A*T-invT 3'
oligoAB360	Bottom (-) strand, 60nt, excise <i>kan</i> from <i>cat</i> , 5' PO <sub>4</sub> <sup>-</sup>	5' PO <sub>4</sub> <sup>-</sup> -GGC CTT TAT TCA CAT TCT TGC CCG CCT GAT GAA TGC TCA TCC GGA ATT ACG TAT GGC AAT 3'
oligoAB380	Bottom (-) strand, 60nt, excise <i>kan</i> from <i>cat</i> , phosphorothioate (*)	5' G*G*C* CTT TAT TCA CAT TCT TGC CCG CCT GAT GAA TGC TCA TCC GGA ATT ACG TAT GGC AAT 3'
oligoAB381	Bottom (-) strand, 60nt, excise <i>kan</i> from <i>cat</i> , phosphorothioate (*), 5' PO <sub>4</sub> <sup>-</sup>	5' PO <sub>4</sub> <sup>-</sup> -G*G*C* CTT TAT TCA CAT TCT TGC CCG CCT GAT GAA TGC TCA TCC GGA ATT ACG TAT GGC AAT 3'
oligoAB365	Bottom (-) strand, 60nt, excise <i>kan</i> from <i>cat</i> , plus 10nt non-homologous	5' AGT AGG TAC GGG CCT TTA TTC ACA TTC TTG CCC GCC TGA TGA ATG CTC ATC CGG AAT TAC GTA TGG CAA TTG CAT CAG TC 3'
oligoAB368	Bottom (-) strand, 60nt, excise <i>kan</i> from <i>cat</i> , plus 35nt non-homologous	5' AGC TGA TAG CAT ATT GAC CTG ACC ATA AGT AAC TAG GCC TTT ATT CAC ATT CTT GCC CGC CTG ATG AAT GCT CAT CCG GAA TTA CGT ATG GCA ATG CGT AGA TCG ATC GAC GAA TTA GCA GCC TAC GAT C 3'
oligoAB378	Bottom (-) strand, 60nt, excise <i>kan</i> from <i>cat</i> , plus 10nt non-homologous, phosphorothioate (*)	5' AGT AGG TAC GGG CCT TTA TTC ACA TTC TTG CCC GCC TGA TGA ATG CTC ATC CGG AAT TAC GTA TGG CAA TTG CAT CA*G* T*C 3'
oligoAB379	Bottom (-) strand, 60nt, excise <i>kan</i> from <i>cat</i> , plus 10nt non-homologous, phosphorothioate (*), 3' invT	5' AGT AGG TAC GGG CCT TTA TTC ACA TTC TTG CCC GCC TGA TGA ATG CTC ATC CGG AAT TAC GTA TGG CAA TTG CAT CA*G* T*C-invT 3'

**Table 3.S3. Oligos used for strain construction.**

oligoAB13	gent R into p206	5' ACC CGG CAT TCG CTG CGC TTA TGG CAG AGC AGG GAA CGG CTT GAA CGA ATT GT 3'	Replace <i>cat</i> with <i>aacC1</i> in pMMB206 to construct pMMBGent
oligoAB31	gent F into p206	5' TCG GTG AAC GCT CTC CTG AGT AGG ACA AAT CCG CCG GAT GAA GGC ACG AAC CCA GTT G 3'	
oligoAB190	E coli endA P0	5' TTC GCT ACG TTG CTG GCT CGT TTT AAC ACG GAG TAA GTG TGT GTA GGC TGG AGC TGC TTC 3'	Construction of <i>endA::frit</i> allele in <i>E. coli</i>
oligoAB191	E coli endA P2	5' GTG GGG TAG GGG TTA ACA AAA AGA ATC CCG CTA GTG TAG GCA TAT GAA TAT CCT CCT TAG TTC CT 3'	
oligoAB193	E coli endA F ck	5' CCG GAG CCA AAA CTC TCT TAC AC 3'	
oligoAB194	E coli endA R ck	5' CTC ACA GGC AGC AAT TGC AAT C 3'	
oligoAB209	recA 500 bp 5' F	5' CGA ATT AGC CTA TGA ATC GGC AC 3'	Amplification of <i>recA</i> to construct pGEM <i>recA</i>
oligoAB210	recA 500 bp 3' R	5' GAA GCT ACT ATT TGA TGA CCG CG 3'	
oligoAB213	recA P0	5' TGA ACG CCA ATT TGG CAA AGG GTC TGT AAT GCG TAT GGG TGT GTA GGC TGG AGC TGC TTC 3'	Deletion of <i>recA</i> by recombineering to construct pGEM <i>recA::frit-cat-frit</i>
oligoAB214	recA P2	5' CTC GCG CCT GGT TAA CAG ACG CAA GGC GCT ATC GAA TGC TCA TAT GAA TAT CCT CCT TAG TTC CT 3'	
oligoAB315	recA-gent F	5' GAA CGC CAA TTT GGC AAA GGG TCT GTA ATG CGT ATG GGG ATG AAG GCA CGA ACC CAG TTG 3'	Deletion of <i>recA</i> by recombineering to construct pGEM <i>recA::gent</i>
oligoAB316	recA-gent R	5' GCG CCT GGT TAA CAG ACG CAA GGC GCT ATC GAA TGC TCG GCT TGA ACG AAT TGT TAG GTG 3'	
oligoAB263	recF 500 bp 5' F	5' GAA TGG CTA TAT CGC GAT ATT CCT G 3'	Amplification of <i>recF</i> to construct pGEM <i>recF</i>
oligoAB264	recF 500 bp 3' R	5' GAC AGG AAT ACC ACG ACC ATC ATC 3'	
oligoAB271	recF P0	5' GAT AAT TAT CAA TAC ATT ATT ATG CCT ATG AAA ATA TGA TGT GTA GGC TGG AGC TGC TTC 3'	Deletion of <i>recA</i> by recombineering to construct pGEM <i>recF::frit-cat-frit</i>
oligoAB272	recF P2	5' TCC ATT AAT TTG TGT TCC ACG TGA AAC ATT CTA TAC ATA TGA ATA TCC TCC TTA GTT CCT 3'	
oligoAB211	mutS 500 bp 5' F	5' CTT CAA CCA GTA TTG AGA AAT GAC CC 3'	Amplification of <i>mutS</i> to construct pGEM <i>mutS</i>
oligoAB212	mutS 500 bp 3' R	5' GCA TAA GGT TGG CCA GGA TC 3'	
oligoAB215	mutS P0	5' TAT TGT TTT CAT AAA AAT CAA TAC CAC CAA CAT GCC TTA TGT GTA GGC TGG AGC TGC TTC 3'	Deletion of <i>mutS</i> by recombineering to construct pGEM <i>mutS::frit-cat-frit</i>
oligoAB216	mutS P2	5' GTA ATA ACT ACA TCA ATT GAT GCT CTC GGC ACA CTC CAG GCA TAT GAA TAT CCT CCT TAG TTC CT 3'	



oligoAB267	recJ 500 bp 5' F	5' GGT TCG ATT TGT ATT CTG CCT ATT TAG 3'	Construction by overlap-extension PCR of <i>recJ::frt-cat-frt</i>
oligoAB268	recJ 500 bp 3' R	5' GCT TAT CAC AAC CTG CTT CAA CC 3'	
oligoAB277	recJ R 5'fuseP0	5' GAA GCA GCT CCA GCC TAC ACA TTA ATC AGC ATG CGT CAG ACT TC 3'	
oligoAB278	recJ F P0fuse3'	5' GAA GTC TGA CGC ATG CTG ATT AAT GTG TAG GCT GGA GCT GCT TC 3'	
oligoAB279	recJ R 3'fuseP2	5' ATC CTA TGA TTA GGC CAG GAT TTT AAA TCC ATA TGA ATA TCC TCC TTA GTT CCT 3'	
oligoAB280	recJ F P2fuse3'	5' AGG AAC TAA GGA GGA TAT TCA TAT GGA TTT AAA ATC CTG GCC TAA TCA TAG GAT 3'	
oligoAB265	<i>xseA</i> 500 bp 5' F	5' GCG CCT CAG TAA GGT ATT GG 3'	Amplification of <i>xseA</i> to construct pGEM <i>xseA</i>
oligoAB266	<i>xseA</i> 500 bp 3' R	5' GAA TGC GGA TCT CTT GGC TG 3'	
oligoAB273	<i>xseA</i> P0	5' ATT GCC AAT ACT GAC CGT GAG TCA GCT GAA TAG ACA AGT TGT GTA GGC TGG AGC TGC TTC 3'	Deletion of <i>xseA</i> by recombineering to construct pGEM <i>xseA::frt-kan-frt</i>
oligoAB274	<i>xseA</i> P2	5' ACC TCA CAA GCA AGA CTT CCT TTT GCT AAA CGG ACC ATA TGA ATA TCC TCC TTA GTT CCT 3'	
oligoAB64	<i>fliA</i> 500 bp 5' F	5' TGA TGA TTT GGA CTA TAT GAT TAT TGA TAC CGC 3'	Amplification of <i>fliA</i> to construct pGEM <i>fliA</i>
oligoAB65	<i>fliA</i> 500 bp 3' R	5' CCC AAC ACC GCA CCT AAA ATT C 3'	
oligoAB149	<i>fliA</i> P0	5' CTA ATA ACT ACA ATC TGC TGT TAT TGT AAG GAG AGT ATC TGT GTA GGC TGG AGC TGC TTC 3'	Deletion of <i>fliA</i> by recombineering to construct pGEM <i>fliA::frt-cat-frt</i>
oligoAB150	<i>fliA</i> P2	5' CAA TCC TAT TAA AGT CAA AGT ATC CAT ACT TAT TTT CAT ATG AAT ATC CTC CTT AGT TCC 3'	
oligoAB241	<i>kan</i> into <i>cat</i> F	5' AGT TTT ATC CGG CCT TTA TTC ACA TTC TTG CCC GCC TGA TTA TGG ACA GCA AGC GAA CCG 3'	Insertion of <i>kan</i> into <i>cat</i> to construct pGEM <i>fliA::cat::kan</i>
oligoAB242	<i>kan</i> into <i>cat</i> R	5' CGT CTT TCA TTG CCA TAC GTA ATT CCG GAT GAG CAT TCT CAG AAG AAC TCG TCA AGA AGG 3'	
oligoAB310	<i>fliA-cat::kan</i> opp F	5' CAA CAA TCC TAT TAA AGT CAA AGT ATC CAT ACT TAT TTT TGT GTA GGC TGG AGC TGC TTC 3'	Deletion of <i>fliA</i> by <i>cat::kan</i> to construct pGEM <i>fliA::cat::kan</i> opposite orientation
oligoAB311	<i>fliA-cat::kan</i> opp R	5' ATA ACT ACA ATC TGC TGT TAT TGT AAG GAG AGT ATC CAT ATG AAT ATC CTC CTT AGT TCC 3'	
oligoAB234	<i>cat</i> F	5' TGT GAC GGA AGA TCA CTT CG 3'	Construction by overlap-extension PCR of <i>fliA::cat-rdxA-rpsL</i>
oligoAB235	<i>catR</i> fuse <i>rdxA</i>	5' CTG CCC CAT GCT CAA ATT GCC CTG CCA CTC ATC GCA GTA C 3'	
oligoAB236	<i>rdxA</i> F fuse <i>cat</i>	5' GTA CTG CGA TGA GTG GCA GGG CAA TTT GAG CAT GGG GCA G 3'	
oligoAB237	<i>rdxA</i> R fuse <i>rpsL</i>	5' CGA AAT TTG ACC AGT CAA ACC GCG TCA CAA CCA AGT AAT CGC ATC AAC 3'	
oligoAB238	<i>rpsL</i> F fuse <i>rdxA</i>	5' GTT GAT GCG ATT ACT TGG TTG TGA CGC GGT TTG ACT GGT CAA ATT TCG 3'	

oligoAB113	rpsL R	5' TTA AGC CTT AGG ACG CTT CAC G 3'	
oligoAB239	fliAup R fuse all	5' TAT TTA TTC TGC GAA GTG ATC TTC CGT CAC AGA TAC TCT CCT TAC AAT AAC AGC AGA TTG 3'	
oligoAB240	fliAdown R fuse all	5' GGC GTG AAG CGT CCT AAG GCT TAA AAA ATA AGT ATG GAT ACT TTG ACT TTA ATA GGA TTG 3'	

oligoAB296	fliA insert start F	5' AAT AAC TAC AAT CTG CTG TTA TTG TAA GGA GAG TAT CGT GTG TGA CGG AAG ATC ACT TCG 3'	Insertion at start of FliA to construct pGEM <i>fliA::cat-rdxA-</i> <i>rpsL</i> start
oligoAB297	fliA insert start R	5' GGG TTT GTT GAT TTA CTT TGC TGT ATG CAG CCA AAG CAT CTT AAG CCT TAG GAC GCT TCA 3'	

oligoAB281	radA 500 bp 5' F	5' TCA CCA ACC AGT GTT TGT GG 3'	Amplification of <i>radA</i> to construct pGEM <i>radA</i>
oligoAB282	radA 500 bp 3' R	5' CTC CTG CAA ACT TCC TTC AGG 3'	

oligoAB386	radA P0	5' AAA TGT ACT AAA TAA AAT GCT TGA ATC AAG GCA AAA ATT TGT GTA GGC TGG AGC TGC TTC 3'	Deletion of <i>radA</i> by recombineering to construct
oligoAB387	radA P2	5' CGT AAA CTT GAA ATC ACT GCA GCC AAC AAA GCC AAA CAT ATG AAT ATC CTC CTT AGT TCC 3'	pGEM <i>radA::frt-gent-frt</i>

oligoAB261	polA(pol) 500 bp 5' F	5' GCA TCT CTT TAG CAG TTG AGG AAG 3'	Amplification of <i>polA</i> (polymerase) to construct
oligoAB262	polA(pol) 500 bp 3' R	5' GTT CGC ACA TTA TAC TTC TCT CGT AG 3'	pGEM <i>polA</i> (polymerase domain)

oligoAB270	polA(pol) P0	5' TTA TTA TTA AAT CCA ATA AAT TAA ACG CTT TTA TGC GCT TGT GTA GGC TGG AGC TGC TTC 3'	Deletion of <i>polA</i> by recombineering to construct
oligoAB269	polA(pol) P2	5' CTG TTC TCG CAG ACA TGG AAA TGC ACG GCG TTC TCC ATA TGA ATA TCC TCC TTA GTT CCT 3'	pGEM <i>polA</i> (polymerase domain):: <i>gent</i>

oligoAB395	priA 500 bp 5' F	5' CGA GTG AAA TGG GAG AGC TAT TC 3'	Amplification of <i>priA</i> to construct pGEM <i>priA</i>
oligoAB396	priA 500 bp 3' R	5' CGC TCC AAC CCC TAT CGA CAT G 3'	

oligoAB401	priA P0	5' CCC GGC CAA TCA GCG AGT CAT GAA TGG CTT AGA AGT TAA TGT GTA GGC TGG AGC TGC TTC 3'	Deletion of <i>priA</i> by recombineering to construct pGEM <i>priA::frt-gent-frt</i>
oligoAB402	priA P2	5' TTG CAT CCT ATG CTG GTT AGC TTT TCG TGG TAA AGG CAT ATG AAT ATC CTC CTT AGT TCC 3'	

## CHAPTER FOUR

### Discussion

#### Genetic engineering of *L. pneumophila* and beyond

A central theme of my thesis is the development of genetic engineering tools for *L. pneumophila*, especially strategies for the generation of unmarked mutations. Specifically, I demonstrate that synthetic oligonucleotides can delete or incorporate sequences when electroporated (Chapter 3); the Flp recombinase can be harnessed for construction of unmarked deletions in *L. pneumophila* (Chapter 2); and improved counter-selection tools can be coupled with more traditional methods of over-lap extension PCR (Appendix B). Some of these tools would need little or no modification for application to other species. Like all methods, including traditional methods of restriction enzyme-based cloning and allelic exchange, each of these methods has particular advantages and caveats.

Prior to incorporating a resistance cassette into the *L. pneumophila* chromosome, a recombinant allele must be constructed either *in vitro* or *in vivo* using recombineering in *E. coli*. The only way to circumvent this step is to use *in vivo* transposon mutagenesis, which results not in any sequence deletion, but only insertion of the resistance cassette. The goal of allele construction is to include sufficient flanking homology to direct a cassette to undergo RecA-mediated recombination at the desired sequence. Particular

regions can be targeted either by *in vitro* transposon mutagenesis, restriction enzyme-based cloning (whether constructing a simple insertion or an insertion-deletion allele), over-lap extension PCR, or recombineering in *E. coli*. Since *L. pneumophila* undergoes natural transformation with linear DNA, allelic exchange vectors are only needed to construct unmarked deletions by traditional methods. Transposon mutagenesis, though well established, has the disadvantage that no native sequences are deleted, and thus risks polar effects or incomplete gene inactivation. Restriction enzyme-based cloning can be used to delete native sequence, is well established, and only requires basic molecular biology training; however, it requires existence of convenient restriction sites or incorporation of new ones. Therefore, reliance on restriction sites complicates design of precise deletions at the exact nucleotides desired, including construction of in-frame deletions. Using over-lap extension PCR, alleles can be constructed at the precise nucleotides desired by primer design. The technique is also theoretically the fastest method, since recombinant alleles can be constructed by two sequential PCR steps in a single day. A significant drawback, however, is that many experimentalists have difficulty assembling the recombinant allele reproducibly: What may theoretically be faster, often results in a troubleshooting delay. In Chapter 2, I propose the use of recombineering in *E. coli* to construct recombinant alleles. Although this method can take extra time, due to the *in vivo* construction in a recombineering-proficient *E. coli* strain (e.g. DY330), followed by purification in a standard cloning strain (e.g. DH5 $\alpha$ ), recombineering has distinct advantages. Chiefly, it allows the investigator to design the allele to the precise nucleotides desired, and it is extremely efficient. That is, hundreds or thousands of recombinant clones are often obtained, and, once the method has been

established in a laboratory, the desired allele is achieved on the first try in nearly every attempt.

After construction of a recombinant allele, all of the methods we employ and have recently used in the laboratory involve natural transformation to introduce the resistance cassette into the chromosome of *L. pneumophila* at some point in the procedure.

Exploiting natural competence is usually chosen out of convenience, but electroporation of constructs should also produce the same results. In fact, electroporation and RecA-dependent recombination may not require circular DNA, since *L. pneumophila* lacks RecBCD, which contribute to the degradation of linear DNA. Other methods of transformation, appropriate for other species, could also supplant the use of natural transformation as used for *Legionella*. Previous work on natural transformation studied optimal conditions (Sexton and Vogel, 2004, Stone and Kwaik, 1999). I have improved existing protocols by utilizing broth grown cells instead of patches on solid medium to increase the proportion of replicating cells—a requirement for natural transformation. Since stationary phase cells also undergo higher frequencies of spontaneous mutation (Figs 2.S1, 3.2, data not shown), use of replicating cultures also reduces the number of undesired mutational events. I also suggest that PCR products are preferred for natural transformation, because even though their transformation frequency is lower than that obtained with circular molecules, nearly all recombinant clones have the desired mutation. Indeed, one of my engineering principals is that, even if a new method does not decrease the total number of days needed to construct a recombinant allele, the technology should increase efficiency. In particular, I aim to decrease the amount of

clone screening required while also increasing the percentage of the time the desired allele is obtained on the first attempt.

After allele construction, natural transformation, and colony purification, a mutant strain that has been isolated can be used to test hypotheses. However, a residual resistance cassette at the engineered locus has several drawbacks. Foremost for laboratory studies is the increased risk of polar effects on downstream genes. Additionally, in *L. pneumophila* and many other species, few resistance cassettes are available for construction, which limits the ability of the investigator to construct multiple deletion mutants or introduce plasmids. Leaving cassettes in a strain also limits downstream applications, since such strains are unethical for use in attenuated live vaccines or environmental applications, such as oil spill clean-up. Therefore, to circumvent problems caused by residual drug resistance markers, several strategies for removing the cassettes from the host strain have been developed.

Traditionally, one of the most common methods to remove resistance cassettes has been to employ allelic exchange vectors with counter-selectable markers. Vectors are constructed with a desired recombinant allele, and once introduced into the chromosome, a merodiploid is obtained using a selectable marker. The strain is then grown under conditions for negative selection of the vector, typically sucrose- or streptomycin-resistance, which then enriches for clones that have undergone a second recombination event. At some frequency, either the native or recombinant allele remains in the chromosome, and the other allele is excised. The frequency of marker loss can vary dependent on vector and species, and thus can occur with reasonable frequency or be

fairly inefficient; another complication is the high spontaneous mutation frequency in most counter-selectable alleles. To circumvent the problems associated with spontaneous point mutations in the counter-selectable marker, I have constructed a suicide vector containing a double counter-selectable cassette (pR6K $\gamma$ *cat-rdxA-rpsL*, Chapter 3) flanked by recommended priming sites and restriction sites.

Since *L. pneumophila* is naturally transformable, the use of the *cat-rdxA-rpsL* cassette is not limited to traditional allelic exchange, however. In Appendix B, for example, I constructed an in-frame mutation in *lpg0273* by first cloning the region flanking the gene and replacing the gene with the *cat-rdxA-rpsL* cassette by recombineering. I have constructed *E. coli* strains for the maintenance of the plasmid (HB101 $\lambda$ *pir endA::FRT*) and the rescue of subclones containing the cassette (HB101 *endA::FRT*) that allow for phenotypic verification of the counter-selectable markers. Once a double counter-selectable allele is constructed and introduced into *L. pneumophila* by natural transformation, a second recombinant allele made by over-lap extension PCR that contains a precise deletion is introduced to *L. pneumophila*; finally, desired in-frame mutant cells are selected on streptomycin- and metronidazol-containing plates. Compared to previous methods, this strategy eliminates the need to construct the more problematic three fragment product by over-lap extension, and it reduces the occurrence of spontaneous mutants which make screening clones more cumbersome.

To eliminate the need for allelic exchange vectors and over-lap extension PCR, phage-based recombination can be exploited to remove resistance cassettes using a synthetic oligo. This strategy is efficient and allows precise deletions by oligo design; on

the other hand it is limited to species that support the method, requires expression of the phage genes, and still relies on a counter-selectable cassette. While *L. pneumophila* does not have a phage recombinase system, the double counter-selectable cassette I designed may have applications in other species, where it could reduce the frequency of spontaneous mutants.

To harness oligos to remove chromosomal cassettes conveniently, but to eliminate the need for the mutant strain to express a phage recombinase, for the first time I describe a strategy of constructing unmarked deletions that appears to depend on conserved replication and repair machinery, but is RecA-independent (Chapter 3). Although this approach is in its infancy and is currently not very efficient, it perhaps has the greatest potential for genetic engineering. Removal of a cassette does not require expression of any exogenous genes; instead, one merely orders a synthetic oligo of desired sequence and transfers it to the bacterial strain by electroporation. Because oligo mutagenesis relies on conserved machinery, it could also be applied to organisms with fewer genetic tools. The method's drawbacks are its low efficiency and reliance on counter-selection. Future work focusing on increasing efficiency and decreasing occurrence of large spontaneous deletions (Fig. 3.9) could make this a future method of choice. The ultimate goal would be to apply this technology for the initial introduction of cassettes, thereby eliminating the need for RecA-dependent incorporation of cassettes into the chromosome.

Motivated by the desire to circumvent the difficulties associated with allelic exchange vectors and counter-selectable cassettes, the last decade has seen a significant rise in the use of site-specific recombinases to excise cassettes. By flanking cassettes



with short *FRT* recognition sequences, the Flp recombinase can excise the intervening sequence. This results in a small ‘scar’ sequence left by the *FRT* site and priming sequences. Therefore, the method may not be ideal for certain applications, although it eliminates the resistance cassette and associated risks of polarity. Another disadvantage is that Flp must be expressed in the desired host strain, usually followed by removal of the expression vector, which demands extra steps. Significant advantages, however, are that Flp is highly active in a large number of species and, once expressed, nearly all *FRT*-flanked cassettes are excised—limiting the amount of clone screening needed. I apply this strategy to *L. pneumophila* in Chapter 2 and, when coupled with recombineering in *E. coli* or over-lap extension PCR for initial allele construction, is my current method of choice for the construction of unmarked deletions in *L. pneumophila*.

### **Oligo-induced mutagenesis**

In Chapter 3, I described the ability of short oligonucleotides to alter the chromosome of *L. pneumophila*, which I applied for engineering, as discussed above, while also striving to understand its underlying mechanism. During the course of my thesis, oligo-induced mutagenesis was also observed in four other species, but was assumed to occur by a mechanism similar to  $\lambda$  Red recombination (Swingle, *et al.*, 2010b). I expanded knowledge of oligo mutagenesis by showing that it occurs in *L. pneumophila* and is a distinct process from previously described mechanisms. A model for oligo-induced mutagenesis in *L. pneumophila* was also proposed (Fig. 3.10). Modifying the annealing/integration model for  $\lambda$  Red recombination (Fig. 1.1), I propose

that oligo mutagenesis does not require direct polymerase extension; rather replication re-start occurs, and the oligo may not be physically incorporated, depending on the end repair processes that resolve the intermediates (Fig 3.10). Several aspects of this model remain to be elucidated, however.

One lingering question is how the D-loop is excised and the remaining gap is filled in using the oligo as a template. The cell has many endonucleases that could be involved in processing of the D-loop intermediate, but perhaps the most likely is nucleotide excision repair (NER). NER is universally present throughout the Bacterial Domain, as well as having analogous systems in both Archaea and Eukaryotes, and thus would be consistent with the observed conservation of oligo mutagenesis (Bryan and Swanson, 2011, Snyder and Champness, 2007a, Swingle, *et al.*, 2010b). A UvrA-B complex binds to undamaged DNA, where it migrates and can detect helix distortions from damaged DNA or unpaired bases. Once a lesion is detected, UvrC associates with the complex and cleaves 8 nucleotides 5' of the damage and 4 nucleotides 3' of the damage (Zou and Van Houten, 1999). This endonuclease activity could excise the D-loop while leaving sufficient overlapping sequence for pairing of the oligo to both the 5' and 3' ends of the chromosomal strand. DNA Pol I could then fill in the gap left by the excised D-loop using the oligo as a template (Fig 3.7; Snyder and Champness, 2007a). The fact that UvrC cleaves a strand further from the damage at the 5' end is consistent with the observation that nuclease protection of oligos at the 3' end yields a more substantial increase in mutation frequency compared with protection of the 5' end (Fig 3.5 vs. Fig 3.6). That is, there is less disposable DNA at the 3' end of an oligo, since it

needs to be maintained for sufficient base-pairing following NER. The role of NER in oligo mutagenesis could easily be tested by construction of an isogenic *uvrA* mutation, since UvrA is absolutely required for NER. Alternate repair processes, such as base excision repair, or other uncharacterized endonucleases could also play a role in excising D-loops; however, many of these pathways repair more specific lesions or are less well conserved between species and therefore are less likely to play a role in oligo mutagenesis than NER.

Yet another aspect of future investigation could be to further understand the role(s) of DNA polymerase(s) in the continuation of nascent strand synthesis following replisome collision with the annealed oligo and the post-replication repair process. The model dictates that the advancing replicative polymerase encounters the annealed oligo, hops/slips over the oligo, and re-starts downstream, as suggested by PriA dependence (Fig 3.7) and increase in mutation frequency with non-extendable oligos (Fig 3.5). The low, but observable, frequency of large deletions enriched for by strong selective pressure, even in the absence of oligo (Fig 3.9D), suggests that annealed homologous DNA may increase the propensity of a deletion event, but is not absolutely required. These observations can all be accounted for by strand slippage by DNA Pol III, as has been suggested by RecA-independent tandem repeat deletions in *E. coli* (Bierne, *et al.*, 1997). To substantiate the evidence that DNA Pol III slippage leads to the observed deletions both with and without oligo, an *E. coli dnaE486* mutant could be tested in the oligo assay (Fig 3.4A), as it has been observed to decrease polymerase fidelity and increase RecA-independent homologous recombination deletion events (Bierne, *et al.*,

1997). Alternatively, or in conjugation with Pol III slippage, it is possible that the translesion polymerases could be involved in circumventing the annealed oligo or in its subsequent repair. As there may be redundancy in translesion synthesis, if phenotypes are not revealed with single mutations, double or triple mutants in Pol IV and Pol V could be analyzed (compared to *E. coli*, *L. pneumophila* appears to have two copies of Pol V, Table 1.1).

In addition to their important polymerase activity, the DNA polymerases could also have a role in repair or excision of the oligo following D-loop processing. The observation that nuclease protection of oligos at the 5' end lead to a decrease in mutation frequency suggests processing of the 5' end is important. The data suggest that the RecJ and/or XseA nuclease(s) contribute to excision of the annealed oligo, since when oligos were protected by phosphorothioate bonds and examined in the nuclease mutant, only a low mutation frequency was observed (Fig 3.6). However, RecJ and XseA are unlikely to be the only nucleases involved in excision/repair since the mutation frequency was not abolished in the double mutant and since unprotected oligos facilitated the same mutation frequency in both wild-type and nuclease mutant cells (Fig 3.6). A likely culprit, then, could be the 5' to 3' exonuclease activity of DNA Pol I, which is normally involved in excision of RNA primers during lagging strand synthesis. Following slippage of DNA Pol III over the annealed oligo, the 5' to 3' exonuclease activity of DNA Pol I could act in conjunction with RecJ and/or XseA to digest the oligo, while the 3' to 5' polymerase activity fills in the gap. Since the 5' to 3' exonuclease domain of Pol I is essential, it would have to be tested in *E. coli* using the appropriate temperature sensitive alleles. In

the less likely scenario that oligos are excised from the 3' end despite potent nuclease-resistant modifications, the 3' to 5' exonuclease activity of Pol I or DnaQ (the 3' to 5' proofreading activity of the Pol III holoenzyme) could facilitate oligo excision. By examining both the polymerase and exonuclease activity of the DNA polymerases, in addition to testing a possible contribution of nucleotide excision repair, a more complete model of oligo-induced mutagenesis could be developed.

### **Alternative models of oligo mutagenesis**

As I have outlined in Chapter 3 and above, I believe the annealing model of oligo mutagenesis is the most likely scenario that explains my results. It is important, however, to consider alternatives. I therefore explore a different model of oligo mutagenesis, modified from another precedent in the  $\lambda$  literature (Poteete, 2008) that suggests that the annealing/integration  $\lambda$  model may not hold as well for recombination that involves the deletion/insertion of large DNA sequences. In particular, it is difficult to imagine how the hydrogen bonding of ~35 nt of homology flanking a ~1 kb cassette sufficiently stabilize a D-loop against the structural forces in the helix needed for recombination to occur. Specifically, Poteete proposed that the Beta protein facilitates annealing of the donor DNA to the lagging strand during replication, but leaves the 3' end of the donor not fully annealed. The advancing replisome from the leading strand could then switch templates, jumping from the chromosomal template to the free 3' end of the donor DNA, thus incorporating the oligo sequence into the nascent strand. Although many of

mechanistic details are not resolved, this model need not invoke the steric limitations that the annealing/integration model entails.

A modification of the template switch model for  $\lambda$  is consistent with the results presented in this thesis (Fig. 4.1). DNA replication exposes the leading and lagging strands while the oligo is transformed. The 5' end of the oligo anneals to the appropriate sequence on the lagging strand, while the 3' terminus remains free, avoiding the need to invoke complete formation of a sterically limited D-loop. During replication from the leading strand, DNA polymerase then switches templates, re-starting on the 3' end of the oligo. After replicating the sequence of the oligo, the replisome undergoes a second template switch to resume replication from chromosomal DNA. Nucleases then digest the intervening sequences not replicated, and single-strand gaps are filled. Data supporting physical annealing and strand bias are also consistent with this model (Figs 3.1, 3.2, 3.4, 3.5; Swingle, *et al.*, 2010b), due to availability of ssDNA on each strand and advancement of polymerases. RecA-independent template switching may, but need not, require PriA for re-start, depending on the experimental system (Dutra and Lovett, 2006, Ozgenc, *et al.*, 2005). Consistent with our data, inactivation of single-stranded exonucleases increases the frequency of mutations from template switching (Dutra and Lovett, 2006). Also consistent with our results is that single-stranded gap filling by DNA Pol I could contribute to this proposed mechanism. An observation that possibly refutes the model is the lack of incorporation of non-homologous DNA (Fig. 3.8); a template switch process may be more promiscuous to replicating and incorporating non-homologous DNA from the donor. Our assay, however, demands rescue of

chloramphenicol resistance, and in-frame insertions of 1-10 amino acids encoded by our non-homologous oligos (Fig. 3.8) may inhibit the enzyme activity of chloramphenicol acetyltransferase (Cat). Due to the contributions of PriA and results showing no incorporation of non-homologous DNA, our data fit the strand annealing model slightly better than the template switch model, but not conclusively so. As such, future work may help distinguish the two.

Distinguishing the single-stranded annealing (Fig. 3.10) and template switch (Fig 4.1) models of oligo mutagenesis would be difficult, given that many of the same components are invoked for not only both mechanisms, but also other aspects of replication and repair. Genetic tests of the contribution of different genes would also be limited in *L. pneumophila*, since many of the proposed processes are essential—although some could be tested in *E. coli* using temperature sensitive alleles, assuming the contribution is the same in the two organisms. Template switching with DNA repeats has been shown to partially depend on the DnaK chaperone, possibly by remodeling the replisome (Goldfless, *et al.*, 2006). Mutations in *dnaK* would likely be pleiotropic, but may help differentiate the two models. Another difference between the two models is the prediction of differing frequencies of incorporating non-homologous sequences. The counter-selection system in Figure 3.9 could be used to test non-homologous incorporation, but data from such experiments would be very indirect and likely complicated by the background level of spontaneous resistance. Future work, therefore, may require new experimental models in organisms with a greater number of tools

available or laborious *in vitro* assays using purified components.

### **Concluding remarks**

Having examined applications of RecA-independent recombination to *L. pneumophila* and possible mechanisms of underlying oligo-induced mutagenesis, it is useful to re-consider the broader biological and evolutionary implications of my observations. In the process of exploring oligo mutagenesis in *L. pneumophila*, I have observed some interesting differences in its replication, recombination, and repair machinery compared to model organisms. Notably, genome sequence analysis predicts that *L. pneumophila* has a non-canonical SOS response system; lacks the replication restart proteins PriBC and DnaT; lacks the site-specific recombinases XerCD; and is missing the RecBCD helicase-nuclease. I also provide *in silico* and experimental evidence that *L. pneumophila* has fewer single-stranded exonucleases and a less responsive methyl-directed mismatch repair system. These observations provide important clues to the biology of the organism and illustrate the limitations of extrapolating data collected in model organisms to other species.

My work is also the first to observe oligo mutagenesis in a naturally transformable organism. *L. pneumophila* lives in both multi-species biofilms and within a broad array of Eukaryotic hosts—environments that might bring the organism in close contact with foreign DNA. Significantly, the same Type IV pili organelle has been shown to be involved in both adhesion to its phagocytic hosts and natural transformation (Stone and Kwaik, 1999). It is thought that the organism's lifecycle and ability to take up



DNA has led to the surprising number of Eukaryotic-like proteins present in the genome—approximately 3.5% of its predicted proteins (Gomez-Valero, *et al.*, 2009). While Eukaryotic-like proteins are present in other intracellular bacteria, *L. pneumophila* appears to contain the widest variety of any known prokaryote (Gomez-Valero, *et al.*, 2009). This diversity of proteins could be a result of the organism's ubiquity and the broad number of phagocytic hosts it can effectively parasitize (Fields, 1996). Due to the divergent nature of Eukaryotic DNA compared to its own genome, however, RecA-mediated recombination may be inefficient at incorporating these foreign sequences into its chromosome. Furthermore, *L. pneumophila* does not appear to contain the machinery for non-homologous end joining. As such, there does not appear to be any major canonical recombination pathway that can adequately account for the observed diversity in the species. It remains possible that a process akin to oligo mutagenesis, with its ability to undergo homologous recombination with short sequences, has therefore contributed to the diversity of *L. pneumophila* by facilitating horizontal gene transfer. A significant avenue of future work would be to more thoroughly test whether exogenous foreign DNA, either in the laboratory or environmental setting, can be a substrate for natural transformation and subsequent incorporation into the genome by a mechanism similar to the annealing model for oligo mutagenesis I describe.

Together with the microorganism's lower nucleolytic potential and less sensitive repair system, oligo-induced mutagenesis may equip *L. pneumophila* to incorporate divergent sequences into the genome, thereby increasing fitness of this intracellular pathogen to thrive in the environment and to infect a range of phagocytic hosts.

Although a possible role in the evolutionary history of *Legionella* is intriguing, since oligo mutagenesis appears to be conserved, it may play an even larger role in remodeling the genomes of species across the Bacterial Domain.

**Figure 4.1**

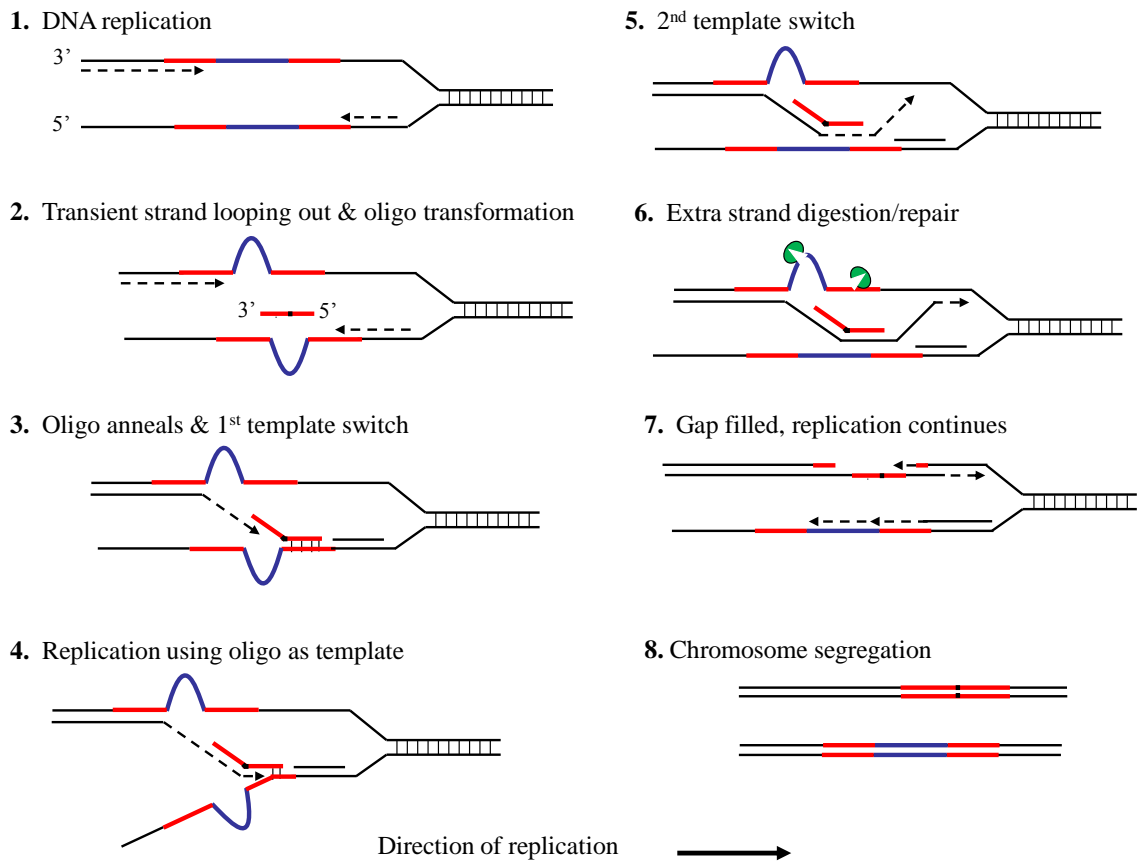


**Figure 4.1.** Template switch model of oligo-induced mutagenesis in *L. pneumophila*, an alternate model to that described in the text and in Figure 3.10. Red line with black center represents an oligo with homology to a chromosomal sequence (red) and a foreign sequence (black). Green Pac-Man characters indicate exonucleases or other unknown repair enzymes.

## APPENDIX A:

### Inhibition of Host Vacuolar H<sup>+</sup>-ATPase Activity by a *Legionella pneumophila* Effector

#### SUMMARY

*Legionella pneumophila* is an intracellular pathogen responsible for Legionnaires' disease. This bacterium uses the Dot/Icm type IV secretion system to inject a large number of bacterial proteins into host cells to facilitate the biogenesis of a phagosome permissive for its intracellular growth. Like many highly adapted intravacuolar pathogens, *L. pneumophila* is able to maintain a neutral pH in the lumen of its phagosome, particularly in the early phase of infection. However, in all cases, the molecular mechanisms underlying this observation remain unknown. In this report, we describe the identification and characterization of a Legionella protein termed SidK that specifically targets host v-ATPase, the multi-subunit machinery primarily responsible for organelle acidification in eukaryotic cells. Our results indicate that after being injected into infected cells by the Dot/Icm secretion system, SidK interacts with VatA, a key component of the proton pump. Such binding leads to the inhibition of ATP hydrolysis and proton translocation. When delivered into macrophages, SidK inhibits vacuole acidification and impairs the ability of the cells to digest non-pathogenic *E. coli*. We also show that a domain located in the N-terminal portion of SidK is responsible for its

interactions with VatA. Furthermore, expression of *sidK* is highly induced when bacteria begin to enter a new growth cycle, correlating well with the potential temporal requirement of its activity during infection. Our results indicate that direct targeting of v-ATPase by secreted proteins constitutes a virulence strategy for *L. pneumophila*, a vacuolar pathogen of macrophages and amoebae.

This work has been published (Xu, *et al.*, 2010), with my contributions including the measurement of vacuolar pH by live cell microscopy and intracellular degradation (Figure A.S2), writing of relevant methods and results, and editing of the entire manuscript.

## **INTRODUCTION**

The delivery of newly formed phagosomes to the lysosomal system by the endocytic pathway is essential for the digestion of phagocytosed materials. To evade such destruction, successful intracellular bacterial pathogens have evolved various mechanisms, including inhibition of phagolysosomal fusion, resistance to lysosomal digestion or the escape to the host cell cytosol. For intravacuolar pathogens, active modification of lipid and protein composition of phagosomal membrane is critical for their survival and replication. Moreover, since lysosomal enzymes often are active only in an acidic environment, regulation of pH in the phagosomal lumen is one common strategy employed by pathogens to avoid lysosomal killing (Huynh and Grinstein, 2007, Ohkuma and Poole, 1978).

*Legionella pneumophila* is a facultative intracellular pathogen responsible for Legionnaires' disease. Upon being phagocytosed, this bacterium orchestrates various cellular processes to initiate a unique trafficking pathway that eventually leads to the formation of a phagosome permissive for its multiplication (Shin and Roy, 2008). The biogenesis and maintenance of the bacterial replicative vacuole is mediated by protein substrates of the Dot/Icm type IV secretion system (Isberg, *et al.*, 2009, Liu, *et al.*, 2008). For example, RalF activates and recruits the small GTPase Arf1 to the bacterial vacuole (Nagai, *et al.*, 2002). Similarly, another small GTPase Rab1 is recruited to the bacterial vacuole by SidM/DrrA, which with LepB (Chen, *et al.*, 2004), completely hijacks the activity of this important regulatory molecule in membrane trafficking (Machner and Isberg, 2006, Murata, *et al.*, 2006). Whereas SidM/DrrA functions to release Rab1 from its GDI and activates the protein by loading it with GTP, LepB promotes the GTPase activity (Ingmundson, *et al.*, 2007). These proteins, along with other effectors such as SidJ that is involved in the recruitment of endoplasmic reticulum (ER) proteins to the bacterial vacuole (Liu and Luo, 2007), are thought to be responsible for the transformation of the nascent phagosome into a vacuole derived from the ER that resembles an immature autophagosome (Amer and Swanson, 2005, Swanson and Isberg, 1995, Tilney, *et al.*, 2001). *L. pneumophila* also actively modulates cell death pathways of infected macrophages, presumably to ensure the well being of the host cell for a complete infection cycle. Inhibition of cell death is mediated through the activation of an NF- $\kappa$ B-dependent induction of antiapoptotic genes and by effectors such as SidF that directly antagonize proapoptotic BNIP3 and Bcl-rambo (Abu-Zant, *et al.*, 2007, Banga, *et al.*, 2007, Losick and Isberg, 2006), and SdhA, an effector of unknown mechanism of

action (Laguna, *et al.*, 2006). Effectors that modulate other cellular processes, including protein synthesis, ubiquitination and lipid metabolism have also been identified, but how the bacterium benefits from the functions of these virulence factors is less clear (Belyi, *et al.*, 2006, Kubori, *et al.*, 2008, Shen, *et al.*, 2009, Weber, *et al.*, 2006). Finally, a recent study indicated that the effector AnkB contributes significantly to bacterial intracellular growth but does not affect any of the above host cellular processes, suggesting the targeting of yet unidentified host pathways by *L. pneumophila* (Al-Khodir, *et al.*, 2008).

The yeast *Saccharomyces cerevisiae* has been widely used to study bacterial effectors, largely due to its genetic manipulability and the conservation of many eukaryotic cellular processes (Siggers and Lesser, 2008). A large number of *L. pneumophila* effectors have been identified by their ability to kill yeast cells (Campodonico, *et al.*, 2005, Shen, *et al.*, 2009) or to interfere with its vesicle trafficking processes (Heidtman, *et al.*, 2009, Shohdy, *et al.*, 2005). In eukaryotic cells, the pH of intracellular compartments is an intricately regulated parameter that is crucial for many biological processes, including membrane trafficking, protein degradation and coupled transport of small molecules (Forgac, 2007). Organellar acidification primarily is mediated by ATP-dependent proton transporters known as the vacuolar H<sup>+</sup>-ATPases or v-ATPases, which is a large multisubunit complex with an approximate molecular mass of 10<sup>3</sup> kDa (Forgac, 2007). The structure of v-ATPases can be divided into two major functional domains: a 570-kDa peripheral subcomplex, known as V<sub>1</sub>, that binds and hydrolyzes ATP, and an integral membrane subcomplex, termed V<sub>0</sub>, that serves as the pore through which protons traverse the membrane bilayer (Forgac, 2007). *L.*

*pneumophila* is able to maintain a neutral luminal pH during infection, particularly within the first 6 hrs after uptake (Horwitz, 1983, Sturgill-Koszycki and Swanson, 2000), a hallmark shared by many intravacuolar pathogens. One such example is *Mycobacterium avium* whose vacuoles fail to acidify below pH 6.3, probably by selectively inhibiting fusion with v-ATPase-containing vesicles or by rapidly removing the complex from its phagosomes (Sturgill-Koszycki, *et al.*, 1994). Interestingly, a recent organelle proteomic study reveals that, in the soil amoebae host *Dictyostelium discoideum*, v-ATPase is associated with the Legionella containing vacuole (LCV) even in early phase of infection (Urwyler, *et al.*, 2009). This finding is contradictory to the well-established notion that in macrophages the bacterial phagosome maintains a neutral luminal pH for several hours, suggesting that the pathogen may initially antagonize the activity of the proton transporter.

Proton transporters from different orders of eukaryotes are highly conserved in structure and function, and some genes of mammalian or plant v-ATPase components can complement the corresponding yeast mutants (Kim, *et al.*, 1999, Lu, *et al.*, 1998). However, whereas in mammals mutations eliminating subunits of v-ATPase generate various phenotypes, ranging from the absence of any severe phenotype to lethality to embryonic development (Finberg, *et al.*, 2005, Inoue, *et al.*, 1999), yeast v-ATPase mutants are viable but only in acidic medium (Nelson and Nelson, 1990). In this study, we have taken the advantage of this conditional phenotype of yeast *vma* mutants to identify *L. pneumophila* proteins that may target the host v-ATPases. Here we report one such protein that inhibits v-ATPase by directly interacting with one component of the



proton transporter.

## **METHODS**

### **Bacterial strains and growth conditions.**

Bacterial strains used in this study are listed in Table A.S2. Strains of *E. coli* were grown in LB and the medium was supplemented with the appropriate antibiotics when necessary. The *L. pneumophila* strain Philadelphia-1 strain Lp02 (Berger and Isberg, 1993) was the parent of all derivatives used in this study. *L. pneumophila* was grown and maintained on CYE medium as previously described (Conover, *et al.*, 2003). When necessary antibiotics were included as described (Conover, *et al.*, 2003). To construct the *sidK* in-frame deletion mutant ZL114, we constructed plasmid pZL886 by cloning two DNA fragments generated by primers PL192/PL193 and PL194/PL195 (Table A.S4) into *SacI/SalI* digested pSR47s (Berger and Isberg, 1993). The primers were designed so that after deletion, only the first and last 15 amino acids are left in the mutant. pZL886 was introduced into Lp02 and the deletion mutant was obtained by following the standard allelic exchange method (Merriam, *et al.*, 1997). To complement the mutation, we inserted the coding region of *sidK* into pJB908 (Bardill, *et al.*, 2005). In complementation experiments, the vector used for expressing the gene of interest was introduced into the wild type strain or mutants and the bacterial cultures grown to the post-exponential phase as determined by optical density of the cultures ( $OD_{600} = 3.3-3.8$ ) as well as an increase of bacterial motility.

### **Plasmid construction.**

The plasmids used in this study are listed in Table A.S3 and the sequences of all primers are in Table A.S4. Plasmids harboring individual full-length *L. pneumophila* hypothetical genes were in Table A.S1. The open reading frame of *sidK* and its derivatives were cloned into pEGFPC1 (Clontech) for expression in mammalian cells. A number of vectors, including pGBKT7 (Clontech), p415ADH, p415TEF, p425TEF and p425GPD (Mumberg, *et al.*, 1995) were used to express *sidK* in yeast either as an untagged form or as GFP fusions (see text for details). To express His<sub>6</sub>-SidK in *L. pneumophila*, we first amplified the multiple cloning site region of pQE30 (Qiagen) with primers QE5'*EcoRV*/QE3'*XbaI* and inserted it into *Ecl136II/XbaI* digested pJB908 (Bardill, *et al.*, 2005). to generate pZL507. The *sidK* gene was then inserted into pZL507 as a *BamHI/XhoI* fragment to give pZL1333. cDNA clones coding for relevant subunits of the v-ATPase were amplified from a human kidney cDNA library (Clontech) or from clones purchased from the ATCC. For expression in mammalian cells, *sidK* or each of these genes was inserted into pEGFPC1 (Clontech) or pFlag-CMV (Sigma). The *vatH* gene (pEF-HA-NBP1) was a gift from Dr. M. Peterlin of University of California, San Francisco. The integrity of all genes was verified by sequencing analysis.

### **Yeast manipulation and screening of *L. pneumophila* proteins that inhibits yeast growth in neutral pH medium.**

Yeast strains used were PJ69-4A (James, *et al.*, 1996), BY4741 (Winzeler, *et al.*, 1999) and their derivatives (Table A.S2). Yeast was grown in YPD medium or in

appropriate amino acid dropout minimal media at 30°C. Using a standard protocol (Gietz, *et al.*, 1995), we transformed plasmids carrying full-length hypothetical *L. pneumophila* genes (Shen, *et al.*, 2009) into yeast strain PJ69-4A (James, *et al.*, 1996) and grew the resulting strains overnight in minimal medium of pH 5.5. After diluting at 1:40 into medium of pH 7.5 buffered with 50 mM MES and 50 mM MOP, the cultures were incubated with vigorous shaking for 24 hrs. Cultures that did not grow to high density were retained for further analysis. For quantitative study of growth, yeast subcultures of  $2 \times 10^6$  cells/ml were made in appropriate Dropout medium and cell growth was monitored by measuring the OD<sub>600</sub> at indicated time points.

To prepare cell lysates for protein analysis, cells from 5 ml overnight cultures were first lysed with a cracking buffer (40 mM Tris-Cl [pH 6.8], 5% SDS, 0.1 mM EDTA, 8 M urea, bromothymol Blue 0.4 mg/ml) with glass beads. Samples were resolved by SDS-PAGE after adding Laemmli buffer.

### **Cell culture and transfection.**

Mouse macrophages were prepared from bone marrow of female A/J mice of 6–10 weeks of age following published protocols (Swanson and Isberg, 1995). U937 cells were cultured in RPMI medium supplemented with 10% fetal bovine/calf serum (FBS) and 5 mM glutamate, and if needed, the cells were differentiated into macrophages with 50 ng/ml phorbol myristic acid (PMA) as described (Swanson and Isberg, 1995). 293T cells were cultured in Dulbecco's modified minimum Eagle's medium (DMEM) supplemented with 10% FBS. For transfection, we grew cells to about 80% confluence

and transfected them with Lipofectamine 2000 (Invitrogen) following manufacturer's instructions. For growth curve experiments, macrophages were plated into 24-well plates at  $2 \times 10^5$  cell per well. For immunoprecipitation and fractionation, about  $2 \times 10^7$  cells plated on standard petri dishes were used. Infection was performed at the indicated MOIs as required by the particular experiments.

### **Protein expression and purification.**

To purify GST-SidK, we inserted the predicted *sidK orf* into pGEX-4T-1 (Qiagen) to generate pZL797. *E. coli* strain XL1Blue containing pZL797 was grown in 1 liter LB to OD<sub>600</sub> of 0.7. After inducing with 0.2 mM IPTG for 6 hrs at 25°C, harvested cells were lysed by passing through a French press twice at 1,500 psi. Cleared supernatant was incubated with glutathione beads (Qiagen) for 2 hrs at 4°C and the beads were washed with 40X bed volume of PBS buffer containing 0.5% Triton X-100. GST-SidK was eluted with PBS containing 10 mM reduced glutathione. When needed, GST tag was removed by Thrombin, a protease that was subsequently removed by benzamidine-Sepharose beads (GE). GST-VatA was purified with a similar procedure.

To purify His<sub>6</sub>-SidK from *L. pneumophila*, we introduced pZL1333 into the non-virulent strain Lp03 (Berger and Isberg, 1993). A 50 ml of saturated culture was diluted into 1 liter AYE broth, when the culture reached exponential growth phase (OD<sub>600</sub> = 0.5), expression of the gene was induced with 0.2 mM IPTG for 16 hrs. Cleared cell lysates were incubated with Ni<sup>2+</sup>-Agrose beads for 2 hrs at 4°C and the beads were washed with 40 times of the bed volume of TBS buffer (50 mM Tris-HCl, 150 mM NaCl, pH 7.4)

containing 10 mM imidazole. The protein was eluted with 200 mM imidazole. After dialyzing against TBS to remove imidazole, the protein was further purified by gel filtration with an FPLC system using a Superdex 200 10/300 GL column (GE Healthcare). TBST buffer (50 mM Tris-Cl, 150 mM NaCl, 0.1% Triton-X100, pH 7.4) was used as eluent and the flow rate was set at 0.4 ml/min. The single peak corresponding to the protein was collected, dialyzed in the appropriate buffer for subsequent use. His<sub>6</sub>-Hsp70 was similarly purified from *E. coli*. Protein concentrations were determined by the Bradford assay; the purity of all proteins was more than 95% as assessed by SDS-PAGE followed by Coomassie bright blue staining (Figs. A.S3 and A.S7).

#### **Affinity chromatograph from cell lysates and *in vitro* protein binding.**

The procedure for affinity pulldown was described elsewhere (Shen, *et al.*, 2009). Briefly, U937 cells collected from 500 ml culture suspended in 3.0 ml PBS containing 5 mM DTT and protease inhibitors (Roche) were lysed with a glass homogenizer (Wheaton). The lysates were subjected to centrifugation at 10,000×g for 10 min at 4°C to remove unbroken cells and nuclei, the post-nuclear supernatant was added to Affigel beads coated with SidK and incubated for 14 hrs at 4°C. We then washed the beads five times with PBS and dissolved bound proteins with SDS sample buffer. After SDS-PAGE, proteins were visualized by silver staining (Bio-Rad). Individual protein bands retained by beads coated by SidK but not by GST were excised, digested with trypsin, and analyzed by matrix-assisted laser desorption/ionization/mass spectrometry (MALDI/MS) (Taplin Biological Mass Spectrometry Facility, Harvard Medical School).

For GST pull down experiments, 10 µg purified GST or GST-VatA was mixed with 2 µg His<sub>6</sub>-SidK in PBS for 4 hrs at 4°C. After adding 40 µl of 50% pre-washed glutathione beads slurry, binding was allowed to proceed for 1 hr. The beads were then washed 5 times with PBS containing 500 mM NaCl. Retained proteins were detected by immunoblot after SDS-PAGE.

### **Coimmunoprecipitation.**

Twenty-four hrs after transfection, cells were collected and lysed in a lysis buffer (0.2% of NP-40, 50 mM Tris-HCl pH = 7.5, 150 mM NaCl, 1 mM EDTA, 15% glycerol, and protease inhibitors (1 mM Na<sub>3</sub>VO<sub>4</sub>, 1 mM PMSF, 10 µg/ml Aprotinin, 2 µg/ml Leupeptin, 0.7 µg/ml Pepstatin)). After removing debris by centrifugation at 10,000 g for 10 min at 4°C, 2 mg protein (approximately 1 ml) was used for immunoprecipitation by adding the appropriate antibody and 30 µl of 40% protein G-sepharose beads (GE Healthcare). After incubating at 4°C on a rotary shaker for 4 hrs, the beads were washed 5 times with the lysis buffer before being dissolved in Laemmli buffer.

For immunoprecipitation with yeast lysates, cells harvested from 50 ml mid-log phase cultures were digested with Zymolyase, and the resulting spheroplasts were lysed with the lysis buffer used for mammalian cells. The lysates containing approximately 2 mg proteins were incubated with appropriate antibody and protein G sepharose for 16 hrs at 4°C. The beads were removed by washing 5 times with the lysis buffer. In both cases, protein associated with beads were dissolved in Laemmli buffer and resolved by SDS-

PAGE. Proteins transferred to nitrocellulose membranes were detected by immunoblot.

### **Antibodies and Western blot.**

Antisera against Legionella, ICDH (isocitrate dehydrogenase) were described in an early study (Liu, *et al.*, 2008). SidK cleaved from GST-SidK were used as an antigen to produce a specific antibody following a standard protocol (Pocono Rabbit Farm and Laboratory, Canadensis, PA). GFP antibody was prepared similarly with purified His<sub>6</sub>-GFP. When necessary, antibodies were affinity-purified against the antigens covalently coupled to an Affigel matrix (Bio-Rad) using standard protocols (Dumenil and Isberg, 2001). Monoclonal or polyclonal antibodies against Flag, Vma1, Vma2, PGK (3-phosphoglycerate kinase), VatA and Hsp70 were purchased from Sigma, Invitrogen, Abcam and Santa Cruz Biotechnology (sc-65521), respectively.

For Western blots, samples resolved by SDS-PAGE were transferred onto nitrocellulose membranes. After blocking with 4% milk in PBS buffer containing 0.2% Tween 20, membranes were incubated with the appropriate primary antibody: anti-SidK, 1:2,500; anti-VatA, 1:10,000; anti-Vma1, 1:1,000; anti-Vma2, 1:1,000; anti-GFP, 1:50,000; anti-PGK, 1: 2000; anti-ICDH, 1:5,000; anti-Hsp70, 1:2000. Horseradish peroxidase conjugated secondary antibodies and enhanced bioluminescence reagents were used to detect the signals (Pierce, Rockford, IL). Alternatively, membranes were incubated with an appropriate IRDye infrared secondary antibody (Li-Cor's Biosciences, Lincoln, Nebraska, USA) and the signals were detected, and if necessary, the intensity of

the bands are quantitated by using the Odyssey infrared imaging system.

### **Preparation of yeast vacuolar membrane vesicles.**

Yeast vacuolar membrane vesicles were prepared according to the standard method (Uchida, *et al.*, 1985) with some modification. Briefly, exponentially growing yeast cells (O.D. = 0.6) were harvested, washed twice with distilled water and digested with zymolyase at 30°C for 90 min in 1 M sorbitol. The spheroplasts were resuspended in 7 volumes of Buffer A (10 mM MES/Tris (pH 6.9), 12% Ficoll 400, and 0.1 mM MgCl<sub>2</sub>), homogenized in a loosely fitting Dounce homogenizer (Wheaton) with 20 strokes, and centrifuged in a swinging bucket rotor at 4,500 g for 10 min. The supernatants were transferred to new centrifuge tubes, and buffer A was layered on the top. After centrifugation at 51,900×g for 40 min, the white layer on the top was collected and resuspended in Buffer A with a homogenizer, and Buffer B (10 mM MES/Tris (pH 6.9), 8% Ficoll 400, and 0.5 mM MgCl<sub>2</sub>) was layered on the top. After similar centrifugation, vacuoles free from lipid granules or other membranous organelles were collected from the top of the tube. Vacuolar membrane vesicles were prepared by diluting the purified vacuoles in a vesicle buffer (10 mM MES/Tris (pH 6.9), 5 mM MgCl<sub>2</sub>, and 25 mM KCl).

### **V-ATPase-mediated ATP hydrolysis assay.**

Equal amount of vacuolar membranes in ATPase buffer (10 mM HEPES, 5 mM MgCl<sub>2</sub>, 125 mM KCl, pH = 7.0) were preincubated for 40 min at room temperature with or without the testing chemicals or proteins. To test the effect of antibody, purified



antibody was added to the reactions for 20 min before the addition of ATP. BSA dissolved in the same buffer as that of SidK was used as a negative control. The reaction was initiated by adding 1 mM of ATP, and samples were withdrawn at indicated time points to measure the production of inorganic phosphate using the malachite green method (Yim, *et al.*, 2003). Briefly, the malachite green reagent was made of 2 volumes of 0.0812% malachite green, 1 volume of 5.72% ammonium molybdate dissolved in 6 M HCl, 1 volume of 2.32% polyvinyl alcohol and 2 volumes of distilled water. 90  $\mu$ l of the malachite green reagent was added to 10  $\mu$ l samples withdrawn at indicated time points. The reactions were allowed to proceed for 2 min and were terminated with 1/10 volume of 34% sodium citrate. After incubation for another 20 min, absorbance at OD<sub>620</sub> nm was measured. A standard curve simultaneously obtained with a series of phosphate solutions of known concentrations was used to determine the amount of phosphate released by the membranes.

#### **Proton translocation activity.**

The ATP-driven proton transport activity was assayed by measuring the uptake of proton in the yeast membrane vesicles using acridine orange (AO) quenching assay (Shiraishi, *et al.*, 2000). Purified vacuolar membrane vesicles were diluted in AO buffer (5 mM HEPES, pH = 7.0, 5 mM MgCl<sub>2</sub>, 150 mM KCl, 6  $\mu$ M AO), and preincubated for 40 min at room temperature with or without the testing chemicals or proteins. The reaction was initiated by adding 2 mM of ATP and quickly mixed. The quenching of acridine orange was monitored by the Spex FluoroMax 3 spectrofluorometer (Jobin

Yvon) with excitation at 493 nm and emission at 525 nm.

### **Measurement of vacuolar pH.**

The pH of *L. pneumophila*-containing phagosomes was determined by fluorescence ratio imaging using 5(6)-carboxyfluorescein-*N*-hydroxysuccinamide ester (FLUOS, Fluka) stained *L. pneumophila* as previously described (Sturgill-Koszycki and Swanson, 2000) with the modifications detailed below. For labeling, *L. pneumophila* were cultured to the post-exponential phase, defined by motility and  $OD_{600} = 3.6 - 4.6$ , washed once with 100 mM potassium phosphate buffer, pH 8.0, and then incubated for 20 min at room temperature with 0.8 mg/ml FLUOS in 4% DMSO in 100 mM potassium phosphate, pH 8.0. This treatment did not affect viability of bacteria as determined by quantifying colony formation.

We infected macrophages plated on 24 mm coverslips with an MOI of ~10. Infections were synchronized by washing infected cells 4 times with RPMI/FBS 60 minutes after uptake. Following an additional 70–180 minutes of incubation, we washed the monolayers 3 times with 37°C Ringers Buffer (RB; 55 mM NaCl, 5 mM KCl, 2 mM CaCl<sub>2</sub>, 1 mM MgCl<sub>2</sub>, 2 mM NaH<sub>2</sub>PO<sub>4</sub>, 10 mM HEPES, and 10 mM glucose, pH 7.2), and placed the samples at a 37°C chamber with 1 ml RB and visualized on an Olympus IX70 inverted microscope. Images were acquired from the attached CoolSNAP HQ2 14-bit CCD camera (Photometrics) and subsequently analyzed using Metamorph Premier v6.3 software (Molecular Devices).

Fluorescence images were obtained at excitation wavelengths of 492 nm and 436 nm and corrected for bias, shading, and background. Individual bacteria were masked by manual thresholding using an addition image of both wavelengths. The mask was then applied to each original corrected image, and the average fluorescence intensity over the masked area of each particle was determined at each wavelength. The pH of each *L. pneumophila*-containing phagosome was calculated from the ratio of the fluorescence intensity at an excitation wavelength of 492 nm to the intensity at excitation 436 nm. The fluorescence intensity ratios from two independent experiments were converted to pH using a single standard curve of quartic function. The standard curve was established using FLUOS-labeled bacteria immobilized on a coverslip coated with poly-(L)-lysine. Samples were processed as above, with greater than 130 bacteria analyzed per pH at 10 incremental values ranging from pH 3.5 to 8.5 in clamping buffer (130 mM KCl, 1 mM MgCl<sub>2</sub>, 15 mM HEPES, 15 mM MES).

Only intact rod-shaped bacteria were evaluated, with greater than 50 bacteria analyzed per coverslip in each of two independent experiments. To verify that *sidK* did not affect lysosomal degradation, the fraction of wild-type and *sidK* mutant bacteria that were degraded was quantified 1 h post-infection by fixed immunofluorescence microscopy as previously described (Dalebroux, *et al.*, 2009) (Fig. A.S2). Heat killed (80°C 20 minutes) wild-type bacteria served as a control for particles that trafficked to an acidic compartment (Joshi, *et al.*, 2001).

### **Protein loading, lysosomal digestion of bacteria and phagosomal pH evaluation.**

We delivered recombinant proteins into macrophages by the syringe loading method (McNeil, 2001) with some modifications: Briefly, cells were washed and collected in ice cold Dulbecco's PBS (DPBS) (Cellgro) by centrifugation (200 g 5 min). We then washed the cells twice with 37°C DPBS containing 1.2 mM CaCl<sub>2</sub> before adding 200 µl warm loading solutions (DPBS containing 1.2 mM CaCl<sub>2</sub> and the protein to be loaded at 0.4 mg/ml) to cell pellet containing 5×10<sup>6</sup> cells. A P-200 micropipettor (Rainin) set at 100 µl was used to pipett the cell suspension for 100 times at 37°C. After pipetting, the mixture was incubated at 37°C for 2 min. After washing twice with warm DPBS containing 1.2 mM CaCl<sub>2</sub>, cells were seeded onto glass coverslips in 24-well plates with a density of 4×10<sup>5</sup> per well and were incubated at 37°C for 12–16 hrs.

The bactericidal activity of macrophages loaded with different proteins was measured according to a published method (Sun-Wada, *et al.*, 2009) with minor modifications. Cells of *E. coli* strain XL1-Blue expressing the mCherry RFP or GFP were added to macrophages at an MOI of 10 for 1 hr at 37°C. The culture supernatant was replaced with fresh tissue culture medium containing 100 µg/ml gentamicin to kill extracellular bacteria. After 1 hr of incubation, the medium was replaced with fresh medium containing 10 µg/ml gentamicin. At indicated time points, cells were washed extensively (5x) with warm PBS and lysed with 0.02% saponin. The lysates were plated on LB plates and colonies were counted after overnight incubation at 37°C.

For the staining with fluorescein dextran, 10 kD fluorescent dextran (Invitrogen) was added to the cells to 0.2 mg/ml; the pH insensitive 10 kD Cascade Blue dextran

(Invitrogen) was added at 0.2 mg/ml as a loading control. After incubating at 37°C for 1 hr, the cells were washed 5 times and incubated at 37°C for an additional 4 hrs before being imaged. For the staining with LysoRed (LysoTracker Red DND-99, Invitrogen), cells of an *E. coli* strain expressing GFP were added to macrophage monolayer at an MOI of 20 for 1 hr at 37°C. After incubating with a medium containing 100 µg/ml gentamicin for 1 hr and then a medium containing 10 µg/ml gentamicin for an additional 8 hrs, a medium containing 50 nM LysoRed was added to the samples for 15 min. Cells were washed 3 times with fresh medium and subjected to imaging analysis immediately under an Olympus X-81 fluorescence microscope. All images were acquired with identical digital imaging parameters (objectives, exposure duration, contrast ratios, etc.) and were similarly processed using the IPLab software package (BD Biosciences).

## **RESULTS**

### **Identification of SidK, a Legionella protein that affects growth of yeast cells in neutral pH medium.**

One of the prominent phenotypes associated with yeast v-ATPase mutants is their inability to grow in neutral pH medium (Nelson and Nelson, 1990). We reasoned that if *L. pneumophila* codes for proteins that inhibit v-ATPase activity, expression of such proteins in a yeast strain would impair its ability to grow in neutral pH medium. To this end, we cloned individual *L. pneumophila* hypothetical genes into pGBKT7 (Clontech) (Shen, *et al.*, 2009). Yeast strains harboring each of the plasmids were tested for their ability to grow in medium with a pH of 7.5. Of the first 97 genes screened (Table A.S1),

one gene that consistently interferes with yeast growth under this condition was obtained (Fig. A.1A and B). This gene (lpg0968), designated SidK is predicted to code for a protein of approximately 65 kDa. It is present in the genomes of all sequenced strains of *L. pneumophila* but has no detectable homology to proteins in the database, nor does it contain predictable domains or motifs suggestive of known biochemical activities. Interestingly, this gene is divergently transcribed from lpg0969, a gene that appears to inhibit yeast growth by interfering with unknown host functions (Heidtman, *et al.*, 2009).

Since the original construct was made by fusing the testing gene to the DNA binding domain of the Gal4 protein on pGBKT7 (Clontech), we attempted to eliminate the potential effect of protein fusion by expressing untagged *sidK* in yeast strain BY4741 (Winzeler, *et al.*, 1999). To this end, we used a series of vectors that differ in copy number and promoter strength (Table A.S3; Mumberg, *et al.*, 1995). The expression of *sidK* on these vectors is proportional to the strength of the promoter, with the GPD (glyceraldehyde-3-phosphate dehydrogenase) promoter giving the highest protein level (Fig. A.1C). Consistent with the protein levels, in 18 hrs after the establishment of subcultures of identical cell density, strains in which SidK was expressed from the GPD promoter almost completely lost the ability to grow in neutral pH medium (Fig. A.1D). On the other hand, only a marginal growth defect was observed when the gene was expressed from the moderate ADH promoter (Fig. A.1C and D, strain 1), indicating that the effect of SidK on yeast growth under this condition is dose-dependent. Taken together, these data indicate that we have identified a *L. pneumophila* gene that affects yeast growth in neutral pH medium, probably by interfering with its v-ATPase activity

directly or with activities relevant to the proton transporter.

**SidK is a substrate of the Dot/Icm system that is delivered into host cytosol during infection.**

To exert an effect on its cellular targets, a bacterial virulence factor must first reach the host cytosol via specialized secretion systems. We thus examined whether SidK is a substrate of the Dot/Icm secretion system. We first employed the Cya assay (Bardill, *et al.*, 2005) by fusing SidK to the carboxyl end of the catalytic domain of the *Bordetella pertusis* cyclic AMP synthetase. Infection of macrophages with a *L. pneumophila* strain expressing Cya fused to the known effector SidJ led to production of high-level cAMP in a Dot/Icm-dependent manner (Fig. A.2A). Importantly, although the Cya-SidK fusion expressed similarly in the wild type and the *dotA* mutant, high levels of cAMP were only detected in infections using the wild type strain (Fig. A.2A), indicating that SidK contains signals recognizable by the Dot/Icm system. Similar results were obtained with the SidC staining assay (VanRheenen, *et al.*, 2006), in which fusion to SidK restores the translocation of the transfer deficient SidC $\Delta$ C100 mutant to wild type levels (Fig. A.2B–D). These results indicate that SidK is a substrate of the Dot/Icm system.

To determine whether SidK is injected into host cells by *L. pneumophila* during infection, we attempted to detect SidK in lysates of infected cells generated by saponin fractionation (VanRheenen, *et al.*, 2006). Despite considerable effort, we were unable to detect this protein in the soluble fraction of lysates of cells infected by *L. pneumophila* for up to 3 hrs (data not shown). Considering the possibility that the amount of

translocated SidK is beyond detection by this method; we used a SidK specific antibody to enrich the protein. After immunoprecipitation, SidK protein was detected in lysates of cells infected with wild-type strain but not with the Dot/Icm deficient mutant or a *sidK* deletion mutant (Fig. A.2E, lanes 2–3). Expression of SidK from a plasmid in the *sidK* deletion mutant restored the delivery of this protein into infected cells (Fig. A.2E, lane 4). Collectively, these results indicate that SidK is a substrate of the Dot/Icm system and is injected into infected cells by *L. pneumophila* during infection. Furthermore, we cannot readily detect SidK in concentrated lysates of infected cells (data not shown), suggesting that the amount of translocated protein is low.

Next, we examined the potential role of *sidK* in *L. pneumophila* infection by constructing an in-frame deletion mutant and tested its intracellular growth. The mutant did not exhibit detectable growth defect in either mouse bone marrow-derived macrophages or *D. discoideum* (Fig. A.S1). These observations extend the list of *L. pneumophila* effectors not essential for its intracellular growth in standard infection models, thus adding another layer to the remarkable potential functional redundancy among substrates of the Dot/Icm system (Isberg, *et al.*, 2009).

Since wild type *L. pneumophila* maintains a neutral pH in its vacuole and SidK appears to interfere with the functions of v-ATPase, we analyzed whether deletion of *sidK* affects luminal pH of LCVs in mouse macrophages. Relevant *L. pneumophila* strains labeled with 5(6)-carboxyfluorescein-*N*-hydroxysuccinamide ester (FLUOS, Fluka) were used to infect macrophages and images obtained from individual phagosomes were used to calculate intravacuolar pH against a standard curve as



described (Sturgill-Koszycki and Swanson, 2000). As expected, vacuoles containing heat-killed bacteria quickly acidified to pH values of about 4, whereas phagosomes harboring wild type *L. pneumophila* maintain a neutral pH at the time points examined (Fig. A.S2-A). Furthermore, although the *dotA* mutant was not lysed by the macrophages in the experimental duration (Fig. A.S2-B), its vacuoles were also acidified, indicating that the Dot/Icm system is required for the biogenesis of a bacterial phagosome of neutral pH. Interestingly, vacuoles containing the *sidK* deletion mutant still are able to block their acidification, thus maintaining a neutral luminal pH in the experimental duration (Fig. A.S2-A). Given the proficient intracellular growth displayed by the mutant (Fig. A.S1), this result was not unexpected. *L. pneumophila* mutants lacking a single effector gene rarely exhibit detectable intracellular growth defect, possibly due to functional redundancy among bacterial and/or host factors (Isberg, *et al.*, 2009, Ninio and Roy, 2007).

**Expression of *sidK* is repressed at stationary phase and is induced within one hour after transition into fresh medium.**

Consistent with the observation that *L. pneumophila* grown at post-exponential phase are more infectious, many substrates of the Dot/Icm system are highly induced when bacterial cultures enter this growth phase (Isberg, *et al.*, 2009). That the luminal pH of LCVs is neutral in the early phase of infection points to the requirement of bacterial factors that target v-ATPase in this period of infection. We thus examined the protein level of SidK at different time points throughout the *L. pneumophila* growth cycle in

broth. In contrast to many substrates of the Dot/Icm transporter whose expression is induced at post-exponential phase, very little SidK was present in *L. pneumophila* grown at this stage (Fig. A.3). Rather, accumulation of SidK was apparent within 1 hr after diluting saturated cultures into fresh medium, and reached the peak 2 hrs after dilution (Fig. A.3B). When the bacterium begins to replicate (approximately 4–5 hrs after dilution), protein level of SidK begins to decrease and became difficult to detect throughout the rest of the growth cycle (Fig. A.3A–B), a pattern consistent with the slow progression of LCVs to lysosomal organelles (Sturgill-Koszycki and Swanson, 2000). We also determined the kinetics of SidK translocation during infection by saponin fractionation. Translocated SidK was not detectable until 3 hrs after infection and the protein is present in the soluble fraction of infected cells in the first 12 hrs of infection (Fig. A.3C).

### **SidK interacts with the host vacuolar ATPase.**

Since mutations affecting various yeast genes not directly involved in v-ATPase function can result in mutants sensitive to neutral pH medium (Sambade, *et al.*, 2005), we furthered our study on the mechanism of action of SidK by identifying its cellular targets with the unbiased affinity chromatograph method. We incubated Affigel beads (Bio-Rad) coated with purified SidK (Fig. A.S3) with PBS soluble fraction of U937 cell lysates. After removing unbound proteins by washing with PBS, proteins retained on the beads were separated by SDS-PAGE and were visualized by silver staining. At least three proteins with molecular weights ranging between 20 kDa and 75 kDa were retained by

beads coated with SidK, but not by uncoated beads (Fig. A.4A, lane 3). By mass spectrometry analysis, we identified these proteins as three components of the mammalian vacuolar H<sup>+</sup>-ATPase: VatA, the ubiquitous VatB<sub>2</sub> subunit and VatE (Fig. A.4A, lane 3). These results indicate v-ATPase is the potential target of SidK.

To further investigate the interactions between v-ATPase and SidK, we transfected mammalian cells with combinations of plasmids that direct the expression of GFP-SidK or Flag-VatA, one essential component of the proton transporter (Forgac, 2007). Lysates of transfected cells were subjected to co-immunoprecipitation (co-IP) with an anti-Flag antibody to detect possible SidK/VatA complexes. GFP-SidK was detected in immunoprecipitates only from cells coexpressing Flag-VatA (Fig. A.4B). No signals were detected in untransfected samples or in samples transfected with plasmids expressing only Flag-VatA or GFP-SidK, indicating that the interactions were specific. Similar results were obtained in reciprocal experiments using the anti-GFP antibody (Fig. A.4C). Furthermore, VatA was detected in precipitates from cells that was transfected only with the plasmid expressing SidK, indicating that this protein interacts with endogenous VatA (Fig. A.4C, lane 3).

The structure and function of v-ATPase from mammals and yeast are highly similar (Forgac, 2007). We thus examined whether SidK interacts with yeast v-ATPase. When lysates of yeast cells expressing GFP or GFP-SidK were immunoprecipitated with a GFP-specific antibody, Vma1 (equivalent of VatA) was detected in precipitates, again only in samples expressing SidK (Fig. A.4D, lane 1 in left panel). Similar results were obtained in reciprocal immunoprecipitation using a Vma1 specific antibody (data not

shown). Taken together, these data establish that v-ATPase is the cellular target of SidK.

**SidK directly interacts with the V<sub>1</sub> (Vma1) subunit of the v-ATPase.**

Under normal physiological condition, components of the V<sub>1</sub> domain of v-ATPases form a stable complex (Forgac, 2007). In agreement with this notion, in immunoprecipitation experiments aiming at detecting interactions between SidK and components of the V<sub>1</sub> complex, positive interactions were observed in many if not all components (data not shown). Thus, we further investigated which subunit of the V<sub>1</sub> domain is directly targeted by SidK. Because some V<sub>1</sub> components are recalcitrant to purification in their soluble form, we used yeast mutants that lack individual V<sub>1</sub> component genes (Winzeler, *et al.*, 1999) to identify the subunit that directly interacts with SidK. We first examined the formation of protein complexes between SidK and two V<sub>1</sub> subunits, Vma1 and Vma2 in these mutants. Vma1 and Vma2 can be coimmunoprecipitated by the SidK antibody in mutants lacking *vma4*, 5, 7, 8, 10 or 13, indicating that none of these subunits is required for the formation of protein complexes between SidK and Vma1 or Vma2 (Fig. A.5A). However, in the absence of Vma1, no interactions between SidK and Vma2 or any other V<sub>1</sub> components were detected (Fig. A.5A, lane 7 and data not shown). Importantly, although at a low level, Vma1 was detected in precipitates obtained by the SidK antibody in the *vma2* mutant (Fig. A.5A, lane 3). Furthermore, when beads coated with SidK were incubated with lysates of different *vma* mutants, Vma1 from the lysates of the *vam2* mutant was retained (Fig. A.5B, lane 3). Under the same condition, SidK coated beads did not retain Vma2 or other

V<sub>1</sub> components expressed in the *vma1* mutant (Fig. A.5B, lane 2 and data not shown). Collectively, these results point to Vma1 as the direct target of SidK. To confirm this conclusion, we purified recombinant mammalian VatA as a GST tagged protein (GST-VatA) and tested its interaction with SidK. As expected, formation of SidK/GST-VatA complexes can be captured by GST beads (Fig. A.5C). From these results, we conclude that SidK targets the v-ATPase by directly interacting with the VatA (Vma1) subunit.

### **A N-terminal domain of SidK is important for binding to Vma1.**

We extended our analysis of the interactions between SidK and VatA by determining the region on SidK important for target binding. To this end, we constructed a series of SidK deletion mutants (Fig. A.6A). To eliminate the potential discrepancy that may arise from the loss of epitopes in these mutants when the polyclonal anti-SidK antibody is used in subsequent experiments, we expressed GFP fusions of these mutants in mammalian cells. Deletion of 30 amino acids from the N-terminus of SidK did not detectably affect its binding with VatA (Fig. A.6B, lane 2). However, although it was expressed at a high level, a mutant missing the first 94 amino acids no longer detectably bound VatA (Fig. A.6B, lane 3). On the other hand, the VatA binding activity of SidK is far more tolerant to deletions in its carboxyl end. A mutant lacking as many as 382 amino acids from this end of SidK still co-precipitated with VatA at a level similar to that of the full-length protein (Fig. A.6B, lane 8). Similar results were obtained in yeast, with the exception of *sidK*ΔC382, which did not bind Vma1, probably due to the different binding affinity of SidK to v-ATPases from these two organisms (Fig. A.S4). Collectively, these

results indicate that a domain that lies within residue 30 to 191 of SidK is important for interacting with VatA.

To determine whether any of the SidK deletion mutants are still active in inhibiting v-ATPase functions, we tested their ability to inhibit yeast growth in neutral pH medium. Our results indicate that under this condition, SidK $\Delta$ N30 consistently inhibits yeast growth, whereas the binding inactive mutant SidK $\Delta$ N94 exhibits very little effect (Fig. A.6C). Similarly, the binding of SidK $\Delta$ C98 and SidK $\Delta$ 286 to VatA is comparable to that of full-length protein and both mutants exhibit detectable inhibition in yeast growth (Fig. A.6C). Although these mutants can be stably expressed in yeast from the GPD promoter, their expression levels are considerably lower than that of full-length SidK (Fig. A.S5). Since high protein level is required for SidK to exert full inhibitory effect on yeast growth (Fig. A.1), the low activity exhibited by these mutants may result from their low protein levels in yeast.

### **SidK inhibits v-ATPase-mediated ATP hydrolysis and proton translocation.**

The V<sub>1</sub> domain of v-ATPase provides the energy required for proton translocation across membranes by binding and hydrolyzing ATP via subunit Vma2 and Vma1, respectively (Stevens and Forgac, 1997). Our observation that SidK directly binds Vma1 prompted us to examine the effect of such binding on ATP hydrolysis. Thus, we followed a standard procedure (Uchida, *et al.*, 1985) to prepare yeast membrane and examined the effect of SidK on its ATPase activity. In this assay, exogenous ATP was added to purified yeast membranes and the release of free phosphate was measured by malachite

green (Yim, *et al.*, 2003). In samples receiving 2  $\mu\text{M}$  BSA, the level of free phosphate steadily increased throughout the experimental duration (Fig. A.7A, open triangles). On the other hand, the addition of 1  $\mu\text{M}$  bafilomycin A1 (Baf A1), a commonly used inhibitor of v-ATPase (Huss and Wiczorek, 2009) led to strong inhibition of ATP hydrolysis, thus low level of free phosphate (Fig. A.7A, diamonds). Importantly, we found that recombinant SidK inhibited v-ATPase activity in a dose-dependent manner. Significant inhibition was observed by 0.1  $\mu\text{M}$  SidK, and a higher amount of protein caused more severe inhibition (Fig. A.7A, closed triangles); 1  $\mu\text{M}$  of SidK exerted inhibition at a level similar to that of Baf A1 (Fig. A.7A, squares). Next, we probed the mechanism of action of SidK by adding its antibody to the reactions. The antibody did not detectably affect SidK activity even when it was two-fold in excess (Fig. A.S6).

To confirm that the observed inhibition of ATP hydrolysis was indeed a result of blocking v-ATPase activity, we did similar experiments with membranes prepared from the *vma1* mutant. For the same amount of membranes, the overall ATP hydrolysis activity of the mutant markedly decreased (compare 3<sup>rd</sup> bar of mutant and 1<sup>st</sup> bar of WT in Fig. A.7B). Moreover, the ATP hydrolysis activity of membranes from the mutant is resistant to Baf A1 or SidK, but not to EDTA and vanadate, two general inhibitors for ATPases (Heneberg, 2009) (Fig. A.7B, mutant 4<sup>th</sup> & 5<sup>th</sup> bar). On the other hand, ATPase activity in membranes prepared from wild type yeast consistently exhibited sensitivity to SidK, again in a dose-dependent manner (Fig. A.7B, wild type 2<sup>nd</sup>-5<sup>th</sup> bar). We also tested the effect of SidK on the ATP hydrolysis activity of mammalian Hsp70, an ATPase structurally distant from the v-ATPase (Sousa and Lafer, 2006). EDTA but not SidK

abolished ATP hydrolysis by this heat shock protein; vanadate also exhibited inhibitory effect, but to a lesser extent (Fig. A.S7). Taken together, these results indicate that binding of SidK to Vma1 leads to specific inhibition of the ATP hydrolysis activity of the proton transporter.

Because v-ATPase-mediated ATP hydrolysis is coupled with proton translocation, and thus the acidification of vesicles (Nishi and Forgac, 2002), inhibition of v-ATPase activity by SidK would block vesicle acidification. To test this hypothesis, we determined the effect of SidK on the sequestration of the lipophilic amine acridine orange (AO) by yeast vesicles. Nonprotonated AO permeates membranes, and, if the pH of the vesicles drops as a result of v-ATPase-mediated proton translocation, it becomes protonated and sequestered, leading to quenching of its fluorescence (Palmgren, 1991). In samples receiving the solvent DMSO that does not affect v-ATPase activity, more AO was trapped in the vesicles as proton translocation was initiated by adding ATP, leading to quenching of fluorescence at 525 nm (Fig. A.7C, diamonds). On the other hand, inclusion of 1  $\mu$ M SidK to the reaction blocked such quenching during the entire experimental duration (Fig. A.7C, squares). The effect of SidK at this concentration is comparable to that of Baf A1, which almost completely blocked AO fluorescence quenching (Fig. A.7C, triangles). From these observations, we conclude that inhibition of ATP hydrolysis activity of v-ATPase by SidK prevents proton translocation.



## **SidK interferes with phagosome acidification and phagolysosomal digestion of bacteria.**

To determine whether SidK affects the functions of v-ATPase *in vivo*, we delivered His<sub>6</sub>-SidK into mouse bone marrow-derived macrophages by syringe loading (McNeil, 2001) and examined the acidification of phagosomes by using the dextran-coupled pH sensitive fluorescein, whose fluorescence drops very sharply at pH values below 5.5 (Han and Burgess, 2009). The pH insensitive Cascade Blue dextran was included in the feeding mixture as a loading control. Macrophages in all samples emitted blue fluorescence signals at similar intensity, indicating that the dyes were equally loaded into the cells (Fig. A.8A, lower panel). Importantly, compared to macrophages receiving BSA, cells loaded with SidK gave significantly stronger green fluorescence signals (Fig. A.8A, upper panel, the first two images). Similarly, compared to cells loaded with BSA, cells treated with the v-ATPase inhibitor Baf A1 also emitted stronger fluorescence signals (Fig. A.8A, upper panel, the right image). These results indicate that SidK interferes with efficient acidification of phagosomes, thus inhibiting the decrease of their luminal pH values. To substantiate this observation, we used LysoRed, which accumulates in acidified organelles to stain protein-loaded macrophages that have been fed with *E. coli* cells expressing GFP for 10 hrs. Strong red fluorescence signals were readily detected in cells loaded with BSA, but not in cells receiving SidK (Fig. A.8B, left panel), further supporting the notion that SidK inhibits phagosomal acidification. No effect was detected in additional controls with two other Legionella effector proteins (data not shown). Moreover, at this time point, we observed that the number of *E. coli* cells in macrophages loaded with SidK was significantly higher than that of cells

containing BSA (Fig. A.8B, middle panel), suggesting that inhibition of phagosomal acidification by SidK impaired the lysosomal digestion of internalized bacteria.

Since macrophages from mice lacking a functional  $\alpha 3$  subunit exhibit delayed digestion of bacteria, we set to more thoroughly examine the effect of SidK on macrophage-mediated lysis of *E. coli* cells. We first determined the survival of *E. coli* in macrophages loaded with different proteins. Macrophages loaded with His<sub>6</sub>-SidK or BSA are capable of killing phagocytosed bacteria, but cells containing SidK were less efficient in the clearance of the bacteria, and such differences became significant 6 hrs after adding the bacteria (Fig. A.8C). Similar results were obtained when macrophages harboring one or more intact *E. coli* cells were scored. In cells receiving His<sub>6</sub>-SidK, more than 90% of the cells harbor intact bacterial cells throughout the 24 hrs experiment duration (Fig. A.8D). However, 8 hrs after adding the bacteria, less than 40% of the macrophages loaded with BSA contained intact bacterial cells and the ratio of such cell population dropped to less than 10% at the 12-hr time point (Fig. A.8D and E). Taken together, these results indicate that SidK can inhibit v-ATPase activity *in vivo* and such inhibition leads to defects in phagosomal acidification and impairment in lysosomal digestion of bacteria by macrophages.

## **DISCUSSION**

Many intracellular bacterial pathogens reside and replicate in phagosomes of unique physiological and biochemical properties. One such property is an actively

regulated pH homeostasis important for successful infection of these pathogens. Since the vacuolar ATPase is the primary cellular machinery involved in controlling vacuolar pH (Nishi and Forgac, 2002), it is believed that pathogens capable of maintaining a neutral phagosomal pH encode specific traits to inhibit the accumulation of the proton transporters on their vacuolar membranes. However, although the importance of maintaining proper phagosomal pH, presumably by actively regulating the activity of v-ATPase, is generally recognized, almost nothing is known concerning the molecular mechanisms responsible for such regulation. Using a screening strategy based on the sensitivity of yeast v-ATPase mutants to neutral pH medium, we have identified SidK, a *L. pneumophila* protein that targets the proton transporter.

A pathogen can employ at least two mechanisms to maintain a neutral luminal pH in its phagosomes: By preventing the accumulation of v-ATPases on the phagosomal membranes or by inhibiting the activity of acquired v-ATPases. Although we have not been able to consistently detect SidK on LCVs, probably because of low protein level and/or poor antibody quality (Fig. A.2 and data not shown), the presence of v-ATPases on LCVs (Urwyler, *et al.*, 2009) strongly suggests that SidK targets the proton pumps on the bacterial phagosomes. This feature differs from vacuoles of *Mycobacterium ovium* that do not contain detectable v-ATPases (Sturgill-Koszycki, *et al.*, 1994). However, these two mechanisms are not mutually exclusive, because in addition to blocking its acquisition, the pathogen may need to antagonize v-ATPases that accidentally associate with its phagosomes. It is worth noting that detecting the association of v-ATPase with specific organelles can be complicated by low abundance of this protein complex on the

membranes. For example, only a few v-ATPases were detected on a phagosome containing a latex bead (Kinchen and Ravichandran, 2008). Similarly, v-ATPases associated with LCVs can be detected by the sensitive mass spectrometry but not by standard immunostaining (data not shown; Urwyler, *et al.*, 2009). Thus, direct targeting of v-ATPase by specific virulence factors could be a mechanism shared by many intravacuolar pathogens.

Our data showed that SidK interacts with v-ATPases by directly binding to the VatA subunit (Fig. A.5). Moreover, this protein appears to have a higher affinity for VatA in the presence of VatB (Fig. A.5A). Such differences may result from the conformation assumed by VatA when it is associated with VatB (Forgac, 2007). Preferably binding to the VatA/VatB and/or the fully assembled v-ATPase complex clearly will result in higher inhibitory efficiency for SidK, as its effect can be diluted by free VatA if these two proteins interact similarly regardless of their statuses. Reversible assembly of the  $V_1$  and  $V_0$  domain is important in regulating v-ATPase activity under different physiological conditions (Forgac, 2007). Whether binding of SidK to v-ATPase causes disassembly of the transporter, block of its rotary movement or other functional mechanisms of the proton transporter remains to be determined. Our biochemical studies indicate that SidK blocks organelle acidification during infection. Two lines of evidence indicate that SidK inhibits v-ATPase *in vivo*. First, macrophages harboring physically delivered recombinant SidK failed to block emission of fluorescence signals by the pH sensitive fluorescein (Fig. A.8A). Second, cells loaded with SidK sequester significantly lower levels of LysoRed, a fluorescence dye that prefers to accumulate in acidic

environments (Fig. A.8B). Moreover, similar to macrophages from mice lacking a subunit of the v-ATPase (Sun-Wada, *et al.*, 2009), cells loaded with SidK displayed a significant delay in the digestion of phagocytosed bacteria (Fig. A.8C–E). Thus, it is clear that by binding to VatA, SidK is able to block phagosomal acidification, thus contributing to the protection of internalized *L. pneumophila* during infection.

Bacterial effectors often enzymatically modify their targets to divert the cellular processes in ways beneficial to the survival of the pathogens (Ninio and Roy, 2007). However, despite considerable effort, we were unable to detect novel post-translational modifications on VatA co-purified with SidK from yeast (data not shown). Moreover, our attempt to determine the mechanism of action of SidK by its antibody is not conclusive because the antibody is able to immunoprecipitate Vma1 or VatA, indicating that it can form a stable complex with these two proteins (Fig. A.5A and data not shown). Although SidK-mediated modifications of VatA or other v-ATPase subunits could substantiate its effect, two lines of evidence indicate the importance of physical binding in the activity of SidK. First, in contrast to other highly effective *L. pneumophila* effectors, such as those involved in inhibiting host protein synthesis or membrane trafficking (Isberg, *et al.*, 2009), a much higher level of SidK is required to significantly inhibit yeast growth in neutral pH medium, a condition that is completely unable to support growth of yeast *vma* mutants (Fig. A.1). For instance, if the effect of SidK was mediated by a highly catalytic mechanism, one would expect more severe inhibition when expressed from the ADH (alcohol dehydrogenase) promoter (Fig. A.1C). Similarly, a considerable amount of SidK is needed to inhibit v-ATPase activity in yeast membranes (Fig. A.7). Second, some

deletion mutants capable of binding VatA still are able to exert inhibitory effect on yeast growth in neutral pH medium (Fig. A.6C). Given the requirement of high-level SidK for full growth inhibition, the loss of inhibitory effect by deletion mutants still competent for binding VatA very likely is a result of lower protein levels (Fig. A.S5). Alternatively, SidK may need other *L. pneumophila* proteins to exert its full activity or our experimental conditions are not optimal for its activity.

In A/J mouse macrophages, vacuoles containing *L. pneumophila* become acidified during the replication phase of infection. Delayed maturation of the LCV promotes intracellular growth, since Baf A1 treatment blocks acidification and acquisition of lysosomal markers and also reduces the bacterial yield (Sturgill-Koszycki and Swanson, 2000). Consistent with the observation that expression of *sidK* peaks early in the lag phase before declining to almost undetectable levels as the bacteria enter the post-exponential phase, translocated SidK did not become detectable until 3 hrs after bacterial uptake. That translocated SidK is still detectable 12 hrs after infection suggests a delayed inhibition of SidK expression during infection or that SidK expresses differently in intracellular bacteria. In *D. discoideum*, the association of v-ATPases with the LCV is detectable from 15 min to 14 hrs after bacterial uptake (Urwyler, *et al.*, 2009). The presence of this transporter in the early phase of infection suggests that the undetected SidK and/or other effectors antagonize its activity. Given the important roles of v-ATPase in vesicular trafficking, particularly in the endocytic pathway (Marshansky and Futai, 2008) that was recently shown to be involved in remodeling the membranes of the LCVs in *D. discoideum* (Urwyler, *et al.*, 2009), prolonged biochemical modifications of

the v-ATPase may interfere with the ability of the bacteria within phagosomes to efficiently acquire nutrients and materials from certain membrane trafficking pathways. Thus, *L. pneumophila* appears to use a combination of strategies to modulate the activities of v-ATPase at different phases of infection for its benefit.

*L. pneumophila* appears to acquire many of its genes important for its interactions with host by horizontal gene transfer, which may account for at least in part the high plasticity of its genomes (Cazalet, *et al.*, 2004, de Felipe, *et al.*, 2005). Although the distinct biochemical activities of these genes can interfere with host cellular processes, a single gene often plays only a small incremental role in its evolution to parasitize its hosts, which may explain the remarkable functional redundancy among effectors of the Dot/Icm system (Isberg, *et al.*, 2009, Ninio and Roy, 2007). For example, at least four proteins are involved in inhibiting host protein synthesis by targeting the elongation factor eEF1A (Belyi, *et al.*, 2008, Shen, *et al.*, 2009). Consistent with this notion, with a few exceptions, deletion of one or more Dot/Icm substrate genes did not cause detectable defect in intracellular growth (Isberg, *et al.*, 2009, Luo and Isberg, 2004, Ninio and Roy, 2007). Thus, our observation that deletion of *sidK* did not impair intracellular growth of *L. pneumophila* or its phagosomal pH is not completely unexpected. It is very likely that multiple Dot/Icm substrates are involved in the modulation of v-ATPase activity. Identification and elucidation of activities of such proteins should pave the way toward further understanding of the mechanisms underlying organelle acidification and of the means whereby it can be disrupted by pathogens.

**Figure A.1**

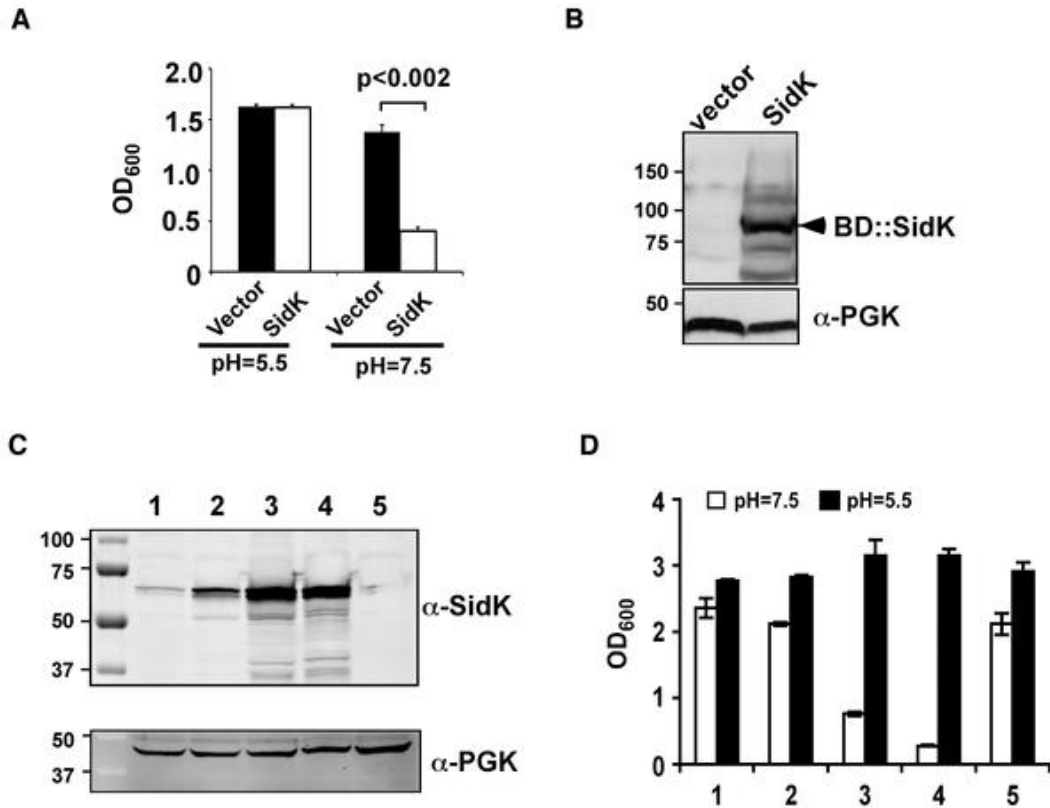


**Figure A.1. Identification of *L. pneumophila* protein that inhibits yeast growth in neutral pH medium.** Yeast strains grown to saturation were diluted in medium buffered to the indicated pH at a density of  $2 \times 10^6$  cells/ml and the subcultures were incubated at 30°C with vigorous shaking. Cell growth was monitored by measuring OD<sub>600</sub> 18–24 hrs after establishing the subcultures. **A.** Growth of a yeast strain expressing SidK fused to the DNA binding domain on pGBKT7. **B.** Expression of the fusion protein. Yeast strains grown to mid-log phase were lysed with a cracking buffer; SDS-PAGE resolved samples were probed with a SidK specific antibody (upper panel). The 3-phosphoglycerate kinase (PGK) was probed as a loading control (lower panel). Relevant protein size markers (in kDa) are indicated. **C.** Expression of SidK from different promoters, samples were prepared and probed as described in B (upper panel), the PGK protein was probed as a loading control (lower panel). **D.** Dose-dependent inhibition of yeast growth in neutral pH medium by SidK. The growth of yeast strains expressing SidK from vectors differing in promoter strength (Materials and Methods) was examined as described in A. Lanes: 1, pADH-SidK(CEN/ARS); 2, pTEF(translation elongation factor 1 $\alpha$ )-SidK(CEN/ARS); 3, pTEF-SidK(2  $\mu$ ); 4, pGPD-SidK(2  $\mu$ ); 5, pGPD. Data shown are one representative experiment done in triplicates with standard variations shown.



**Figure A.2. SidK is translocated into infected cells by the Dot/Icm transporter. A.** SidK promoted the translocation of the pertussis toxin Cya into host cells. Differentiated U937 cells were infected with indicated *L. pneumophila* strains at an MOI of 5 for 1 hr. Cyclic AMP present in lysates of infected cells was measured by ELISA. Lower panel, expression of Cya fusions in *L. pneumophila* detected with a Cya specific antibody. **B–D.** Fusion to SidK restores the translocation of the transfer deficient Sid $\Delta$ C100. U937 macrophages were infected with bacteria expressing SidC, Sid $\Delta$ C100 or Sid $\Delta$ C100::SidK for one hr; *L. pneumophila* and SidC was differently labeled by immunostaining. At least 150 vacuoles in triple samples were scored in each experiment. Representative images of vacuoles harboring *sidC* $\Delta$ C100 (C) or *sidC* $\Delta$ C100::*sidK*(D); bacteria were labeled in red and SidC was stained in green. **E.** Dot/Icm-dependent translocation of SidK into infected cells. U937 cells were infected with indicated *L. pneumophila* strains at an MOI of 5 for 3 hrs. Cleared supernatant obtained with 0.2% saponin was subjected to immunoprecipitation with a SidK specific antibody. Proteins associated with the precipitates were detected by the SidK antibody (upper panel). The Hsp70 in the cell lysates was probed as a loading control and the cytosolic protein ICDH was probed to assess the integrity of the bacterial cells. Note that SidK is present in pellets of all infections except for the deletion mutant (3<sup>rd</sup> lane, lower panel). Lanes: 1, Lp02(*dot/icm*<sup>+</sup>); 2, Lp03(*dot/icm*<sup>-</sup>); 3, Lp02 $\Delta$ sidK; 4, Lp02 $\Delta$ sidK/pSidK. \*, bacterial lysate. The sizes (in kDa) of relevant protein markers are labeled on the left side of the blots.

Figure A.2

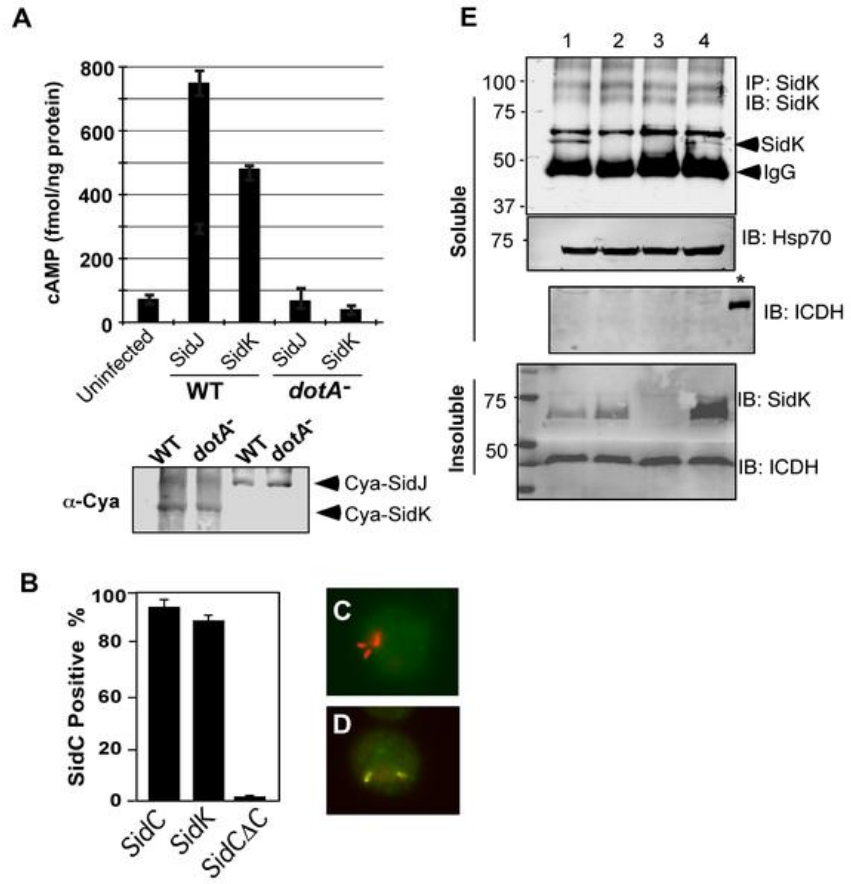


**Figure A.3**

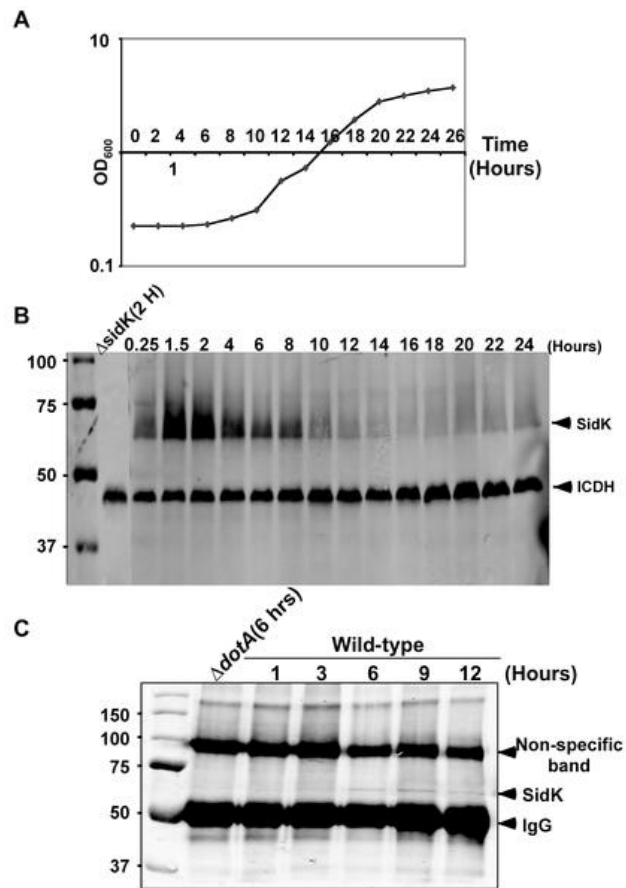


**Figure A.3. Expression of *sidK* is induced within hours at the initial phase of bacterial growth.** **A.** The growth cycle of *L. pneumophila* in AYE broth. Cultures grown at stationary phase was diluted 1:20 into fresh medium and the growth of bacteria was monitored by measuring OD<sub>600</sub> at indicated time points. **B.** The expression of SidK at different bacterial growth phase. Lysates were prepared from equal amount of cells withdrawn at the indicated time points and were resolved by SDS-PAGE, the level of SidK was detected by immunoblot with a specific antibody. Lysates of the *sidK* deletion mutant grown for 2 hrs after dilution was used as a control. The metabolic protein isocitrate dehydrogenase (ICDH) was probed as a loading control. **C.** Kinetics of SidK translocation during infection. Lysates of U937 cells infected by the *dotA* mutant or wild type *L. pneumophila* for indicated time were immunoprecipitated with  $\alpha$ -SidK and probed by immunoblot. Note the non-specific band about 100 kDa can serve as a loading control. The sizes (in kDa) of relevant protein markers were labeled on the left side of the blots.

**Figure A.4. The vacuolar H<sup>+</sup>-ATPase is the cellular target of SidK.** **A.** Subunits of the v-ATPase V<sub>1</sub> domain were retained by agarose beads coated with SidK. Affigel beads blocked with Tris-HCl buffer (lane 1) or coated with SidK (lane 3) were incubated with mammalian cell lysates. SidK coated beads incubated with lysis buffer (lane 2) served as a second control. After washing with lysis buffer, proteins separated by SDS-PAGE were visualized by silver staining; bands only retained by the SidK coated beads were identified by MALDI/mass spectrometry analysis. **B.** SidK and VatA form protein complexes in mammalian cells. Lysates of 293T cells transfected to express GFP-SidK or/and Flag-VatA were subjected to immunoprecipitation with an anti-Flag antibody, the presence of SidK in precipitated proteins was detected with GFP specific antibody. **C.** SidK forms protein complexes with endogenous VatA. Lysates of cells transfected with combinations of plasmids were precipitated with a SidK specific antibody, and proteins bound to beads were detected for VatA. Note that VatA also was precipitated in cells only transfected to express GFP-SidK (lane 3). **D.** SidK formed complexes with Vma1 of yeast v-ATPase. Lysates of yeast strains expressing GFP or GFP-SidK were coimmunoprecipitated with an anti-GFP antibody, and the presence of Vma1 in the precipitates was detected. In all cases, 5% (50 µg) of total protein was probed as input controls. Relevant protein size markers (in kDa) were indicated.

Figure A.4

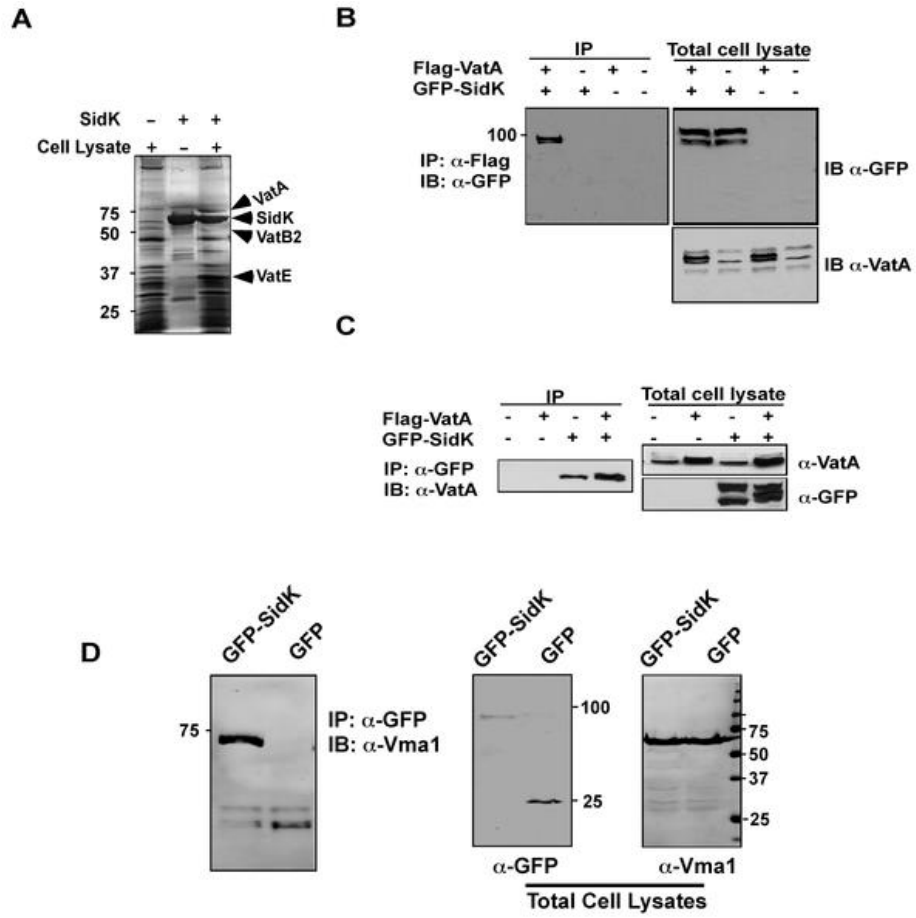


**Figure A.5**

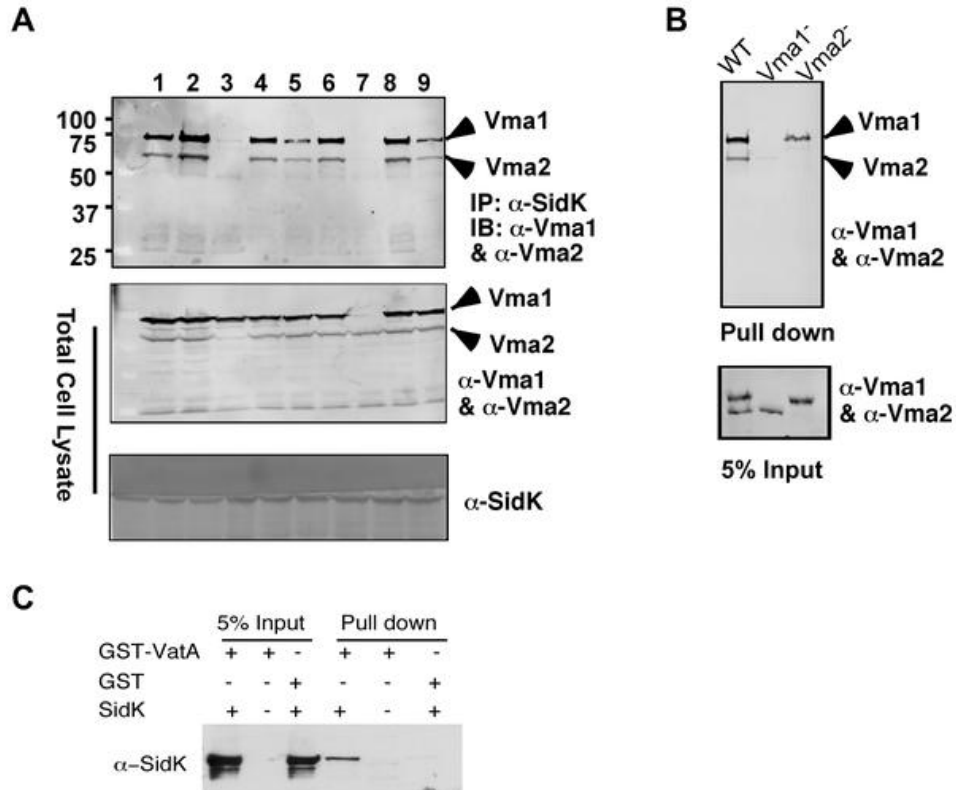


**Figure A.5. SidK directly interacts with VatA, the ATP hydrolyzing subunit of v-ATPase.** **A.** SidK interacts with Vma1 in the absence of other  $V_1$  subunits. Lysates of individual *vma* mutant expressing SidK were coimmunoprecipitated with the anti-SidK antibody and the presence of Vma1 and Vma2 in the precipitates were detected with specific antibodies. Lanes: 1,  $\Delta vma4$ ; 2, wild type; 3,  $\Delta vma2$ ; 4,  $\Delta vma5$ ; 5,  $\Delta vma7$ ; 6,  $\Delta vma8$ ; 7,  $\Delta vma1$ ; 8,  $\Delta vma10$ ; 9,  $\Delta vma13$ . The presence of SidK, Vma1 and Vma2 in the samples were probed with 5% proteins used for immunoprecipitation. **B.** SidK coated beads retained Vma1. Affigel beads coated with SidK were incubated with cell lysates of wild type  $\Delta vma1$  or  $\Delta vma2$  mutant. Proteins associated with the beads after extensive wash were probed for Vma1 and Vma2. 5% of lysates was used to probe for the presence of these proteins. Relevant protein size markers (in kDa) were indicated. **C.** SidK directly interacts with VatA. His<sub>6</sub>-SidK was incubated with GST-VatA or GST in PBS and potential protein complexes captured with glutathione beads were detected with specific antibody.

**Figure A.6**

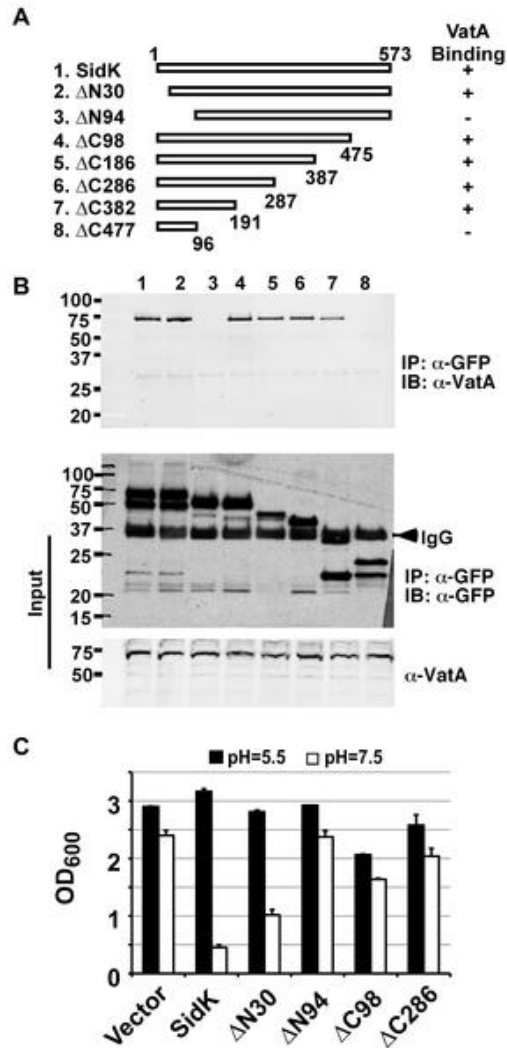


**Figure A.6. SidK binds to VatA via a N-terminal domain.** **A.** Diagrams of *sidK* truncation mutants. The numbers at the ends of the bars are the numbers of remaining amino acids for the mutants. +: binds VatA; -, no longer binds VatA. **B.** Interactions between VatA and the SidK deletion mutants. Lysates of 293T cells expressing each of the mutants fused to GFP were subjected to coimmunoprecipitation with an anti-GFP antibody and the presence of VatA in the precipitates were probed. The middle panel shows protein levels of the mutants probed with a GFP specific antibody after immunoprecipitation. Note that the several mutants that no longer interact with Vma1 still code for stable proteins. Endogenous VatA also was probed as input controls (lower panel). **C.** Inhibition of yeast growth in neutral pH medium by SidK mutants. Indicated mutants (without any tag) were cloned into p425GPD and yeast growth was assayed as described in Fig. A.1.

Figure A.7

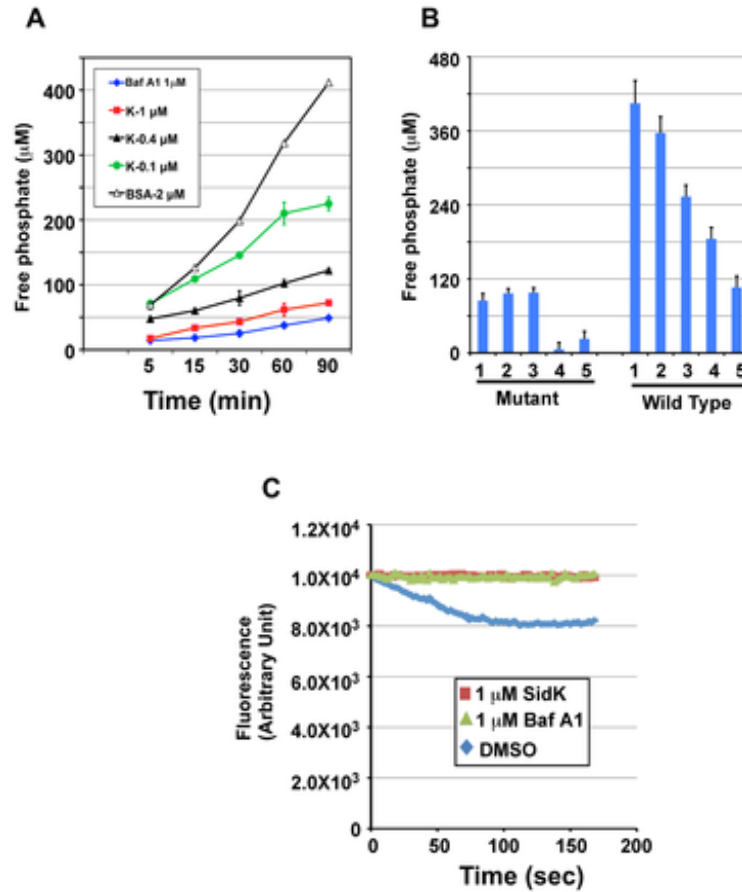


**Figure A.7. SidK inhibits v-ATPase-mediated ATP hydrolysis and proton translocation.** **A.** SidK inhibits ATP hydrolysis in yeast vesicle membranes. BSA, Baf A1 or three different concentrations of His<sub>6</sub>-SidK was incubated with yeast vesicle membranes, ATP was added to initiate the reaction. The concentration of free phosphate in samples withdrawn at indicated time points was determined by the malachite green method (Materials and Methods). **B.** SidK specifically inhibits ATPase activity of v-ATPase. Yeast vesicle membranes prepared from wild type or the *vma1* mutant were used for similar assays. Note that SidK and the v-ATPase specific inhibitor Baf A1 block ATPase activity in membranes from the wild type but not the *vma1* mutant. Lanes (mutant): 1, 1  $\mu$ M SidK; 2, 1  $\mu$ M Baf A1; 3, 1  $\mu$ M BSA; 4, 10 mM EDTA; 5, 1 mM vanadate. Lanes (wild type): 1, 1  $\mu$ M BSA; 2, 0.1  $\mu$ M SidK; 3, 0.4  $\mu$ M SidK; 4, 1  $\mu$ M SidK; 5, 1  $\mu$ M Baf A1. **C.** SidK prevents v-ATPase-mediated proton translocation. ATP was added to reactions containing vacuolar membrane vesicles, acridine orange and the indicated reagents that had been preincubated for 40 min at room temperature. The quenching of acridine orange fluorescence was monitored as described in Experimental Procedures.



**Figure A.8. Macrophages loaded with SidK are defective in phagosomal acidification and lysosomal digestion of bacteria.** **A–B.** Phagosomal acidification in macrophages assessed by pH sensitive fluorescein dextran and LysoRed staining. Mouse bone marrow-derived macrophages were loaded with His<sub>6</sub>-SidK or BSA by syringe loading. Treated cells were incubated with a mixture of fluorescein dextran and cascade blue dextran (0.2 mg/ml) for 1 h, washed 5 times and incubated at 37°C for 4 hrs before being imaged. As a control, Baf A1 (250 nM) was added 40 min before taking the images (A). *E. coli* cells expressing GFP were incubated with loaded macrophages at an MOI of 20 for 1 hr at 37°C. After incubating with gentamicin for 8 hrs, cells were stained with LysoRed (50 nM) for 15 min. Images were acquired using a fluorescence microscope with identical parameters (B). Bar, 5 μm. **C.** SidK affects bacterial killing by macrophages. Loaded macrophages were fed with *E. coli* cells expressing mCherry RFP at an MOI of 10 for 1 hr at 37°C. Samples were treated with gentamicin for 1 h and were extensively washed. Viable *E. coli* cells were evaluated by plating macrophage lysates on bacteriological media at indicated time points. **D.** Digestion of bacteria by macrophages. Samples prepared similarly as C were used to evaluate the ratios of macrophages that contain intact *E. coli* cells. Cells harboring one or more bacterial cells were quantitated at indicated time points. Experiments were performed in triplicates and at least 200 cells were examined each sample. The *P* values of the relevant data points are indicated. Similar results were obtained in more than three independent experiments. **E.** Representative images of macrophages fed with fluorescent *E. coli* cells. Samples at indicated time points were processed and analyzed under a fluorescence microscope and images of typical cells were acquired. Bar, 5 μm.

Figure A.8

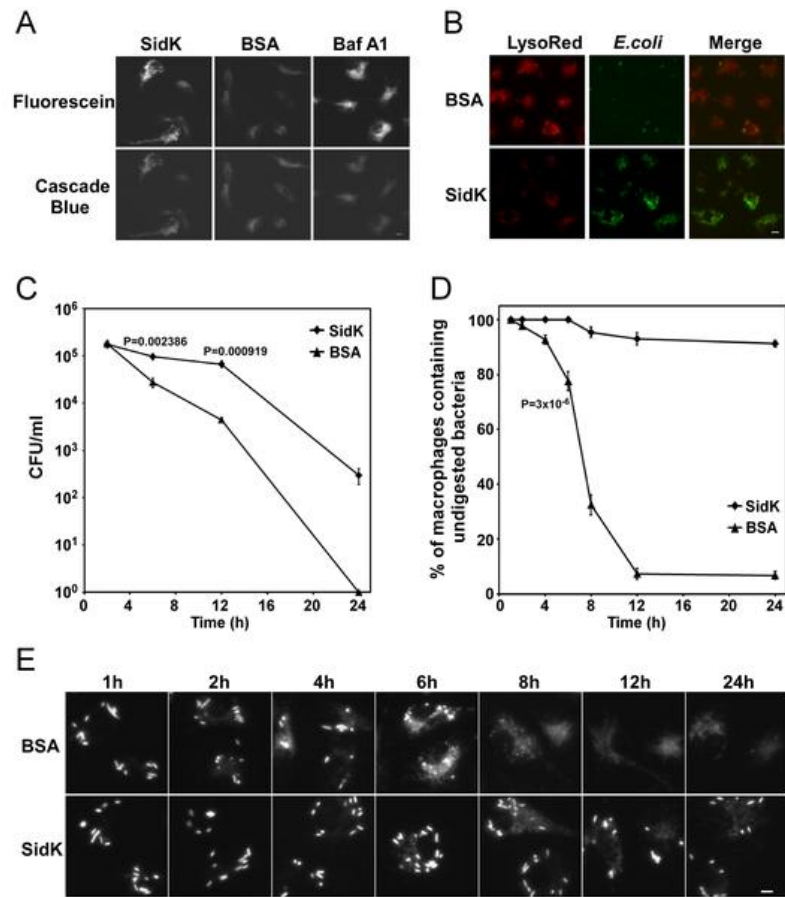


**Table A.S1. *L. pneumophila* proteins tested for conferring yeast sensitivity to neutral pH.**

Number	Lpg number	Number	Lpg number	Number	Lpg number
1	lpg0008	34	lpg1496	67	lpg2424
2	lpg0012	35	lpg1602	68	lpg2464
3	lpg0086	36	lpg1666	69	lpg2523
4	lpg0096	37	lpg1683	70	lpg2526
5	lpg0149	38	lpg1684	71	lpg2527
6	lpg0150	39	lpg1687	72	lpg2529
7	lpg0196	40	lpg1705	73	lpg2568
8	lpg0269	41	lpg1717	74	lpg2582
9	lpg0284	42	lpg1751	75	lpg2603
10	lpg0360	43	lpg1809	76	lpg2622
11	lpg0634	44	lpg1949	77	lpg2627
12	lpg0642	45	lpg1958	78	lpg2637
13	lpg0696	46	lpg1963	79	lpg2719
14	lpg0771	47	lpg1969	80	lpg2744
15	lpg0774	48	lpg1979	81	lpg2745
16	lpg0788	49	lpg1986	82	lpg2758
17	lpg0944	50	Lpg2050	83	lpg2759
18	lpg0968	51	lpg2148	84	lpg2804
19	lpg0969	52	lpg2155	85	lpg2826
20	lpg0974	53	lpg2160	86	lpg2844
21	lpg1073	54	lpg2161	87	lpg2853
22	lpg1109	55	lpg2166	88	lpg2856
23	lpg1129	56	lpg2220	89	lpg2864
24	lpg1145	57	lpg2223	90	lpg2877
25	lpg1148	58	lpg2239	91	lpg2879
26	lpg1183	59	lpg2242	92	lpg2912
27	lpg1227	60	lpg2248	93	lpg2913
28	lpg1228	61	lpg2313	94	lpg2939
29	lpg1234	62	lpg2399	95	lpg2959
30	lpg1265	63	lpg2400	96	lpg2976
31	lpg1329	64	lpg2410	97	lpg3000
32	lpg1354	65	lpg2422		
33	lpg1481	66	lpg2423		

**Table A.S2. Bacterial and yeast strains used in this study.**

Strains	Genotype, relevant markers	Reference
<i>E. coli</i>		
XL1-Blue	<i>recA1 endA1 gyrA96 thi-1 hsdR17 supE44 relA1 lac [F' proAB lacI<sup>q</sup>ZM15 Tn10(Tet<sup>r</sup>)]</i>	Stratagene
DH5α(λpir)	<i>supE44 dlacU169(φ80lacZΔM15) hsdR17 recA1 endA1 gyrA96 thi-1 relA1 pir tet::Mu recA</i>	Our collection
<i>L. pneumophila</i>		
Lp02	Philadelphia-1 <i>rpsL hsdR thyA</i>	(Berger and Isberg, 1993)
ZL25	LP02Δ <i>sidC</i>	(Luo and Isberg, 2004)
ZL25(pZL199)	LP02Δ <i>sidC</i> (pZLSidC)	(VanRheenen, <i>et al.</i> , 2006)
ZL25(pZL204)	LP02Δ <i>sidC</i> (pSidCΔC100)	(VanRheenen, <i>et al.</i> , 2006)
ZL370	LP02Δ <i>sidC</i> (pZL204::K)	This study
ZL371	LP03(pZL204::K)	(VanRheenen, <i>et al.</i> , 2006)
Lp03	Lp02( <i>dotA</i> <sup>-</sup> )	(Berger and Isberg, 1993)
Lp02(pJB908)	Lp02(pJB908)	(Liu and Luo, 2007)
ZL14	Lp03(pJB908)	(Liu and Luo, 2007)
ZL114	Lp02Δ <i>sidK</i>	This study
ZL115	Lp02Δ <i>sidK</i> (pJB908)	This study
ZL207	Lp02Δ <i>sidK</i> (pJB908::K)	This study
ZL156	Lp02(pJB2581::K)	This study
ZL157	Lp03(pJB2581::K)	This study
ZL269	Lp03ΔK , pZL507::K	This study
Yeast		
PJ69-4A	<i>MATa GALI-HIS3 GAL2-ADE8 GAL7-lacZ leu2 ura3 his3 gal4 gal80</i>	(James, <i>et al.</i> , 1996)
BY4741	<i>MATa his3 1 leu2 0 met15 0 ura3 0</i>	(Winzeler, <i>et al.</i> , 1999)
BY4741	<i>vma1Δ::KanMX</i>	(Winzeler, <i>et al.</i> , 1999)
BY4741	<i>Vma2Δ::KanMX</i>	(Winzeler, <i>et al.</i> , 1999)
BY4741	<i>Vma4Δ::KanMX</i>	(Winzeler, <i>et al.</i> , 1999)
BY4741	<i>Vma5Δ::KanMX</i>	(Winzeler, <i>et al.</i> , 1999)
BY4741	<i>Vma7Δ::KanMX</i>	(Winzeler, <i>et al.</i> , 1999)
BY4741	<i>Vma8Δ::KanMX</i>	(Winzeler, <i>et al.</i> , 1999)
BY4741	<i>Vma10Δ::KanMX</i>	(Winzeler, <i>et al.</i> , 1999)
BY4741	<i>Vma13Δ::KanMX</i>	(Winzeler, <i>et al.</i> , 1999)

**Table A.S3. Plasmids used in this study.**

Plasmid	Relevant phenotypes	Sources
pQE30	Amp	Qiagen
pJB908	Amp, <i>thy</i> <sup>+</sup>	(Bardill, <i>et al.</i> , 2005)
pJB2581	Cm, Amp	(Bardill, <i>et al.</i> , 2005)
pGEX-4T-1	Amp	Qiagen
pZL204	Amp, <i>thy</i> <sup>+</sup> SidCΔ <i>C100</i> on pJB908	(Luo and Isberg, 2004)
pZL507	For expression His <sub>6</sub> -tagged protein <i>L. pneumophila</i>	This study
pEGFPC-1	For expressing C-terminal GFP fusion proteins	Clontech
p415-ADH	Amp, <i>leu</i> <sup>+</sup> , ADH promoter	(Mumberg, <i>et al.</i> , 1995)
p415-TEF	Amp, <i>leu</i> <sup>+</sup> , TEF promoter	(Mumberg, <i>et al.</i> , 1995)
p425-GPD	Amp, <i>leu</i> <sup>+</sup> , GPD promoter	(Mumberg, <i>et al.</i> , 1995)
p425-TEF	Amp, <i>leu</i> <sup>+</sup> , TEF promoter	(Mumberg, <i>et al.</i> , 1995)
pGBKT7	Km, <i>trp</i> <sup>+</sup>	Clontech
pZL796	pZL204::K, BamHI, XbaI	This study
pZL797	pGEX-4T-1::K, BamHI, XbaI	This study
pZL812	pGBKT7::K, EcoRI, BamHI	This study
pZL863	pEGFPc1::K, BglII, EcoRI	This study
pZL864	pCMVFlagM-VatA, BglII, SalI	This study
pZL866	pSR47s::SidK-knockout	This study
pZL1048	pQE-30::Hsp70, BamHI/SalI	This study
pZL1109	pCMVFlagM::VatC, BglII, SalI	This study
pZL1264	pEGFPc1::K-C1, BglII/BamHI, PstI	This study
pZL1265	pEGFPc1::K-C2, BglII/BamHI, PstI	This study
pZL1266	pEGFPc1::K-C3, BglII/BamHI, PstI	This study
pZL1272	pEGFPc1::K-N2, BglII/BamHI, EcoRI	This study
pZL1273	pEGFPc1::K-N1, BglII/BamHI, EcoRI	This study
pZL1281	pEGFPc1::K-C4, BglII/BamHI, EcoRI	This study
pZL1282	pEGFPc1::K-C5, BglII/BamHI, EcoRI	This study
pZL1283	pEGFPc1::K-N30, BglII/BamHI, EcoRI	This study
pZL1333	pZL507::K, BamHI, SalI/XhoI	This study
pZL1463	p415-ADH::K, BamHI, SalI/XhoI	This study

PZL1508	p416-ADH::Flag-Vma5, BamHI, Sall/XhoI	This study
pZL1517	p415-ADH::GFP-K, BamHI/BglII, Sall/XhoI	This study
pZL1518	p415-ADH::GFP-KN30, BamHI/BglII, Sall/XhoI	This study
pZL1519	p415-ADH::GFP-KC2, BamHI/BglII, PstI	This study
pZL1520	p415-ADH::GFP-KC3, BamHI/BglII, PstI	This study
pZL1521	p415-ADH::GFP-KC4, BamHI/BglII,PstI	This study
pZL1543	p415-ADH::GFP-KN1, BamHI/BglII, Sall/XhoI	This study
pZL1544	p415-ADH::GFP-KN2, BamHI/BglII, Sall/XhoI	This study
pZL1546	p415-ADH::GFP-KC5, BamHI/BglII, PstI	This study
pZL1572	p415-ADH::GFP, BamHI/BglII, Sall	This study
pZL1585	p415-TEF::K, BamHI, Sall/XhoI	This study
pZL1586	p425-GPD::K, BamHI, Sall/XhoI	This study
pZL1587	p425-TEF::K, BamHI, Sall/XhoI	This study
pZL1593	p425-GPD::KN1, BamHI, Sall/XhoI	This study
pZL1594	p425-GPD::KC1, BamHI, Sall/XhoI	This study
pZL1596	p425-GPD::KC3, BamHI, Sall/XhoI	This study
pZL1628	p425-GPD::KN30, BamHI, PstI	This study
pZL1645	p416-ADH::Flag-Vma4, BamHI, Sall/XhoI	This study

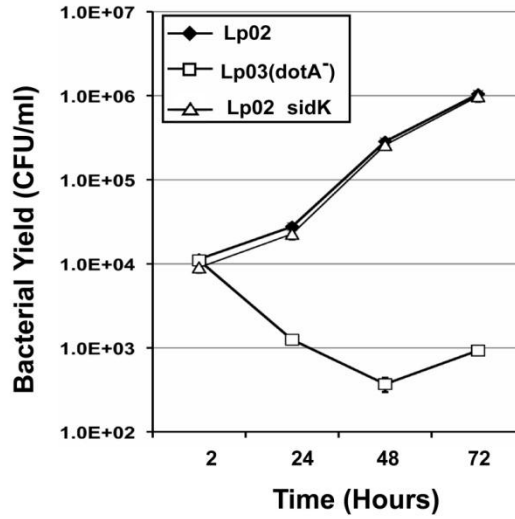
---

**Table A.S4. Primers used in this study.**

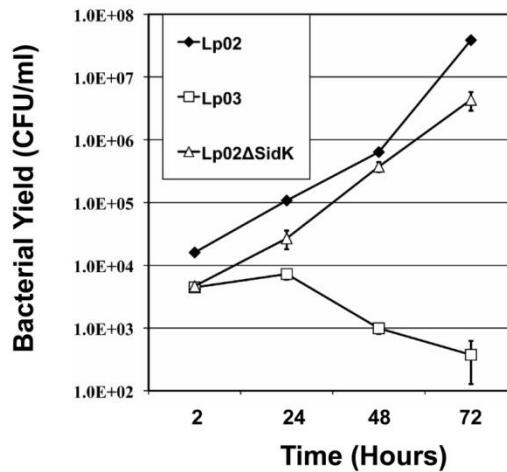
Primer	Sequence (Restriction enzyme sites are underlined)	Note
QE3	CTCT <u>CTAGAG</u> TTCTTTACGATGCCATTGGG	QE3'XbaI
QE5	CTAGGATATCCGGAAATGTTGAATACTCATAC	QE5'EcoRV
PL130	CTGGGATCCTTGTCTTTTATCAAGGTAGG	sidK5'BamHI
PL131	CTGT <u>CTAGAT</u> TAAAGGCTTAGGCTTTCTT	sidK3'XbaI
PL142	CTGGA <u>ATTCT</u> TGTCTTTTATCAAGGTAG	sidK5'EcoRI
PL143	CGCGGATCCTTAAAGGCTTAGGCTTTC	sidK3'BamHI
PL177	CTAGAGATCTATGGATTTTTCCAAGCTACC	VatA 5'BglII
PL178	CCTGGT <u>CGAC</u> CTTCTAATCTTCAAGGCTAC	VatA 3'SalI
PL192	CCTGGT <u>CGAC</u> CGCAAAGAACCGGGAAGAG	sidK up SalI knock-out
PL193	CTAGGATCCCAGAACCTGTGTGGATC	sidK up BamHI knock-out
PL194	CTAGGATCCAGCCACCCATTTTTATAACC	sidK down BamHI knock-out
PL195	CTAGAGCTCGCTTTATCTCTGTTTCAGG	sidK down SacI knock-out
PL208	CTAGAGATCTAACTGAGTCTGGCTTATAATCTG	VatC1FBglII
PL209	CCTGGT <u>CGACT</u> CACTTGAATCCAGCAAGTTG	VatC1RSalI
PL312	CTGGGATCCGCCAAAGCCGCGCGATCGG	Hsp70 5' BamHI
PL313	CTGGT <u>CGAC</u> CTAATCTACCTCCTCAATGG	Hsp70 3' SalI
PL391	ACCGGATCCATGTCTTTTATCAAGGTAGG	sidK 5'BamHI
PL494	GCC <u>CTGCAG</u> TAAAGGCTTAGGCTTTCTTCC	sidK 3' PstI
PL495	AGGCT <u>CGAG</u> TAAAGGCTTAGGCTTTCTTCCTG	sidK 3' XhoI
PL526	GCCGGATCCATGAGATGCATGCAAATATAGATC	sidK-N30 5' BamHI
PL528	CCAGGATCCATGGTTTCATCAATTAGTCCC	sidK-N100 5' BamHI
PL416	GCCGGATCCATGATAGATGAACAATATCACCTG	sidK-N200 5' BamHI
PL529	ACCGGATCCATGATCAGGAAATTGAAGTG	sidK-N300 5' BamHI
PL530	CGGCTGCAGTTACCCAAGAAGCTAATACAATTC	sidK-C100 3' PstI
PL531	CA <u>ACTGCAG</u> TACTATGGAGTAATATCTTC	sidK-C200 3' PstI
PL532	AGGCTGCAGTTAATCCAGGCCAAATTTACC	sidK-C300 3' PstI
PL533	GTGCTGCAGTTATGAAACAAGCCGAGCAATTC	sidK-C400 3' PstI
PL534	GT <u>CCTGCAG</u> TTATGAAACAAGCCGAGCAATTC	sidK-C500 3' PstI
PL556	GGCGGATCCATGGACTACAAAGACGATGACGA CAAGGCTACTGCGTTATATACTGC	M2-Vma5 5'BamHI
PL564	GCACTCGAGTTATTCGTTAGCCATTGCGAGC	sidK-C4 3'XhoI
PL565	CGGCTCGAGTTAATCCAGGCCAAATTTACC	sidK-C3 3'XhoI
PL571	TCAAGATCTATGGTGAGCAAGGGCGAGGAG	GFP 5'BglII
PL572	GACGGATCCATGGACTACAAAGACGATGACGAC AAGTCCTCCGCTATTACTGCTTTGAC	M2-Vma4 5'BamHI
PL574	GCCG <u>CTGACT</u> CAATCAAAGAACTTTCTTG	Vma4 3'XhoI

Figure A.S1

A



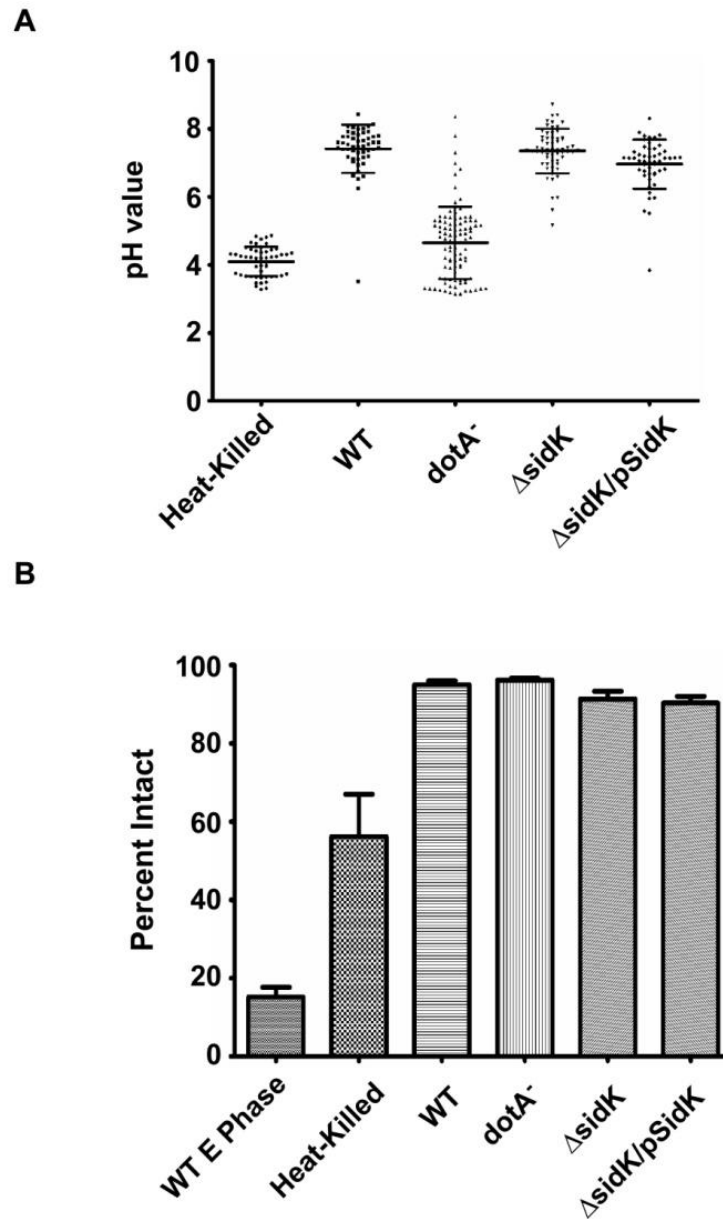
B



**Figure A.S1.** Deletion of *sidK* did not affect intracellular growth of *L. pneumophila*. Indicated bacterial strains grown to post-exponential phase were used to infect mouse macrophages (A) or *Dictyostelium discoideum* (B). Infections were synchronized 1 h after uptake and the total bacterial counts at indicated time points were determined by lysing infected cells with 0.02% saponin and plating appropriately diluted lysates on CYE plates. Data shown are one representative experiment done in triplicates. Similar results are obtained in more than three independent experiments.

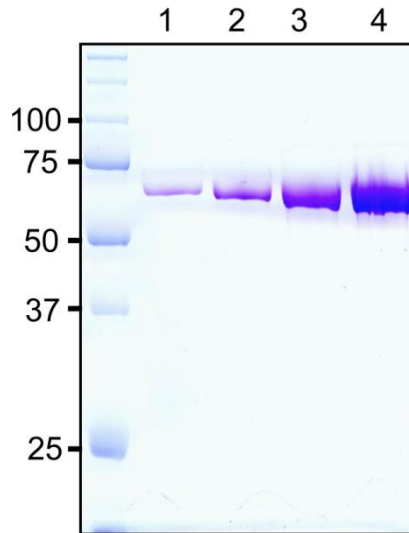


Figure A.S2



**Figure A.S2.** Vacuoles containing the *sidK* deletion mutant maintain a neutral luminal pH. Mouse macrophages were infected with indicated *L. pneumophila* strains for 2 hours and vacuolar pH of the phagosomes was measured as described in Materials and Methods (A). The integrity of the internalized bacteria also was examined (B). More than 50 vacuoles were scored for each coverslip. Similar results were obtained in two independent experiments.

**Figure A.S3**



**Figure A.S3.** Purification of SidK from *L. pneumophila*. A derivative of the avirulent strain Lp03 containing pZL1333 that direct the expression of His<sub>6</sub>-SidK was grown in AYE broth and the expression of the protein was induced with IPTG for 16 hours. His<sub>6</sub>-SidK was first purified by a Ni<sup>2+</sup> column followed by FPLC with an AKTA system. Fractions containing the protein were pooled and dialysed in TBS buffer. Image shown are different amount of His<sub>6</sub>-SidK resolved SDS-PAGE and stained by Coomassie bright blue staining. Lanes: 1, 1 μg; 2, 2 μg; 3, 4 μg; 4, 8 μg.

**Figure A.S4**

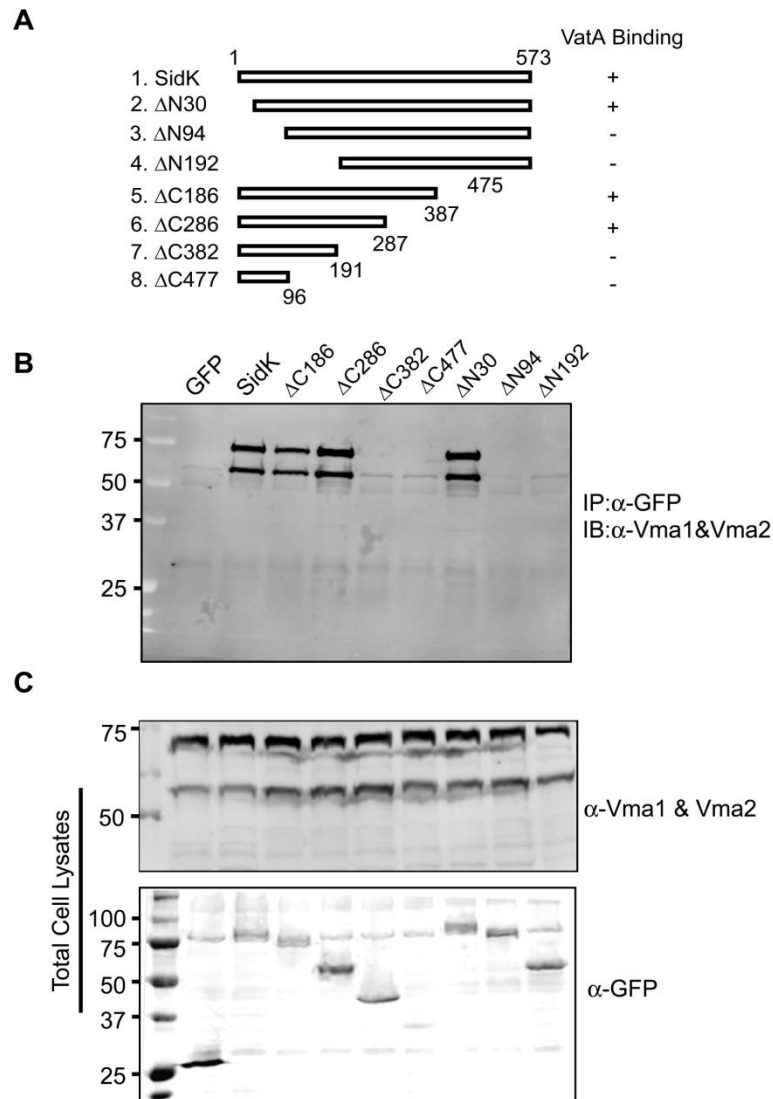


**Figure A.S4.** Interactions between v-ATPase and SidK deletion mutants in yeast. The indicated SidK deletion mutants (A) were expressed in yeast as GFP fusions. Total cell lysates were subjected to co-immunoprecipitation with a GFP specific antibody and the presence of Vma1 and Vma2 in the precipitates was detected by immunoblot (B). The presence of Vma1 and Vma2 in the cell lysates was detected (C, upper panel) and the expression of the SidK truncations was evaluated with the GFP specific antibody (B, lower panel).

**Figure A.S5**

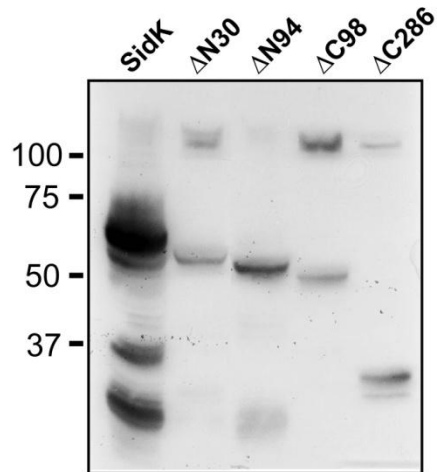


**Figure A.S5.** Expression of *sidK* mutants in yeast. Indicated mutants were cloned into p425GPD, a start codon (ATG) was added to N-terminal deletion mutant. Samples were processed as described for Fig. 1 and proteins were detected with an anti-SidK antibody.

**Figure A.S6**

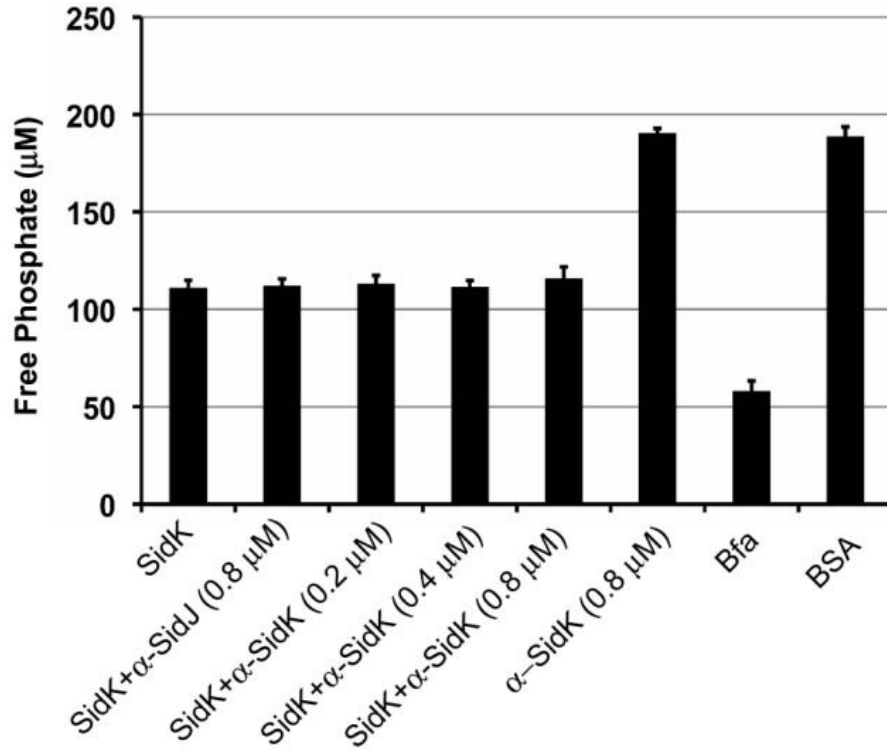


**Figure A.S6.** The SidK specific antibody did not affect SidK activity. v-ATPase assays were performed as described in Fig. 7A. 0.4 µM of SidK was used in each reaction. Indicated amount of antibody specific for SidJ or SidK was added 20 min after the addition of SidK. Reactions were allowed to proceed for 60 min and the release of free phosphate was measured.

**Figure A.S7**

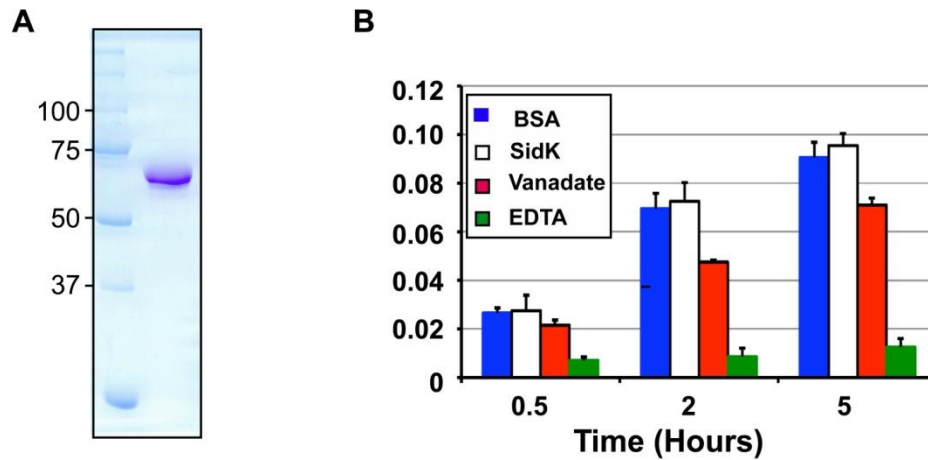


**Figure A.S7.** SidK does not affect ATPase activity of Hsp70. Mammalian Hsp70 was purified from *E. coli* as a His<sub>6</sub>-tagged protein (A). 0.5 ug of purified protein was incubated with 2 mM ATP and the indicated compounds or proteins for various periods of time (X-axis). Hydrolysis of ATP was monitored by measuring released free phosphate with malachite green (B). Similar results were obtained in two experiments done in triplicates. Concentrations of testing materials: BSA, 1  $\mu$ M; SidK, 1  $\mu$ M; Vanadate, 1 mM; EDTA, 10 mM.

## APPENDIX B:

### ***L. pneumophila* major facilitator superfamily protein Lpg0273 provides protection from toxic concentrations of nicotinic acid**

#### SUMMARY

High concentrations of nicotinic acid inhibit growth and stimulate differentiation of *Legionella pneumophila* from the replicative to transmissive phase. In response to nicotinic acid, the bacteria induce expression of the gene *lpg0273*, which is predicted to encode a major facilitator superfamily protein. Indeed, Lpg0273 likely functions as an efflux pump to combat toxic accumulation of nicotinic acid or related metabolites, as judged by the response of the corresponding mutant bacteria to nicotinic acid.

#### INTRODUCTION

The ability of *L. pneumophila* to differentiate between replicative and transmissive forms is critical for its ability to efficiently infect its phagocytic hosts (Molofsky and Swanson, 2004). Central to this transition is the LetA/S two-component system, which is predicted to sense environmental triggers and relay the message to subsequent regulatory components (Edwards, *et al.*, 2010, Hammer, *et al.*, 2002, Lynch, *et al.*, 2003). Nicotinic acid can trigger the analogous two-component systems that regulate virulence in *Bordetella* (Cotter and DiRita, 2000, Cummings, *et al.*, 2006, McPheat, *et al.*, 1983, Miller, *et al.*, 1989, Schneider and Parker, 1982) and multi-drug

resistance in *E. coli* (Eguchi, *et al.*, 2003, Masuda and Church, 2002, Masuda and Church, 2003, Nishino, *et al.*, 2003, Nishino and Yamaguchi, 2001, Utsumi, *et al.*, 1994). Since the concentrations of nicotinic acid needed to trigger these responses are generally considered to be non-physiologic, nicotinic acid may be a surrogate for some other environmental signal.

Edwards (2008) recently demonstrated that nicotinic acid can also stimulate the differentiation of *L. pneumophila* from the replicative to transmissive phase in a LetA/S-dependent manner. For example, nicotinic acid induces the virulence-associated traits of macrophage cytotoxicity and lysosome evasion. Microarray analysis of the *L. pneumophila* response to 5 mM nicotinic acid revealed a transcriptional profile unique from cells that had naturally transitioned to the post-exponential phase. The two most highly induced genes, *lpg0272* and *lpg0273*, are annotated as a cysteine transferase and a major facilitator superfamily (MFS) transporter, respectively (Fig. B.1). Protein alignment of Lpg0273 (Altschul, *et al.*, 1997) shows the most significant similarity to a putative MFS from the phylogenetically related *Coxiella burnetii* (ZP\_02219825.1). Structural prediction (Kelley and Sternberg, 2009) yields significant homology to the solved structure of the MFS multi-drug transporter EmrD from *E. coli* (Yin, *et al.*, 2006). To test more directly whether Lpg0273 or Lpg0272 might equip *L. pneumophila* to respond to nicotinic acid, isogenic mutants were constructed and their growth characterized after exposure to a range of concentrations of NA.



## METHODS

### Bacterial strains and plasmids.

*L. pneumophila* strain Lp02 and derivatives were cultured as previously described (Byrne and Swanson, 1998); *E. coli* DH5 $\alpha$ , HB101 and derivatives were cultured using standard laboratory conditions. Chloramphenicol (5 and 25  $\mu$ g/ml), gentamycin (10  $\mu$ g/ml), ampicillin (100  $\mu$ g/ml), streptomycin (0.5 and 1 mg/ml), and metronidazole (10  $\mu$ g/ml) were used for selection of *L. pneumophila* and *E. coli*, respectively. A shuttle vector for IPTG-inducible expression of *lpg0273* was constructed by standard methods using pMMBGent (pMB741). An isogenic mutant of *lpg0272* in strain Lp02 was generated by constructing recombinant alleles in *E. coli* after cloning into pGEM T easy (Promega, Madison, WI) and replacing the desired sequence with a resistance cassette by recombineering (Bryan, *et al.*, 2011). An in-frame unmarked deletion in *lpg0273* was made by first replacing the first 1200 bp of the coding sequence with a *cat-rdxA-rpsL* cassette by recombineering and verifying the phenotype in HB101  $\lambda$ *pir endA::frt* (MB740) (Bryan, *et al.*, 2011, Bryan and Swanson, 2011). The recombinant selectable/double counter-selectable allele was then transferred to Lp02 by natural transformation (Sexton and Vogel, 2004), yielding *lpg0273::cat-rdxA-rpsL* (MB866). To remove the cassette, an allele containing a precise 1200 bp deletion was constructed by overlap-extension PCR, transferred to MB866 by natural transformation, and the mutant strain selected on metronidazole- and streptomycin-containing plates. The resulting in-frame deletion was confirmed by antibiotic resistance phenotype, PCR, and sequencing.

### **Growth curves.**

Bacterial strains were cultured to mid-exponential phase in AYET. Cultures were back-diluted and their cell density normalized in triplicate using a dilution factor of 0.00696. A Bioscreen Growth Curve Analyzer, set at continuous shaking at medium amplitude, measured optical density at 600 nm every hour over a 48 hour time period.

## **RESULTS**

To substantiate the transcriptional response of *L. pneumophila* to nicotinic acid and to more directly test whether the putative *lpg0272-3* operon contributes to nicotinic acid metabolism, isogenic mutations in each gene were constructed and their growth phenotype in response to a range of concentrations of nicotinic acid analyzed. The growth behavior of cells containing mutations in *lpg0272* did not appreciably differ from wild-type cells (data not shown). However, a mutant with an in-frame deletion of *lpg0273* was consistently more sensitive to nicotinic acid than wild-type cells, as assessed by OD<sub>600</sub> (Fig. B.2). The growth defect showed a consistent dose-response relationship and was complemented by providing *lpg0273* in *trans* (Fig. B.2). Furthermore, both mutant and wild-type *L. pneumophila* induced to express *lpg0273* displayed a slight growth advantage compared to vector control cells, even in the absence of nicotinic acid (Fig. B.2).

## DISCUSSION

Gene annotation and protein prediction suggest Lpg0273 belongs to the major facilitator superfamily of proteins (Altschul, *et al.*, 1997, Chien, *et al.*, 2004, Kelley and Sternberg, 2009, Wass, *et al.*, 2010). Moreover, it is structurally similar to the multi-drug efflux pump EmrD (Kelley and Sternberg, 2009, Yin, *et al.*, 2006). Previous data from our lab revealed that *lpg0273* is up-regulated when replicating *L. pneumophila* are exposed to nicotinic acid (Edwards, 2008). Here, I show that plasmid-born *lpg0273* confers a growth advantage to cells when exposed to nicotinic acid (Fig. B.2). The heightened, but not complete, sensitivity of the *lpg0273* mutant to nicotinic acid is consistent with its function as a contributing, but not sole, transporter of nicotinic acid or related metabolites. The mild growth advantage to cells over-expressing *lpg0273* in the absence of nicotinic acid suggest that this putative transporter may contribute to other aspects of metabolism, perhaps efflux of toxic compounds or nutrient uptake.

**Table B.1. Bacterial strains and plasmids.**

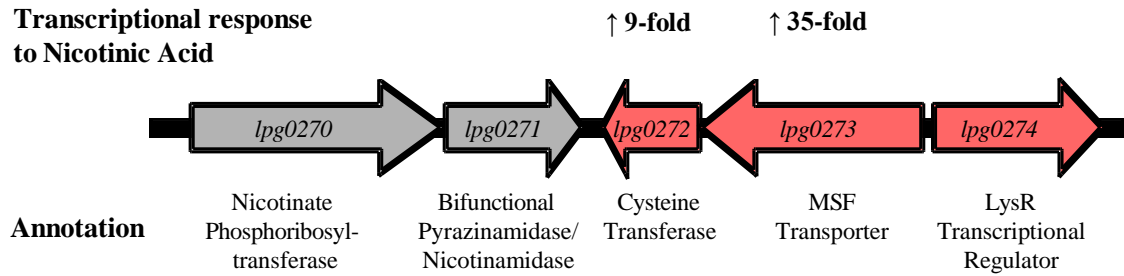
Strain	Genotype or plasmid	Source
<i>E. coli</i> and plasmids		
DH5 $\alpha$	<i>supE44 ΔlacU169 (80 lacZΔM15) hsdR17 recA1 endA1 gyrA96 thi-1 relA1</i>	Laboratory collection
DY330	W3110 <i>ΔlacU169 gal490 λcI857 Δ(cro-bioA)</i>	(Yu, <i>et al.</i> , 2000)
	pGEM-T easy	Promega
	pKD3 ( <i>FRT-cat-FRT</i> allele)	(Datsenko and Wanner, 2000)
MB739	HB101 <i>endA::frt</i>	(Bryan and Swanson, 2011)
MB741	DH5 $\alpha$ pMMBGent	(Bryan and Swanson, 2011)
MB776	HB101 <i>λpir endA::frt pR6KcatrdxArpsL</i>	(Bryan and Swanson, 2011)
MB870	DH5 $\alpha$ pGEMlpg0272-3	This work
MB871	DH5 $\alpha$ pGEMlpg0272:: <i>FRT-cat-FRT</i>	This work
MB872	HB101 <i>endA::frt pGEMlpg0273::cat-rdxA-rpsL</i>	This work
MB873	DH5 $\alpha$ pMMBGent-lpg0273	This work
<i>L. pneumophila</i>		
MB110	Lp02 wild type, <i>thyA, hsdR, rpsL</i> (Str <sup>R</sup> )	(Berger and Isberg, 1993)
MB864	Lp02 <i>Δlpg0272::FRT-cat-FRT</i>	This work
MB865	Lp02 <i>Δlpg0272::FRT</i>	This work
MB866	Lp02 <i>lpg0273::cat-rdxA-rpsL</i>	This work
MB867	Lp02 <i>Δlpg0273</i>	This work
MB860	Lp02 pMMBGent	This work
MB861	Lp02 pMMBGent-lpg0273	This work
MB862	Lp02 <i>Δlpg0273</i> pMMBGent	This work
MB863	Lp02 <i>Δlpg0273</i> pMMBGent-lpg0273	This work

\*Kaoru Harada contributed to construction of strains in this table.

**Figure B.1**

**A.**

**Transcriptional response  
to Nicotinic Acid**



**B.**

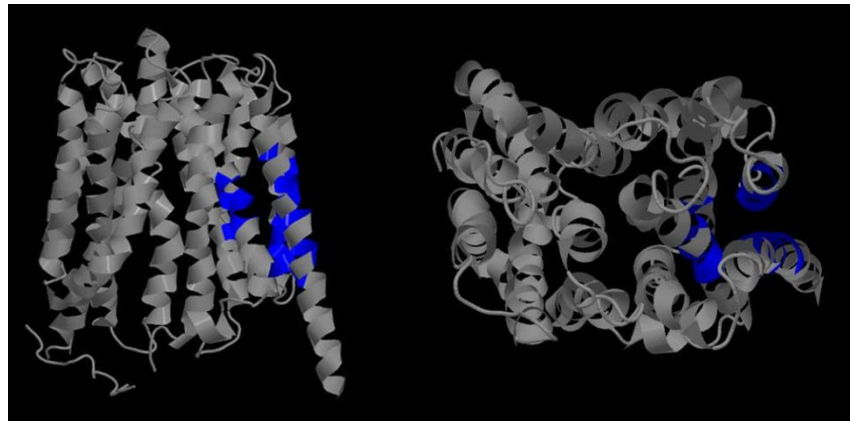


**Figure B.1.** **A)** Chromosomal locus of *lpg0272-3* and transcriptional response upon supplementing wild-type cells with 5 mM nicotinic acid. Adapted from (Edwards, 2008). **B).** Predicted structure of Lpg0273 and ligand binding site (blue) using 3DLigandSite prediction software (Wass, *et al.*, 2010) showing predicted transmembrane helices typical of Major Facilitator Superfamily proteins.

**Figure B.2**

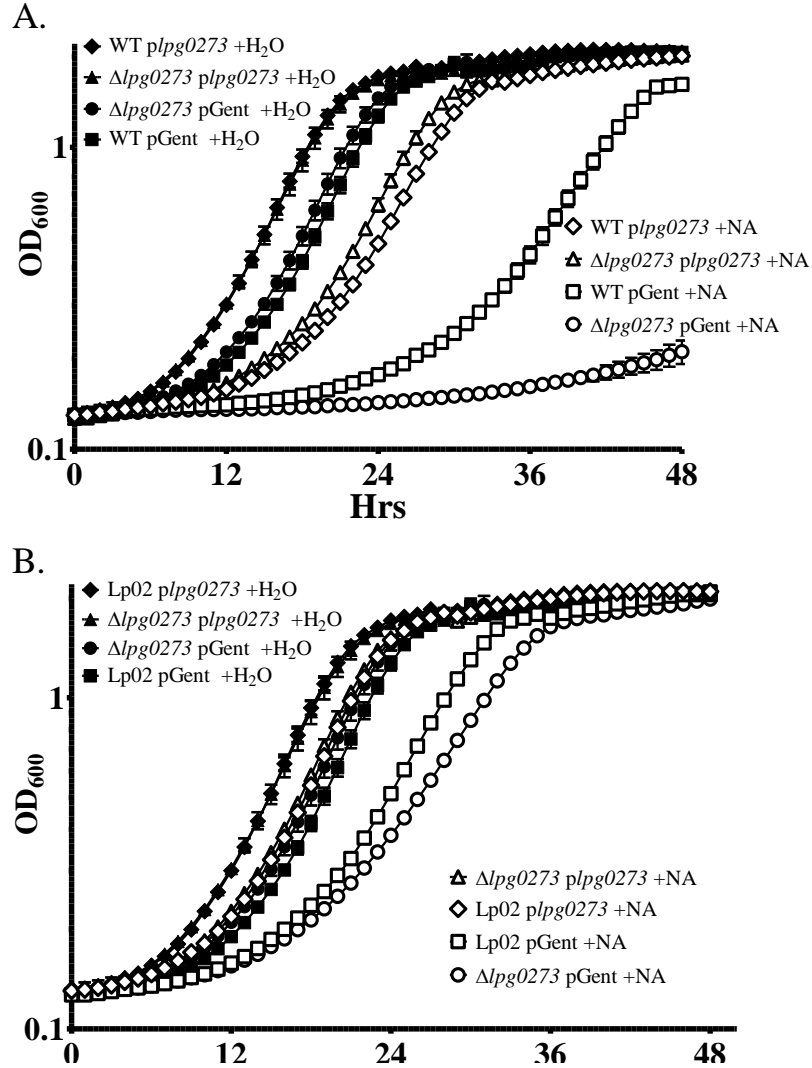


**Figure B.2.** Broth growth curves reveal increased sensitivity to nicotinic acid for an *lpg0273* mutant. Indicated strains were cultured overnight in AYET, cell density normalized, and OD<sub>600</sub> followed for 48 h in a Bioscreen Growth Curve Analyzer. All strains were grown in the presence of 200  $\mu$ M IPTG. NA indicates 5mM (A) or 2.5mM (B) nicotinic acid. Data is representative of at least three independent experiments, and represents the mean  $\pm$  SD of triplicate wells of a single experiment. Kaoru Harada contributed to preliminary experiments for these data.

## BIBLIOGRAPHY

- Abu-Zant, A., S. Jones, R. Asare, J. Suttles, C. Price, J. Graham, and Y. A. Kwaik.** 2007. Anti-apoptotic signalling by the Dot/Icm secretion system of *L. pneumophila*. *Cell Microbiol* 9:246-64.
- Al-Khodor, S., C. T. Price, F. Habyarimana, A. Kalia, and Y. Abu Kwaik.** 2008. A Dot/Icm-translocated ankyrin protein of *Legionella pneumophila* is required for intracellular proliferation within human macrophages and protozoa. *Mol Microbiol* 70:908-23.
- Altschul, S. F., E. M. Gertz, R. Agarwala, A. A. Schaffer, and Y. K. Yu.** 2009. PSI-BLAST pseudocounts and the minimum description length principle. *Nucleic Acids Res* 37:815-24.
- Altschul, S. F., T. L. Madden, A. A. Schaffer, J. Zhang, Z. Zhang, W. Miller, and D. J. Lipman.** 1997. Gapped BLAST and PSI-BLAST: a new generation of protein database search programs. *Nucleic Acids Res* 25:3389-402.
- Amer, A. O., and M. S. Swanson.** 2005. Autophagy is an immediate macrophage response to *Legionella pneumophila*. *Cell Microbiol* 7:765-78.
- Baba, T., T. Ara, M. Hasegawa, Y. Takai, Y. Okumura, M. Baba, K. A. Datsenko, M. Tomita, B. L. Wanner, and H. Mori.** 2006. Construction of *Escherichia coli* K-12 in-frame, single-gene knockout mutants: the Keio collection. *Mol Syst Biol* 2:2006 0008.
- Banga, S., P. Gao, X. Shen, V. Fiscus, W. X. Zong, L. Chen, and Z. Q. Luo.** 2007. *Legionella pneumophila* inhibits macrophage apoptosis by targeting pro-death members of the Bcl2 protein family. *Proc Natl Acad Sci U S A* 104:5121-6.
- Bardill, J. P., J. L. Miller, and J. P. Vogel.** 2005. IcmS-dependent translocation of SdeA into macrophages by the *Legionella pneumophila* type IV secretion system. *Mol Microbiol* 56:90-103.
- Barras, F., and M. G. Marinus.** 1989. The great GATC: DNA methylation in *E. coli*. *Trends Genet* 5:139-43.

- Baskerville, A., A. B. Dowsett, R. B. Fitzgeorge, P. Hambleton, and M. Broster.** 1983. Ultrastructure of pulmonary alveoli and macrophages in experimental Legionnaires' disease. *J Pathol* 140:77-90.
- Beam, C. E., C. J. Saveson, and S. T. Lovett.** 2002. Role for *radA/sms* in recombination intermediate processing in *Escherichia coli*. *J Bacteriol* 184:6836-44.
- Belyi, Y., R. Niggeweg, B. Opitz, M. Vogelsgesang, S. Hippenstiel, M. Wilm, and K. Aktories.** 2006. *Legionella pneumophila* glucosyltransferase inhibits host elongation factor 1A. *Proc Natl Acad Sci U S A* 103:16953-8.
- Belyi, Y., I. Tabakova, M. Stahl, and K. Aktories.** 2008. Lgt: a family of cytotoxic glucosyltransferases produced by *Legionella pneumophila*. *J Bacteriol* 190:3026-35.
- Benin, A. L., R. F. Benson, and R. E. Besser.** 2002. Trends in legionnaires disease, 1980-1998: declining mortality and new patterns of diagnosis. *Clin Infect Dis* 35:1039-46.
- Berger, K. H., and R. R. Isberg.** 1993. Two distinct defects in intracellular growth complemented by a single genetic locus in *Legionella pneumophila*. *Mol Microbiol* 7:7-19.
- Bierne, H., D. Vilette, S. D. Ehrlich, and B. Michel.** 1997. Isolation of a *dnaE* mutation which enhances RecA-independent homologous recombination in the *Escherichia coli* chromosome. *Mol Microbiol* 24:1225-34.
- Blakely, G., G. May, R. McCulloch, L. K. Arciszewska, M. Burke, S. T. Lovett, and D. J. Sherratt.** 1993. Two related recombinases are required for site-specific recombination at *dif* and *cer* in *E. coli* K12. *Cell* 75:351-61.
- Bruggemann, H., C. Cazalet, and C. Buchrieser.** 2006. Adaptation of *Legionella pneumophila* to the host environment: role of protein secretion, effectors and eukaryotic-like proteins. *Curr Opin Microbiol* 9:86-94.
- Bryan, A., K. Harada, and M. S. Swanson.** 2011. Efficient generation of unmarked deletions in *Legionella pneumophila*. *Appl Environ Microbiol* 77: *In press*.
- Bryan, A., P. Roesch, L. Davis, R. Moritz, S. Pellett, and R. A. Welch.** 2006. Regulation of type 1 fimbriae by unlinked FimB- and FimE-like recombinases in uropathogenic *Escherichia coli* strain CFT073. *Infect Immun* 74:1072-83.
- Bryan, A., and M. S. Swanson.** 2011. Oligonucleotides stimulate genomic alterations of *Legionella pneumophila*. *Mol Microbiol* *In press*.



- Burdett, V., C. Baitinger, M. Viswanathan, S. T. Lovett, and P. Modrich.** 2001. *In vivo* requirement for RecJ, ExoVII, ExoI, and ExoX in methyl-directed mismatch repair. *Proc Natl Acad Sci U S A* 98:6765-70.
- Byrd, T. F., and M. A. Horwitz.** 1989. Interferon gamma-activated human monocytes downregulate transferrin receptors and inhibit the intracellular multiplication of *Legionella pneumophila* by limiting the availability of iron. *J Clin Invest* 83:1457-65.
- Byrne, B., and M. S. Swanson.** 1998. Expression of *Legionella pneumophila* virulence traits in response to growth conditions. *Infect Immun* 66:3029-34.
- Bzymek, M., and S. T. Lovett.** 2001. Instability of repetitive DNA sequences: the role of replication in multiple mechanisms. *Proc Natl Acad Sci U S A* 98:8319-25.
- Campodonico, E. M., L. Chesnel, and C. R. Roy.** 2005. A yeast genetic system for the identification and characterization of substrate proteins transferred into host cells by the *Legionella pneumophila* Dot/Icm system. *Mol Microbiol* 56:918-33.
- Canceill, D., and S. D. Ehrlich.** 1996. Copy-choice recombination mediated by DNA polymerase III holoenzyme from *Escherichia coli*. *Proc Natl Acad Sci U S A* 93:6647-52.
- Cazalet, C., S. Jarraud, Y. Ghavi-Helm, F. Kunst, P. Glaser, J. Etienne, and C. Buchrieser.** 2008. Multigenome analysis identifies a worldwide distributed epidemic *Legionella pneumophila* clone that emerged within a highly diverse species. *Genome Res* 18:431-41.
- Cazalet, C., C. Rusniok, H. Bruggemann, N. Zidane, A. Magnier, L. Ma, M. Tichit, S. Jarraud, C. Bouchier, F. Vandenesch, F. Kunst, J. Etienne, P. Glaser, and C. Buchrieser.** 2004. Evidence in the *Legionella pneumophila* genome for exploitation of host cell functions and high genome plasticity. *Nat Genet* 36:1165-73.
- Chase, J. W., and C. C. Richardson.** 1977. *Escherichia coli* mutants deficient in exonuclease VII. *J Bacteriol* 129:934-47.
- Chen, D. Q., S. S. Huang, and Y. J. Lu.** 2006. Efficient transformation of *Legionella pneumophila* by high-voltage electroporation. *Microbiol Res* 161:246-51.
- Chen, J., K. S. de Felipe, M. Clarke, H. Lu, O. R. Anderson, G. Segal, and H. A. Shuman.** 2004. *Legionella* effectors that promote nonlytic release from protozoa. *Science* 303:1358-61.

- Chen, J. M., D. N. Cooper, C. Ferec, H. Kehrer-Sawatzki, and G. P. Patrinos.** 2010. Genomic rearrangements in inherited disease and cancer. *Semin Cancer Biol* 20:222-33.
- Chien, M., I. Morozova, S. Shi, H. Sheng, J. Chen, S. M. Gomez, G. Asamani, K. Hill, J. Nuara, M. Feder, J. Rineer, J. J. Greenberg, V. Steshenko, S. H. Park, B. Zhao, E. Teplitskaya, J. R. Edwards, S. Pampou, A. Georghiou, I. C. Chou, W. Iannuccilli, M. E. Ulz, D. H. Kim, A. Geringer-Sameth, C. Goldsberry, P. Morozov, S. G. Fischer, G. Segal, X. Qu, A. Rzhetsky, P. Zhang, E. Cayanis, P. J. De Jong, J. Ju, S. Kalachikov, H. A. Shuman, and J. J. Russo.** 2004. The genomic sequence of the accidental pathogen *Legionella pneumophila*. *Science* 305:1966-8.
- Cianciotto, N. P.** 2009. Many substrates and functions of type II secretion: lessons learned from *Legionella pneumophila*. *Future Microbiol* 4:797-805.
- Conover, G. M., I. Derre, J. P. Vogel, and R. R. Isberg.** 2003. The *Legionella pneumophila* LidA protein: a translocated substrate of the Dot/Icm system associated with maintenance of bacterial integrity. *Mol Microbiol* 48:305-21.
- Corrette-Bennett, S. E., and S. T. Lovett.** 1995. Enhancement of RecA strand-transfer activity by the RecJ exonuclease of *Escherichia coli*. *J Biol Chem* 270:6881-5.
- Coscolla, M., and F. Gonzalez-Candelas.** 2007. Population structure and recombination in environmental isolates of *Legionella pneumophila*. *Environ Microbiol* 9:643-56.
- Costantino, N., and D. L. Court.** 2003. Enhanced levels of lambda Red-mediated recombinants in mismatch repair mutants. *Proc Natl Acad Sci U S A* 100:15748-53.
- Cotter, P. A., and V. J. DiRita.** 2000. Bacterial virulence gene regulation: an evolutionary perspective. *Annu Rev Microbiol* 54:519-65.
- Court, D. L., J. A. Sawitzke, and L. C. Thomason.** 2002. Genetic engineering using homologous recombination. *Annu Rev Genet* 36:361-88.
- Cox, M. M.** 1983. The FLP protein of the yeast 2-microns plasmid: expression of a eukaryotic genetic recombination system in *Escherichia coli*. *Proc Natl Acad Sci U S A* 80:4223-7.
- Cummings, C. A., H. J. Bootsma, D. A. Relman, and J. F. Miller.** 2006. Species- and strain-specific control of a complex, flexible regulon by *Bordetella BvgAS*. *J Bacteriol* 188:1775-85.

- Dalebroux, Z. D., R. L. Edwards, and M. S. Swanson.** 2009. SpoT governs *Legionella pneumophila* differentiation in host macrophages. *Mol Microbiol* 71:640-58.
- Datsenko, K. A., and B. L. Wanner.** 2000. One-step inactivation of chromosomal genes in *Escherichia coli* K-12 using PCR products. *Proc Natl Acad Sci U S A* 97:6640-5.
- Datta, S., N. Costantino, X. Zhou, and D. L. Court.** 2008. Identification and analysis of recombineering functions from Gram-negative and Gram-positive bacteria and their phages. *Proc Natl Acad Sci U S A* 105:1626-31.
- de Felipe, K. S., S. Pampou, O. S. Jovanovic, C. D. Pericone, S. F. Ye, S. Kalachikov, and H. A. Shuman.** 2005. Evidence for acquisition of *Legionella type IV* secretion substrates via interdomain horizontal gene transfer. *J Bacteriol* 187:7716-26.
- Declerck, P.** 2009. Biofilms: the environmental playground of *Legionella pneumophila*. *Environ Microbiol* 12:557-66.
- Diederren, B. M., J. A. Kluytmans, C. M. Vandembroucke-Grauls, and M. F. Peeters.** 2008. Utility of real-time PCR for diagnosis of Legionnaires' disease in routine clinical practice. *J Clin Microbiol* 46:671-7.
- Doleans, A., H. Aurell, M. Reyrolle, G. Lina, J. Freney, F. Vandenesch, J. Etienne, and S. Jarraud.** 2004. Clinical and environmental distributions of *Legionella* strains in France are different. *J Clin Microbiol* 42:458-60.
- Dominguez, N. M., K. T. Hackett, and J. P. Dillard.** 2010. XerCD-mediated site-specific recombination leads to loss of the 57-kilobase gonococcal genetic island. *J Bacteriol* 193:377-88.
- Dumenil, G., and R. R. Isberg.** 2001. The *Legionella pneumophila* IcmR protein exhibits chaperone activity for IcmQ by preventing its participation in high-molecular-weight complexes. *Mol Microbiol* 40:1113-27.
- Dutra, B. E., and S. T. Lovett.** 2006. Cis and trans-acting effects on a mutational hotspot involving a replication template switch. *J Mol Biol* 356:300-11.
- Dutra, B. E., V. A. Sutera, Jr., and S. T. Lovett.** 2007. RecA-independent recombination is efficient but limited by exonucleases. *Proc Natl Acad Sci U S A* 104:216-21.
- Edelstein, P. H.** 2008. Legionnaires Disease: History and Clinical Findings. In K. H. a. M. S. Swanson (ed.), *Legionella: Molecular Microbiology*. Caister Academic Press, Norfolk, U.K.

- Edelstein, P. H., and N. P. Cianciotto.** 2005. *Legionella*, p. 2711-2724. In G. L. Mandell, E. Bennet, and R. Dolin (ed.), Principles and Practice of Infectious Disease, 6th ed, vol. 2. Elsevier, Philadelphia, PA.
- Edwards, R. L.** 2008. Metabolic Cues and Regulatory Proteins That Govern *Legionella pneumophila* Differentiation and Virulence. Univeristy of Michigan, Ann Arbor, MI.
- Edwards, R. L., M. Jules, T. Sahr, C. Buchrieser, and M. S. Swanson.** 2010. The *Legionella pneumophila* LetA/LetS two-component system exhibits rheostat-like behavior. *Infect Immun* 78:2571-83.
- Eguchi, Y., T. Oshima, H. Mori, R. Aono, K. Yamamoto, A. Ishihama, and R. Utsumi.** 2003. Transcriptional regulation of drug efflux genes by EvgAS, a two-component system in *Escherichia coli*. *Microbiology* 149:2819-28.
- Ellis, H. M., D. Yu, T. DiTizio, and D. L. Court.** 2001. High efficiency mutagenesis, repair, and engineering of chromosomal DNA using single-stranded oligonucleotides. *Proc Natl Acad Sci U S A* 98:6742-6.
- Falco, S. C., Y. Li, J. R. Broach, and D. Botstein.** 1982. Genetic properties of chromosomally integrated 2 mu plasmid DNA in yeast. *Cell* 29:573-84.
- Fields, B. S.** 1996. The molecular ecology of legionellae. *Trends Microbiol* 4:286-90.
- Finberg, K. E., C. A. Wagner, M. A. Bailey, T. G. Paunescu, S. Breton, D. Brown, G. Giebisch, J. P. Geibel, and R. P. Lifton.** 2005. The B1-subunit of the H(+) ATPase is required for maximal urinary acidification. *Proc Natl Acad Sci U S A* 102:13616-21.
- Forgac, M.** 2007. Vacuolar ATPases: rotary proton pumps in physiology and pathophysiology. *Nat Rev Mol Cell Biol* 8:917-29.
- Foy, H., C. Broome, P. Hayes, I. Allan, M. Cooney, and R. Tobe.** 1979. Legionnaires' disease in a prepaid medical-care group in Seattle 1963--75. *Lancet* 1:767-70.
- Gabbai, C. B., and K. J. Marians.** Recruitment to stalled replication forks of the PriA DNA helicase and replisome-loading activities is essential for survival. *DNA Repair (Amst)* 9:202-9.
- Gao, F., and C. T. Zhang.** 2007. DoriC: a database of oriC regions in bacterial genomes. *Bioinformatics* 23:1866-7.

- Gietz, R. D., R. H. Schiestl, A. R. Willems, and R. A. Woods.** 1995. Studies on the transformation of intact yeast cells by the LiAc/SS-DNA/PEG procedure. *Yeast* 11:355-60.
- Goedhart, J., and T. W. Gadella, Jr.** 2005. Analysis of oligonucleotide annealing by electrophoresis in agarose gels using sodium borate conductive medium. *Anal Biochem* 343:186-7.
- Goldfless, S. J., A. S. Morag, K. A. Belisle, V. A. Suttera, Jr., and S. T. Lovett.** 2006. DNA repeat rearrangements mediated by DnaK-dependent replication fork repair. *Mol Cell* 21:595-604.
- Golic, K. G., and S. Lindquist.** 1989. The FLP recombinase of yeast catalyzes site-specific recombination in the *Drosophila* genome. *Cell* 59:499-509.
- Gomez-Valero, L., C. Rusniok, and C. Buchrieser.** 2009. *Legionella pneumophila*: population genetics, phylogeny and genomics. *Infect Genet Evol* 9:727-39.
- Goodwin, A., D. Kersulyte, G. Sisson, S. J. Veldhuyzen van Zanten, D. E. Berg, and P. S. Hoffman.** 1998. Metronidazole resistance in *Helicobacter pylori* is due to null mutations in a gene (*rdxA*) that encodes an oxygen-insensitive NADPH nitroreductase. *Mol Microbiol* 28:383-93.
- Grogan, D. W., and K. R. Stengel.** 2008. Recombination of synthetic oligonucleotides with prokaryotic chromosomes: substrate requirements of the *Escherichia coli*/Lambda-Red and *Sulfolobus acidocaldarius* recombination systems. *Mol Microbiol* 69:1255-65.
- Hall-Baker, P. A., E. Nieves, R. A. Jajosky, D. A. Adams, P. Sharp, W. J. Anderson, J. J. Aponte, A. E. Aranas, S. B. Katz, M. Mayes, M. S. Wodajo, D. H. Onweh, J. Baillie, and M. Park.** 2010. Summary of Notifiable Diseases --- United States, 2008. *MMWR Morb Mortal Wkly Rep* 57:1-94.
- Hammer, B. K., E. S. Tateda, and M. S. Swanson.** 2002. A two-component regulator induces the transmission phenotype of stationary-phase *Legionella pneumophila*. *Mol Microbiol* 44:107-18.
- Han, E. S., D. L. Cooper, N. S. Persky, V. A. Suttera, Jr., R. D. Whitaker, M. L. Montello, and S. T. Lovett.** 2006. RecJ exonuclease: substrates, products and interaction with SSB. *Nucleic Acids Res* 34:1084-91.
- Han, J., and K. Burgess.** 2009. Fluorescent indicators for intracellular pH. *Chem Rev* 110:2709-28.

- Hayden, R. T., J. R. Uhl, X. Qian, M. K. Hopkins, M. C. Aubry, A. H. Limper, R. V. Lloyd, and F. R. Cockerill.** 2001. Direct detection of *Legionella* species from bronchoalveolar lavage and open lung biopsy specimens: comparison of LightCycler PCR, *in situ* hybridization, direct fluorescence antigen detection, and culture. *J Clin Microbiol* 39:2618-26.
- Heidtman, M., E. J. Chen, M. Y. Moy, and R. R. Isberg.** 2009. Large-scale identification of *Legionella pneumophila* Dot/Icm substrates that modulate host cell vesicle trafficking pathways. *Cell Microbiol* 11:230-48.
- Heneberg, P.** 2009. Use of protein tyrosine phosphatase inhibitors as promising targeted therapeutic drugs. *Curr Med Chem* 16:706-33.
- Horwitz, M. A.** 1983. The Legionnaires' disease bacterium (*Legionella pneumophila*) inhibits phagosome-lysosome fusion in human monocytes. *J Exp Med* 158:2108-26.
- Hubber, A., and C. R. Roy.** 2010. Modulation of host cell function by *Legionella pneumophila* type IV effectors. *Annu Rev Cell Dev Biol* 26:261-83.
- Huber, K. E., and M. K. Waldor.** 2002. Filamentous phage integration requires the host recombinases XerC and XerD. *Nature* 417:656-9.
- Huen, M. S., X. T. Li, L. Y. Lu, R. M. Watt, D. P. Liu, and J. D. Huang.** 2006. The involvement of replication in single stranded oligonucleotide-mediated gene repair. *Nucleic Acids Res* 34:6183-94.
- Huss, M., and H. Wiczorek.** 2009. Inhibitors of V-ATPases: old and new players. *J Exp Biol* 212:341-6.
- Huynh, K. K., and S. Grinstein.** 2007. Regulation of vacuolar pH and its modulation by some microbial species. *Microbiol Mol Biol Rev* 71:452-62.
- Ikeda, H., and T. Matsumoto.** 1979. Transcription promotes recA-independent recombination mediated by DNA-dependent RNA polymerase in *Escherichia coli*. *Proc Natl Acad Sci U S A* 76:4571-5.
- Ingmundson, A., A. Delprato, D. G. Lambright, and C. R. Roy.** 2007. *Legionella pneumophila* proteins that regulate Rab1 membrane cycling. *Nature* 450:365-9.
- Inoue, H., T. Noumi, M. Nagata, H. Murakami, and H. Kanazawa.** 1999. Targeted disruption of the gene encoding the proteolipid subunit of mouse vacuolar H(+)-ATPase leads to early embryonic lethality. *Biochim Biophys Acta* 1413:130-8.

- Isberg, R. R., T. J. O'Connor, and M. Heidtman.** 2009. The *Legionella pneumophila* replication vacuole: making a cosy niche inside host cells. *Nat Rev Microbiol* 7:13-24.
- James, P., J. Halladay, and E. A. Craig.** 1996. Genomic libraries and a host strain designed for highly efficient two-hybrid selection in yeast. *Genetics* 144:1425-36.
- Johnsborg, O., V. Eldholm, and L. S. Havarstein.** 2007. Natural genetic transformation: prevalence, mechanisms and function. *Res Microbiol* 158:767-78.
- Joshi, A. D., S. Sturgill-Koszycki, and M. S. Swanson.** 2001. Evidence that Dot-dependent and -independent factors isolate the *Legionella pneumophila* phagosome from the endocytic network in mouse macrophages. *Cell Microbiol* 3:99-114.
- Kelley, L. A., and M. J. Sternberg.** 2009. Protein structure prediction on the Web: a case study using the Phyre server. *Nat Protoc* 4:363-71.
- Kim, W., C. Y. Wan, and T. A. Wilkins.** 1999. Functional complementation of yeast *vma1* delta cells by a plant subunit A homolog rescues the mutant phenotype and partially restores vacuolar H(+)-ATPase activity. *Plant J* 17:501-10.
- Kinchen, J. M., and K. S. Ravichandran.** 2008. Phagosome maturation: going through the acid test. *Nat Rev Mol Cell Biol* 9:781-95.
- Klemm, P.** 1986. Two regulatory *fim* genes, *fimB* and *fimE*, control the phase variation of type 1 fimbriae in *Escherichia coli*. *EMBO J* 5:1389-93.
- Ko, K. S., S. K. Hong, H. K. Lee, M. Y. Park, and Y. H. Kook.** 2003. Molecular evolution of the *dotA* gene in *Legionella pneumophila*. *J Bacteriol* 185:6269-77.
- Kubori, T., A. Hyakutake, and H. Nagai.** 2008. *Legionella* translocates an E3 ubiquitin ligase that has multiple U-boxes with distinct functions. *Mol Microbiol* 67:1307-19.
- Kuzminov, A.** 1999. Recombinational repair of DNA damage in *Escherichia coli* and bacteriophage lambda. *Microbiol Mol Biol Rev* 63:751-813, table of contents.
- Lacks, S., and B. Greenberg.** 1977. Complementary specificity of restriction endonucleases of *Diplococcus pneumoniae* with respect to DNA methylation. *J Mol Biol* 114:153-68.
- Laguna, R. K., E. A. Creasey, Z. Li, N. Valtz, and R. R. Isberg.** 2006. A *Legionella pneumophila*-translocated substrate that is required for growth within

macrophages and protection from host cell death. Proc Natl Acad Sci U S A 103:18745-50.

- LeBlanc, J. J., R. J. Davidson, and P. S. Hoffman.** 2006. Compensatory functions of two alkyl hydroperoxide reductases in the oxidative defense system of *Legionella pneumophila*. J Bacteriol 188:6235-44.
- Lesic, B., and L. G. Rahme.** 2008. Use of the lambda Red recombinase system to rapidly generate mutants in *Pseudomonas aeruginosa*. BMC Mol Biol 9:20.
- Li, X. T., N. Costantino, L. Y. Lu, D. P. Liu, R. M. Watt, K. S. Cheah, D. L. Court, and J. D. Huang.** 2003. Identification of factors influencing strand bias in oligonucleotide-mediated recombination in *Escherichia coli*. Nucleic Acids Res 31:6674-87.
- Liu, L., M. C. Rice, M. Drury, S. Cheng, H. Gamper, and E. B. Kmiec.** 2002. Strand bias in targeted gene repair is influenced by transcriptional activity. Mol Cell Biol 22:3852-63.
- Liu, Y., P. Gao, S. Banga, and Z. Q. Luo.** 2008. An *in vivo* gene deletion system for determining temporal requirement of bacterial virulence factors. Proc Natl Acad Sci U S A 105:9385-90.
- Liu, Y., and Z. Q. Luo.** 2007. The *Legionella pneumophila* effector SidJ is required for efficient recruitment of endoplasmic reticulum proteins to the bacterial phagosome. Infect Immun 75:592-603.
- Losick, V. P., and R. R. Isberg.** 2006. NF-kappaB translocation prevents host cell death after low-dose challenge by *Legionella pneumophila*. J Exp Med 203:2177-89.
- Lovett, S. T.** 2005. Filling the gaps in replication restart pathways. Mol Cell 17:751-2.
- Lovett, S. T.** 2006. Replication arrest-stimulated recombination: Dependence on the RecA paralog, RadA/Sms and translesion polymerase, DinB. DNA Repair 5:1421-7.
- Lovett, S. T., R. L. Hurley, V. A. Suttera, Jr., R. H. Aubuchon, and M. A. Lebedeva.** 2002. Crossing over between regions of limited homology in *Escherichia coli*. RecA-dependent and RecA-independent pathways. Genetics 160:851-9.
- Lu, X., H. Yu, S. H. Liu, F. M. Brodsky, and B. M. Peterlin.** 1998. Interactions between HIV1 Nef and vacuolar ATPase facilitate the internalization of CD4. Immunity 8:647-56.



- Luneberg, E., B. Mayer, N. Daryab, O. Kooistra, U. Zahringer, M. Rohde, J. Swanson, and M. Frosch.** 2001. Chromosomal insertion and excision of a 30 kb unstable genetic element is responsible for phase variation of lipopolysaccharide and other virulence determinants in *Legionella pneumophila*. *Mol Microbiol* 39:1259-71.
- Luo, Z. Q., and R. R. Isberg.** 2004. Multiple substrates of the *Legionella pneumophila* Dot/Icm system identified by interbacterial protein transfer. *Proc Natl Acad Sci U S A* 101:841-6.
- Lurie-Weinberger, M. N., L. Gomez-Valero, N. Merault, G. Glockner, C. Buchrieser, and U. Gophna.** 2010. The origins of eukaryotic-like proteins in *Legionella pneumophila*. *Int J Med Microbiol* 300:470-81.
- Lusetti, S. L., and M. M. Cox.** 2002. The bacterial RecA protein and the recombinational DNA repair of stalled replication forks. *Annu Rev Biochem* 71:71-100.
- Lynch, D., N. Fieser, K. Glogler, V. Forsbach-Birk, and R. Marre.** 2003. The response regulator LetA regulates the stationary-phase stress response in *Legionella pneumophila* and is required for efficient infection of *Acanthamoeba castellanii*. *FEMS Microbiol Lett* 219:241-8.
- Machner, M. P., and R. R. Isberg.** 2006. Targeting of host Rab GTPase function by the intravacuolar pathogen *Legionella pneumophila*. *Dev Cell* 11:47-56.
- Marra, A., S. J. Blander, M. A. Horwitz, and H. A. Shuman.** 1992. Identification of a *Legionella pneumophila* locus required for intracellular multiplication in human macrophages. *Proc Natl Acad Sci U S A* 89:9607-11.
- Marshansky, V., and M. Futai.** 2008. The V-type H<sup>+</sup>-ATPase in vesicular trafficking: targeting, regulation and function. *Curr Opin Cell Biol* 20:415-26.
- Marston, B., J. Plouffe, T. J. File, B. Hackman, S. Salstrom, H. Lipman, M. Kolczak, and R. Breiman.** 1997. Incidence of community-acquired pneumonia requiring hospitalization: results of a population-based active surveillance study in Ohio. *Arch Intern Med* 157:1709-18.
- Masuda, N., and G. M. Church.** 2002. *Escherichia coli* gene expression responsive to levels of the response regulator EvgA. *J Bacteriol* 184:6225-34.
- Masuda, N., and G. M. Church.** 2003. Regulatory network of acid resistance genes in *Escherichia coli*. *Mol Microbiol* 48:699-712.

- McClain, M. S., M. C. Hurley, J. K. Brieland, and N. C. Engleberg.** 1996. The *Legionella pneumophila* hel locus encodes intracellularly induced homologs of heavy-metal ion transporters of *Alcaligenes* spp. *Infect Immun* 64:1532-40.
- McNeil, P. L.** 2001. Direct introduction of molecules into cells. *Curr Protoc Cell Biol* Chapter 20:Unit 20 1.
- McPheat, W. L., A. C. Wardlaw, and P. Novotny.** 1983. Modulation of *Bordetella pertussis* by nicotinic acid. *Infect Immun* 41:516-22.
- Merriam, J. J., R. Mathur, R. Maxfield-Boumil, and R. R. Isberg.** 1997. Analysis of the *Legionella pneumophila* *fliI* gene: intracellular growth of a defined mutant defective for flagellum biosynthesis. *Infect Immun* 65:2497-501.
- Miller, J. F., C. R. Roy, and S. Falkow.** 1989. Analysis of *Bordetella pertussis* virulence gene regulation by use of transcriptional fusions in *Escherichia coli*. *J Bacteriol* 171:6345-8.
- Modrich, P.** 1991. Mechanisms and biological effects of mismatch repair. *Annu Rev Genet* 25:229-53.
- Molofsky, A. B., L. M. Shetron-Rama, and M. S. Swanson.** 2005. Components of the *Legionella pneumophila* flagellar regulon contribute to multiple virulence traits, including lysosome avoidance and macrophage death. *Infect Immun* 73:5720-34.
- Molofsky, A. B., and M. S. Swanson.** 2004. Differentiate to thrive: lessons from the *Legionella pneumophila* life cycle. *Mol Microbiol* 53:29-40.
- Molofsky, A. B., and M. S. Swanson.** 2003. *Legionella pneumophila* CsrA is a pivotal repressor of transmission traits and activator of replication. *Mol Microbiol* 50:445-61.
- Morschhauser, J., S. Michel, and P. Staib.** 1999. Sequential gene disruption in *Candida albicans* by FLP-mediated site-specific recombination. *Mol Microbiol* 32:547-56.
- Mulazimoglu, L., and V. L. Yu.** 2001. Can Legionnaires disease be diagnosed by clinical criteria? A critical review. *Chest* 120:1049-53.
- Mumberg, D., R. Muller, and M. Funk.** 1995. Yeast vectors for the controlled expression of heterologous proteins in different genetic backgrounds. *Gene* 156:119-22.
- Murata, T., A. Delprato, A. Ingmundson, D. K. Toomre, D. G. Lambright, and C. R. Roy.** 2006. The *Legionella pneumophila* effector protein DrrA is a Rab1 guanine nucleotide-exchange factor. *Nat Cell Biol* 8:971-7.

- Murphy, K. C., and M. G. Marinus.** 2010. RecA-independent single-stranded DNA oligonucleotide-mediated mutagenesis. *F1000 Biol Rep* 2:56.
- Nagai, H., J. C. Kagan, X. Zhu, R. A. Kahn, and C. R. Roy.** 2002. A bacterial guanine nucleotide exchange factor activates ARF on *Legionella* phagosomes. *Science* 295:679-82.
- Nelson, H., and N. Nelson.** 1990. Disruption of genes encoding subunits of yeast vacuolar H(+)-ATPase causes conditional lethality. *Proc Natl Acad Sci U S A* 87:3503-7.
- Newton, H. J., D. K. Ang, I. R. van Driel, and E. L. Hartland.** 2010. Molecular pathogenesis of infections caused by *Legionella pneumophila*. *Clin Microbiol Rev* 23:274-98.
- Nielsen, K., P. Hindersson, N. Hoiby, and J. M. Bangsberg.** 2000. Sequencing of the *rpoB* gene in *Legionella pneumophila* and characterization of mutations associated with rifampin resistance in the Legionellaceae. *Antimicrob Agents Chemother* 44:2679-83.
- Ninio, S., and C. R. Roy.** 2007. Effector proteins translocated by *Legionella pneumophila*: strength in numbers. *Trends Microbiol* 15:372-80.
- Nishi, T., and M. Forgac.** 2002. The vacuolar (H<sup>+</sup>)-ATPases--nature's most versatile proton pumps. *Nat Rev Mol Cell Biol* 3:94-103.
- Nishino, K., Y. Inazumi, and A. Yamaguchi.** 2003. Global analysis of genes regulated by EvgA of the two-component regulatory system in *Escherichia coli*. *J Bacteriol* 185:2667-72.
- Nishino, K., and A. Yamaguchi.** 2001. Overexpression of the response regulator *evgA* of the two-component signal transduction system modulates multidrug resistance conferred by multidrug resistance transporters. *J Bacteriol* 183:1455-8.
- O'Gorman, S., D. T. Fox, and G. M. Wahl.** 1991. Recombinase-mediated gene activation and site-specific integration in mammalian cells. *Science* 251:1351-5.
- Ogata, H., B. La Scola, S. Audic, P. Renesto, G. Blanc, C. Robert, P. E. Fournier, J. M. Claverie, and D. Raoult.** 2006. Genome sequence of *Rickettsia bellii* illuminates the role of amoebae in gene exchanges between intracellular pathogens. *PLoS Genet* 2:e76.
- Ohkuma, S., and B. Poole.** 1978. Fluorescence probe measurement of the intralysosomal pH in living cells and the perturbation of pH by various agents. *Proc Natl Acad Sci U S A* 75:3327-31.

- Oppenheim, A. B., A. J. Rattray, M. Bubunenko, L. C. Thomason, and D. L. Court.** 2004. *In vivo* recombineering of bacteriophage lambda by PCR fragments and single-strand oligonucleotides. *Virology* 319:185-9.
- Ortigao, J. F., H. Rosch, H. Selter, A. Frohlich, A. Lorenz, M. Montenarh, and H. Seliger.** 1992. Antisense effect of oligodeoxynucleotides with inverted terminal internucleotidic linkages: a minimal modification protecting against nucleolytic degradation. *Antisense Res Dev* 2:129-46.
- Ozgenç, A. I., E. S. Szekeres, and C. W. Lawrence.** 2005. In vivo evidence for a *recA*-independent recombination process in *Escherichia coli* that permits completion of replication of DNA containing UV damage in both strands. *J Bacteriol* 187:1974-84.
- Palmgren, M. G.** 1991. Acridine orange as a probe for measuring pH gradients across membranes: mechanism and limitations. *Anal Biochem* 192:316-21.
- Parekh-Olmedo, H., M. Drury, and E. B. Kmiec.** 2002. Targeted nucleotide exchange in *Saccharomyces cerevisiae* directed by short oligonucleotides containing locked nucleic acids. *Chem Biol* 9:1073-84.
- Pasculle, A. W., J. C. Feeley, R. J. Gibson, L. G. Cordes, R. L. Myerowitz, C. M. Patton, G. W. Gorman, C. L. Carmack, J. W. Ezzell, and J. N. Dowling.** 1980. Pittsburgh pneumonia agent: direct isolation from human lung tissue. *J Infect Dis* 141:727-32.
- Poteete, A. R.** 2008. Involvement of DNA replication in phage lambda Red-mediated homologous recombination. *Mol Microbiol* 68:66-74.
- Poteete, A. R., and A. C. Fenton.** 1993. Efficient double-strand break-stimulated recombination promoted by the general recombination systems of phages lambda and P22. *Genetics* 134:1013-21.
- Poteete, A. R., and A. C. Fenton.** 2000. Genetic requirements of phage lambda red-mediated gene replacement in *Escherichia coli* K-12. *J Bacteriol* 182:2336-40.
- Price, C. T., S. Al-Khodor, T. Al-Quadani, M. Santic, F. Habyarimana, A. Kalia, and Y. A. Kwaik.** 2009. Molecular mimicry by an F-box effector of *Legionella pneumophila* hijacks a conserved polyubiquitination machinery within macrophages and protozoa. *PLoS Pathog* 5:e1000704.
- Radecke, S., F. Radecke, I. Peter, and K. Schwarz.** 2006. Physical incorporation of a single-stranded oligodeoxynucleotide during targeted repair of a human chromosomal locus. *J Gene Med* 8:217-28.

- Ranallo, R. T., S. Barnoy, S. Thakkar, T. Urick, and M. M. Venkatesan.** 2006. Developing live *Shigella* vaccines using lambda Red recombineering. *FEMS Immunol Med Microbiol* 47:462-9.
- Rangarajan, S., R. Woodgate, and M. F. Goodman.** 2002. Replication restart in UV-irradiated *Escherichia coli* involving pols II, III, V, PriA, RecA and RecFOR proteins. *Mol Microbiol* 43:617-28.
- Sambade, M., M. Alba, A. M. Smardon, R. W. West, and P. M. Kane.** 2005. A genomic screen for yeast vacuolar membrane ATPase mutants. *Genetics* 170:1539-51.
- Saveson, C. J., and S. T. Lovett.** 1997. Enhanced deletion formation by aberrant DNA replication in *Escherichia coli*. *Genetics* 146:457-70.
- Schneider, D. R., and C. D. Parker.** 1982. Effect of pyridines on phenotypic properties of *Bordetella pertussis*. *Infect Immun* 38:548-53.
- Schweizer, H. P.** 2003. Applications of the *Saccharomyces cerevisiae* FLP-FRT system in bacterial genetics. *J Mol Microbiol Biotechnol* 5:67-77.
- Seitz, E. M., J. P. Brockman, S. J. Sandler, A. J. Clark, and S. C. Kowalczykowski.** 1998. RadA protein is an archaeal RecA protein homolog that catalyzes DNA strand exchange. *Genes Dev* 12:1248-53.
- Senecoff, J. F., R. C. Bruckner, and M. M. Cox.** 1985. The FLP recombinase of the yeast 2-micron plasmid: characterization of its recombination site. *Proc Natl Acad Sci U S A* 82:7270-4.
- Sexton, J. A., and J. P. Vogel.** 2004. Regulation of hypercompetence in *Legionella pneumophila*. *J Bacteriol* 186:3814-25.
- Shen, X., S. Banga, Y. Liu, L. Xu, P. Gao, I. Shamovsky, E. Nudler, and Z. Q. Luo.** 2009. Targeting eEF1A by a *Legionella pneumophila* effector leads to inhibition of protein synthesis and induction of host stress response. *Cell Microbiol* 11:911-26.
- Shin, S., and C. R. Roy.** 2008. Host cell processes that influence the intracellular survival of *Legionella pneumophila*. *Cell Microbiol* 10:1209-20.
- Shiraishi, Y., J. Nagai, T. Murakami, and M. Takano.** 2000. Effect of cisplatin on H<sup>+</sup> transport by H<sup>+</sup>-ATPase and Na<sup>+</sup>/H<sup>+</sup> exchanger in rat renal brush-border membrane. *Life Sci* 67:1047-58.

- Shohdy, N., J. A. Efe, S. D. Emr, and H. A. Shuman.** 2005. Pathogen effector protein screening in yeast identifies *Legionella* factors that interfere with membrane trafficking. *Proc Natl Acad Sci U S A* 102:4866-71.
- Siggers, K. A., and C. F. Lesser.** 2008. The Yeast *Saccharomyces cerevisiae*: a versatile model system for the identification and characterization of bacterial virulence proteins. *Cell Host Microbe* 4:8-15.
- Slade, D., A. B. Lindner, G. Paul, and M. Radman.** 2009. Recombination and replication in DNA repair of heavily irradiated *Deinococcus radiodurans*. *Cell* 136:1044-55.
- Snyder, L., and W. Champness.** 2007a. DNA Repair and Mutagenesis, p. 459-497, *Molecular Genetics of Bacteria*, 3rd ed. ASM Press, Washington D.C.
- Snyder, L., and W. Champness.** 2007b. Molecular Mechanisms of Homologous Recombination, p. 429-457, *Molecular genetics of bacteria*, 3rd ed. ASM Press, Washington, D.C.
- Sousa, R., and E. M. Lafer.** 2006. Keep the traffic moving: mechanism of the Hsp70 motor. *Traffic* 7:1596-603.
- Sporri, R., N. Joller, U. Albers, H. Hilbi, and A. Oxenius.** 2006. MyD88-dependent IFN-gamma production by NK cells is key for control of *Legionella pneumophila* infection. *J Immunol* 176:6162-71.
- Stahl, M. M., L. Thomason, A. R. Poteete, T. Tarkowski, A. Kuzminov, and F. W. Stahl.** 1997. Annealing vs. invasion in phage lambda recombination. *Genetics* 147:961-77.
- Stevens, T. H., and M. Forgac.** 1997. Structure, function and regulation of the vacuolar (H<sup>+</sup>)-ATPase. *Annu Rev Cell Dev Biol* 13:779-808.
- Stone, B. J., and Y. Abu Kwaik.** 1998. Expression of multiple pili by *Legionella pneumophila*: identification and characterization of a type IV pilin gene and its role in adherence to mammalian and protozoan cells. *Infect Immun* 66:1768-75.
- Stone, B. J., and Y. A. Kwaik.** 1999. Natural competence for DNA transformation by *Legionella pneumophila* and its association with expression of type IV pili. *J Bacteriol* 181:1395-402.
- Sturgill-Koszycki, S., P. H. Schlesinger, P. Chakraborty, P. L. Haddix, H. L. Collins, A. K. Fok, R. D. Allen, S. L. Gluck, J. Heuser, and D. G. Russell.** 1994. Lack of acidification in *Mycobacterium* phagosomes produced by exclusion of the vesicular proton-ATPase. *Science* 263:678-81.

- Sturgill-Koszycki, S., and M. S. Swanson.** 2000. *Legionella pneumophila* replication vacuoles mature into acidic, endocytic organelles. *J Exp Med* 192:1261-72.
- Su, S. S., R. S. Lahue, K. G. Au, and P. Modrich.** 1988. Mismatch specificity of methyl-directed DNA mismatch correction in vitro. *J Biol Chem* 263:6829-35.
- Su, S. S., and P. Modrich.** 1986. *Escherichia coli* mutS-encoded protein binds to mismatched DNA base pairs. *Proc Natl Acad Sci U S A* 83:5057-61.
- Sun-Wada, G. H., H. Tabata, N. Kawamura, M. Aoyama, and Y. Wada.** 2009. Direct recruitment of H<sup>+</sup>-ATPase from lysosomes for phagosomal acidification. *J Cell Sci* 122:2504-13.
- Swanson, M. S., and R. R. Isberg.** 1995. Association of *Legionella pneumophila* with the macrophage endoplasmic reticulum. *Infect Immun* 63:3609-20.
- Swingle, B., E. Markel, and S. Cartinhour.** 2010a. Oligonucleotide recombination: A hidden treasure. *Bioengineered Bugs* 1:265-268.
- Swingle, B., E. Markel, N. Costantino, M. G. Bubunenko, S. Cartinhour, and D. L. Court.** 2010b. Oligonucleotide recombination in Gram-negative bacteria. *Mol Microbiol* 75:138-48.
- Templeton, K. E., S. A. Scheltinga, P. Sillekens, J. W. Crielaard, A. P. van Dam, H. Goossens, and E. C. Claas.** 2003. Development and clinical evaluation of an internally controlled, single-tube multiplex real-time PCR assay for detection of *Legionella pneumophila* and other *Legionella* species. *J Clin Microbiol* 41:4016-21.
- Thomas, C. M., and K. M. Nielsen.** 2005. Mechanisms of, and barriers to, horizontal gene transfer between bacteria. *Nat Rev Microbiol* 3:711-21.
- Thomason, L., D. L. Court, M. Bubunenko, N. Costantino, H. Wilson, S. Datta, and A. Oppenheim.** 2007a. Recombineering: genetic engineering in bacteria using homologous recombination. *Curr Protoc Mol Biol* 78:1.16.1–1.16.24.
- Thomason, L. C., N. Costantino, D. V. Shaw, and D. L. Court.** 2007b. Multicopy plasmid modification with phage lambda Red recombineering. *Plasmid* 58:148-58.
- Tilney, L. G., O. S. Harb, P. S. Connelly, C. G. Robinson, and C. R. Roy.** 2001. How the parasitic bacterium *Legionella pneumophila* modifies its phagosome and transforms it into rough ER: implications for conversion of plasma membrane to the ER membrane. *J Cell Sci* 114:4637-50.

- Uchida, E., Y. Ohsumi, and Y. Anraku.** 1985. Purification and properties of H<sup>+</sup>-translocating, Mg<sup>2+</sup>-adenosine triphosphatase from vacuolar membranes of *Saccharomyces cerevisiae*. *J Biol Chem* 260:1090-5.
- Urwyler, S., Y. Nyfeler, C. Ragaz, H. Lee, L. N. Mueller, R. Aebersold, and H. Hilbi.** 2009. Proteome analysis of *Legionella* vacuoles purified by magnetic immunoseparation reveals secretory and endosomal GTPases. *Traffic* 10:76-87.
- Utsumi, R., S. Katayama, M. Taniguchi, T. Horie, M. Ikeda, S. Igaki, H. Nakagawa, A. Miwa, H. Tanabe, and M. Noda.** 1994. Newly identified genes involved in the signal transduction of *Escherichia coli* K-12. *Gene* 140:73-7.
- van Kessel, J. C., and G. F. Hatfull.** 2007. Recombineering in *Mycobacterium tuberculosis*. *Nat Methods* 4:147-52.
- VanRheenen, S. M., Z. Q. Luo, T. O'Connor, and R. R. Isberg.** 2006. Members of a *Legionella pneumophila* family of proteins with ExoU (phospholipase A) active sites are translocated to target cells. *Infect Immun* 74:3597-606.
- Viguera, E., D. Canceill, and S. D. Ehrlich.** 2001. Replication slippage involves DNA polymerase pausing and dissociation. *EMBO J* 20:2587-95.
- Vincent, C. D., J. R. Friedman, K. C. Jeong, E. C. Buford, J. L. Miller, and J. P. Vogel.** 2006. Identification of the core transmembrane complex of the *Legionella* Dot/Icm type IV secretion system. *Mol Microbiol* 62:1278-91.
- Viswanathan, M., V. Burdett, C. Baitinger, P. Modrich, and S. T. Lovett.** 2001. Redundant exonuclease involvement in *Escherichia coli* methyl-directed mismatch repair. *J Biol Chem* 276:31053-8.
- Viswanathan, M., and S. T. Lovett.** 1998. Single-strand DNA-specific exonucleases in *Escherichia coli*. Roles in repair and mutation avoidance. *Genetics* 149:7-16.
- Vogel, J. P., H. L. Andrews, S. K. Wong, and R. R. Isberg.** 1998. Conjugative transfer by the virulence system of *Legionella pneumophila*. *Science* 279:873-6.
- Volodin, A. A., O. N. Voloshin, and R. D. Camerini-Otero.** 2005. Homologous recombination and RecA protein: towards a new generation of tools for genome manipulations. *Trends Biotechnol* 23:97-102.
- Wass, M. N., L. A. Kelley, and M. J. Sternberg.** 2010. 3DLigandSite: predicting ligand-binding sites using similar structures. *Nucleic Acids Res* 38:W469-73.



- Weber, S. S., C. Ragaz, K. Reus, Y. Nyfeler, and H. Hilbi.** 2006. *Legionella pneumophila* exploits PI(4)P to anchor secreted effector proteins to the replicative vacuole. PLoS Pathog 2:e46.
- Whitchurch, C. B., T. Tolker-Nielsen, P. C. Ragas, and J. S. Mattick.** 2002. Extracellular DNA required for bacterial biofilm formation. Science 295:1487.
- Whitfield, N. N., B. G. Byrne, and M. S. Swanson.** 2009. Mouse Macrophages are Permissive to Motile *Legionella* Species that Fail to Trigger Pyroptosis. Infect Immun.
- Winn, W., and R. Myerowitz.** 1981. The Pathology of the *Legionella* Pneumonias: A Review of 74 Cases and the Literature. Human Pathology 12:401-422.
- Winzeler, E. A., D. D. Shoemaker, A. Astromoff, H. Liang, K. Anderson, B. Andre, R. Bangham, R. Benito, J. D. Boeke, H. Bussey, A. M. Chu, C. Connelly, K. Davis, F. Dietrich, S. W. Dow, M. El Bakkoury, F. Foury, S. H. Friend, E. Gentalen, G. Giaever, J. H. Hegemann, T. Jones, M. Laub, H. Liao, N. Liebundguth, D. J. Lockhart, A. Lucau-Danila, M. Lussier, N. M'Rabet, P. Menard, M. Mittmann, C. Pai, C. Rebischung, J. L. Revuelta, L. Riles, C. J. Roberts, P. Ross-MacDonald, B. Scherens, M. Snyder, S. Sookhai-Mahadeo, R. K. Storms, S. Veronneau, M. Voet, G. Volckaert, T. R. Ward, R. Wysocki, G. S. Yen, K. Yu, K. Zimmermann, P. Philippsen, M. Johnston, and R. W. Davis.** 1999. Functional characterization of the *S. cerevisiae* genome by gene deletion and parallel analysis. Science 285:901-6.
- Xu, L., X. Shen, A. Bryan, S. Banga, M. S. Swanson, and Z. Q. Luo.** 2010. Inhibition of host vacuolar H<sup>+</sup>-ATPase activity by a *Legionella pneumophila* effector. PLoS Pathog 6:e1000822.
- Yim, L., M. Martinez-Vicente, M. Villarroya, C. Aguado, E. Knecht, and M. E. Armengod.** 2003. The GTPase activity and C-terminal cysteine of the *Escherichia coli* MnmE protein are essential for its tRNA modifying function. J Biol Chem 278:28378-87.
- Yin, Y., X. He, P. Szewczyk, T. Nguyen, and G. Chang.** 2006. Structure of the multidrug transporter EmrD from *Escherichia coli*. Science 312:741-4.
- Yoshizawa, S., K. Tateda, T. Matsumoto, F. Gondaira, S. Miyazaki, T. J. Standiford, and K. Yamaguchi.** 2005. *Legionella pneumophila* evades gamma interferon-mediated growth suppression through interleukin-10 induction in bone marrow-derived macrophages. Infect Immun 73:2709-17.

- Yu, D., H. M. Ellis, E. C. Lee, N. A. Jenkins, N. G. Copeland, and D. L. Court.** 2000. An efficient recombination system for chromosome engineering in *Escherichia coli*. Proc Natl Acad Sci U S A 97:5978-83.
- Yu, V. L., J. F. Plouffe, M. C. Pastoris, J. E. Stout, M. Schousboe, A. Widmer, J. Summersgill, T. File, C. M. Heath, D. L. Paterson, and A. Cheresky.** 2002. Distribution of *Legionella* species and serogroups isolated by culture in patients with sporadic community-acquired legionellosis: an international collaborative survey. J Infect Dis 186:127-8.
- Zhang, Y., F. Buchholz, J. P. Muyrers, and A. F. Stewart.** 1998. A new logic for DNA engineering using recombination in *Escherichia coli*. Nat Genet 20:123-8.
- Zou, Y., and B. Van Houten.** 1999. Strand opening by the UvrA(2)B complex allows dynamic recognition of DNA damage. EMBO J 18:4889-901.